

# World Journal of *Gastroenterology*

*World J Gastroenterol* 2019 November 7; 25(41): 6172-6288



**REVIEW**

- 6172** Disease monitoring strategies in inflammatory bowel diseases: What do we mean by “tight control”?  
*Goncz L, Bessissow T, Lakatos PL*

**ORIGINAL ARTICLE****Basic Study**

- 6190** Therapeutic potential of menstrual blood stem cells in treating acute liver failure  
*Cen PP, Fan LX, Wang J, Chen JJ, Li LJ*
- 6205** Yinchenhao decoction attenuates obstructive jaundice-induced liver injury and hepatocyte apoptosis by suppressing protein kinase RNA-like endoplasmic reticulum kinase-induced pathway  
*Wu YL, Li ZL, Zhang XB, Liu H*
- 6222** MiR-32-5p aggravates intestinal epithelial cell injury in pediatric enteritis induced by *Helicobacter pylori*  
*Feng J, Guo J, Wang JP, Chai BF*

**Retrospective Study**

- 6238** Bacterobilia in pancreatic surgery-conclusions for perioperative antibiotic prophylaxis  
*Krüger CM, Adam U, Adam T, Kramer A, Heidecke CD, Makowiec F, Riediger H*
- 6248** Tumor-infiltrating platelets predict postoperative recurrence and survival in resectable pancreatic neuroendocrine tumor  
*Xu SS, Xu HX, Wang WQ, Li S, Li H, Li TJ, Zhang WH, Liu L, Yu XJ*
- 6258** Blood parameters score predicts long-term outcomes in stage II-III gastric cancer patients  
*Lin JX, Tang YH, Wang JB, Lu J, Chen QY, Cao LL, Lin M, Tu RH, Huang CM, Li P, Zheng CH, Xie JW*

**Observational Study**

- 6273** Increased circulating circular RNA\_103516 is a novel biomarker for inflammatory bowel disease in adult patients  
*Ye YL, Yin J, Hu T, Zhang LP, Wu LY, Pang Z*



**ABOUT COVER**

Editorial board member of *World Journal of Gastroenterology*, Wan-Long Chuang, MD, PhD, Doctor, Professor, Hepatobiliary Division, Department of Internal Medicine, Kaohsiung Medical University Hospital, Kaohsiung Medical University, Kaohsiung 807, Taiwan.

**AIMS AND SCOPE**

The primary aim of *World Journal of Gastroenterology* (WJG, *World J Gastroenterol*) is to provide scholars and readers from various fields of gastroenterology and hepatology with a platform to publish high-quality basic and clinical research articles and communicate their research findings online.

WJG mainly publishes articles reporting research results and findings obtained in the field of gastroenterology and hepatology and covering a wide range of topics including gastroenterology, hepatology, gastrointestinal endoscopy, gastrointestinal surgery, gastrointestinal oncology, and pediatric gastroenterology.

**INDEXING/ABSTRACTING**

The WJG is now indexed in Current Contents®/Clinical Medicine, Science Citation Index Expanded (also known as SciSearch®), Journal Citation Reports®, Index Medicus, MEDLINE, PubMed, PubMed Central, and Scopus. The 2019 edition of Journal Citation Report® cites the 2018 impact factor for WJG as 3.411 (5-year impact factor: 3.579), ranking WJG as 35<sup>th</sup> among 84 journals in gastroenterology and hepatology (quartile in category Q2). CiteScore (2018): 3.43.

**RESPONSIBLE EDITORS FOR THIS ISSUE**

Responsible Electronic Editor: *Yu-Jie Ma*

Proofing Production Department Director: *Yun-Xiaojuan Wu*

**NAME OF JOURNAL**

*World Journal of Gastroenterology*

**ISSN**

ISSN 1007-9327 (print) ISSN 2219-2840 (online)

**LAUNCH DATE**

October 1, 1995

**FREQUENCY**

Weekly

**EDITORS-IN-CHIEF**

Subrata Ghosh, Andrzej S Tarnawski

**EDITORIAL BOARD MEMBERS**

<http://www.wjgnet.com/1007-9327/editorialboard.htm>

**EDITORIAL OFFICE**

Ze-Mao Gong, Director

**PUBLICATION DATE**

November 7, 2019

**COPYRIGHT**

© 2019 Baishideng Publishing Group Inc

**INSTRUCTIONS TO AUTHORS**

<https://www.wjgnet.com/bpg/gerinfo/204>

**GUIDELINES FOR ETHICS DOCUMENTS**

<https://www.wjgnet.com/bpg/GerInfo/287>

**GUIDELINES FOR NON-NATIVE SPEAKERS OF ENGLISH**

<https://www.wjgnet.com/bpg/gerinfo/240>

**PUBLICATION MISCONDUCT**

<https://www.wjgnet.com/bpg/gerinfo/208>

**ARTICLE PROCESSING CHARGE**

<https://www.wjgnet.com/bpg/gerinfo/242>

**STEPS FOR SUBMITTING MANUSCRIPTS**

<https://www.wjgnet.com/bpg/GerInfo/239>

**ONLINE SUBMISSION**

<https://www.f6publishing.com>



## Disease monitoring strategies in inflammatory bowel diseases: What do we mean by “tight control”?

Lorant Gonczi, Talat Bessissow, Peter Laszlo Lakatos

**ORCID number:** Lorant Gonczi (0000-0002-8819-6460); Talat Bessissow (0000-0003-2610-1910); Peter Laszlo Lakatos (0000-0002-3948-6488).

**Author contributions:** All authors equally contributed to this paper with conception and design of the study, literature review and analysis, drafting and critical revision and editing, and final approval of the final version; Bessissow T reviewed and language edited the submitted version of the manuscript.

**Conflict-of-interest statement:** Authors declare no conflict of interest.

**Open-Access:** This article is an open-access article which was selected by an in-house editor and fully peer-reviewed by external reviewers. It is distributed in accordance with the Creative Commons Attribution Non Commercial (CC BY-NC 4.0) license, which permits others to distribute, remix, adapt, build upon this work non-commercially, and license their derivative works on different terms, provided the original work is properly cited and the use is non-commercial. See: <http://creativecommons.org/licenses/by-nc/4.0/>

**Manuscript source:** Invited Manuscript

**Received:** September 8, 2019

**Peer-review started:** September 8, 2019

**First decision:** September 19, 2019

**Revised:** September 26, 2019

**Accepted:** October 30, 2019

**Lorant Gonczi, Peter Laszlo Lakatos**, First Department of Medicine, Semmelweis University, Budapest H-1083, Hungary

**Talat Bessissow, Peter Laszlo Lakatos**, Division of Gastroenterology, McGill University Health Centre, Montreal H3G 1A4, Quebec, Canada

**Corresponding author:** Peter Laszlo Lakatos, DSc, FRCP (C), MD, Full Professor, Staff Physician, Division of Gastroenterology, McGill University Health Centre, 1650 Cedar Avenue, Montreal H3G 1A4, Quebec, Canada. [peter.lakatos@mcgill.ca](mailto:peter.lakatos@mcgill.ca)

**Telephone:** +1-514-9341934

**Fax:** +1-514-9344452

### Abstract

In recent years, there has been a critical change in treatment paradigms in inflammatory bowel diseases (IBD) triggered by the arrival of new effective treatments aiming to prevent disease progression, bowel damage and disability. The insufficiency of symptomatic disease control and the well-known discordance between symptoms and objective measures of disease activity lead to the need of reviewing conventional treatment algorithms and developing new concepts of optimal therapeutic strategy. The treat-to-target strategies, defined by the selecting therapeutic targets in inflammatory bowel disease consensus recommendation, move away from only symptomatic disease control and support targeting composite therapeutic endpoints (clinical and endoscopic remission) and timely assessment. Emerging data suggest that early therapy using a treat-to-target approach and an algorithmic therapy escalation using regular disease monitoring by clinical and biochemical markers (fecal calprotectin and C-reactive protein) leads to improved outcomes. This review aims to present the emerging strategies and supporting evidence in the current therapeutic paradigm of IBD including the concepts of “early intervention”, “treat-to-target” and “tight control” strategies. We also discuss the real-world experience and applicability of these new strategies and give an overview on the future perspectives and areas in need of further research and potential improvement regarding treatment targets and (“tight”) disease monitoring strategies.

**Key words:** Crohn’s disease; Ulcerative colitis; Treat-to-target; Tight control; Monitoring; Biomarker

©The Author(s) 2019. Published by Baishideng Publishing Group Inc. All rights reserved.

**Article in press:** October 30, 2019  
**Published online:** November 7, 2019

**P-Reviewer:** Sipos F, Triantafyllou K, Tsuchiya K, Wenzl HH

**S-Editor:** Tang JZ

**L-Editor:** A

**E-Editor:** Ma YJ



**Core tip:** Inflammatory bowel diseases are chronic, progressive, immune-mediated disorders leading to disability and cumulative intestinal damage. There has been a major change in treatment paradigms favouring an early introduction of highly effective therapies, applying a treat-to-target approach to target composite clinical and endoscopic therapeutic endpoints and using close monitoring of objective markers of inflammation (with clinical, endoscopic and biomarker assessment) to direct therapeutic decisions until these goals are reached. Although several data support the benefit of ‘treat-to-target’ and “tight control” strategies so far, these approaches require further validation assessing long-term outcomes and more precise definition of therapeutic targets (for both endoscopic and biomarker monitoring).

**Citation:** Gonczi L, Bessissow T, Lakatos PL. Disease monitoring strategies in inflammatory bowel diseases: What do we mean by “tight control”? *World J Gastroenterol* 2019; 25(41): 6172-6189

**URL:** <https://www.wjgnet.com/1007-9327/full/v25/i41/6172.htm>

**DOI:** <https://dx.doi.org/10.3748/wjg.v25.i41.6172>

## INTRODUCTION

Inflammatory bowel diseases (IBD) are chronic immune-mediated inflammatory disorders that primarily affect the gastrointestinal tract and if uncontrolled, lead to disabling conditions that impact severely on the patient’s physical health and quality of life. The incidence and prevalence of IBD is increasing worldwide, putting significant burden on both individuals and the health care system<sup>[1]</sup>. The past two decades have brought substantial advances in the pharmacological management of IBD by the introduction of immunosuppressive agents, biologics and lately small molecules. Numerous new drugs with different mechanisms of action have emerged, however determining the specific role of each drug in the therapeutic armamentarium of IBD has become challenging. In addition to the burst of novel therapeutic options, probably the second most important result of the past years is the observation that most therapeutic approaches driven only by symptomatic control of disease activity probably failed to change the natural course of the disease<sup>[2-5]</sup>.

The availability of new, effective therapies with biologics and the insufficiency of symptomatic disease control inherently lead to the need of reviewing conventional treatment algorithms and developing new concepts of optimal therapeutic strategy. This review aims to present the emerging trends and evidence in the current therapeutic paradigm of IBD including “early intervention”, “treating to target” and “tight control” as three pillars of a modern, individualized therapeutic approach in IBD management.

## THE EVOLUTION OF TREATMENT STRATEGIES—EARLY INTERVENTION AND RISK STRATIFICATION

The treatment approach and the positioning of available therapies in the management of IBD has evolved significantly. It has now been widely acknowledged that IBD is a progressive disease and in the absence of timely and effective treatment causes cumulative structural damage and disability to the gastrointestinal tract alongside the disease course, especially in Crohn’s disease (CD)<sup>[6-8]</sup>. The Lémann score is the first disability index for CD providing comprehensive assessment of structural bowel damage (strictures, abscesses, fistulas, and surgical requirements)<sup>[7]</sup>. In ulcerative colitis (UC), there is less evidence whether ongoing inflammation necessarily leads to permanent bowel damage, however data suggests that UC also present a progressive nature in about one-fifth of patients (proctitis or left-sided colitis progressing to extensive colitis over time)<sup>[3,9]</sup>. This recognition led to the revision of conventional “step-up” treatment approaches based on the idea that the introduction of more efficacious therapies early in the disease course can potentially modify the disease trajectory.

TOP-DOWN<sup>[10]</sup> was the first trial to assess and compare different treatment algorithms in IBD. In this landmark study, treatment-naïve CD patients were randomly assigned to “top-down” strategy [start with a combination of biological

therapy and immunosuppressant-early combined immunosuppression (ECI)] compared with the standard “step-up” management (start with steroids and step up to immunosuppressant and biologics if necessary). Authors found that ECI was more effective than conventional management for achieving corticosteroid-free remission at week 52 (61.5 *vs* 42.2%;  $P = 0.0278$ ). A subsequent trial proving the superiority of combined immunosuppression in biologic naïve CD patients was the SONIC<sup>[11]</sup> trial. Results showed a clear benefit for ECI in terms of corticosteroid-free clinical remission at week 26. The REACT<sup>[12]</sup> study was designed to validate the efficacy, safety and generalizability of the top-down algorithm-based therapy in community GI practices. In this study, 1982 patients with CD were randomized to receive either ECI or conventional “step-up” therapy. The composite endpoint of hospitalization, surgery and serious disease related complications was lower in patients treated with ECI strategy at 24 mo (27.7 and 35.1%,  $P < 0.001$ ). However, the primary outcome, the proportion of patients in corticosteroid-free remission at 12 mo, was not superior (66% *vs* 61.9%;  $P = 0.52$ ). A notable limitation to the REACT study is that although the trial is supposed to investigate the effects of “early” introduction of combined immunosuppression, a large proportion of patients had longstanding disease or prior respective surgery, and had been treated with biologics and/or immunosuppressants. The very recent CALM<sup>[13]</sup> trial also verified the benefits of early introduction and quick escalation of immunosuppressive and biologic therapies when meeting treatment failure criteria (either clinical or biomarker). Despite certain limitations and methodological differences, the above results suggest that highly effective therapy initiated early in the course can potentially lead to better outcomes without a significant increase in drug-related risk (concept of “window of opportunity”).

It is important to recognize that a significant proportion of IBD patients have mild disease course. Population-based data suggests that 40% of patients with CD have a clinically indolent disease, and approximately half of the patients with CD will present non-complicated (B1) disease behavior 10 years after diagnosis<sup>[8]</sup>. In both CD and UC, potentially indolent disease must be distinguished from severe disease, assuring the opportunity of early intensive therapy for the latter one, while those with indolent disease might benefit from a slower escalation of therapeutic steps, avoiding potential overtreatment. With the introduction of multiple new therapies, the identification of populations with high risk of severe disease course gained a growing interest. Predictive factors have been identified in population-based cohorts for CD, including younger age at disease onset, smoking, extensive small bowel disease, perianal disease, deep ulceration on endoscopy, prior surgery, corticosteroid use at diagnosis, and extra-intestinal manifestations<sup>[14,15]</sup>. In the case of UC, patients with pancolitis, deep ulcers on endoscopy and non-smoking status are at higher risk for colectomy<sup>[16]</sup>. Prediction models for assessing the probability of advanced disease 5 and 10 years after diagnosis have been developed in both CD and UC, however external validation of these prediction tools are still warranted<sup>[16-18]</sup>.

## THE CONCEPT OF TREAT-TO-TARGET

The concept of “treat-to-target” has been studied and applied thoroughly in chronic diseases, such as diabetes or rheumatoid arthritis for several years and resulted in improved outcomes. For IBD patients, this concept originated from the observation that current symptom oriented therapeutic strategies failed to alter the natural progression of IBD according to the results of many population-based studies, even though immunosuppressives and biologicals have been introduced<sup>[2-5,19-21]</sup>. This could at least partly be the results of the frequent and widely acknowledged discordance between symptoms and objective measures of disease activity, especially in CD. In a post-hoc analysis of the SONIC trial, half of the patients who were in clinical remission had evidence of residual disease activity, based on endoscopic assessment or C-reactive protein (CRP) measurement, whereas other patients with endoscopic and CRP normalization still had persistent clinical symptoms<sup>[22]</sup>. In the case of UC, symptoms usually correlate better with endoscopic activity compared to CD, although a significant proportion of patients in clinical remission still have endoscopic activity and the normalization of stool frequency does not always follow endoscopic healing<sup>[23]</sup>. Switching the therapeutic endpoints from clinical remission to endoscopic healing has been increasingly supported by post-hoc analyses of pivotal clinical trials. Achieving mucosal healing was shown to predict long-term steroid free remission and better outcomes in terms of surgical and hospitalization requirements<sup>[10,24-27]</sup>.

The treat-to-target concept in IBD was developed by the selecting therapeutic targets in inflammatory bowel disease (STRIDE) committee, a group of international IBD experts established by the International Organization for the Study of



Inflammatory Bowel Diseases in 2015. The treat-to-target implies the identification of a predefined goal in the context of the patient's individual needs to be achieved by the therapy, followed by regular monitoring and treatment optimization if needed, until this goal is achieved. The definition of recommended treatment targets were performed based on an evidence-based expert consensus process<sup>[28]</sup>.

In CD, the treat-to-target recommendations are composite endpoints of clinical (defined as resolution of abdominal pain and altered bowel habit) and endoscopic remission (defined as resolution of ulceration). For patients who could not be adequately assessed by ileocolonoscopy, resolution of inflammation based on cross-sectional imaging is the desired target. The primary target recommendations for UC also consist of clinical (defined as resolution of rectal bleeding and normalisation of bowel habit) and endoscopic endpoints (defined as resolution of friability and ulceration at flexible sigmoidoscopy or colonoscopy). Biochemical targets [CRP or fecal calprotectin (FCAL)] and histopathology were not recommended as adjunctive endpoints. The use of biomarkers (CRP and FCAL) are recommended in both CD and UC for disease monitoring, and persistent failure of normalization should prompt further endoscopic or radiologic evaluation, regardless of symptoms. Imaging modalities are considered having a complementary role to endoscopy in CD, and they are not recommended for disease assessment in UC<sup>[28]</sup>.

## INSTRUMENTS OF TIGHT CONTROL IN DISEASE MONITORING

At the time of the development of STRIDE, supporting evidence for target recommendations were available only from retrospective studies and post-hoc analyses of randomized clinical trials. Emerging prospective and clinical trial data with long-term outcomes of the application of the treat-to-target concept have been published, which will help further understanding of the treat-to-target approach and adjusting and optimizing the various targets in everyday clinical practice. The importance of timely assessment of disease activity has been clearly emphasized in the STRIDE creating the concept of "tight" disease control. The CALM<sup>[13]</sup> trial was the first randomized study to show that tight disease monitoring using objective markers of inflammation and timely escalation of therapy in patients with early CD leads to better clinical and endoscopic outcomes compared to symptom-driven management alone. Objective measurement of inflammatory activity requires invasive and costly procedures, such as ileocolonoscopy or cross-sectional imaging. Levels of CRP and FCAL are among the most widely investigated non-invasive markers of inflammation in IBD. In recent years, the most significant adjustment to the STRIDE recommendations is the increasing role of biomarkers (CRP and FCAL) in treatment decisions based on the supporting results of the CALM trial. In the following sections we aim to give a detailed description and review of current evidence on each therapeutic target and their role in a "tight control" disease management (see [Table 1](#)).

### Clinical targets

Although resolution of symptoms alone is not a sufficient therapeutic endpoint, it is still necessary to properly monitor and treat symptoms of the disease. Multiple clinical scoring systems have been developed in clinical practice; the Crohn's Disease Activity Index (CDAI) and Harvey Bradshaw Index (HBI) being the most widely used in CD, and the partial Mayo score (pMayo) and the Simple Clinical Colitis Activity Index in UC<sup>[29-32]</sup>.

The CDAI, HBI or pMayo scores are composite clinical scores, meaning that they include laboratory features, disease characteristics or the general assessment of the physician. As the STRIDE recommendation outlined the resolution of clinical symptoms as a separate therapeutic target, it is logical to develop independent clinical measures that reliably assess symptoms coming directly from a patient. A "patient reported outcome" (PRO) is a report from the patient's perspective about the status of their symptoms and perceived response to therapy. According to the FDA guidance, creating a PRO must involve generation of items based on qualitative patient interviews and thorough testing for responsiveness and internal consistency<sup>[33]</sup>. Although composite clinical scores such as the CDAI and HBI indices include patient-reported severity of symptoms, their development was not conducted in accordance with these stringent requirements. In the absence of a well-characterized PRO items for IBD, the STRIDE program recommends the use of a two-item interim PRO that should be resolution of abdominal pain and normalization of bowel habit for CD, and in the case of UC, resolution of rectal bleeding and normalization of bowel habit. Assessment of clinical targets should be tailored to the patient's individual needs,

**Table 1** Selected studies supporting the use of clinical, biochemical, endoscopic, histological and combined targets since the publication of selecting therapeutic targets in inflammatory bowel disease consensus

Study	Study type	Treatment targets evaluated	Patient population	Compared patient groups	Outcomes
Colombel <i>et al</i> <sup>[13]</sup> (CALM)	Randomized clinical trial	Combined clinical and biomarker	CD- 244 patients	Incremental therapy escalation based on "tight control" with biomarker (CRP and FCAL) and clinical assessment every 12 wk <i>vs</i> "clinical management" with only clinical assessment	Outcomes at 48 wk: Mucosal healing (CDEIS < 4 and no deep ulcerations), 45.9% <i>vs</i> 30.3%; <i>P</i> = 0.010 steroid free remission, 59.8% <i>vs</i> 39.3%; <i>P</i> < 0.001 deep remission (CDAI < 150, CDEIS < 4 and no deep ulcers), 36.9% <i>vs</i> 23.0%; <i>P</i> = 0.014 biological remission (FCAL < 250 µg/g, CRP < 5 mg/L, and CDEIS < 4), 29.5% <i>vs</i> 15.6; <i>P</i> = 0.006
Ungaro <i>et al</i> <sup>[55]</sup> (CALM – long term extension)	Randomized clinical trial	Endoscopy	CD – 122 patients	Endoscopic remission (CDEIS < 4 and no deep ulcerations) at 1 yr <i>vs</i> NOT Deep remission (CDAI < 150, CDEIS < 4 and no deep ulcers) at 1 yr <i>vs</i> NOT	Composite of major adverse outcomes reflecting CD progression: New internal fistula/abscess, stricture, perianal fistula/abscess, CD hospitalization, or CD surgery (median 3 yr follow-up after end of CALM): aHR = 0.44, 95%CI: 0.20-0.96, <i>P</i> = 0.038 aHR = 0.25, 95%CI: 0.09-0.72, <i>P</i> = 0.01
Shah <i>et al</i> <sup>[38]</sup>	Meta-analysis	Endoscopy	CD – 673 patients (12 studies included)	Achieving MH at first endoscopic assessment after therapy initiation <i>vs</i> NOT	Outcomes reported at ≥ 50 wk: Clinical remission [OR] 2.80, 95%CI: 1.91-4.10 maintenance of mucosal healing [OR] 14.30, 95%CI: 5.57-36.74 resective surgery [OR] 2.22, 95%CI: 0.86-5.69
Shah <i>et al</i> <sup>[39]</sup>	Meta-analysis	Endoscopy	UC – 2073 patients (13 studies included)	Achieving MH at first endoscopic assessment after therapy initiation <i>vs</i> NOT	Outcomes reported at ≥ 50 wk: clinical remission [OR] 4.50, 95%CI: 2.12-9.52 avoiding colectomy [OR] 4.15, 95%CI: 2.53-6.81 maintenance of mucosal healing [OR] 8.40, 95%CI: 3.13-22.53 long-term corticosteroid-free clinical remission [OR] 9.70, 95%CI: 0.94-99.67
Park <i>et al</i> <sup>[70]</sup>	Meta-analysis	Histology	UC – 13 studies included	Histological remission <i>vs</i> NO histological remission at baseline Histological remission <i>vs</i> NO histological remission at baseline among patients in combined clinical and endoscopic remission	Outcomes up to 12 mo follow-up: Clinical relapse/ exacerbation [RR] 0.48, 95%CI: 0.39–0.60 Clinical relapse/ exacerbation [RR] 0.81, 95%CI: 0.70–0.94
Bryant <i>et al</i> <sup>[68]</sup>	Prospective	Histology	UC – 91 patients	Histological remission <i>vs</i> NO histological remission at baseline	Outcomes reported over a median 72 mo follow-up: corticosteroid use [HR] 0.42, 95%CI: 0.2–0.9; <i>P</i> = 0.02 acute severe colitis requiring hospitalization [HR] 0.21, 95%CI: 0.1–0.7; <i>P</i> = 0.02

Lasson <i>et al</i> <sup>[93]</sup>	Prospective, Randomized	Biomarker	UC – 91 patients	Monthly FCAL measurement: Dose-escalation of 5-ASA in patients with FCAL > 300 µg/g <i>vs</i> NO intervention	18 mo follow-up: Fewer clinical relapses observed in intervention group, 28.6% <i>vs</i> 57.1%; <i>P</i> <0.05
Zhulina <i>et al</i> <sup>[52]</sup>	Prospective	Biomarker	CD – 49 patients; UC – 55 patients	First clinical relapse <i>vs</i> NO relapse in patients with clinical remission at baseline	2 yr of follow-up: Doubling of faecal calprotectin level between two consecutively samples 3 mo apart predicted relapse [HR] 2.01, 95%CI: 1.53-2.65
Sollelis <i>et al</i> <sup>[94]</sup>	Prospective	Combined clinical and biomarker	CD – 40 patients	Clinical and biomarker remission at 12 wk (CDAI < 150 and CRP ≤ 2.9 mg/L and FCAL < 300 µg/g) <i>vs</i> NOT	Predictive power for corticosteroid-free clinical remission at 52 wk: Sensitivity = 69.2% (42.0-87.4) specificity = 100.0% (84.9-100.0) PPV = 100.0% (100.0-100.0) NPV = 87.1% (75.3-98.9)

CD: Crohn's disease; UC: Ulcerative colitis; CRP: C-reactive protein; FCAL: Fecal calprotectin; CDAI: Crohn's Disease Activity Index; CDEIS: Crohn's Disease Endoscopic Index of Severity; 5-ASA: 5-aminosalicylic acid; RR: Relative risk; HR: Hazard ratio; OR: Odds ratio; CI: Confidence interval; NPV: Negative predictive value; PPV: Positive predictive value; aHR: Adjusted hazard ratio.

with a minimum of every 3 mo during active disease and every 6-12 mo after symptom resolution for both CD and UC<sup>[28]</sup> (see Table 2).

Since the STRIDE recommendations, newer PRO tools, including more clinical variables (abdominal pain and urgency for UC) in accordance with FDA guidance, have been developed, however their applicability in clinical trial design or everyday clinical practice still remain to be validated<sup>[34-36]</sup>. Various other PROs have already been used in clinical trials reporting depression, anxiety, disability and other quality of life parameters, however available data on these PROs in IBD are yet limited. The IBD disability index (IBD-DI), developed in accordance with the WHO International Classification of Functioning is a validated tool to measure disability, and shows good correlation with clinical disease activity<sup>[37]</sup>. Future studies will assess the role of IBD-DI as a potential clinical target.

### Endoscopic targets

Numerous recent studies support the STRIDE recommendation to target endoscopic healing, since several clinical trials (post-hoc analysis) and population-based studies have demonstrated that achieving mucosal healing is associated with improving outcomes, such as lower rates of hospitalizations, disease relapse, and lower surgery requirements<sup>[24-27]</sup>. In a systematic review and meta-analysis of 12 studies, endoscopic remission (or mucosal healing) on the first post-treatment endoscopy was associated with a higher rates of long-term clinical remission [pooled odds ratio (OR) = 2.80, 95%CI: 1.91-4.10], maintenance of mucosal healing (14.30, 95%CI: 5.57-36.74), and lower risk of surgery (2.22, 95%CI: 0.86-5.69) in patients with CD<sup>[38]</sup>. The same meta-analysis of 13 studies was performed for UC, resulting that mucosal healing on the first post-treatment endoscopy was associated with long-term (52 wk) clinical remission [OR = 4.50, 95%CI: 2.12-9.52], avoiding colectomy (4.15, 95%CI: 2.53-6.81), achieving long-term corticosteroid-free clinical remission (9.70, 95%CI: 0.94-99.67), and long-term mucosal healing (8.40, 95%CI: 3.13-22.53)<sup>[39]</sup>. The feasibility of applying a treat-to-target approach in regard to mucosal healing was studied by Bouguen *et al*<sup>[40]</sup>. Sixty-seven CD patients with endoscopic lesions underwent two to four subsequent endoscopies with a median follow-up of 76 wk. Factors associated with achieving mucosal healing were fewer than 26 wk between endoscopic procedures [hazard ratio (HR) = 2.21; 95%CI: 1.16-4.26; *P* = 0.016] and adjustment to medical therapy when mucosal healing was not observed (2.35; 95%CI: 1.2-4.94; *P* = 0.012), concluding that serial endoscopic procedures and treatment optimizations accordingly are feasible in clinical practice and high rates of MH can be achieved.

Although, the predictive value of early mucosal healing and the need for applying endoscopic targets as primary therapeutic endpoints is clear, the definition for optimal endoscopic targets is lacking. The STRIDE recommendations specify endoscopic targets as resolution of ulceration in CD and resolution of ulceration and friability in UC assessed at 6-9 mo and 3-6 mo after commencing therapy, respectively<sup>[28]</sup> (Table 2). The definition of mucosal healing is however highly

**Table 2** Intervals of clinical, biomarker, and endoscopic assessment in the treat-to-target and tight control framework

	Active disease/at flare	Clinical remission
<b>Crohn's disease</b>		
Clinical evaluation (PRO, CDAI, HBI indices)	3 mo [STRIDE and CALM protocol] <sup>[28,13]</sup>	6-12 mo [STRIDE] <sup>[28]</sup> 3 mo [CALM protocol] <sup>[13]</sup>
Endoscopic evaluation	6-9 mo after therapy initiation [STRIDE] <sup>[28]</sup>	Based on screening recommendations in deep remission Prompted by clinical symptoms or (consecutive) biomarker positivity – FCAL <sup>[52,53]</sup>
Biomarker evaluation (CRP and FCAL)	3 mo (FCAL + CRP) [CALM protocol] <sup>[13,94]</sup> Approximately 12-14 wk after therapy initiation (CRP) <sup>[95,96]</sup> Approximately 14 wk after therapy initiation (FCAL) <sup>[94,97,98]</sup>	3 mo (FCAL + CRP) [CALM protocol] <sup>[13]</sup> (2)-3 mo (FCAL) <sup>[52,53]</sup> 3 mo (CRP) <sup>[99]</sup>
<b>Ulcerative colitis</b>		
Clinical evaluation (PRO, CDAI, HBI indices)	3 mo [STRIDE] <sup>[28]</sup>	6-12 mo [STRIDE] <sup>[28]</sup>
Endoscopic evaluation	3-6 mo after therapy initiation [STRIDE] <sup>[28]</sup>	Based on screening recommendations in deep remission Prompted by clinical symptoms or (consecutive) biomarker positivity – FCAL <sup>[52,53]</sup>
Biomarker evaluation (CRP and FCAL)	Approximately 10 wk after therapy initiation (FCAL) <sup>[100]</sup>	(2)-3 mo <sup>[51-53,101]</sup>

<sup>1</sup>Using C-reactive protein alone has only moderate predictive value in identifying relapse in patients with clinical remission. PRO: Patient reported outcome; CDAI: Crohn's Disease Activity Index; HBI: Harvey Bradshaw Index; CRP: C-reactive protein; FCAL: Fecal calprotectin; STRIDE: Selecting therapeutic targets in inflammatory bowel disease.

heterogenous, especially in CD. The most commonly accepted definition of endoscopic healing is the disappearance of all ulcerative lesions, however this definition does not allow for the interpretation of partial resolution of mucosal inflammation. A different solution would be the use of reproducible endoscopic activity scores capable of depicting precise degree of endoscopic activity and subsequent changes. Widely used endoscopic scores in CD are the Crohn's disease Endoscopic Index of Severity (CDEIS) and Simple Endoscopic Score for Crohn's disease (SES-CD), and Rutgeerts' score for post-surgical evaluation of endoscopic recurrence. In UC, the endoscopic Mayo score and the Ulcerative Colitis Endoscopic Index of Severity (UCEIS) are most frequently used. However, the proper definition of "optimal" or "targeted" degree of endoscopic healing is lacking.

A post-hoc analysis of the SCONIC trial tried to identify an optimal definition for endoscopic healing/remission that would predict long term outcomes in CD. Mucosal healing (resolution of ulcers) and endoscopic response (defined as a decrease from baseline SES-CD or CDEIS by at least 50%) at week 26 showed the best performance in identifying those most likely to be in corticosteroid-free clinical remission at week 50, however AUC values were fairly modest in either case, moreover a higher decrease from baseline SES-CD or CDEIS scores did not show better predictive performance<sup>[41]</sup>. This further strengthens the fact that the desired degree of endoscopic healing to reach superior long-term outcomes or the absence of endoscopic improvement which should prompt therapy change is largely unknown. The same problem applies for clinical trial design where the absence of validated definitions of endoscopic healing leads to the arbitrary choice of endoscopic endpoints by investigators. Recently, the International Organization for the Study of Inflammatory Bowel Disease (IOIBD) reviewed endoscopic scoring systems and achieved consensus on definitions of endoscopic remission and response in CD. Expert investigators chose a > 50% decrease in SES-CD or CDIES for the definition of endoscopic response, and an SES-CD 0-2 for the definition of endoscopic remission<sup>[42]</sup>. Of note, these recommendations are yet to be subjected to thorough validation and prospective testing before widely incorporated into clinical trial endpoints or everyday clinical practice.

Although endoscopic healing is a critical target in UC, the scoring systems and endoscopic criteria of healing also warrant revision. Generally, a Mayo 0 or 1 endoscopic score is considered to be endoscopic remission, however new data show that a score of 0 is associated with lower risk of clinical relapse compared with a score of 1<sup>[43,44]</sup>. Updates in the endoscopic Mayo score incorporating disease extent correlate well with clinical and endoscopic outcomes and may improve the applicability and accuracy of the most widely used scoring system<sup>[45]</sup>. The UCEIS is also accurate and responsive, and takes ulcer size and depth in consideration, parameters that are not captured by the endoscopic Mayo score, however the assessment of friability is excluded from the UCEIS<sup>[46]</sup>. Recently, the IOIBD suggested the use of UCEIS of 0 as the definition of endoscopic remission and a decrease in Mayo endoscopic score ≥ 1



grade or a decrease in UCEIS  $\geq 2$  points for the definition of endoscopic response in UC<sup>[47]</sup>.

### Biochemical targets

The most broadly used and thoroughly studied biomarkers are the serum CRP and FCAL. In general, elevated CRP levels in CD are associated with clinical disease activity and endoscopic inflammation<sup>[48]</sup>. Compelling results show that early normalization of CRP is associated with therapeutic response in CD and in patients having an elevated CRP concentration at baseline, changes in CRP may provide useful information in monitoring treatment response. However, CRP is not a specific marker of intestinal inflammation with an overall specificity of 0.49 (95%CI: 0.72–0.98) in CD, moreover, approximately 20% of patients do not present with an elevated CRP during disease flare<sup>[49]</sup>. Much less data support the applicability of CRP measurements in UC as many patients with UC do not have elevated CRP levels. However, serial measurements may be useful for assessment of treatment response in patients with severe colitis.

FCAL is a highly sensitive marker of endoscopic disease activity in both UC and CD<sup>[49]</sup>. However, identifying the optimal FCAL concentration cut-off values best predictive of disease activity is challenging. D’Haens *et al*<sup>[50]</sup> suggested a fecal calprotectin cut-off value of 250  $\mu\text{g/g}$ , as levels above this concentration predicted large ulcers in CD (sensitivity 60%, specificity 80%) and active mucosal disease (Mayo score  $> 0$ ) in UC (sensitivity 71%, specificity 100%). A recent study also demonstrated that during the regular monitoring of FCP levels, two consecutive FCAL measurements of  $> 300 \mu\text{g/g}$  with 1-mo interval were identified as the best predictor of disease flare (61.5% sensitivity and 100% specificity)<sup>[51]</sup>. Furthermore, two recent studies showed that patients had significantly higher FCAL levels as soon as 3 mo before disease flare<sup>[51,52]</sup>. Zhulina *et al*<sup>[52]</sup> reported that doubling of faecal calprotectin level between two consecutively collected samples 3 mo apart was associated with a 101% increased risk of relapse (HR = 2.01; 95%CI: 1.53–2.65;  $P < 0.001$ ). A systematic analysis of six studies has shown that increased levels of FCAL on at least two consecutive measurements were associated with a higher risk of relapse within 2–3 mo in asymptomatic patients<sup>[53]</sup>. In predicting relapse after surgery, evidence suggests that FCAL may be best utilized as a monitoring strategy for postoperative recurrence, with values  $< 100 \mu\text{g/mg}$  strongly suggesting no recurrent disease<sup>[54]</sup> (see [Table 2](#)).

Biochemical targets (CRP or FCAL) were not recommended by STRIDE as primary treat-to-target endpoints due to lack of sufficient evidence in support of their use at the time the guidance. However, their use is recommended in both CD and UC as adjunctive measure to monitor disease activity<sup>[28]</sup>. The use of biomarkers for disease monitoring has the advantage of being non-invasive and relatively inexpensive. The above results suggest that after identifying the appropriate cut-off levels, the combined measurement of these biomarkers (FCAL and CRP) could very much help disease monitoring and decision making about the optimal timing of endoscopy. Significant progress has been made since the STRIDE recommendations in this regard.

The most compelling evidence for the tailored use of biomarkers in tight disease monitoring derives from the CALM<sup>[13]</sup> study, seeking whether it is appropriate to intensify therapy in patients based on close monitoring of inflammatory biomarkers (CRP and/or FCAL). The CALM study is the first randomized trial to demonstrate that in patients with early CD, therapy based on biochemical targets in addition to clinical targets (tight control arm) is associated with higher endoscopic remission at 1 year compared with therapy based on clinical targets alone (clinical management arm). Treatment in both arms was escalated in a stepwise manner from no treatment to adalimumab induction, followed by adalimumab every other week, adalimumab every week, and lastly to both weekly adalimumab and daily azathioprine. Evaluations were performed at 12, 24, and 36 wk and escalation was based on meeting one of the following failure criteria; tight control group: faecal calprotectin  $\geq 250 \mu\text{g/g}$ , CRP  $\geq 5\text{mg/L}$ , CDAI  $\geq 150$  or prednisone use in the previous week; clinical management group: CDAI decrease of  $< 100$  points compared with baseline or CDAI  $\geq 200$ , or prednisone use in the previous week. For the tight control arm, even if patients were symptomatically well, treatment was escalated if biomarkers were raised. The primary outcome at 48 wk after randomisation was mucosal healing (CDEIS  $< 4$  and no deep ulcerations). A significantly higher proportion of patients achieved the primary endpoint (46% *vs* 30%; adjusted risk difference 16.1%, 95%CI: 3.9–28.3;  $P = 0.010$ ) when applying a tight control strategy, compared to symptom-driven clinical management. In addition, fewer CD-related hospitalizations occurred in the tight control arm (13.2 *vs* 28.0 events/100 patient-years;  $P = 0.021$ ). Subsequent follow-up data of the CALM study on 122 patients for 3 additional years revealed that endoscopic remission [adjusted hazard ratio = 0.44, 95%CI: 0.20–0.96] and combined endoscopic and clinical (deep) remission (0.25, 95%CI: 0.09–0.72) at 1 year were

associated with lower risk of adverse events such as new internal fistula/abscess, stricture, perianal fistula/abscess, hospitalization, or surgery in long-term follow-up<sup>[55]</sup>. These data further strengthen the STRIDE recommendations for targeting combined endoscopic and clinical remission and adds the importance of the timely assessment and aiming for normalization of biochemical markers.

Therapeutic drug monitoring (TDM) is an integral component of tight disease monitoring in IBD. Numerous studies have shown that optimal levels of anti-TNF agents are associated with clinical and endoscopic remission, and conversely, low drug levels are associated with reduced clinical efficacy, suboptimal control of inflammation, and higher risk of disease flares<sup>[56-58]</sup>. The most evidence support the role of drug Trough Level (TL) and anti-drug antibody (ADA) evaluations ideally in patients losing response to biologic therapy– *i.e.*, reactive TDM in the case of suspected loss of response (LOR)<sup>[59-61]</sup>. The use of reactive TDM is based on a widely known algorithmic approach, originally developed to assess treatment failure (LOR) in patients treated with anti-TNF agents (see Table 3). There are currently insufficient data to determine the exact role of TDM in other newer biologics, such as vedolizumab or ustekinumab.

Results of clinical trials investigating the benefit of proactive/routine drug monitoring have been however somewhat disappointing. In the TAXIT (Trough Level Adapted Infliximab Treatment) trial, no difference in the primary outcomes (clinical remission at 1 year) was observed between patients randomly assigned to a drug-monitoring group in which infliximab dosing was continuously adjusted, (drug levels within 3–7 µg/mL), or to a conventional therapy group, with infliximab dosing based on clinical symptoms alone (69% *vs* 66%;  $P = 0.686$ )<sup>[62]</sup>. The TAILORIX (Tailored treatment with infliximab for active CD) trial also studied CD patients receiving infliximab and subsequent dose-escalation guided by infliximab levels, biomarkers and clinical symptoms *vs* clinical symptoms alone. No significant difference was observed between the patient groups for the primary outcome of steroid-free clinical remission at 22 and 54 wk<sup>[63-65]</sup>. Although other single cohort or retrospective studies show potential benefits of proactive TDM<sup>[66]</sup>, based on the above trials it is questionable whether routine proactive monitoring of aTNF agents lead to improving outcomes, or TDM measurements can be reserved optimally for assessment of therapeutic failure. Observational studies also show that measuring drug and anti-drug antibody levels can guide decisions for anti-TNF withdrawal or restart after a drug holiday<sup>[67]</sup>. Further reviewing the available evidence on TDM is beyond the scope of this article.

### Histologic targets

Histologic remission, which means resolution of inflammation on microscopical/histological examination of the colonic mucosa, was not recommended as a target by the STRIDE recommendation due to lack of sufficient evidence. Lately, histological assessment in UC has an emerging role in clinical trials. Recent studies consistently suggest that achieving histologic remission may demonstrate better prognostic value in long-term outcomes (relapse-free survival, corticosteroid use, and hospitalization) than endoscopy<sup>[68,69]</sup>. In a meta-analysis of 15 studies, the risk of UC exacerbation was lower with histologic remission compared with patients with histological activity but in endoscopic and clinical remission [pooled OR = 0.81, 95% CI: 0.70–0.94]<sup>[70]</sup>. Several histologic scoring systems are available in UC, the Nancy index and the Robarts Histopathology Index (RHI) being properly validated and showing good correlation with endoscopic disease activity and biomarkers, however optimal endpoints in histologic healing are yet to be determined<sup>[71]</sup>. In the case of CD, there are very few data to support histologic remission as a treatment target. The lack of a validated histologic scoring systems to identify remission and the risk of sampling error due to the manifestation of CD (skip-lesions) limit the applicability of histologic assessment.

### Imaging targets

Several study demonstrated that cross-sectional imaging have superior diagnostic accuracy compared to ileocolonoscopy in extensive ileal, stricturing or penetrating CD, and have a higher impact on therapeutic decisions in appropriate patients<sup>[72]</sup>. The STRIDE consensus recommended resolution of lesions in cross-sectional imaging as not a universal target, although imaging modalities should have a complementary role in patients with CD who cannot be adequately assessed by colonoscopy. Further data in CD patients using imaging modalities to target resolution of inflammation have been reported since the publication of STRIDE. In a retrospective analysis, complete resolution of small bowel lesions on CTE or MRE was associated with a decrease in hospitalization [(HR), 0.28, 95% CI: 0.15–0.50] and surgery (0.34, 95% CI: 0.18–0.63) over a median of 9 years observed period<sup>[73]</sup>. Patients with transmural

**Table 3** Therapeutic drug monitoring-based algorithm for handling patients with treatment failure on biologic therapy<sup>[59-61]</sup>

	Detectable anti-drug antibodies	Undetectable anti-drug antibodies
Sub-therapeutic anti-TNF drug levels	Change to different TNF-inhibitor.	Intensify the treatment regimen of the currently used TNF-inhibitor.
Therapeutic anti-TNF drug levels	(Repeat assessments of anti-TNF drug and anti-drug antibodies over time) Switch to another biological agent with a different mechanism of action.	Switch to another biological agent with a different mechanism of action.

TNF: Tumor necrosis factor.

healing on MRE presented lower rates of therapy escalation, hospital admission and surgery at 1 year in a prospective cohort<sup>[74]</sup>. In a retrospective study, fast-track MRI examinations coupled with clinical and biomarker activity assessment had a significant impact on patient management, leading to better patient stratification and earlier optimization of the therapy (medical or surgical)<sup>[75]</sup>. Abdominal ultrasound (US) is a safe and inexpensive diagnostic modality, and shows comparable overall diagnostic performance to MRI and CT modalities in ileal CD<sup>[72]</sup>. Recently, several US indices have been developed for assessing disease activity, however further validation of these tools and their impact in disease monitoring need more research<sup>[76]</sup>.

Cross-sectional imaging modalities are not recommended by the STRIDE in the evaluation of UC, considering that it is primarily a mucosal disease. However, the MaRIA MRI index or diffusion-weighted MRI modalities studied mainly in patients with CD, have high sensitivity in detecting mucosal lesions, thus could have potential applicability in UC<sup>[77]</sup>. The lack of invasiveness and radiation exposure makes MRI an attractive diagnostic tool, although further investigation is definitely warranted however to demonstrate long-term outcomes in MRI guided therapeutic strategies.

## TREATMENT DE-ESCALATION

As a result of the changing treatment paradigms, there has been an exponential increase in the exposure to immunosuppressive and biologic agents. Several long-term trials have shown that discontinuation of therapy is associated with high relapse rates, suggesting that cessation of biologics can be considered only in selected patients. It is important to recognize that tight control management strategies could also help identifying those patients through proper disease monitoring strategies and not only promote therapy escalation but de-escalation as well. The STORI (infliximab discontinuation in CD patients in stable Remission on combined therapy with Immunosuppressors) trial showed that the relapse rate within a 1 year of discontinuation was approximately 50%, however, patients having  $\leq 2$  risk factors, including male gender, elevated leukocytes, an elevated CRP level, elevated FC level, and decreased hemoglobin showed only a 15% risk of relapse<sup>[78]</sup>. Safety signals were not different between patient groups in the CALM<sup>[13]</sup> study despite a higher exposure to combined immunosuppression in the tight control arm, nevertheless, safety concerns regarding combined immunosuppression and the huge increase in drug related costs makes it necessary to develop appropriate de-escalation strategies for selected patients, and determine the exact role of biomarkers and endoscopy in this area as well.

## REAL-WORD EXPERIENCE WITH TREAT-TO-TARGET STRATEGIES

Although the treat-to-target and tight control strategies seem to achieve improved long-term outcomes in CD and UC, certain factors can limit the applicability and acceptance of these new paradigms in clinical practice. Although there are reports of these new strategies to be properly translated in clinical practice in several IBD centers, some studies propose significant gaps in the implementation of treat-to-target strategies<sup>[79,80]</sup>. The overall increase in doctor-patient visits, laboratory testing, and endoscopies could be “burdensome” for both patients and physicians and could potentially slow the uptake of treat-to-target strategies, especially in community gastroenterology services. In contrast to the STRIDE recommendations, which advocate for endoscopic evaluation after 3 mo of therapy start in active UC,

endoscopy was performed in only 47% of such patients within 3 mo, and in 68% within 6 mo in a recent Australian multicenter study of IBD outpatient services<sup>[80]</sup>. In the same study, a clinician survey was performed showing that 80% of respondents had heard of the “treat-to-target” concept, 61% were familiar with the recommendations, but only 64% considered it relevant to local clinical practice.

It is important for individual IBD centers to assess and measure local therapeutic strategies and processes, and evaluate whether they are in concordance with current expert recommendations and consensus Quality of Care standards<sup>[81,82]</sup>. A study by Reinglas *et al*<sup>[83]</sup> is one of the few reporting a detailed assessment of patient evaluation strategies, disease monitoring, treatment decisions, disease-related outcomes from a tertiary care IBD center in Canada. Results confirmed the application of objective patient re-evaluation and monitoring (ileocolonoscopy or colonoscopy was performed in 79% of all IBD patients within the past 2 years from a chosen time point), timely access to diagnostic procedures and accelerated treatment pathways. Another example for the application of tight control strategies is from Hungary, where a harmonized monitoring strategy is mandatory with serial clinical (CDAI and pMayo scores) and laboratory (CBC and CRP) assessments reported every 3 mo as requested by the Hungarian National Health Fund for patients receiving biologic therapies<sup>[84]</sup>.

A properly working platform for rapid patient access (in case of flare or other IBD related emergency situations) is equally important in the framework of “tight control” management. A special emphasis on providing rapid patient access could potentially help avoiding undesirable outcomes such as steroid dependency, frequent Emergency Department (ED) visits or emergency hospitalizations/surgeries. Several data show that inadequate ‘patient access’ to treating physician or healthcare services is frequently a source of dissatisfaction among patients<sup>[85]</sup>. Our group performed a detailed analysis of patient access, diagnostic procedures, resource utilization, and outcome parameters after the implementation of a new Rapid Access Clinic service at the McGill University Health Centre tertiary care IBD center. Patients presenting with flare had a fast-track clinical and biomarker evaluation (CRP and FCAL measured in 91% and 73%) within a median of 2 d. Patient evaluations by an IBD specialist instead of the ED services led to a more optimal resource utilization (fewer cross-sectional imaging and fewer hospitalizations) in the majority of cases<sup>[86]</sup>.

Targeting MH as treatment endpoint and the tight control strategies may result in a potential increase in healthcare costs because of the more frequent use of diagnostic procedures and services and more importantly the increased rate of therapy escalations (dose intensification of biologics). Whether these additional costs could be balanced by the reduction of other healthcare expenditures associated with the long-term remission could also have major influence on the real-world application of the treat-to-target strategies. A decision analysis model performed by Ananthakrishnan *et al*<sup>[87]</sup> using existing clinical trial data demonstrated that targeting MH was more effective at a 2 year endpoint (QALY 0.71) compared to convention clinical management strategies (QALY 0.69) with an incremental cost-effectiveness ratio (ICER) of \$ 47,278/QALY gained. A similar cost-effectiveness analysis of the CALM trial was also performed. At 48 wk, the tight control arm produced a total of £ 13296 in direct medical costs and a QALY of 0.684, while the same results were £ 12627 and 0.652 for the clinical management arm. The difference in costs (£ 669) divided by the difference in QALY (0.032) produced an ICER of £ 20913 per QALY gained which is within the acceptable range that is considered cost-effective (\$ 50–100000/QALY gained)<sup>[88,89]</sup>. Further investigations are however needed to determine the cost-effectiveness of treat-to-target strategies in reducing disease progression, taking into account proper de-escalation strategies as well.

## FUTURE PERSPECTIVES AND UNANSWERED QUESTIONS—EXPERT OPINION

In recent years, there has been a critical change in the treatment paradigms with the arrival of biologic agents. Many studies showed that the introduction of highly effective treatments in selected patients early in the disease course is crucial in achieving deep remission and avoiding disease complications. An important limitation to the landmark clinical trials evaluating the early use of biologics and immunosuppressives is that they only measured clinical outcomes as primary endpoints and endoscopic data are usually available in a subgroup of patients, except for the CALM study. In this regard, the CURE<sup>[90]</sup> study is currently underway and is evaluating the impact of early adalimumab therapy on the disease course in CD, including mucosal healing. Personalization of the therapeutic strategy by proper early patient stratification have an increasingly important role in selecting patients who



benefit from early aggressive therapy.

The other pillar of achieving sustained deep remission is a stringent patient follow-up and timely re-evaluation. The current focus on objective parameters as treatment targets is an important step towards that direction, as proposed by the STRIDE guidance. Since the STRIDE recommendations have been published, an increasing amount of clinical data emerged on the use of various targets and subsequent long-term outcomes, thus the re-evaluation of the recommendations and targets (*e.g.*, the role of biomarkers) is warranted.

Recent long-term follow-up data of the CALM study show that endoscopic and deep remission at 1 year prevents disease progression in early CD<sup>[55]</sup>, however further clinical trials are needed to demonstrate the long-term superiority of treating to endoscopic remission. The REACT2 trial (Enhanced Algorithm for Crohn's Treatment Incorporating Early Combination Therapy trial) assesses the exact role of endoscopy in the tight control concept by comparing an enhanced treat-to-target strategy featuring early use and rapid escalation of combined antimetabolite/adalimumab therapy based on timely endoscopic evaluations with a traditional step-care algorithm with symptom driven treatment escalation (ClinicalTrials.gov: NCT01698307)<sup>[91]</sup>. In addition, a unified definition of endoscopic response/remission tailored to the everyday clinical practice is missing, especially in CD.

The evidence is clearly increasing on the role of biomarkers, supported by the positive results of the CALM study. Biomarkers emerge as treatment targets as they can guide treatment escalations, leading to superior endoscopic and clinical outcomes, which is the foundation of the tight control concept. However, more evidence is needed to determine the optimal role and cut-offs of biomarkers in monitoring disease control. Using directly the "therapeutic failure" from the CALM study solely based on biomarker positivity to prompt therapy escalation in certain cases would potentially be overly stringent in everyday clinical practice, leading to frequent overtreatment. Long term cost-efficacy has to be established as well. Further data is needed to evaluate the role of different biomarkers, especially used as composite (biomarker and endoscopic) "treatment failure" criteria.

Other elements of the treat-to-target and tight control strategies, such as the adequate intervals of patient monitoring also need clarification. Although the STRIDE specifies recommendations for timing of clinical and endoscopic evaluations, data on optimal biomarker follow-up intervals are partly conflictive. Moreover, patients in different clinical scenarios—active disease, clinical remission or at relapse, mild(er) or complex complicated disease—may require different disease monitoring strategy and intervals. Biomarker evaluations were performed every 12 wk in the CALM, and other studies reported that FCAL may predict clinical flare as soon as approximately 3 mo before symptoms occur. These data may suggest an optimal interval of approximately 3 mo for biomarker monitoring in patients with clinically controlled disease, however detailed recommendations for patient monitoring intervals—including clinical, biochemical and endoscopic evaluation as well— is urgently needed (see Table 2).

Although there has been a significant increase and earlier exposure to immunosuppressive and biologic agents in IBD recently, population-based data on long-term outcomes show somewhat controversial results and prompt caution when translating clinical trial results into clinical practice. The Epi-IBD<sup>[5]</sup> cohort is a prospective population-based inception cohort of unselected CD patients from 29 European centres. Although significant geographic differences were observed in medication timing and exposures (in Western Europe 33% of patients received biological therapy and 66% immunomodulators; in Eastern Europe 14% and 54%, respectively,  $P < 0.01$ ), the course of disease—including rates of patients undergoing surgery, developing stricturing or penetrating disease phenotype or being hospitalized— did not differ between in Western and Eastern Europe. Similar results are being reported from two very recent administrative database analyses from Canada. Data from Murthy *et al*<sup>[92]</sup> showed that the introduction of anti-TNF therapy failed to modify the trend of IBD-related hospitalizations and surgeries in both CD and UC between 1995 and 2012. This suggests that disease monitoring in real life practice is suboptimal and in the future, using new, algorithm-based therapeutic strategies as standard of care may translate into improved outcomes as observed in pivotal clinical trials<sup>[12,28]</sup>.

## CONCLUSION

Data favoring the treat-to-target strategies and tight patient control still continue to accumulate and results from ongoing trials will further clarify its long-term

implications. Early and effective treatment with optimal patient stratification and monitoring using treat-to-target and tight control concepts is emerging as superior therapeutic strategy. The use of biologic agents should be optimized with timely monitoring, appropriate treatment escalation and de-escalation strategies are both warranted in selected patients. Finally, improving patient-physician communication and patient access to IBD specific healthcare services to receive proper evaluation in urgent IBD related situations is vital in the framework of tight control management. These approaches however require further validation with more precise definition of therapeutic targets (endoscopic, biomarker) in prospective studies of newly diagnosed patients with assessment of long-term outcomes.

## REFERENCES

- 1 Ng SC, Shi HY, Hamidi N, Underwood FE, Tang W, Benchimol EI, Panaccione R, Ghosh S, Wu JCY, Chan FKL, Sung JJY, Kaplan GG. Worldwide incidence and prevalence of inflammatory bowel disease in the 21st century: a systematic review of population-based studies. *Lancet* 2018; **390**: 2769-2778 [PMID: 29050646 DOI: 10.1016/S0140-6736(17)32448-0]
- 2 Peyrin-Biroulet L, Loftus EV, Colombel JF, Sandborn WJ. Long-term complications, extraintestinal manifestations, and mortality in adult Crohn's disease in population-based cohorts. *Inflamm Bowel Dis* 2011; **17**: 471-478 [PMID: 20725943 DOI: 10.1002/ibd.21417]
- 3 Torres J, Billioud V, Sachar DB, Peyrin-Biroulet L, Colombel JF. Ulcerative colitis as a progressive disease: the forgotten evidence. *Inflamm Bowel Dis* 2012; **18**: 1356-1363 [PMID: 22162423 DOI: 10.1002/ibd.22839]
- 4 Bouguen G, Peyrin-Biroulet L. Surgery for adult Crohn's disease: what is the actual risk? *Gut* 2011; **60**: 1178-1181 [PMID: 21610273 DOI: 10.1136/gut.2010.234617]
- 5 Burisch J, Kiudelis G, Kupcinskas L, Kievit HAL, Andersen KW, Andersen V, Salupere R, Pedersen N, Kjeldsen J, D'Incà R, Valpiani D, Schwartz D, Odes S, Olsen J, Nielsen KR, Vegh Z, Lakatos PL, Toca A, Turcan S, Katsanos KH, Christodoulou DK, Fumery M, Gower-Rousseau C, Chetcuti Zammit S, Ellul P, Eriksson C, Halfvarson J, Magro FJ, Duricova D, Bortlik M, Fernandez A, Hernández V, Myers S, Sebastian S, Oksanen P, Collin P, Goldis A, Misra R, Arebi N, Kaimakliotis IP, Nikuina I, Belousova E, Brinar M, Cukovic-Cavka S, Langholz E, Munkholm P, Epi-IBD group. Natural disease course of Crohn's disease during the first 5 years after diagnosis in a European population-based inception cohort: an Epi-IBD study. *Gut* 2018 [PMID: 29363534 DOI: 10.1136/gutjnl-2017-315568]
- 6 Peyrin-Biroulet L, Cieza A, Sandborn WJ, Coenen M, Chowers Y, Hibi T, Kostanjsek N, Stucki G, Colombel JF; International Programme to Develop New Indexes for Crohn's Disease (IPNIC) group. Development of the first disability index for inflammatory bowel disease based on the international classification of functioning, disability and health. *Gut* 2012; **61**: 241-247 [PMID: 21646246 DOI: 10.1136/gutjnl-2011-300049]
- 7 Pariente B, Mary JY, Danese S, Chowers Y, De Cruz P, D'Haens G, Loftus EV, Louis E, Panés J, Schölmerich J, Schreiber S, Vecchi M, Branche J, Bruining D, Fiorino G, Herzog M, Kamm MA, Klein A, Lewin M, Meunier P, Ordas I, Strauch U, Tontini GE, Zagdanski AM, Bonifacio C, Rimola J, Nachury M, Leroy C, Sandborn W, Colombel JF, Cosnes J. Development of the Lémann index to assess digestive tract damage in patients with Crohn's disease. *Gastroenterology* 2015; **148**: 52-63.e3 [PMID: 25241327 DOI: 10.1053/j.gastro.2014.09.015]
- 8 Solberg IC, Vatn MH, Høie O, Stray N, Sauar J, Jahnsen J, Moum B, Lygren I; IBSEN Study Group. Clinical course in Crohn's disease: results of a Norwegian population-based ten-year follow-up study. *Clin Gastroenterol Hepatol* 2007; **5**: 1430-1438 [PMID: 18054751 DOI: 10.1016/j.cgh.2007.09.002]
- 9 Solberg IC, Lygren I, Jahnsen J, Aadland E, Høie O, Cvancarova M, Bernklev T, Henriksen M, Sauar J, Vatn MH, Moum B; IBSEN Study Group. Clinical course during the first 10 years of ulcerative colitis: results from a population-based inception cohort (IBSEN Study). *Scand J Gastroenterol* 2009; **44**: 431-440 [PMID: 19101844 DOI: 10.1080/00365520802600961]
- 10 D'Haens G, Baert F, van Assche G, Caenepeel P, Vergauwe P, Tuynman H, De Vos M, van Deventer S, Stitt L, Donner A, Vermeire S, Van De Mierop FJ, Coche JR, van der Woude J, Ochsenkühn T, van Bodegraven AA, Van Hooftgem PP, Lambrecht GL, Mana F, Rutgeerts P, Feagan BG, Hommes D; Belgian Inflammatory Bowel Disease Research Group; North-Holland Gut Club. Early combined immunosuppression or conventional management in patients with newly diagnosed Crohn's disease: an open randomised trial. *Lancet* 2008; **371**: 660-667 [PMID: 18295023 DOI: 10.1016/S0140-6736(08)60304-9]
- 11 Colombel JF, Sandborn WJ, Reinisch W, Mantzaris GJ, Kornbluth A, Rachmilewitz D, Lichtiger S, D'Haens G, Diamond RH, Broussard DL, Tang KL, van der Woude CJ, Rutgeerts P; SONIC Study Group. Infliximab, azathioprine, or combination therapy for Crohn's disease. *N Engl J Med* 2010; **362**: 1383-1395 [PMID: 20393175 DOI: 10.1056/NEJMoa0904492]
- 12 Khanna R, Bressler B, Levesque BG, Zou G, Stitt LW, Greenberg GR, Panaccione R, Bitton A, Paré P, Vermeire S, D'Haens G, MacIntosh D, Sandborn WJ, Donner A, Vandervoort MK, Morris JC, Feagan BG; REACT Study Investigators. Early combined immunosuppression for the management of Crohn's disease (REACT): a cluster randomised controlled trial. *Lancet* 2015; **386**: 1825-1834 [PMID: 26342731 DOI: 10.1016/S0140-6736(15)00068-9]
- 13 Colombel JF, Panaccione R, Bossuyt P, Lukas M, Baert F, Vaňásek T, Danalioglu A, Novacek G, Armuzzi A, Hébuterne X, Travis S, Danese S, Reinisch W, Sandborn WJ, Rutgeerts P, Hommes D, Schreiber S, Neimark E, Huang B, Zhou Q, Mendez P, Petersson J, Wallace K, Robinson AM, Thakkar RB, D'Haens G. Effect of tight control management on Crohn's disease (CALM): a multicentre, randomised, controlled phase 3 trial. *Lancet* 2018; **390**: 2779-2789 [PMID: 29096949 DOI: 10.1016/S0140-6736(17)32641-7]
- 14 Beaugerie L, Seksik P, Nion-Larmurier I, Gendre JP, Cosnes J. Predictors of Crohn's disease. *Gastroenterology* 2006; **130**: 650-656 [PMID: 16530505 DOI: 10.1053/j.gastro.2005.12.019]
- 15 Lakatos PL, Czeglédi Z, Szamosi T, Banai J, David G, Zsigmond F, Pandur T, Erdelyi Z, Gemela O, Papp J, Lakatos L. Perianal disease, small bowel disease, smoking, prior steroid or early azathioprine/biological

- therapy are predictors of disease behavior change in patients with Crohn's disease. *World J Gastroenterol* 2009; **15**: 3504-3510 [PMID: 19630105 DOI: 10.3748/wjg.15.3504]
- 16 **Solberg IC**, Høivik ML, Cvancarova M, Moum B; IBSEN Study Group. Risk matrix model for prediction of colectomy in a population-based study of ulcerative colitis patients (the IBSEN study). *Scand J Gastroenterol* 2015; **50**: 1456-1462 [PMID: 26139389 DOI: 10.3109/00365521.2015.1064991]
  - 17 **Solberg IC**, Cvancarova M, Vatn MH, Moum B; IBSEN Study Group. Risk matrix for prediction of advanced disease in a population-based study of patients with Crohn's Disease (the IBSEN Study). *Inflamm Bowel Dis* 2014; **20**: 60-68 [PMID: 24280875 DOI: 10.1097/01.MIB.0000436956.78220.67]
  - 18 **Guizzetti L**, Zou G, Khanna R, Dulai PS, Sandborn WJ, Jairath V, Feagan BG. Development of Clinical Prediction Models for Surgery and Complications in Crohn's Disease. *J Crohns Colitis* 2018; **12**: 167-177 [PMID: 29028958 DOI: 10.1093/ecco-jcc/jjx130]
  - 19 **Allen PB**, Peyrin-Biroulet L. Moving towards disease modification in inflammatory bowel disease therapy. *Curr Opin Gastroenterol* 2013; **29**: 397-404 [PMID: 23695427 DOI: 10.1097/MOG.0b013e3283622914]
  - 20 **Sandborn WJ**, Hanauer S, Van Assche G, Panés J, Wilson S, Petersson J, Panaccione R. Treating beyond symptoms with a view to improving patient outcomes in inflammatory bowel diseases. *J Crohns Colitis* 2014; **8**: 927-935 [PMID: 24713173 DOI: 10.1016/j.crohns.2014.02.021]
  - 21 **Magro F**, Rodrigues A, Vieira AI, Portela F, Cremers I, Cotter J, Correia L, Duarte MA, Tavares ML, Lago P, Ministro P, Peixe P, Lopes S, Garcia EB. Review of the disease course among adult ulcerative colitis population-based longitudinal cohorts. *Inflamm Bowel Dis* 2012; **18**: 573-583 [PMID: 21793126 DOI: 10.1002/ibd.21815]
  - 22 **Peyrin-Biroulet L**, Reinisch W, Colombel JF, Mantzaris GJ, Kornbluth A, Diamond R, Rutgeerts P, Tang LK, Cornillie FJ, Sandborn WJ. Clinical disease activity, C-reactive protein normalisation and mucosal healing in Crohn's disease in the SONIC trial. *Gut* 2014; **63**: 88-95 [PMID: 23974954 DOI: 10.1136/gutjnl-2013-304984]
  - 23 **Jharap B**, Sandborn WJ, Reinisch W, D'Haens G, Robinson AM, Wang W, Huang B, Lazar A, Thakkar RB, Colombel JF. Randomised clinical study: discrepancies between patient-reported outcomes and endoscopic appearance in moderate to severe ulcerative colitis. *Aliment Pharmacol Ther* 2015; **42**: 1082-1092 [PMID: 26381802 DOI: 10.1111/apt.13387]
  - 24 **Baert F**, Moortgat L, Van Assche G, Caenepeel P, Vergauwe P, De Vos M, Stokkers P, Hommes D, Rutgeerts P, Vermeire S, D'Haens G; Belgian Inflammatory Bowel Disease Research Group; North-Holland Gut Club. Mucosal healing predicts sustained clinical remission in patients with early-stage Crohn's disease. *Gastroenterology* 2010; **138**: 463-468 [PMID: 19818785 DOI: 10.1053/j.gastro.2009.09.056]
  - 25 **Colombel JF**, Rutgeerts P, Reinisch W, Esser D, Wang Y, Lang Y, Marano CW, Strauss R, Oddens BJ, Feagan BG, Hanauer SB, Lichtenstein GR, Present D, Sands BE, Sandborn WJ. Early mucosal healing with infliximab is associated with improved long-term clinical outcomes in ulcerative colitis. *Gastroenterology* 2011; **141**: 1194-1201 [PMID: 21723220 DOI: 10.1053/j.gastro.2011.06.054]
  - 26 **Colombel JF**, Rutgeerts PJ, Sandborn WJ, Yang M, Camez A, Pollack PF, Thakkar RB, Robinson AM, Chen N, Mulani PM, Chao J. Adalimumab induces deep remission in patients with Crohn's disease. *Clin Gastroenterol Hepatol* 2014; **12**: 414-22.e5 [PMID: 23856361 DOI: 10.1016/j.cgh.2013.06.019]
  - 27 **Froslie KF**, Jahnsen J, Moum BA, Vatn MH; IBSEN Group. Mucosal healing in inflammatory bowel disease: results from a Norwegian population-based cohort. *Gastroenterology* 2007; **133**: 412-422 [PMID: 17681162 DOI: 10.1053/j.gastro.2007.05.051]
  - 28 **Peyrin-Biroulet L**, Sandborn W, Sands BE, Reinisch W, Bemelman W, Bryant RV, D'Haens G, Dotan I, Dubinsky M, Feagan B, Fiorino G, Gearry R, Krishnareddy S, Lakatos PL, Loftus EV, Marteau P, Munkholm P, Murdoch TB, Ordás I, Panaccione R, Riddell RH, Ruel J, Rubin DT, Samaan M, Siegel CA, Silverberg MS, Stoker J, Schreiber S, Travis S, Van Assche G, Danese S, Panes J, Bouguen G, O'Donnell S, Pariente B, Winer S, Hanauer S, Colombel JF. Selecting Therapeutic Targets in Inflammatory Bowel Disease (STRIDE): Determining Therapeutic Goals for Treat-to-Target. *Am J Gastroenterol* 2015; **110**: 1324-1338 [PMID: 26303131 DOI: 10.1038/ajg.2015.233]
  - 29 **Best WR**, Becktel JM, Singleton JW. Rederived values of the eight coefficients of the Crohn's Disease Activity Index (CDAI). *Gastroenterology* 1979; **77**: 843-846 [PMID: 467941 DOI: 10.1016/0016-5085(79)90384-6]
  - 30 **Harvey RF**, Bradshaw JM. A simple index of Crohn's-disease activity. *Lancet* 1980; **1**: 514 [PMID: 6102236 DOI: 10.1016/s0140-6736(80)92767-1]
  - 31 **Walmsley RS**, Ayres RC, Pounder RE, Allan RN. A simple clinical colitis activity index. *Gut* 1998; **43**: 29-32 [PMID: 9771402 DOI: 10.1136/gut.43.1.29]
  - 32 **Rutgeerts P**, Sandborn WJ, Feagan BG, Reinisch W, Olson A, Johanns J, Travers S, Rachmilewitz D, Hanauer SB, Lichtenstein GR, de Villiers WJ, Present D, Sands BE, Colombel JF. Infliximab for induction and maintenance therapy for ulcerative colitis. *N Engl J Med* 2005; **353**: 2462-2476 [PMID: 16339095 DOI: 10.1056/NEJMoa050516]
  - 33 **FDA Guidance for Industry**. Patient-Reported Outcome Measures: Use in Medical Product Development to Support Labeling Claims. Cited 27 August 2019. Available from: <http://www.fda.gov/downloads/Drugs/Guidances/UCM193282.pdf>
  - 34 **de Jong MJ**, Roosen D, Degens JHRJ, van den Heuvel TRA, Romberg-Camps M, Hameeteman W, Bodelier AGL, Romanko I, Lukas M, Winkens B, Markus T, Masclee AAM, van Tubergen A, Jonkers DMAE, Pierik MJ. Development and Validation of a Patient-reported Score to Screen for Mucosal Inflammation in Inflammatory Bowel Disease. *J Crohns Colitis* 2019; **13**: 555-563 [PMID: 30476099 DOI: 10.1093/ecco-jcc/jjy196]
  - 35 **Higgins PDR**, Harding G, Leidy NK, DeBusk K, Patrick DL, Viswanathan HN, Fitzgerald K, Donelson SM, Cyrille M, Ortmeier BG, Wilson H, Revicki DA, Globe G. Development and validation of the Crohn's disease patient-reported outcomes signs and symptoms (CD-PRO/SS) diary. *J Patient Rep Outcomes* 2017; **2**: 24 [PMID: 29770803 DOI: 10.1186/s41687-018-0044-7]
  - 36 **Higgins PDR**, Harding G, Revicki DA, Globe G, Patrick DL, Fitzgerald K, Viswanathan H, Donelson SM, Ortmeier BG, Chen WH, Leidy NK, DeBusk K. Development and validation of the Ulcerative Colitis patient-reported outcomes signs and symptoms (UC-pro/SS) diary. *J Patient Rep Outcomes* 2017; **2**: 26 [PMID: 29888745 DOI: 10.1186/s41687-018-0049-2]
  - 37 **Gower-Rousseau C**, Sarter H, Savoye G, Tavernier N, Fumery M, Sandborn WJ, Feagan BG, Duhamel A, Guillon-Dellac N, Colombel JF, Peyrin-Biroulet L; International Programme to Develop New Indexes for Crohn's Disease (IPNIC) group; International Programme to Develop New Indexes for Crohn's Disease

- (IPNIC) group. Validation of the Inflammatory Bowel Disease Disability Index in a population-based cohort. *Gut* 2017; **66**: 588-596 [PMID: [26646934](#) DOI: [10.1136/gutjnl-2015-310151](#)]
- 38 **Shah SC**, Colombel JF, Sands BE, Narula N. Systematic review with meta-analysis: mucosal healing is associated with improved long-term outcomes in Crohn's disease. *Aliment Pharmacol Ther* 2016; **43**: 317-333 [PMID: [26607562](#) DOI: [10.1111/apt.13475](#)]
- 39 **Shah SC**, Colombel JF, Sands BE, Narula N. Mucosal Healing Is Associated With Improved Long-term Outcomes of Patients With Ulcerative Colitis: A Systematic Review and Meta-analysis. *Clin Gastroenterol Hepatol* 2016; **14**: 1245-1255.e8 [PMID: [26829025](#) DOI: [10.1016/j.cgh.2016.01.015](#)]
- 40 **Bouguen G**, Levesque BG, Pola S, Evans E, Sandborn WJ. Endoscopic assessment and treating to target increase the likelihood of mucosal healing in patients with Crohn's disease. *Clin Gastroenterol Hepatol* 2014; **12**: 978-985 [PMID: [24246770](#) DOI: [10.1016/j.cgh.2013.11.005](#)]
- 41 **Ferrante M**, Colombel JF, Sandborn WJ, Reinisch W, Mantzaris GJ, Kornbluth A, Rachmilewitz D, Lichtiger S, D'Haens GR, van der Woude CJ, Danese S, Diamond RH, Oortwijn AF, Tang KL, Miller M, Cornillie F, Rutgeerts PJ; International Organization for the Study of Inflammatory Bowel Diseases. Validation of endoscopic activity scores in patients with Crohn's disease based on a post hoc analysis of data from SONIC. *Gastroenterology* 2013; **145**: 978-986.e5 [PMID: [23954314](#) DOI: [10.1053/j.gastro.2013.08.010](#)]
- 42 **Vuitton L**, Marteau P, Sandborn WJ, Levesque BG, Feagan B, Vermeire S, Danese S, D'Haens G, Lowenberg M, Khanna R, Fiorino G, Travis S, Mary JY, Peyrin-Biroulet L. IOIBD technical review on endoscopic indices for Crohn's disease clinical trials. *Gut* 2016; **65**: 1447-1455 [PMID: [26353983](#) DOI: [10.1136/gutjnl-2015-309903](#)]
- 43 **Barreiro-de Acosta M**, Vallejo N, de la Iglesia D, Uribarri L, Bastón I, Ferreira-Iglesias R, Lorenzo A, Domínguez-Muñoz JE. Evaluation of the Risk of Relapse in Ulcerative Colitis According to the Degree of Mucosal Healing (Mayo 0 vs 1): A Longitudinal Cohort Study. *J Crohns Colitis* 2016; **10**: 13-19 [PMID: [26351390](#) DOI: [10.1093/ecco-jcc/jjv158](#)]
- 44 **Boal Carvalho P**, Dias de Castro F, Rosa B, Moreira MJ, Cotter J. Mucosal Healing in Ulcerative Colitis--When Zero is Better. *J Crohns Colitis* 2016; **10**: 20-25 [PMID: [26438714](#) DOI: [10.1093/ecco-jcc/jjv180](#)]
- 45 **Lobatón T**, Bessisow T, De Hertogh G, Lemmens B, Maedler C, Van Assche G, Vermeire S, Bisschops R, Rutgeerts P, Bitton A, Afif W, Marcus V, Ferrante M. The Modified Mayo Endoscopic Score (MMES): A New Index for the Assessment of Extension and Severity of Endoscopic Activity in Ulcerative Colitis Patients. *J Crohns Colitis* 2015; **9**: 846-852 [PMID: [26116558](#) DOI: [10.1093/ecco-jcc/jjv111](#)]
- 46 **Ikeya K**, Hanai H, Sugimoto K, Osawa S, Kawasaki S, Iida T, Maruyama Y, Watanabe F. The Ulcerative Colitis Endoscopic Index of Severity More Accurately Reflects Clinical Outcomes and Long-term Prognosis than the Mayo Endoscopic Score. *J Crohns Colitis* 2016; **10**: 286-295 [PMID: [26581895](#) DOI: [10.1093/ecco-jcc/jjv210](#)]
- 47 **Vuitton L**, Peyrin-Biroulet L, Colombel JF, Pariente B, Pineton de Chambrun G, Walsh AJ, Panes J, Travis SP, Mary JY, Marteau P. Defining endoscopic response and remission in ulcerative colitis clinical trials: an international consensus. *Aliment Pharmacol Ther* 2017; **45**: 801-813 [PMID: [28112419](#) DOI: [10.1111/apt.13948](#)]
- 48 **Solem CA**, Loftus EV, Tremaine WJ, Harmsen WS, Zinsmeister AR, Sandborn WJ. Correlation of C-reactive protein with clinical, endoscopic, histologic, and radiographic activity in inflammatory bowel disease. *Inflamm Bowel Dis* 2005; **11**: 707-712 [PMID: [16043984](#) DOI: [10.1097/01.mib.0000173271.18319.53](#)]
- 49 **Mosli MH**, Zou G, Garg SK, Feagan SG, MacDonald JK, Chande N, Sandborn WJ, Feagan BG. C-Reactive Protein, Fecal Calprotectin, and Stool Lactoferrin for Detection of Endoscopic Activity in Symptomatic Inflammatory Bowel Disease Patients: A Systematic Review and Meta-Analysis. *Am J Gastroenterol* 2015; **110**: 802-819 [PMID: [25964225](#) DOI: [10.1038/ajg.2015.120](#)]
- 50 **D'Haens G**, Ferrante M, Vermeire S, Baert F, Noman M, Moortgat L, Geens P, Iwens D, Aerden I, Van Assche G, Van Olmen G, Rutgeerts P. Fecal calprotectin is a surrogate marker for endoscopic lesions in inflammatory bowel disease. *Inflamm Bowel Dis* 2012; **18**: 2218-2224 [PMID: [22344983](#) DOI: [10.1002/ibd.22917](#)]
- 51 **De Vos M**, Louis EJ, Jahnsen J, Vandervoort JG, Noman M, Dewit O, D'haens GR, Franchimont D, Baert FJ, Torp RA, Henriksen M, Potvin PM, Van Hooft PP, Hindryckx PM, Moreels TG, Collard A, Karlens LN, Kittang E, Lambrecht G, Grimstad T, Koch J, Lygren I, Coche JC, Mana F, Van Gossom A, Belaiche J, Cool MR, Fontaine F, Maisin JM, Muls V, Neuville B, Staessen DA, Van Assche GA, de Lange T, Solberg IC, Vander Cruyssen BJ, Vermeire SA. Consecutive fecal calprotectin measurements to predict relapse in patients with ulcerative colitis receiving infliximab maintenance therapy. *Inflamm Bowel Dis* 2013; **19**: 2111-2117 [PMID: [23883959](#) DOI: [10.1097/MIB.0b013e31829b2a37](#)]
- 52 **Zhulina Y**, Cao Y, Amcoff K, Carlson M, Tysk C, Halfvarson J. The prognostic significance of faecal calprotectin in patients with inactive inflammatory bowel disease. *Aliment Pharmacol Ther* 2016; **44**: 495-504 [PMID: [27402063](#) DOI: [10.1111/apt.13731](#)]
- 53 **Heida A**, Park KT, van Rhee PF. Clinical Utility of Fecal Calprotectin Monitoring in Asymptomatic Patients with Inflammatory Bowel Disease: A Systematic Review and Practical Guide. *Inflamm Bowel Dis* 2017; **23**: 894-902 [PMID: [28511198](#) DOI: [10.1097/MIB.0000000000001082](#)]
- 54 **Wright EK**, Kamm MA, De Cruz P, Hamilton AL, Ritchie KJ, Krejany EO, Leach S, Gorelik A, Liew D, Prideaux L, Lawrance IC, Andrews JM, Bampton PA, Jakobovits SL, Florin TH, Gibson PR, Debinski H, Macrae FA, Samuel D, Kronborg I, Radford-Smith G, Selby W, Johnston MJ, Woods R, Elliott PR, Bell SJ, Brown SJ, Connell WR, Day AS, Desmond PV, Gearry RB. Measurement of fecal calprotectin improves monitoring and detection of recurrence of Crohn's disease after surgery. *Gastroenterology* 2015; **148**: 938-947.e1 [PMID: [25620670](#) DOI: [10.1053/j.gastro.2015.01.026](#)]
- 55 **Ungaro RC**, Yzet C, Bossuyt P, Baert FJ, Vanasek T, D'Haens GR, Joustra VW, Panaccione R, Novacek G, Armuzzi A, Golovchenko O, Olga P, Goldis A, Travis SP, Hebuterne X, Ferrante M, Rogler G, Fumery M, Danese S, Rydzewska G, Pariente B, Hertervig E, Stanciu C, Grimaud J, Diculescu M, Peyrin-Biroulet L, Laharie D, Wright JP, Gomollon F, Gubonina I, Schreiber S, Motoya S, Hellström PM, Halfvarson J, Colombel JF. Sa1812 Endoscopic and deep remission at 1 year prevents disease progression in early Crohn's disease: long-term data from CALM. *Gastroenterology* 2019; **6** Suppl 1: S411 [DOI: [10.1016/S0016-5085\(19\)37879-5](#)]
- 56 **Cornillie F**, Hanauer SB, Diamond RH, Wang J, Tang KL, Xu Z, Rutgeerts P, Vermeire S. Postinduction serum infliximab trough level and decrease of C-reactive protein level are associated with durable sustained response to infliximab: a retrospective analysis of the ACCENT I trial. *Gut* 2014; **63**: 1721-1727 [PMID: [24474383](#) DOI: [10.1136/gutjnl-2012-304094](#)]



- 57 **Bortlik M**, Duricova D, Malickova K, Machkova N, Bouzkova E, Hrdlicka L, Komarek A, Lukas M. Infliximab trough levels may predict sustained response to infliximab in patients with Crohn's disease. *J Crohns Colitis* 2013; **7**: 736-743 [PMID: [23200919](#) DOI: [10.1016/j.crohns.2012.10.019](#)]
- 58 **Mazor Y**, Almog R, Kopylov U, Ben Hur D, Blatt A, Dahan A, Waterman M, Ben-Horin S, Chowers Y. Adalimumab drug and antibody levels as predictors of clinical and laboratory response in patients with Crohn's disease. *Aliment Pharmacol Ther* 2014; **40**: 620-628 [PMID: [25039584](#) DOI: [10.1111/apt.12869](#)]
- 59 **Affif W**, Loftus EV, Faubert WA, Kane SV, Bruining DH, Hanson KA, Sandborn WJ. Clinical utility of measuring infliximab and human anti-chimeric antibody concentrations in patients with inflammatory bowel disease. *Am J Gastroenterol* 2010; **105**: 1133-1139 [PMID: [20145610](#) DOI: [10.1038/ajg.2010.9](#)]
- 60 **Roblin X**, Rinaudo M, Del Tedesco E, Phelip JM, Genin C, Peyrin-Biroulet L, Paul S. Development of an algorithm incorporating pharmacokinetics of adalimumab in inflammatory bowel diseases. *Am J Gastroenterol* 2014; **109**: 1250-1256 [PMID: [24913041](#) DOI: [10.1038/ajg.2014.146](#)]
- 61 **Papamichael K**, Cheifetz AS. Use of anti-TNF drug levels to optimise patient management. *Frontline Gastroenterol* 2016; **7**: 289-300 [PMID: [28839870](#) DOI: [10.1136/flgastro-2016-100685](#)]
- 62 **Vande Casteele N**, Ferrante M, Van Assche G, Ballet V, Compernelle G, Van Steen K, Simoons S, Rutgeerts P, Gils A, Vermeire S. Trough concentrations of infliximab guide dosing for patients with inflammatory bowel disease. *Gastroenterology* 2015; **148**: 1320-9.e3 [PMID: [25724455](#) DOI: [10.1053/j.gastro.2015.02.031](#)]
- 63 **D'Haens G**, Vermeire S, Lambrecht G, Baert F, Bossuyt P, Pariente B, Buisson A, Bouhnik Y, Filippi J, Vander Woude J, Van Hooft P, Moreau J, Louis E, Franchimont D, De Vos M, Mana F, Peyrin-Biroulet L, Brix H, Allez M, Caenepeel P, Aubourg A, Oldenburg B, Pierik M, Gils A, Chevrete S, Laharie D; GETAID. Increasing Infliximab Dose Based on Symptoms, Biomarkers, and Serum Drug Concentrations Does Not Increase Clinical, Endoscopic, and Corticosteroid-Free Remission in Patients With Active Luminal Crohn's Disease. *Gastroenterology* 2018; **154**: 1343-1351.e1 [PMID: [29317275](#) DOI: [10.1053/j.gastro.2018.01.004](#)]
- 64 **Papamichael K**, Juncadella A, Wong D, Rakowsky S, Sattler LA, Campbell JP, Vaughn BP, Cheifetz AS. Proactive Therapeutic Drug Monitoring of Adalimumab Is Associated With Better Long-term Outcomes Compared With Standard of Care in Patients With Inflammatory Bowel Disease. *J Crohns Colitis* 2019; **13**: 976-981 [PMID: [30689771](#) DOI: [10.1093/ecco-jcc/jjz018](#)]
- 65 **Papamichael K**, Chachu KA, Vajravelu RK, Vaughn BP, Ni J, Osterman MT, Cheifetz AS. Improved Long-term Outcomes of Patients With Inflammatory Bowel Disease Receiving Proactive Compared With Reactive Monitoring of Serum Concentrations of Infliximab. *Clin Gastroenterol Hepatol* 2017; **15**: 1580-1588.e3 [PMID: [28365486](#) DOI: [10.1016/j.cgh.2017.03.031](#)]
- 66 **Fernandes SR**, Bernardo S, Simões C, Correia L, Santos PM, Gonçalves AR, Valente A, Baldaia C, Tato Marinho R. DOP59 Proactive infliximab drug monitoring is superior to conventional management in inflammatory bowel disease. *J Crohns Colitis* 2019; **13** Suppl 1: S064-S065 [DOI: [10.1093/ecco-jcc/jjy222.093](#)]
- 67 **Papamichael K**, Vande Casteele N, Gils A, Tops S, Hauenstein S, Singh S, Princen F, Van Assche G, Rutgeerts P, Vermeire S, Ferrante M. Long-term outcome of patients with Crohn's disease who discontinued infliximab therapy upon clinical remission. *Clin Gastroenterol Hepatol* 2015; **13**: 1103-1110 [PMID: [25478919](#) DOI: [10.1016/j.cgh.2014.11.026](#)]
- 68 **Bryant RV**, Burger DC, Delo J, Walsh AJ, Thomas S, von Herbay A, Buchel OC, White L, Brain O, Keshav S, Warren BF, Travis SP. Beyond endoscopic mucosal healing in UC: histological remission better predicts corticosteroid use and hospitalisation over 6 years of follow-up. *Gut* 2016; **65**: 408-414 [PMID: [25986946](#) DOI: [10.1136/gutjnl-2015-309598](#)]
- 69 **Christensen B**, Hanauer SB, Erlich J, Kassim O, Gibson PR, Turner JR, Hart J, Rubin DT. Histologic Normalization Occurs in Ulcerative Colitis and Is Associated With Improved Clinical Outcomes. *Clin Gastroenterol Hepatol* 2017; **15**: 1557-1564.e1 [PMID: [28238954](#) DOI: [10.1016/j.cgh.2017.02.016](#)]
- 70 **Park S**, Abdi T, Gentry M, Laine L. Histological Disease Activity as a Predictor of Clinical Relapse Among Patients With Ulcerative Colitis: Systematic Review and Meta-Analysis. *Am J Gastroenterol* 2016; **111**: 1692-1701 [PMID: [27725645](#) DOI: [10.1038/ajg.2016.418](#)]
- 71 **Magro F**, Lopes J, Borralho P, Lopes S, Coelho R, Cotter J, Castro FD, Sousa HT, Salgado M, Andrade P, Vieira AI, Figueiredo P, Caldeira P, Sousa A, Duarte MA, Ávila F, Silva J, Moleiro J, Mendes S, Giestas S, Ministro P, Sousa P, Gonçalves R, Gonçalves B, Oliveira A, Rosa I, Rodrigues M, Chagas C, Dias CC, Afonso J, Geboes K, Carneiro F; Portuguese IBD Study Group (GEDII). Comparison of different histological indexes in the assessment of UC activity and their accuracy regarding endoscopic outcomes and faecal calprotectin levels. *Gut* 2019; **68**: 594-603 [PMID: [29437913](#) DOI: [10.1136/gutjnl-2017-315545](#)]
- 72 **Panés J**, Bouzas R, Chaparro M, García-Sánchez V, Gisbert JP, Martínez de Guereñu B, Mendoza JL, Paredes JM, Quiroga S, Ripollés T, Rimola J. Systematic review: the use of ultrasonography, computed tomography and magnetic resonance imaging for the diagnosis, assessment of activity and abdominal complications of Crohn's disease. *Aliment Pharmacol Ther* 2011; **34**: 125-145 [PMID: [21615440](#) DOI: [10.1111/j.1365-2036.2011.04710.x](#)]
- 73 **Deepak P**, Fletcher JG, Fidler JL, Barlow JM, Sheedy SP, Kolbe AB, Harmsen WS, Loftus EV, Hansel SL, Becker BD, Bruining DH. Radiological Response Is Associated With Better Long-Term Outcomes and Is a Potential Treatment Target in Patients With Small Bowel Crohn's Disease. *Am J Gastroenterol* 2016; **111**: 997-1006 [PMID: [27166131](#) DOI: [10.1038/ajg.2016.177](#)]
- 74 **Fernandes SR**, Rodrigues RV, Bernardo S, Cortez-Pinto J, Rosa I, da Silva JP, Gonçalves AR, Valente A, Baldaia C, Santos PM, Correia L, Venâncio J, Campos P, Pereira AD, Velosa J. Transmural Healing Is Associated with Improved Long-term Outcomes of Patients with Crohn's Disease. *Inflamm Bowel Dis* 2017; **23**: 1403-1409 [PMID: [28498158](#) DOI: [10.1097/MIB.0000000000001143](#)]
- 75 **Ilias A**, Lovasz BD, Gonczi L, Kurti Z, Vegh Z, Sumegi LD, Golovics PA, Rudas G, Lakatos PL. Optimizing Patient Management in Crohn's Disease in a Tertiary Referral Center: the Impact of Fast-Track MRI on Patient Management and Outcomes. *J Gastrointest Liver Dis* 2018; **27**: 391-397 [PMID: [30574621](#) DOI: [10.15403/jgld.2014.1121.274.oem](#)]
- 76 **Bots S**, Nylund K, Löwenberg M, Gecse K, Gilja OH, D'Haens G. Ultrasound for Assessing Disease Activity in IBD Patients: A Systematic Review of Activity Scores. *J Crohns Colitis* 2018; **12**: 920-929 [PMID: [29684200](#) DOI: [10.1093/ecco-jcc/jjy048](#)]
- 77 **Laurent V**, Naudé S, Vuitton L, Zallot C, Baumann C, Girard-Gavanier M, Peyrin-Biroulet L. Accuracy of Diffusion-weighted Magnetic Resonance Colonography in Assessing Mucosal Healing and the Treatment Response in Patients with Ulcerative Colitis. *J Crohns Colitis* 2017; **11**: 716-723 [PMID: [28365486](#) DOI: [10.1016/j.cgh.2017.03.031](#)]

- 27932450 DOI: [10.1093/ecco-jcc/jjw211](https://doi.org/10.1093/ecco-jcc/jjw211)]
- 78 **Louis E**, Mary JY, Vernier-Massouille G, Grimaud JC, Bouhnik Y, Laharie D, Dupas JL, Pillant H, Picon L, Veyrac M, Flamant M, Savoye G, Jian R, Devos M, Porcher R, Pintaud G, Piver E, Colombel JF, Lemann M; Groupe D'etudes Thérapeutiques Des Affections Inflammatoires Digestives. Maintenance of remission among patients with Crohn's disease on antimetabolite therapy after infliximab therapy is stopped. *Gastroenterology* 2012; **142**: 63-70.e5 [PMID: [21945953](https://pubmed.ncbi.nlm.nih.gov/21945953/) DOI: [10.1053/j.gastro.2011.09.034](https://doi.org/10.1053/j.gastro.2011.09.034)]
  - 79 **Bryant RV**, Costello SP, Schoeman S, Sathananthan D, Knight E, Lau SY, Schoeman MN, Mountfield R, Tee D, Travis SPL, Andrews JM. Limited uptake of ulcerative colitis "treat-to-target" recommendations in real-world practice. *J Gastroenterol Hepatol* 2018; **33**: 599-607 [PMID: [28806471](https://pubmed.ncbi.nlm.nih.gov/28806471/) DOI: [10.1111/jgh.13923](https://doi.org/10.1111/jgh.13923)]
  - 80 **Römkens TE**, Gijsbers K, Kievit W, Hoentjen F, Drenth JP. Treatment Targets in Inflammatory Bowel Disease: Current Status in Daily Practice. *J Gastrointest Liver Dis* 2016; **25**: 465-471 [PMID: [27981302](https://pubmed.ncbi.nlm.nih.gov/27981302/) DOI: [10.15403/jgld.2014.1121.254.ken](https://doi.org/10.15403/jgld.2014.1121.254.ken)]
  - 81 **Bitton A**, Vutcovici M, Lytvyak E, Kachan N, Bressler B, Jones J, Lakatos PL, Sewitch M, El-Matary W, Melmed G, Nguyen G; QI consensus group; Promoting Access and Care through Centers of Excellence-PACE program). Selection of Quality Indicators in IBD: Integrating Physician and Patient Perspectives. *Inflamm Bowel Dis* 2019; **25**: 403-409 [PMID: [30169582](https://pubmed.ncbi.nlm.nih.gov/30169582/) DOI: [10.1093/ibd/izy259](https://doi.org/10.1093/ibd/izy259)]
  - 82 **Fiorino G**, Allocca M, Chaparro M, Coenen S, Fidalgo C, Younge L, Gisbert JP. 'Quality of Care' Standards in Inflammatory Bowel Disease: A Systematic Review. *J Crohns Colitis* 2019; **13**: 127-137 [PMID: [30423033](https://pubmed.ncbi.nlm.nih.gov/30423033/) DOI: [10.1093/ecco-jcc/jjy140](https://doi.org/10.1093/ecco-jcc/jjy140)]
  - 83 **Reinglas J**, Restellini S, Gonczi L, Kurti Z, Verdon C, Nene S, Kohen R, Afif W, Bessissow T, Wild G, Seidman E, Bitton A, Lakatos PL. Harmonization of quality of care in an IBD center impacts disease outcomes: Importance of structure, process indicators and rapid access clinic. *Dig Liver Dis* 2019; **51**: 340-345 [PMID: [30591367](https://pubmed.ncbi.nlm.nih.gov/30591367/) DOI: [10.1016/j.dld.2018.11.013](https://doi.org/10.1016/j.dld.2018.11.013)]
  - 84 **Gonczi L**, Gecse KB, Vegh Z, Kurti Z, Rutka M, Farkas K, Golovics PA, Lovasz BD, Banai J, Bene L, Gasztonyi B, Kristof T, Lakatos L, Miheller P, Nagy F, Palatka K, Papp M, Patai A, Salamon A, Szamosi T, Szepes Z, Toth GT, Vincze A, Szalay B, Molnar T, Lakatos PL. Long-term Efficacy, Safety, and Immunogenicity of Biosimilar Infliximab After One Year in a Prospective Nationwide Cohort. *Inflamm Bowel Dis* 2017; **23**: 1908-1915 [PMID: [28922253](https://pubmed.ncbi.nlm.nih.gov/28922253/) DOI: [10.1097/MIB.0000000000001237](https://doi.org/10.1097/MIB.0000000000001237)]
  - 85 **Gonczi L**, Kurti Z, Verdon C, Reinglas J, Kohen R, Morin I, Chavez K, Bessissow T, Afif W, Wild G, Seidman E, Bitton A, Lakatos PL. Perceived Quality of Care is Associated with Disease Activity, Quality of Life, Work Productivity, and Gender, but not Disease Phenotype: A Prospective Study in a High-volume IBD Centre. *J Crohns Colitis* 2019; **13**: 1138-1147 [PMID: [30793162](https://pubmed.ncbi.nlm.nih.gov/30793162/) DOI: [10.1093/ecco-jcc/jjz035](https://doi.org/10.1093/ecco-jcc/jjz035)]
  - 86 **Reinglas J**, Nene S, Gonczi L, Kurti Z, Restellini S, Kohen R, Afif W, Bessissow T, Wild G, Seidman E, Bitton A, Lakatos P. P452 Impact of implementing a rapid access clinic in a high-volume inflammatory bowel disease centre: accessibility, resource utilisation and outcomes. *J Crohns Colitis* 2019; **13** Suppl 1: S337-S337 [DOI: [10.1093/ecco-jcc/jjz22.576](https://doi.org/10.1093/ecco-jcc/jjz22.576)]
  - 87 **Ananthakrishnan AN**, Korzenik JR, Hur C. Can mucosal healing be a cost-effective endpoint for biologic therapy in Crohn's disease? A decision analysis. *Inflamm Bowel Dis* 2013; **19**: 37-44 [PMID: [22416019](https://pubmed.ncbi.nlm.nih.gov/22416019/) DOI: [10.1002/ibd.22951](https://doi.org/10.1002/ibd.22951)]
  - 88 **Panaccione R**, Colombel JF, Bossuyt P, Baert F, Vanasek T, Danalioglu A, Novacek G, Armuzzi A, Reinisch W, Johnson S, Buessing M, Neimark E, Petersson J, M Robinson A, Thakkar RB, Lee WJ, Skup M, D'Haens G. DOP065 Long-term costeffectiveness of tight control for Crohn's disease with adalimumab-based treatment: economic evaluation beyond 48 wk of CALM trial. *J Crohns Colitis* 2018; **12** Suppl 1: S074-S075 [DOI: [10.1093/ecco-jcc/jjx180.102](https://doi.org/10.1093/ecco-jcc/jjx180.102)]
  - 89 **Hirth RA**, Chernew ME, Miller E, Fendrick AM, Weissert WG. Willingness to pay for a quality-adjusted life year: in search of a standard. *Med Decis Making* 2000; **20**: 332-342 [PMID: [10929856](https://pubmed.ncbi.nlm.nih.gov/10929856/) DOI: [10.1177/0272989X0002000310](https://doi.org/10.1177/0272989X0002000310)]
  - 90 Changing the course of Crohn's Disease With an Early Use of Adalimumab (CURE). Cited: 7 September 2019 ClinicalTrials.gov Identifier: NCT03306446. Available from: <https://clinicaltrials.gov/ct2/show/record/NCT03306446>
  - 91 Enhanced Algorithm for Crohn's Treatment Incorporating Early Combination Therapy (REACT2) Cited: 7 September 2019 ClinicalTrials.gov Identifier: NCT01698307. Available from: <https://clinicaltrials.gov/ct2/show/NCT01698307>
  - 92 **Murthy SK**, Begum J, Benchimol EI, Bernstein CN, Kaplan GG, McCurdy JD, Singh H, Targownik L, Taljaard M. Introduction of anti-TNF therapy has not yielded expected declines in hospitalisation and intestinal resection rates in inflammatory bowel diseases: a population-based interrupted time series study. *Gut* 2019 [PMID: [31196874](https://pubmed.ncbi.nlm.nih.gov/31196874/) DOI: [10.1136/gutjnl-2019-318440](https://doi.org/10.1136/gutjnl-2019-318440)]
  - 93 **Lasson A**, Öhman L, Stotzer PO, Isaksson S, Überbacher O, Ung KA, Strid H. Pharmacological intervention based on fecal calprotectin levels in patients with ulcerative colitis at high risk of a relapse: A prospective, randomized, controlled study. *United European Gastroenterol J* 2015; **3**: 72-79 [PMID: [25653861](https://pubmed.ncbi.nlm.nih.gov/25653861/) DOI: [10.1177/2050640614560785](https://doi.org/10.1177/2050640614560785)]
  - 94 **Solleis E**, Quinard RM, Bouguen G, Goutte M, Goutorbe F, Bouvier D, Pereira B, Bommelaer G, Buisson A. Combined evaluation of biomarkers as predictor of maintained remission in Crohn's disease. *World J Gastroenterol* 2019; **25**: 2354-2364 [PMID: [31148906](https://pubmed.ncbi.nlm.nih.gov/31148906/) DOI: [10.3748/wjg.v25.i19.2354](https://doi.org/10.3748/wjg.v25.i19.2354)]
  - 95 **Reinisch W**, Wang Y, Oddens BJ, Link R. C-reactive protein, an indicator for maintained response or remission to infliximab in patients with Crohn's disease: a post-hoc analysis from ACCENT I. *Aliment Pharmacol Ther* 2012; **35**: 568-576 [PMID: [22251435](https://pubmed.ncbi.nlm.nih.gov/22251435/) DOI: [10.1111/j.1365-2036.2011.04987.x](https://doi.org/10.1111/j.1365-2036.2011.04987.x)]
  - 96 **Kiss LS**, Szamosi T, Molnar T, Miheller P, Lakatos L, Vincze A, Palatka K, Barta Z, Gasztonyi B, Salamon A, Horvath G, Tóth GT, Farkas K, Banai J, Tulassay Z, Nagy F, Szenes M, Veres G, Lovasz BD, Vegh Z, Golovics PA, Szathmari M, Papp M, Lakatos PL; Hungarian IBD Study Group. Early clinical remission and normalisation of CRP are the strongest predictors of efficacy, mucosal healing and dose escalation during the first year of adalimumab therapy in Crohn's disease. *Aliment Pharmacol Ther* 2011; **34**: 911-922 [PMID: [21883326](https://pubmed.ncbi.nlm.nih.gov/21883326/) DOI: [10.1111/j.1365-2036.2011.04827.x](https://doi.org/10.1111/j.1365-2036.2011.04827.x)]
  - 97 **Molander P**, af Björkstén CG, Mustonen H, Haapamäki J, Vauhkonen M, Kolho KL, Färkkilä M, Sipponen T. Fecal calprotectin concentration predicts outcome in inflammatory bowel disease after induction therapy with TNFα blocking agents. *Inflamm Bowel Dis* 2012; **18**: 2011-2017 [PMID: [22223566](https://pubmed.ncbi.nlm.nih.gov/22223566/) DOI: [10.1002/ibd.22863](https://doi.org/10.1002/ibd.22863)]
  - 98 **Sipponen T**, Björkstén CG, Färkkilä M, Nuutinen H, Savilahti E, Kolho KL. Faecal calprotectin and lactoferrin are reliable surrogate markers of endoscopic response during Crohn's disease treatment. *Scand J*

- Gastroenterol* 2010; **45**: 325-331 [PMID: 20034360 DOI: 10.3109/00365520903483650]
- 99 **Consigny Y**, Modigliani R, Colombel JF, Dupas JL, Lémann M, Mary JY; Groupe d'Etudes Thérapeutiques des Affections Inflammatoires Digestives (GETAID). A simple biological score for predicting low risk of short-term relapse in Crohn's disease. *Inflamm Bowel Dis* 2006; **12**: 551-557 [PMID: 16804391 DOI: 10.1097/01.ibd.0000225334.60990.5b]
- 100 **De Vos M**, Dewit O, D'Haens G, Baert F, Fontaine F, Vermeire S, Franchimont D, Moreels T, Staessen D, Terriere L, Vander Cruyssen B, Louis E, behalf of BIRD. Fast and sharp decrease in calprotectin predicts remission by infliximab in anti-TNF naïve patients with ulcerative colitis. *J Crohns Colitis* 2012; **6**: 557-562 [PMID: 22398050 DOI: 10.1016/j.crohns.2011.11.002]
- 101 **Jauregui-Amezaga A**, López-Cerón M, Aceituno M, Jimeno M, Rodríguez de Miguel C, Pinó-Donnay S, Zabalza M, Sans M, Ricart E, Ordás I, González-Suárez B, Cuatrecasas M, Llach J, Panés J, Pellise M. Accuracy of advanced endoscopy and fecal calprotectin for prediction of relapse in ulcerative colitis: a prospective study. *Inflamm Bowel Dis* 2014; **20**: 1187-1193 [PMID: 24874457 DOI: 10.1097/MIB.0000000000000069]



## Basic Study

# Therapeutic potential of menstrual blood stem cells in treating acute liver failure

Pan-Pan Cen, Lin-Xiao Fan, Jie Wang, Jia-Jia Chen, Lan-Juan Li

**ORCID number:** Pan-Pan Cen (0000-0002-6593-6606); Lin-Xiao Fan (0000-0002-3387-3188); Jie Wang (0000-0003-0335-8246); Jia-Jia Chen (0000-0001-9701-8677); Lan-Juan Li (0000-0001-6945-0593).

**Author contributions:** Cen PP and Chen JJ conceived and designed the research; Cen PP, Fan LX, and Wang J performed the experiments, and collected the data; Cen PP and Fan LX analyzed the data; Cen PP wrote the paper; all authors reviewed the paper; Li LJ provided financial support and gave final approval of the manuscript.

**Supported by** the State Key Laboratory for Diagnosis and Treatment of Infectious Disease; The First Affiliated Hospital of Zhejiang University School of Medicine, No. 2015KF04.

**Institutional review board statement:** This study was approved by the Institutional Review Board of the First Affiliated Hospital of Zhejiang University School of Medicine.

**Institutional animal care and use committee statement:** This study was approved by the Animal Care Ethics Committee of the First Affiliated Hospital of Zhejiang University School of Medicine (reference number: ZJU2015-511-09).

**Conflict-of-interest statement:** No competing financial interests exist.

**Data sharing statement:** (1) The copyright on any open access

**Pan-Pan Cen**, Department of Infectious Diseases, Hangzhou First People's Hospital, Zhejiang University School of Medicine, Hangzhou 310006, Zhejiang Province, China

**Lin-Xiao Fan, Jie Wang, Jia-Jia Chen, Lan-Juan Li**, State Key Laboratory for Diagnosis and Treatment of Infectious Diseases; National Clinical Research Center for Infectious Diseases; The First Affiliated Hospital, Zhejiang University School of Medicine, Hangzhou 310003, Zhejiang Province, China

**Corresponding author:** Lan-Juan Li, MD, PhD, Professor, Senior Researcher, State Key Laboratory for Diagnosis and Treatment of Infectious Diseases; National Clinical Research Center for Infectious Diseases; First Affiliated Hospital of Zhejiang University School of Medicine, 48 Qingchun Road, Shangcheng District, Hangzhou 310003, Zhejiang Province, China. [ljli@zju.edu.cn](mailto:ljli@zju.edu.cn)

**Telephone:** +86-571-87236759

## Abstract

### BACKGROUND

Acute liver failure (ALF) is a significant and complex hepatic insult that may rapidly progress to life-threatening conditions. Recently, menstrual blood stem cells (MenSCs) have been identified as a group of easily accessible mesenchymal stem cells with the advantages of non-invasive acquisition, low immunogenicity, a greater capacity of self-renewal and multi-lineage differentiation, making them promising candidates for stem cell-based therapy to revolutionize the treatment strategies for liver failure.

### AIM

To investigate the therapeutic potential of MenSCs for treating ALF in pigs and to dynamically trace the biodistribution of transplanted cells.

### METHODS

MenSCs were labeled *in vitro* with PKH26, a lipophilic fluorescent dye. The treatment group received immediate transplantation of PKH26-labelled MenSCs ( $2.5 \times 10^6$ /kg) *via* the portal vein after D-galactosamine injection, and the control group underwent sham operation. The survival time, liver function, and hepatic pathological changes were compared between the two groups. Three major organs (liver, lungs and spleen) were extracted from animals and imaged directly with the *In vivo* Imaging System (IVIS) at the predetermined time points. The regions of interest were drawn to quantify the cell uptake in different organs.

### RESULTS

article in a journal published by BPG is retained by the authors; (2) Authors grant BPG the license to publish the article and identify itself as the original publisher; and (3) Authors grant any third party the right to use the article freely as long as its integrity is maintained and its original authors, citation details, and publisher are identified.

**ARRIVE guidelines statement:** The authors have read the ARRIVE guidelines, and the manuscript was prepared and revised according to the ARRIVE guidelines.

**Open-Access:** This article is an open-access article which was selected by an in-house editor and fully peer-reviewed by external reviewers. It is distributed in accordance with the Creative Commons Attribution Non Commercial (CC BY-NC 4.0) license, which permits others to distribute, remix, adapt, build upon this work non-commercially, and license their derivative works on different terms, provided the original work is properly cited and the use is non-commercial. See: <http://creativecommons.org/licenses/by-nc/4.0/>

**Manuscript source:** Unsolicited manuscript

**Received:** August 12, 2019

**Peer-review started:** August 12, 2019

**First decision:** August 27, 2019

**Revised:** September 11, 2019

**Accepted:** October 17, 2019

**Article in press:** October 17, 2019

**Published online:** November 7, 2019

**P-Reviewer:** Nacif LS, Shimizu Y

**S-Editor:** Wang J

**L-Editor:** Ma JY

**E-Editor:** Ma YJ



The labelling procedure did not affect the morphology, viability or multipotential differentiation of MenSCs. Biochemical analysis showed that the levels of alanine aminotransferase (ALT), aspartate aminotransferase (AST), total bilirubin (TBIL) and prothrombin time (PT) measured at selected time points 24 h after transplantation were significantly decreased in the treatment group ( $P < 0.05$ ). The survival time of ALF animals was prolonged in the treatment group compared with the control group ( $75.75 \pm 5.11$  h vs  $53.75 \pm 2.37$  h, log rank,  $P < 0.001$ ). The liver pathological tissue in the MenSC treatment group showed obviously increased numbers of remaining hepatocytes and a comparatively slight necrotic degree and area. In addition, the IVIS imaging revealed that PKH26-positive MenSCs were clearly retained in the liver initially and then diffused through the systemic circulation. Interestingly, the signal intensity in the liver increased obviously at 36 h, which corresponded to the biochemical result that liver function deteriorated most rapidly at 24 - 36 h.

## CONCLUSION

Our study demonstrates the therapeutic efficacy and homing ability of transplanted MenSCs in a large animal model of ALF and suggests that MenSC transplantation could be a promising strategy for treating ALF.

**Key words:** Menstrual blood stem cell; Acute liver failure; Cell transplantation; Homing; Labelling

©The Author(s) 2019. Published by Baishideng Publishing Group Inc. All rights reserved.

**Core tip:** In this study, we investigated for the first time the therapeutic potential of intraportally transplanted menstrual blood stem cells (MenSCs) in treating pigs with acute liver failure, and showed that MenSC treatment improved liver function and coagulation, alleviated the progression of liver injury, and prolonged the survival time of pigs. Additionally, *ex vivo* imaging also demonstrated the ability of MenSCs to home to pathological hepatic environments after transplantation. MenSC transplantation has the potential to be used as an available source for treating acute liver failure in future clinical therapy.

**Citation:** Cen PP, Fan LX, Wang J, Chen JJ, Li LJ. Therapeutic potential of menstrual blood stem cells in treating acute liver failure. *World J Gastroenterol* 2019; 25(41): 6190-6204

**URL:** <https://www.wjgnet.com/1007-9327/full/v25/i41/6190.htm>

**DOI:** <https://dx.doi.org/10.3748/wjg.v25.i41.6190>

## INTRODUCTION

Acute liver failure (ALF) is a significant and complex hepatic insult that may rapidly progress to life-threatening multiple organ failure. The survival prognosis of ALF is extremely poor with a high short-term mortality of 70% - 80%<sup>[1]</sup>. Liver transplantation is considered the ultimate therapeutic option for these patients, but its clinical use is hindered by organ shortage, high cost, surgical risk, and postoperative complications. Thus, stem cell transplantation, as the most cutting-edge medical technique, offers a new hope for revolutionizing the treatment strategies for liver failure<sup>[2,3]</sup>.

Stem cells, with a capacity of self-renewal and multi-lineage differentiation, have become vital players in liver regeneration. In recent years, many studies have shown that stem cell-based therapy may alleviate fibrosis, reduce liver inflammation, promote hepatocyte regeneration, and subsequently improve the liver function of ALF patients<sup>[4]</sup>. Mesenchymal stem cells (MSCs) are defined as adherent, fibroblast-like adult stem cells with characteristic surface phenotypes and multipotential differentiation. Compared with embryonic stem cells and induced pluripotent stem cells, MSCs have less tumorigenicity and involve no ethical issues. They have been identified in a wide range of adult tissues, such as bone marrow, placenta, umbilical cord, adipose tissue, skeletal muscle, cornea, synovial membrane, *etc*<sup>[5]</sup>. However, the application potential of these cell lines is partly restricted by proliferative activity, limited sources, and the invasiveness of acquiring the cells.

In 2007, the Medistem group first isolated a highly proliferating adherent cell



population from menstrual blood with non-haematopoietic markers, termed menstrual blood stem cells (MenSCs)<sup>[6]</sup>. Subsequent studies have demonstrated that MenSCs possess robust replicative capacity, multipotential differentiation, and angiogenesis and vascularization pathways<sup>[7]</sup>. Since they are isolated from menstrual blood, MenSCs have a high level of immune privilege and easy access for acquisition<sup>[8,9]</sup>. Moreover, MenSCs express pluripotency factors, making them easily reprogrammed into disease-specific pluripotent stem cells<sup>[10]</sup>. These characteristics make them an ideal tool for regenerative medicine. To date, MenSCs have shown promising results for diverse diseases, including liver fibrosis<sup>[11]</sup>, muscular dystrophy<sup>[12]</sup>, stroke<sup>[13]</sup>, and glioma<sup>[14]</sup>, in several animal models and pre-clinical studies. Recently, MenSCs in the treatment of an ALF mouse model have been evaluated<sup>[15]</sup>; however, little is known about the therapeutic effect of MenSCs in treating ALF in large animal models, and the potential mechanisms involved are not yet completely understood. Optimizing stem cell-based therapies would require a safe, sensitive, high-efficiency labeling method to dynamically monitor cellular viability, biodistribution, differentiation capacity and long-term fate after engraftment. PKH26, a lipophilic tracer dye, is an easy-to-use and good biocompatible fluorescent marker with high sensitivity, which can bond tightly to the cell membrane and be specific to original cells, thereby passing all progenies with division<sup>[16,17]</sup>.

In this study, we aimed to evaluate the therapeutic potential of intraportal transplanted MenSCs in treating pigs with ALF and used a fluorescent dye (PKH26) to achieve real-time visualization for the biological distribution of infused stem cells.

## MATERIALS AND METHODS

### *Isolation and culturing of MenSCs*

The donors of menstrual blood signed written informed consent for the studies. MenSCs were isolated from the menstrual blood of healthy donors during the first day of menstruation as previously reported<sup>[18]</sup>. Briefly, mononuclear cells were collected by Ficoll-Paque (1.077 g/mL; Fisher Scientific, NH) density-gradient centrifugation according to the manufacturer's instructions. The cells were suspended in menstrual stem cell culture medium (S-Evans Biosciences, China) overnight at 37 °C in 5% humidified CO<sub>2</sub> until the medium was replaced to remove non-adherent cells by washing with 1x phosphate buffered saline (1x PBS). About one million primary cells were isolated from 5mL menstrual blood. When cells reached 80%-90% confluence, they were subcultured and used for experiments during passages 3 to 5.

### *Phenotypic analysis via flow cytometry*

Surface markers of cultured MenSCs were analyzed using a flow cytometer (FC500MCL, Beckman Coulter, United States). The third and fifth passages of MenSCs ( $5 \times 10^5$  cells/100  $\mu$ L) were incubated directly with phycoerythrin (PE) or allophycocyanin (APC)-conjugated mouse monoclonal antibodies against human CD9, CD29, CD41a, CD44, CD59, CD 73, CD90, CD105, CD14, CD34, CD45, CD117, and human leukocyte antigen (HLA)-DR (BD Biosciences, CA, United States) for 30 min in the dark at 4 °C, followed by washing and resuspension in PBS twice. Flow cytometry was conducted using a FACSCalibur system (FC500, Beckman Coulter, United States). Data were analyzed using FlowJo Version 10.05.

### *PKH26 labeling of MenSCs*

Cells were labeled with the fluorescent dye PKH26 (Sigma-Aldrich, United States) before transplantation according to the manufacturer's protocol. MenSCs ( $2 \times 10^7$ ) were washed twice in serum-free medium after trypsinization and resuspended in 1mL of the dilution buffer. Before labeling, 4  $\mu$ L stock solution of PKH26 was diluted with an equal volume of the dilution buffer and then immediately incubated with the cell suspension for 4 min at 25 °C. The labeling process was terminated by adding 2 mL fetal bovine serum. The cells were finally washed twice in complete culture medium, and the labelling ratio was counted under a confocal microscope (Carl Zeiss, Germany).

### *Cell viability and multipotential differentiation*

Cell viability was assessed by a cell counting kit-8 (CCK-8). Briefly, PKH26-labelled MenSCs (PKH26-MenSCs) and unlabelled MenSCs were separately seeded at a density of 1000 cells per well in 96-well plates. Ten microliters of CCK-8 reagent (Dojindo Laboratories, Japan) was added to 6 wells of each group every 24 h, and the cells were incubated for 1 h at 37 °C in 5% CO<sub>2</sub>. The absorbance at 450 nm was measured by a spectrophotometer (Beckman Coulter, United States), and the growth curve was drawn to compare cell proliferation ability between the two groups. To

induce osteogenic differentiation, PKH26-MenSCs and unlabeled MenSCs were cultured in commercially available osteogenesis differentiation medium (Cyagen Biosciences, United States). On day 21, cells were stained with alizarin red S. To induce adipogenic differentiation, each group of cells was cultured in a commercially available adipogenesis differentiation medium purchased from Cyagen. On day 21, lipid droplets were visualized by oil red O.

### **ALF induction and cell transplantation**

The experiments were approved by the Animal Care Ethics Committee of the First Affiliated Hospital of Zhejiang University School of Medicine, Hangzhou, China on July 20<sup>th</sup>, 2015 (reference number: ZJU2015-511-09). A flow chart of the experimental design is presented in [Figure 1](#). Forty male Bama experimental miniature pigs (Jiagan Biotechnology, China) with an average weight of 8–12 kg were used in this study. All animals were fed in a single cage in a temperature-controlled environment (20–25 °C) with a 12 h light/12 h dark cycle and acclimatized for 7 d prior to the experiments. Sedation was induced with atropine (0.05 mg/kg), tramadol (2 mg/kg) and midazolam (0.1 mg/kg) by intramuscular injection. After anesthetized by intravenous injection of propofol (2.5 mg/kg/h), the animals were placed in the right lateral position and sterilized on their jugular skin. Then, an incision was made along the medial margin of the sternocleidomastoid followed by exposing and separating the external jugular vein. After the distal end of the vessel was ligated with sutures, the vessel was inserted into a double channel catheter (7 Fr). Finally, the wound was closed in layers, a sterile dressing was carried out. Twenty-four hours after jugular vein catheterization, ALF was induced with [D-galactosamine (D-gal), Hanhong Chemical, Shanghai, China] at a dose of 1.0 g/kg as previously described by our laboratory<sup>[19,20]</sup>. The animals were randomly allocated to two groups: Group I ( $n = 20$ ), a treatment group, received an immediate intraportal transplantation of PKH26-MenSCs ( $2.5 \times 10^6$  /kg) suspended in 30 mL normal saline after D-gal injection. Specifically, after locating the portal vein, a puncture needle (18G) pierced the portal vein slowly under B-ultrasound guidance. When a free flow of blood appeared in the needle, PKH26- MenSCs were infused into the portal vein. Group II ( $n = 20$ ), a sham operation group, received an equal volume of normal saline without MenSCs. No additional medical support was provided during the entire course of the experiment. Survival time was recorded until death without any human intervention.

### **Dynamic tracing of PKH26- MenSCs**

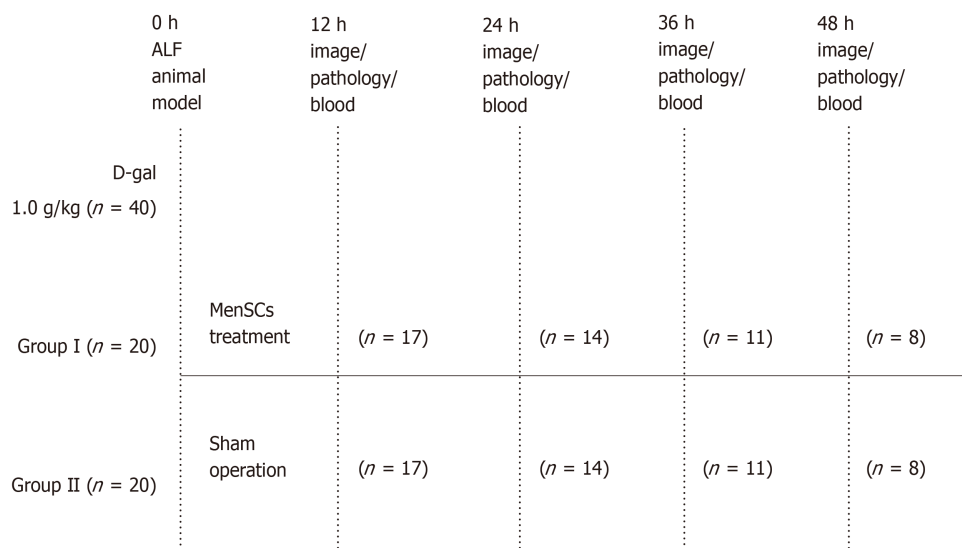
For dynamic tracing and imaging studies, immediately after the animals were sacrificed by propofol overdose, three major organs (the liver, spleen, and lungs) were isolated and placed into the In vivo Imaging System (IVIS) chamber (PerkinElmer, United States) and images were acquired using a CCD camera (Ex = 580 nm, Em = 535 nm, Exposure time = 5 s) at 12 h after transplantation, and then at 24 h, 36 h, and 48 h. The regions of interest (ROI) were drawn to quantify the cell uptake in different organs by calculating the total photon emission efficiency.

### **Blood sampling and pathological examination**

The mental status, appetite, and activity of the animals during the experiment were closely observed. Blood samples were collected using a jugular vein catheter after D-gal administration and every 12 h thereafter. At the predetermined time points, 2 mL whole blood was sampled in coagulation tubes, and prothrombin time (PT) was measured in the emergency laboratory of the First Affiliated Hospital of Zhejiang University. Another set of blood samples (3 mL whole blood) was centrifuged in BD Vacutainer SST tubes to collect serum for biochemical analysis with an automated biochemical analyzer (Abbott Aeroset, United States). Tissue samples of liver were collected to assess the effect of MenSC treatment on liver apoptosis and necrosis. At the set time points, following the imaging of the animals, sections of liver were preserved in 4% buffered formalin for 24 h, and then embedded in paraffin for haematoxylin and eosin (H&E) staining. Apoptosis of hepatocytes was assessed by terminal deoxynucleotidyl transferase-mediated dUTP nick-end labeling (TUNEL) assay (Roche, Germany).

### **Statistical analysis**

All data were analyzed using SPSS for Windows version 19.0 (SPSS, Chicago, IL, United States) and GraphPad Prism 5 (GraphPad, San Diego, CA, United States). Continuous variables were compared with Student's *t* test and expressed as the mean  $\pm$  SE. The survival of animals was analyzed by a Kaplan-Meier graph and compared by log-rank tests. Statistical significance was taken as  $P < 0.05$ . A statistical review of the study was performed by a biomedical statistician.



**Figure 1 Experimental design.** Acute liver failure (ALF) was induced in forty animals with D-galactosamine (D-gal) at a dose of 1.0 g/kg. The treatment group (Group I,  $n = 20$ ) received cell transplantation and the control group (Group II,  $n = 20$ ) received a sham operation. Animals from both groups were sacrificed every 12 h. Blood samples were collected for biochemical analysis. Three major organs (the lungs, liver, and spleen) were isolated and immediately imaged with the In vivo Imaging System. Then liver tissues were collected for pathological examination. ALF: Acute liver failure; MenSCs: Menstrual blood stem cells; D-gal: D-galactosamine; IVIS: In vivo Imaging System.

## RESULTS

### *Morphology and phenotypic profile of MenSCs*

Plastic-adherent MenSCs were successfully isolated from menstrual blood and expanded rapidly with a short doubling time of 24 - 36 h. They presented with a fibroblast-like spindle shape, formed a monolayer and grew adhering to the wall in a spiral or radial arrangement. The phenotypic analysis by flow cytometry showed that the third and fifth passages of MenSCs were positive for CD9, CD29, CD73, CD90, CD105, CD44, and CD59, but were negative for haematopoietic stem cell markers, such as CD34, CD45, and CD117, as well as the immune activation marker HLA-DR (Figure 2). These findings were consistent with the general characteristics of classic MenSCs.

### *Cell labeling*

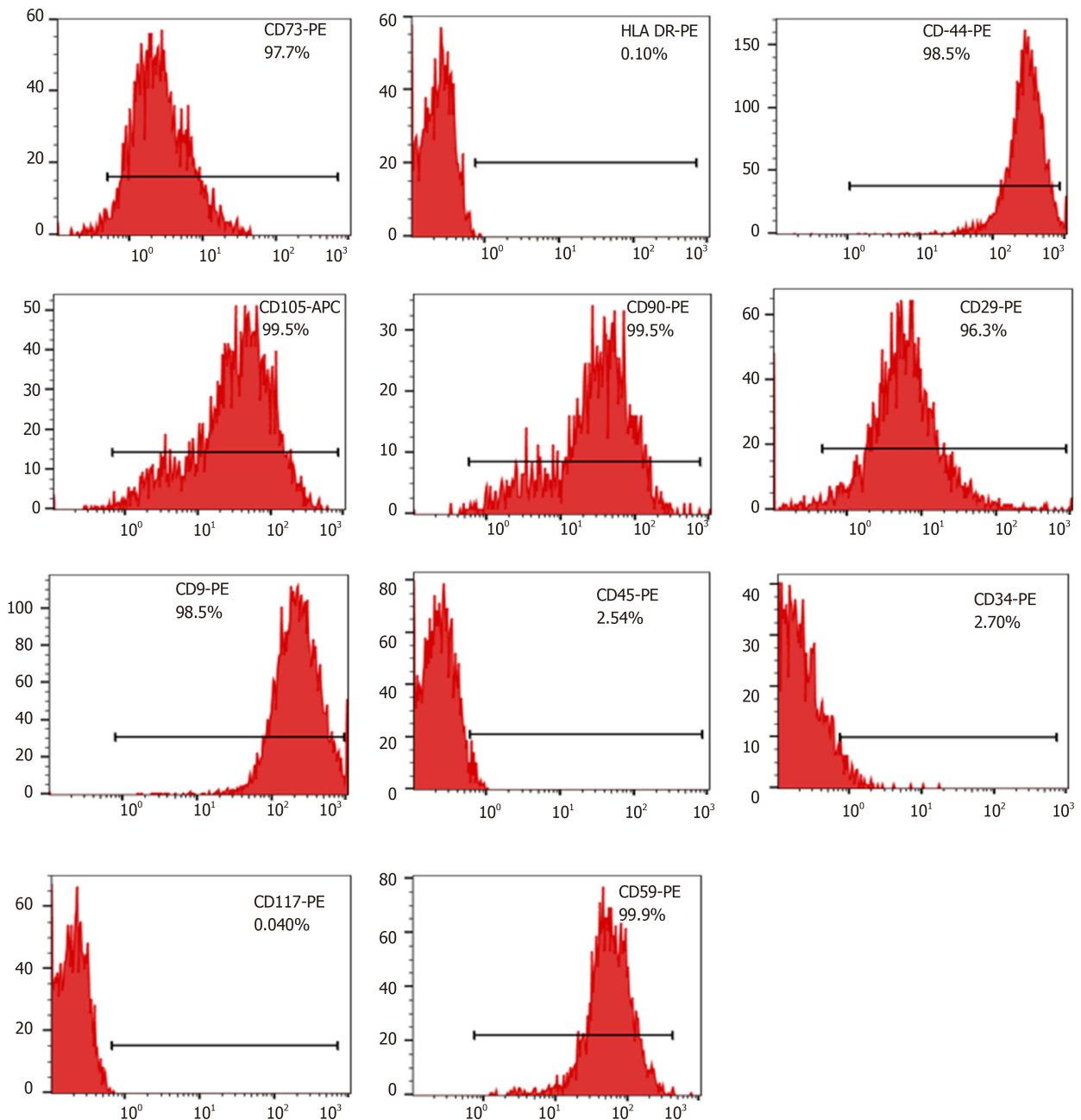
The PKH26 labeled cell members of MenSCs emitted strong red fluorescence with a clear cell configuration under a confocal microscope, and nuclei were stained with DAPI. The labeling rate of PKH26 was more than 95%. After serial passages, the fluorescent signal intensity from the PKH26-MenSCs decreased with time but could also be detected (Figure 3).

### *Effects of PKH26 on the cytomorphology, viability and multipotential differentiation of MenSCs*

PKH26-MenSCs presented with long, spindle-shaped, fibroblast-like adherent growth, and no remarkable morphological changes were found, which indicated that the labelling procedure did not impair cytomorphology. To assess the effect of PKH26 on the viability of MenSCs, CCK-8 assays were conducted and a cell growth curve generated. No significant difference between the PKH26-MenSCs and unlabeled MenSCs was observed on d 1 to d 7 ( $n = 6$ ,  $P > 0.05$ ), confirming that PKH26 dye had no effect on cell viability. After 3 wk of induction of adipogenic and osteogenic differentiation *in vitro*, bone nodules formed by osteogenically differentiated PKH26-MenSCs were visualized by alizarin red S staining. Adipogenic differentiation was identified by oil red O staining. Differentiated PKH26-MenSCs produced intracytoplasmic lipid droplets and stained positive (Figure 4). These results indicated that PKH26 had no adverse effect on the multipotential differentiation ability.

### *Dynamic tracing of transplanted PKH26-MenSCs*

After MenSC transplantation, no serious adverse reaction was observed. Three major organs (the liver, spleen, and lungs), in which almost all transplanted MenSCs were predicted to be retained, were extracted from the animals at the predetermined time points and then imaged in the IVIS. The *ex vivo* imaging showed that most of the



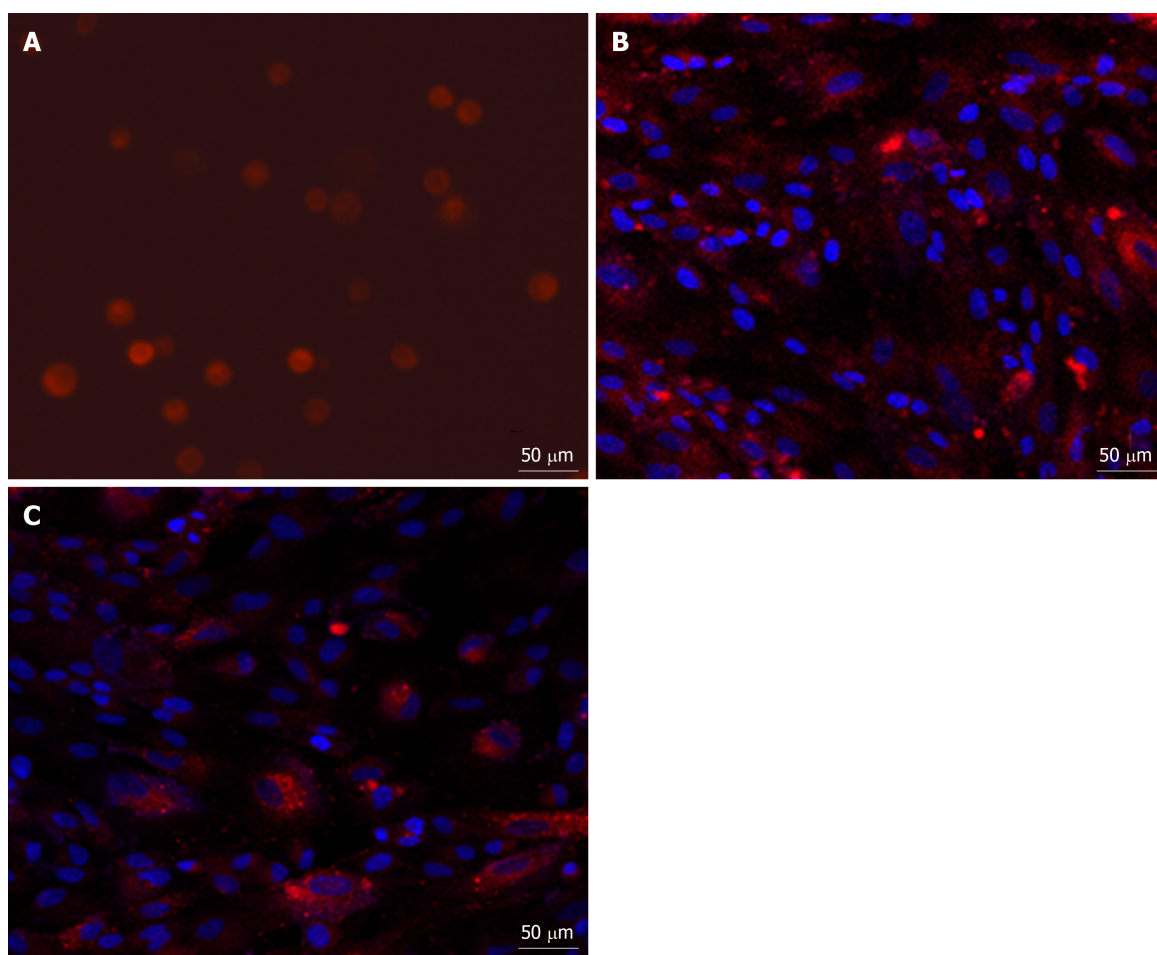
**Figure 2 Phenotypic profile of menstrual blood stem cells isolated from menstrual blood.** Surface markers of cultured menstrual blood stem cells (MenSCs) were analyzed using a flowcytometer at the third and fifth passages. MenSCs: Menstrual blood stem cells.

strong red fluorescence emitted from PKH26-MenSCs was distributed in the hepatic periportal area, and a small part was accumulated in the centrilobular regions. A weak signal was also detected in the lungs, and little signal was observed in the spleen (Figure 5A-F). At 12 h after transplantation, the ROI analysis revealed that the number of photons emitted from the liver was  $1.55 \times 10^{10} \pm 2.97 \times 10^8$  p/s, and dropped to  $7.74 \times 10^9 \pm 1.23 \times 10^8$  p/s at 24 h ( $P < 0.001$ ). However, the signal intensity of the liver significantly increased to  $3.65 \times 10^{10} \pm 1.38 \times 10^8$  p/s at 36 h ( $P < 0.001$ ), and attenuated at 48 h after transplantation (Figure 5G).

### Survival

Portal vein puncture was well-tolerated in all experimental animals. Compared with the sham operation group, symptoms of hepatic encephalopathy, such as anorexia, dysphoria and limb tremors, in animals with MenSC treatment occurred obviously later. In the sham operation group, none of the animals survived more than 63 h (survival time,  $53.75 \pm 2.37$  h). After the transplantation of  $2.5 \times 10^6$ /kg MenSCs *via* the intrahepatic portal vein in the treatment group, the survival time was significantly prolonged ( $75.75 \pm 5.11$  h, log rank,  $P < 0.001$ ) (Figure 6A).





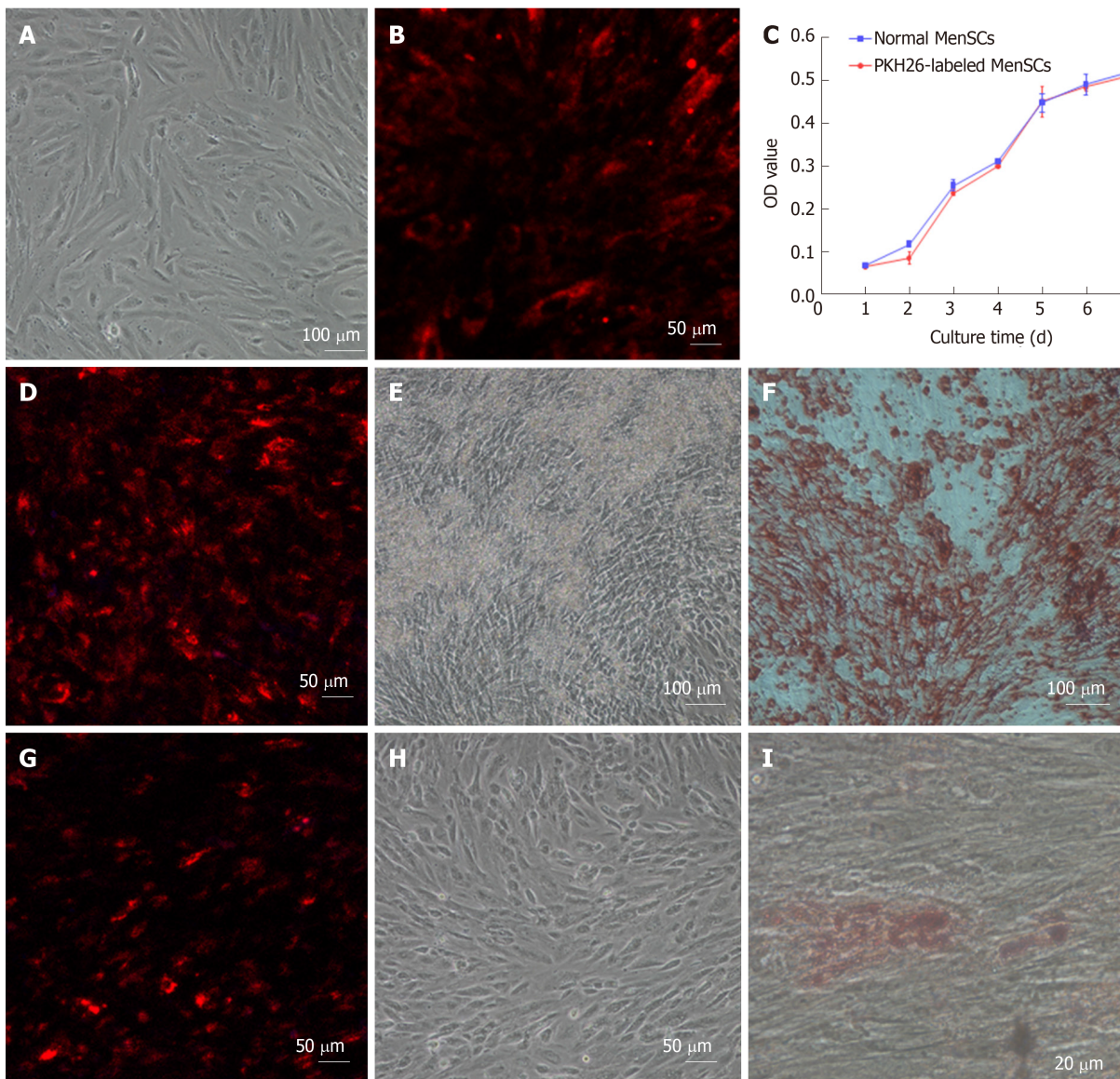
**Figure 3** Fluorescence micrograph of PKH26-labelled menstrual blood stem cells. A: The third passage of PKH26-labelled menstrual blood stem cells (MenSCs) was resuspended and exhibited red fluorescence ( $\times 20$ ); B: When the labelled MenSCs were cultured *in vitro*, most of the cells were able to grow adhering to the wall ( $\times 20$ ); C: After serial passages, the fluorescent signal intensity from the cells decreased with time ( $\times 20$ , passage 8). MenSCs: Menstrual blood stem cells.

### Biochemical and hematological parameters

Continuous progression of ALF was observed in the sham operation group, manifesting as a dynamical increase in PT and the levels of alanine aminotransferase (ALT), aspartate aminotransferase (AST), and total bilirubin (TBIL). The liver function of ALF animals without MenSC treatment deteriorated most rapidly at 24 h to 36 h after D-gal administration, and the phenomenon of enzyme-jaundice separation appeared at 48 h, indicating a wide range of hepatocyte necrosis. In the treatment group, biochemical parameters and coagulation function were similarly worsened as early as 24 h after ALF induction ( $P > 0.05$ ). After 24 h, the deterioration trend was comparatively slowing down. The levels of ALT, AST, TBIL and PT measured at selected time points 24 h after transplantation were significantly lower than those in animals in the sham operation group ( $P < 0.05$ ). No significant changes occurred in the serum albumin level in either group. Compared with the sham operation group, MenSC transplanted *via* the portal vein significantly improved the liver function of D-gal-induced ALF (Figure 6B-C).

### Histological features

Liver tissues were collected for H&E staining to examine hepatic pathological changes. ALF was confirmed by the observation of massive necrosis, large areas of hemorrhage and inflammatory infiltration, hepatocyte apoptosis and vacuolar degeneration at 48 h after ALF induction in the liver tissues of the control group. Hepatic lobular structure was completely collapsed. In contrast, the liver pathological tissue in the MenSC treatment group showed obviously increased numbers of remaining hepatocytes and hepatic parenchymal cells and a comparatively slight necrotic degree and area. Positively labeled apoptotic hepatocytes were observed by TUNEL in the experimental groups at 36 h. However, the number of apoptotic cells was significantly lower in the post-mortem liver tissues of the MenSC treatment group than in the control group (Figure 7).



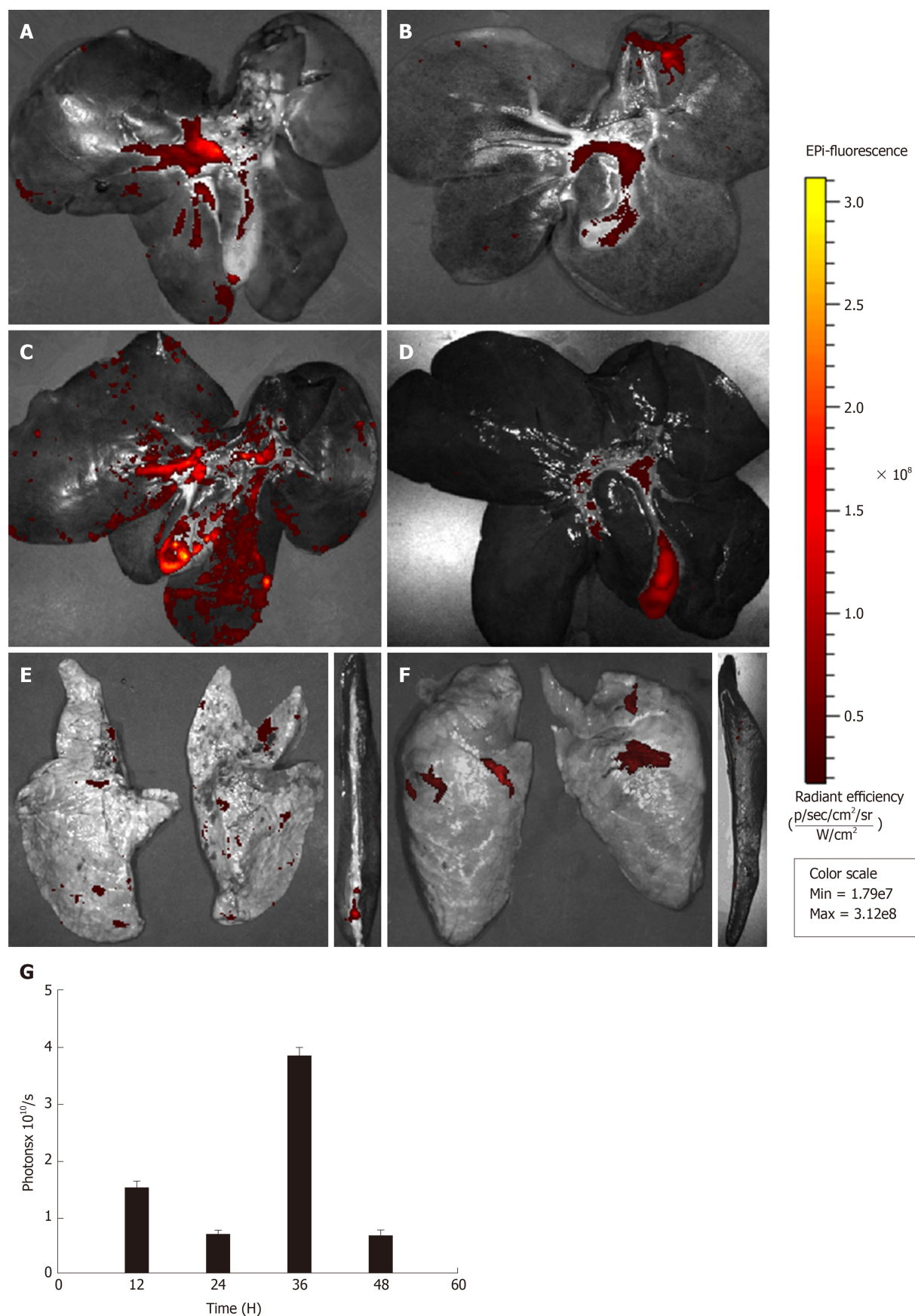
**Figure 4** Effect of PKH26 on the cytomorphology, viability and multipotential differentiation of menstrual blood stem cells. A: Morphology of the fifth passage of menstrual blood stem cells (MenSCs) without PKH26 labelling ( $\times 10$ ); B: the fifth passage of MenSCs with PKH26 labelling after 3 d ( $\times 20$ ); C: Viability of PKH26-labelled MenSCs and non-labelled normal MenSCs; D: Osteogenic differentiation of PKH26-labelled MenSCs under a confocal microscope ( $\times 20$ ); E: Bone nodules formed by differentiated osteocytes were visualized ( $\times 10$ ); F: PKH26-labelled MenSCs underwent osteogenic differentiation after alizarin red S staining ( $\times 10$ ); G: Adipogenic differentiation of PKH26-labelled MenSCs under a confocal microscope ( $\times 20$ ); H: Differentiated adipocytes were visualized before oil red O staining ( $\times 10$ ); I: Differentiated adipocytes contained lipid droplets after oil red O staining ( $\times 40$ ). MenSCs: Menstrual blood stem cells.

## DISCUSSION

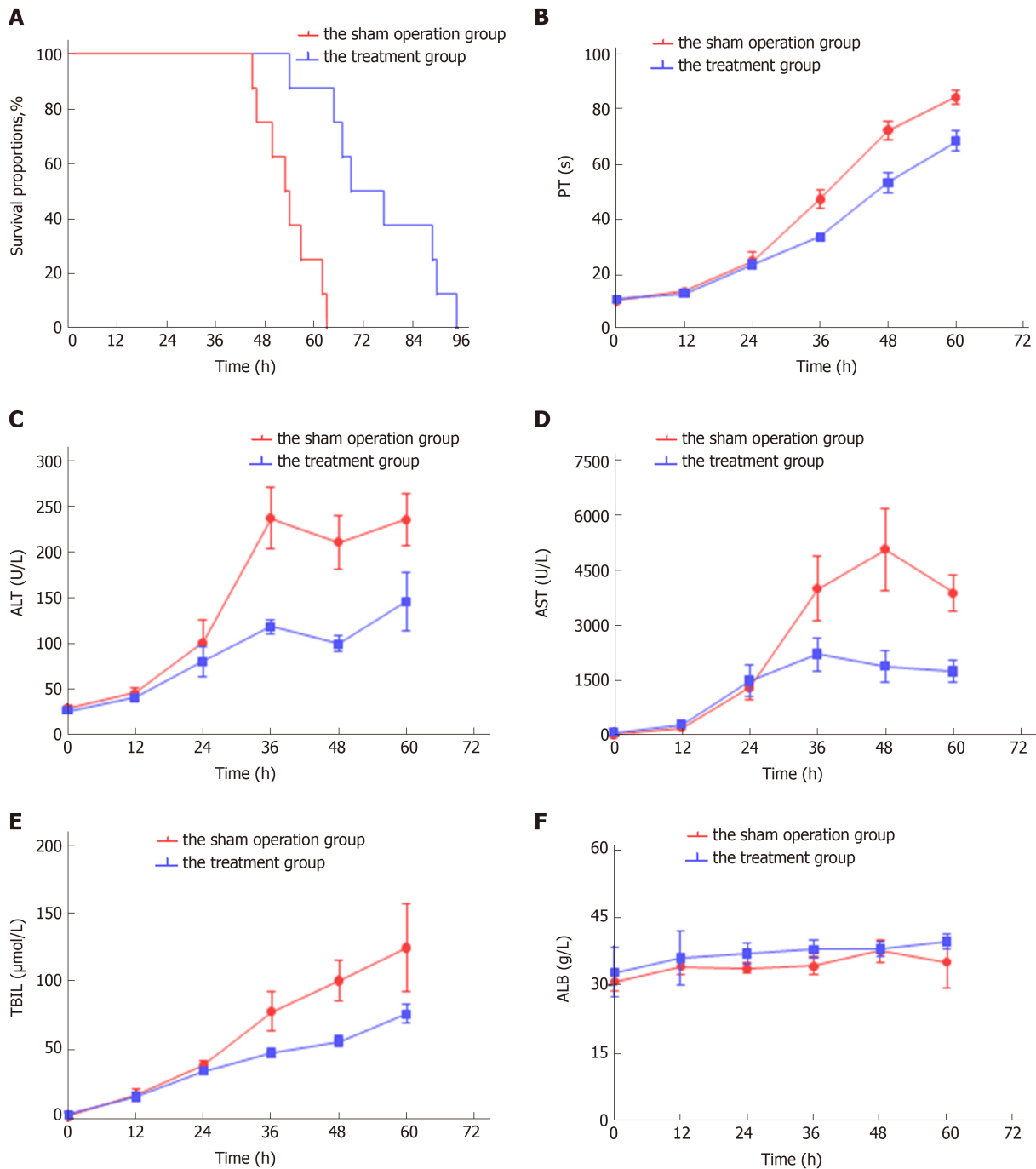
MSC transplantation has opened new frontiers in regenerative medicine with the possibility of repairing damaged tissues. There has been an increasing need for an ideal cell population that provides a high proliferation rate, easy access and sufficient doses of lower-passage MSCs. As a refreshing, non-invasive, and plentiful source of stem cells, MenSCs have shown promising effects in several pre-clinical models<sup>[21,22]</sup>. However, the therapeutic effect of MenSCs in ALF has not been well studied, although it is significant. Therefore, in this study, we investigated the efficacy of intraportally transplanted MenSCs in treating pigs with ALF, and a fluorescent dye (PKH26) was used to evaluate their homing ability in the injured liver and to dynamically monitor the biological distribution of infused stem cells.

Choosing an appropriate animal model is vital in estimating the efficacy of cell transplantation. In our study, D-gal was used to establish the ALF porcine model because the drug possesses a specific hepatotoxicity, controllable dose, and potential reversibility, and has been widely used for large animal studies<sup>[19,23]</sup>. Obviously, the pig model was more acceptable and suitable for further clinical research. The dose of D-gal for ALF induction was an issue of crucial importance. After D-gal (1.0 g/kg)





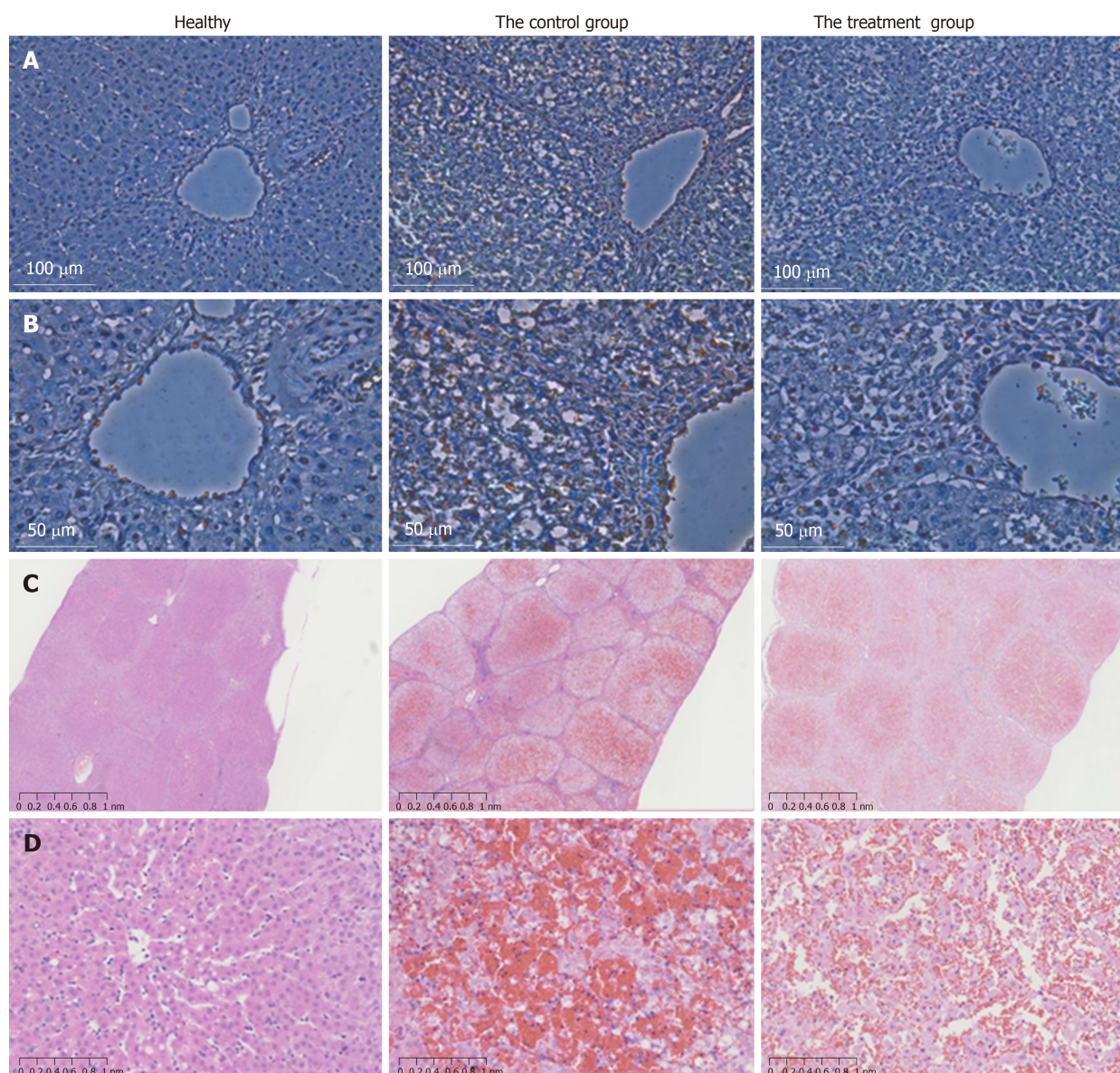
**Figure 5** *Ex vivo* images showing the dynamic biodistribution of transplanted PKH26-labelled menstrual blood stem cells in different organs by the *in vivo* imaging system. A: At 12 h after transplantation, strong red fluorescence emitted from PKH26-labelled menstrual blood stem cells (MenSCs) was detected in the liver; B: The fluorescence intensity of the liver weakened at 24 h; C: The fluorescence intensity of the liver increased notably at 36 h; D: Finally, the signal faded after 48 h; E: At 24 h after transplantation, a weak signal was detected in the lungs and the spleen; F: At 48 h after transplantation, a weak signal was also detected in the lungs, but it was seldom observed in the spleen; G: A graph showing the total photon emission efficiency in the liver at all time points. MenSCs: Menstrual blood stem cells; IVIS: *In vivo* Imaging System.



**Figure 6** Efficacy of intraportally transplanted menstrual blood stem cells in treating pigs with acute liver failure. A: Survival time of the treatment group and the sham operation group ( $P < 0.001$ ); B: Dynamic changes in the biochemical in the two groups; C: Dynamic changes in the hematological parameters in the two groups. MenSCs: Menstrual blood stem cells; ALF: Acute liver failure; PT: Prothrombin time; ALT: Alanine aminotransferase; AST: Aspartate aminotransferase; TBIL: Total bilirubin; ALB: Albumin.

administration, the biochemical indices of the sham operation group showed a stable toxic effect. The most rapid deterioration period of liver function and coagulation was established 24 - 36 h after modeling, and enzyme-jaundice separation appeared at 48 h, indicating a mass of hepatocyte necrosis. However, in the low-dose groups ( $< 1.0$  g/kg), there was a high disparity in survival time, indicating that the ALF progressed differently in animals. The lower dose may not satisfy the process of ALF. In addition, it is a stable and exact ALF large animal model established by our laboratory, and some significant work has been published based on the ALF model<sup>[20,24]</sup>. Therefore, the D-gal-induced ALF porcine model in our study was supposed to be reliable and steady. The selection of transplantation methods is also vital. Several studies have demonstrated the feasibility and superiority of intraportal transplantation for cell survival compared to the peripheral vein route<sup>[24,25]</sup>. Thus, we used this approach to transplant MenSCs into the animals.





**Figure 7** TUNEL assay and H&E staining of liver tissues after acute liver failure induction. A: Apoptotic hepatocytes were stained red. At 36 h after ALF induction, the number of apoptotic cells was significantly lower in the menstrual blood stem cell (MenSC) treatment group than in the control group ( $\times 20$ ); B: High magnification images were shown ( $\times 40$ ); C: The livers of the ALF pigs without MenSC treatment showed a typical ALF histology with extensive haemorrhage, hepatocyte necrosis and adipose degeneration at 48 h. In contrast, ALF pigs with MenSC transplantation showed increased numbers of remaining hepatocytes and hepatic parenchymal cells ( $\times 2$ ); D: High magnification images were shown ( $\times 20$ ). MenSC treatment alleviated the progression of liver injury. ALF: acute liver failure; MenSC: menstrual blood stem cell.

Our study explored the clinical potential of MenSCs in the treatment of ALF. The result revealed that the survival time was significantly prolonged, and the levels of ALT, AST, TBIL and PT were obviously decreased in the treatment group, which was also confirmed by the pathological improvements in pigs with MenSC transplant. These findings indicated that the immediate transplantation of MenSCs *via* the portal vein effectively improved liver function and coagulation, alleviated the progression of liver injury, and prolonged survival time. As a most commonly used type of MSC for cell therapy, human bone marrow mesenchymal stem cell (BMMSC) transplantation has been proven effective in preventing death from ALF in a porcine model<sup>[25]</sup>. Compared to bone marrow mesenchymal stem cells (BMMSCs), MenSCs presented a higher expression of ICM-1 and IL-8, which indicates that MenSCs may have superiority in anti-inflammatory actions<sup>[10,21]</sup>. Additionally, it was also observed that MenSCs proliferated faster and possessed a higher capacity of homing to injured sites than BMMSCs<sup>[26]</sup>. Nevertheless, whether MenSCs can ensure the long-term survival of individuals with ALF needs to be further studied. MenSC therapy may serve as a bridge to liver transplantation in ALF patients. Therefore, to achieve the optimal effectiveness of MenSC therapy, cell preconditioning, the timing of cell grafting, the

therapeutic dose, and the delivery route need to be further investigated.

To date, near-infrared dyes have been utilized for dynamically tracing stem cells *in vivo* with improved signal detection capacity<sup>[27-30]</sup>. To achieve real-time monitoring of infused stem cells, we labeled the cells with PKH26. The advantage of the labeling method in our study mainly lies in its simplicity and high efficiency, with no need for additional genetic manipulation. Some studies have demonstrated the feasibility of PKH26 for the *in vivo* imaging of grafted stem cells in rat liver<sup>[31,32]</sup>. Therefore, PKH26 is a suitable cell dye to be used for tracing. The IVIS imaging revealed that the transplanted MenSCs were initially clearly retained in the liver and then diffused through the systemic circulation, leading to a decrease in the signal at 24 h after transplantation. Interestingly, the ability of MenSCs to home to pathological hepatic environments was confirmed by the notably increased signal intensity of the ROI in the liver at 36 h, which corresponded to the biochemical result that liver function deteriorated most rapidly at 24 - 36 h, supporting the concept that the damaged liver may release some chemotactic factors to mobilize stem cells migration to the injured position<sup>[33,34]</sup>. The homing mechanisms of MenSCs in the pathological hepatic environments have remained unclear and need to be explored. So far, MenSCs have been reported to function via antiapoptotic effects<sup>[35]</sup>, anti-inflammatory effects<sup>[36]</sup>, immunomodulation<sup>[37]</sup>, angiogenesis<sup>[14]</sup>, and the mobilization of endogenous stem cells<sup>[38]</sup>. Some groups have demonstrated that the mechanisms of direct differentiation and cell replacement could not explain the function compensation<sup>[39,40]</sup>. The paracrine effects of MenSCs may play a pivotal role in tissue regeneration. Additionally, cell fusion also contributes to the therapeutic effect<sup>[37]</sup>. To better translate from bench to bedside, we should furnish deeper insights into the therapeutic mechanism and optimize stem-cell-based therapies.

ALF is a life-threatening liver disease with an extremely high mortality due to lack of effective treatment methods. However, few preclinical studies have reported the therapeutic effect of MenSCs in treating ALF in large animal models, although MenSCs have shown promising properties in tissue regeneration. Hence, our research provided feasibility and preliminary basis for future exploration and clinical application. Since the clinical trials of MenSCs are a drop in the bucket, there is still a long way to go before they are applied in clinical practice and translate to the medicine. We need to take into account their *in-vivo* survival time, long-term safety, standard collection procedure, and heterogeneity derived from diverse donors before MenSC transplantation becomes a clinical strategy for treating ALF<sup>[41]</sup>.

The current study has some limitations. First, we established the ALF porcine model by D-gal. The model focused on drug-induced liver failure and cannot reflect the diversity of causes for liver failure in human patients. Furthermore, the survival time in the animals was short in our study, so we did not carry out further experiments to confirm the *in-vivo* differentiation of MenSCs. The therapeutic dose, the quality of MenSCs, the delivery route and the timing of grafting may lead to the result.

In summary, the effectiveness and dynamic biodistribution of immediate intraportal transplantation of MenSCs were investigated in a large animal model of ALF for the first time. These findings suggest that MenSC transplantation may be considered an alternative approach for treating ALF.

## ARTICLE HIGHLIGHTS

### Research background

Acute liver failure (ALF) is a rapidly progressing liver disorder with extremely poor survival prognosis due to lack of effective treatment methods. In recent years, stem cell-based therapy has emerged as a new hope for revolutionizing the treatment of ALF. Thus, seeking for an ideal cell line for transplantation is of great importance.

### Research motivation

Menstrual blood stem cells (MenSCs) are a group of easily accessible mesenchymal stem cells with advantages of a high level of immune privilege, robust replicative capacity and multipotential differentiation. However, little is known about the therapeutic effect of MenSCs in treating ALF in large animal models. MenSC transplantation could be a promising strategy for treating ALF.

### Research objectives

The aim of this study was to investigate the efficacy of MenSCs for treating ALF in pigs and to dynamically trace the biodistribution of transplanted cells.

### Research methods

MenSCs were labelled *in vitro* with the fluorescent dye PKH26. Phenotypic analysis of MenSCs



was performed using a flow cytometer. Cell viability was assessed by CCK-8. Cell multipotential differentiation was assessed by osteogenic and adipogenic differentiation. ALF porcine model was induced with D-galactosamine at a dose of 1.0 g/kg. The treatment group received transplantation of PKH26-labelled MenSCs *via* the portal vein under B-ultrasound guidance. The liver, lungs and spleen of sacrificed animals were imaged with the In vivo Imaging System (IVIS) using a CCD camera.

### Research results

The labelling procedure did not affect the morphology, viability or multipotential differentiation of MenSCs. The survival time was significantly prolonged, and the levels of ALT, AST, TBIL and PT were obviously decreased in the treatment group compared with the control group. The liver pathological tissue in MenSC treatment group showed obviously increased numbers of remaining hepatocytes and a comparatively slight necrotic degree and area. The IVIS imaging revealed that PKH26-positive MenSCs were clearly retained in the liver initially and then diffused through the systemic circulation. The homing ability of MenSCs was confirmed by the markedly increased signal intensity in the liver at 36 h after transplantation. However, to achieve the optimal effectiveness of MenSC therapy, the therapeutic dose, cell preconditioning, the timing of cell grafting and the delivery route need to be further investigated.

### Research conclusions

This study showed that the immediate transplantation of MenSCs *via* the portal vein effectively improved liver function and coagulation, alleviated the progression of liver injury, and prolonged survival time. The study also demonstrated the ability of MenSCs to home to pathological hepatic environments after transplantation.

### Research perspectives

The therapeutic effect and homing ability of intraportally transplanted MenSCs in a porcine ALF model have been confirmed. MenSC transplantation may be a promising strategy for treating ALF.

## REFERENCES

- Cardoso FS, Marcelino P, Bagulho L, Karvellas CJ. Acute liver failure: An up-to-date approach. *J Crit Care* 2017; **39**: 25-30 [PMID: 28131021 DOI: 10.1016/j.jcrc.2017.01.003]
- Peng L, Xie DY, Lin BL, Liu J, Zhu HP, Xie C, Zheng YB, Gao ZL. Autologous bone marrow mesenchymal stem cell transplantation in liver failure patients caused by hepatitis B: short-term and long-term outcomes. *Hepatology* 2011; **54**: 820-828 [PMID: 21608000 DOI: 10.1002/hep.24434]
- Vassilopoulos G, Wang PR, Russell DW. Transplanted bone marrow regenerates liver by cell fusion. *Nature* 2003; **422**: 901-904 [PMID: 12665833 DOI: 10.1038/nature01539]
- Forbes SJ, Newsome PN. New horizons for stem cell therapy in liver disease. *J Hepatol* 2012; **56**: 496-499 [PMID: 21798218 DOI: 10.1016/j.jhep.2011.06.022]
- Hu C, Li L. In Vitro and In Vivo Hepatic Differentiation of Adult Somatic Stem Cells and Extraembryonic Stem Cells for Treating End Stage Liver Diseases. *Stem Cells Int* 2015; **2015**: 871972 [PMID: 26347063 DOI: 10.1155/2015/871972]
- Meng X, Ichim TE, Zhong J, Rogers A, Yin Z, Jackson J, Wang H, Ge W, Bogin V, Chan KW, Thébaud B, Riordan NH. Endometrial regenerative cells: a novel stem cell population. *J Transl Med* 2007; **5**: 57 [PMID: 18005405 DOI: 10.1186/1479-5876-5-57]
- Bockeria L, Bogin V, Bockeria O, Le T, Alekian B, Woods EJ, Brown AA, Ichim TE, Patel AN. Endometrial regenerative cells for treatment of heart failure: a new stem cell enters the clinic. *J Transl Med* 2013; **11**: 56 [PMID: 23510656 DOI: 10.1186/1479-5876-11-56]
- Gargett CE, Schwab KE, Zillwood RM, Nguyen HP, Wu D. Isolation and culture of epithelial progenitors and mesenchymal stem cells from human endometrium. *Biol Reprod* 2009; **80**: 1136-1145 [PMID: 19228591 DOI: 10.1095/biolreprod.108.075226]
- Mutlu L, Hufnagel D, Taylor HS. The endometrium as a source of mesenchymal stem cells for regenerative medicine. *Biol Reprod* 2015; **92**: 138 [PMID: 25904012 DOI: 10.1095/biolreprod.114.126771]
- Verdi J, Tan A, Shoaie-Hassani A, Seifalian AM. Endometrial stem cells in regenerative medicine. *J Biol Eng* 2014; **8**: 20 [PMID: 25097665 DOI: 10.1186/1754-1611-8-20]
- Chen L, Zhang C, Chen L, Wang X, Xiang B, Wu X, Guo Y, Mou X, Yuan L, Chen B, Wang J, Xiang C. Human Menstrual Blood-Derived Stem Cells Ameliorate Liver Fibrosis in Mice by Targeting Hepatic Stellate Cells via Paracrine Mediators. *Stem Cells Transl Med* 2017; **6**: 272-284 [PMID: 28170193 DOI: 10.5966/sctm.2015-0265]
- Cui CH, Uyama T, Miyado K, Terai M, Kyo S, Kiyono T, Umezawa A. Menstrual blood-derived cells confer human dystrophin expression in the murine model of Duchenne muscular dystrophy via cell fusion and myogenic transdifferentiation. *Mol Biol Cell* 2007; **18**: 1586-1594 [PMID: 17314403 DOI: 10.1091/mbc.E06-09-0872]
- Borlongan CV, Kaneko Y, Maki M, Yu SJ, Ali M, Allickson JG, Sanberg CD, Kuzmin-Nichols N, Sanberg PR. Menstrual blood cells display stem cell-like phenotypic markers and exert neuroprotection following transplantation in experimental stroke. *Stem Cells Dev* 2010; **19**: 439-452 [PMID: 19860544 DOI: 10.1089/scd.2009.0340]
- Han X, Meng X, Yin Z, Rogers A, Zhong J, Rillema P, Jackson JA, Ichim TE, Minev B, Carrier E, Patel AN, Murphy MP, Min WP, Riordan NH. Inhibition of intracranial glioma growth by endometrial regenerative cells. *Cell Cycle* 2009; **8**: 606-610 [PMID: 19197154 DOI: 10.4161/cc.8.4.7731]
- Fathi-Kazerooni M, Tavosidana G, Taghizadeh-Jahed M, Khanjani S, Golshahi H, Gargett CE, Edalatkhah H, Kazemnejad S. Comparative restoration of acute liver failure by menstrual blood stem cells compared with bone marrow stem cells in mice model. *Cytotherapy* 2017; **19**: 1474-1490 [PMID: 28170193 DOI: 10.1016/j.jcyt.2017.01.003]

- 29107739 DOI: [10.1016/j.jcyt.2017.08.022](https://doi.org/10.1016/j.jcyt.2017.08.022)]
- 16 **Rosen AB**, Kelly DJ, Schuldt AJ, Lu J, Potapova IA, Doronin SV, Robichaud KJ, Robinson RB, Rosen MR, Brink PR, Gaudette GR, Cohen IS. Finding fluorescent needles in the cardiac haystack: tracking human mesenchymal stem cells labeled with quantum dots for quantitative in vivo three-dimensional fluorescence analysis. *Stem Cells* 2007; **25**: 2128-2138 [PMID: [17495112](https://pubmed.ncbi.nlm.nih.gov/17495112/) DOI: [10.1634/stemcells.2006-0722](https://doi.org/10.1634/stemcells.2006-0722)]
  - 17 **Shao-Fang Z**, Hong-Tian Z, Zhi-Nian Z, Yuan-Li H. PKH26 as a fluorescent label for live human umbilical mesenchymal stem cells. *In Vitro Cell Dev Biol Anim* 2011; **47**: 516-520 [PMID: [21805232](https://pubmed.ncbi.nlm.nih.gov/21805232/) DOI: [10.1007/s11626-011-9424-5](https://doi.org/10.1007/s11626-011-9424-5)]
  - 18 **Mou XZ**, Lin J, Chen JY, Li YF, Wu XX, Xiang BY, Li CY, Ma JM, Xiang C. Menstrual blood-derived mesenchymal stem cells differentiate into functional hepatocyte-like cells. *J Zhejiang Univ Sci B* 2013; **14**: 961-972 [PMID: [24190442](https://pubmed.ncbi.nlm.nih.gov/24190442/) DOI: [10.1631/jzus.B1300081](https://doi.org/10.1631/jzus.B1300081)]
  - 19 **Li LJ**, Du WB, Zhang YM, Li J, Pan XP, Chen JJ, Cao HC, Chen Y, Chen YM. Evaluation of a bioartificial liver based on a nonwoven fabric bioreactor with porcine hepatocytes in pigs. *J Hepatol* 2006; **44**: 317-324 [PMID: [16356580](https://pubmed.ncbi.nlm.nih.gov/16356580/) DOI: [10.1016/j.jhep.2005.08.006](https://doi.org/10.1016/j.jhep.2005.08.006)]
  - 20 **Zhou N**, Li J, Zhang Y, Lu J, Chen E, Du W, Wang J, Pan X, Zhu D, Yang Y, Chen Y, Cao H, Li L. Efficacy of coupled low-volume plasma exchange with plasma filtration adsorption in treating pigs with acute liver failure: A randomised study. *J Hepatol* 2015; **63**: 378-387 [PMID: [25814048](https://pubmed.ncbi.nlm.nih.gov/25814048/) DOI: [10.1016/j.jhep.2015.03.018](https://doi.org/10.1016/j.jhep.2015.03.018)]
  - 21 **Ulrich D**, Muralitharan R, Gargett CE. Toward the use of endometrial and menstrual blood mesenchymal stem cells for cell-based therapies. *Expert Opin Biol Ther* 2013; **13**: 1387-1400 [PMID: [23930703](https://pubmed.ncbi.nlm.nih.gov/23930703/) DOI: [10.1517/14712598.2013.826187](https://doi.org/10.1517/14712598.2013.826187)]
  - 22 **Rodrigues MC**, Lippert T, Nguyen H, Kaelber S, Sanberg PR, Borlongan CV. Menstrual Blood-Derived Stem Cells: In Vitro and In Vivo Characterization of Functional Effects. *Adv Exp Med Biol* 2016; **951**: 111-121 [PMID: [27837558](https://pubmed.ncbi.nlm.nih.gov/27837558/) DOI: [10.1007/978-3-319-45457-3\\_9](https://doi.org/10.1007/978-3-319-45457-3_9)]
  - 23 **Lv G**, Zhao L, Zhang A, Du W, Chen Y, Yu C, Pan X, Zhang Y, Song T, Xu J, Chen Y, Li L. Bioartificial liver system based on choanoid fluidized bed bioreactor improve the survival time of fulminant hepatic failure pigs. *Biotechnol Bioeng* 2011; **108**: 2229-2236 [PMID: [21455934](https://pubmed.ncbi.nlm.nih.gov/21455934/) DOI: [10.1002/bit.23150](https://doi.org/10.1002/bit.23150)]
  - 24 **Cao H**, Yang J, Yu J, Pan Q, Li J, Zhou P, Li Y, Pan X, Li J, Wang Y, Li L. Therapeutic potential of transplanted placental mesenchymal stem cells in treating Chinese miniature pigs with acute liver failure. *BMC Med* 2012; **10**: 56 [PMID: [22673529](https://pubmed.ncbi.nlm.nih.gov/22673529/) DOI: [10.1186/1741-7015-10-56](https://doi.org/10.1186/1741-7015-10-56)]
  - 25 **Li J**, Zhang L, Xin J, Jiang L, Li J, Zhang T, Jin L, Li J, Zhou P, Hao S, Cao H, Li L. Immediate intraportal transplantation of human bone marrow mesenchymal stem cells prevents death from fulminant hepatic failure in pigs. *Hepatology* 2012; **56**: 1044-1052 [PMID: [22422600](https://pubmed.ncbi.nlm.nih.gov/22422600/) DOI: [10.1002/hep.25722](https://doi.org/10.1002/hep.25722)]
  - 26 **Luz-Crawford P**, Torres MJ, Noël D, Fernandez A, Toupet K, Alcayaga-Miranda F, Tejedor G, Jorgensen C, Illanes SE, Figueroa FE, Djouad F, Khoury M. The immunosuppressive signature of menstrual blood mesenchymal stem cells entails opposite effects on experimental arthritis and graft versus host diseases. *Stem Cells* 2016; **34**: 456-469 [PMID: [26528946](https://pubmed.ncbi.nlm.nih.gov/26528946/) DOI: [10.1002/stem.2244](https://doi.org/10.1002/stem.2244)]
  - 27 **Ma HC**, Shi XL, Ren HZ, Yuan XW, Ding YT. Targeted migration of mesenchymal stem cells modified with CXCR4 to acute failing liver improves liver regeneration. *World J Gastroenterol* 2014; **20**: 14884-14894 [PMID: [25356048](https://pubmed.ncbi.nlm.nih.gov/25356048/) DOI: [10.3748/wjg.v20.i40.14884](https://doi.org/10.3748/wjg.v20.i40.14884)]
  - 28 **Ezzat T**, Dhar DK, Malago M, Olde Damink SW. Dynamic tracking of stem cells in an acute liver failure model. *World J Gastroenterol* 2012; **18**: 507-516 [PMID: [22363116](https://pubmed.ncbi.nlm.nih.gov/22363116/) DOI: [10.3748/wjg.v18.i6.507](https://doi.org/10.3748/wjg.v18.i6.507)]
  - 29 **Jiang H**, Cheng Z, Tian M, Zhang H. In vivo imaging of embryonic stem cell therapy. *Eur J Nucl Med Mol Imaging* 2011; **38**: 774-784 [PMID: [21107558](https://pubmed.ncbi.nlm.nih.gov/21107558/) DOI: [10.1007/s00259-010-1667-y](https://doi.org/10.1007/s00259-010-1667-y)]
  - 30 **Chen J**, Wang C, Lü S, Wu J, Guo X, Duan C, Dong L, Song Y, Zhang J, Jing D, Wu L, Ding J, Li D. In vivo chondrogenesis of adult bone-marrow-derived autologous mesenchymal stem cells. *Cell Tissue Res* 2005; **319**: 429-438 [PMID: [15672263](https://pubmed.ncbi.nlm.nih.gov/15672263/) DOI: [10.1007/s00441-004-1025-0](https://doi.org/10.1007/s00441-004-1025-0)]
  - 31 **Ikeda E**, Yagi K, Kojima M, Yagyu T, Ohshima A, Sobajima S, Tadokoro M, Katsube Y, Isoda K, Kondoh M, Kawase M, Go MJ, Adachi H, Yokota Y, Kirita T, Ohgushi H. Multipotent cells from the human third molar: feasibility of cell-based therapy for liver disease. *Differentiation* 2008; **76**: 495-505 [PMID: [18093227](https://pubmed.ncbi.nlm.nih.gov/18093227/) DOI: [10.1111/j.1432-0436.2007.00245.x](https://doi.org/10.1111/j.1432-0436.2007.00245.x)]
  - 32 **Zhan Y**, Wang Y, Wei L, Chen H, Cong X, Fei R, Gao Y, Liu F. Differentiation of hematopoietic stem cells into hepatocytes in liver fibrosis in rats. *Transplant Proc* 2006; **38**: 3082-3085 [PMID: [17112904](https://pubmed.ncbi.nlm.nih.gov/17112904/) DOI: [10.1016/j.transproceed.2006.08.132](https://doi.org/10.1016/j.transproceed.2006.08.132)]
  - 33 **Yagi H**, Soto-Gutierrez A, Parekkadan B, Kitagawa Y, Tompkins RG, Kobayashi N, Yarmush ML. Mesenchymal stem cells: Mechanisms of immunomodulation and homing. *Cell Transplant* 2010; **19**: 667-679 [PMID: [20525442](https://pubmed.ncbi.nlm.nih.gov/20525442/) DOI: [10.3727/096368910X508762](https://doi.org/10.3727/096368910X508762)]
  - 34 **Cho JW**, Lee CY, Ko Y. Therapeutic potential of mesenchymal stem cells overexpressing human forkhead box A2 gene in the regeneration of damaged liver tissues. *J Gastroenterol Hepatol* 2012; **27**: 1362-1370 [PMID: [22432472](https://pubmed.ncbi.nlm.nih.gov/22432472/) DOI: [10.1111/j.1440-1746.2012.07137.x](https://doi.org/10.1111/j.1440-1746.2012.07137.x)]
  - 35 **Chen L**, Xiang B, Wang X, Xiang C. Exosomes derived from human menstrual blood-derived stem cells alleviate fulminant hepatic failure. *Stem Cell Res Ther* 2017; **8**: 9 [PMID: [28115012](https://pubmed.ncbi.nlm.nih.gov/28115012/) DOI: [10.1186/s13287-016-0453-6](https://doi.org/10.1186/s13287-016-0453-6)]
  - 36 **Xiang B**, Chen L, Wang X, Zhao Y, Wang Y, Xiang C. Transplantation of Menstrual Blood-Derived Mesenchymal Stem Cells Promotes the Repair of LPS-Induced Acute Lung Injury. *Int J Mol Sci* 2017; **18** [PMID: [28346367](https://pubmed.ncbi.nlm.nih.gov/28346367/) DOI: [10.3390/ijms18040689](https://doi.org/10.3390/ijms18040689)]
  - 37 **Lv Y**, Xu X, Zhang B, Zhou G, Li H, Du C, Han H, Wang H. Endometrial regenerative cells as a novel cell therapy attenuate experimental colitis in mice. *J Transl Med* 2014; **12**: 344 [PMID: [25475342](https://pubmed.ncbi.nlm.nih.gov/25475342/) DOI: [10.1186/s12967-014-0344-5](https://doi.org/10.1186/s12967-014-0344-5)]
  - 38 **Drago H**, Marín GH, Sturla F, Roque G, Mártire K, Díaz Aquino V, Lamonega R, Gardiner C, Ichim T, Riordan N, Raimondi JC, Bossi S, Samadikuchaksaraei A, van Leeuwen M, Tau JM, Núñez L, Larsen G, Spretz R, Mansilla E. The next generation of burns treatment: intelligent films and matrix, controlled enzymatic debridement, and adult stem cells. *Transplant Proc* 2010; **42**: 345-349 [PMID: [20172347](https://pubmed.ncbi.nlm.nih.gov/20172347/) DOI: [10.1016/j.transproceed.2009.11.031](https://doi.org/10.1016/j.transproceed.2009.11.031)]
  - 39 **Shi D**, Zhang J, Zhou Q, Xin J, Jiang J, Jiang L, Wu T, Li J, Ding W, Li J, Sun S, Li J, Zhou N, Zhang L, Jin L, Hao S, Chen P, Cao H, Li M, Li L, Chen X, Li J. Quantitative evaluation of human bone mesenchymal stem cells rescuing fulminant hepatic failure in pigs. *Gut* 2017; **66**: 955-964 [PMID: [26884426](https://pubmed.ncbi.nlm.nih.gov/26884426/) DOI: [10.1136/gutjnl-2015-311146](https://doi.org/10.1136/gutjnl-2015-311146)]
  - 40 **Wu X**, Luo Y, Chen J, Pan R, Xiang B, Du X, Xiang L, Shao J, Xiang C. Transplantation of human menstrual blood progenitor cells improves hyperglycemia by promoting endogenous progenitor



- differentiation in type 1 diabetic mice. *Stem Cells Dev* 2014; **23**: 1245-1257 [PMID: [24499421](#) DOI: [10.1089/scd.2013.0390](#)]
- 41 **Chen L**, Qu J, Xiang C. The multi-functional roles of menstrual blood-derived stem cells in regenerative medicine. *Stem Cell Res Ther* 2019; **10**: 1 [PMID: [30606242](#) DOI: [10.1186/s13287-018-1105-9](#)]



## Basic Study

# Yinchenhao decoction attenuates obstructive jaundice-induced liver injury and hepatocyte apoptosis by suppressing protein kinase RNA-like endoplasmic reticulum kinase-induced pathway

Yan-Li Wu, Zhong-Lian Li, Xi-Bo Zhang, Hao Liu

**ORCID number:** Yan-Li Wu (0000-0001-6560-0443); Zhong-Lian Li (0000-0001-5211-7612); Xi-Bo Zhang (0000-0003-4153-6445); Hao Liu (0000-0002-6062-1656).

**Author contributions:** Wu YL and Li ZL designed the research; Wu YL and Liu H performed the research; Wu YL and Zhang XB analyzed the data; Wu YL and Li ZL composed the paper.

**Supported by** the National Natural Science Foundation of China, No. 81273952.

**Institutional animal care and use committee statement:** The experimental protocol was approved by the Animal Research Committee of Tianjin Nankai Hospital.

**Conflict-of-interest statement:** The authors declare that they have no conflicts of interest.

**Data sharing statement:** No additional data are available.

**ARRIVE guidelines statement:** The authors have read the ARRIVE guidelines and prepared the manuscript accordingly.

**Open-Access:** This article is an open-access article which was selected by an in-house editor and fully peer-reviewed by external reviewers. It is distributed in accordance with the Creative Commons Attribution Non Commercial (CC BY-NC 4.0) license, which permits others to

**Yan-Li Wu**, Graduate School of Tianjin Medical University, Tianjin 300070, China

**Zhong-Lian Li, Xi-Bo Zhang**, Department of Hepatobiliary and Pancreatic Surgery, Tianjin Nankai Hospital, Tianjin 300100, China

**Hao Liu**, Graduate School of Tianjin Medical University, Tianjin 300070, China.

**Corresponding author:** Zhong-Lian Li, MD, PhD, Chief Doctor, Doctor, Professor, Surgeon, Department of Hepatobiliary and Pancreatic Surgery, Tianjin Nankai Hospital, No. 6, Changjiang Street, Nankai District, Tianjin 300100, China. [nkylzl@163.com](mailto:nkylzl@163.com)

**Telephone:** +86-22-27435237

**Fax:** +86-22-27435237

## Abstract

### BACKGROUND

Chronic biliary obstruction results in ischemia and hypoxia of hepatocytes, and leads to apoptosis. Apoptosis is very important in regulating the homeostasis of the hepatobiliary system. Endoplasmic reticulum (ER) stress is one of the signaling pathways that induce apoptosis. Moreover, the protein kinase RNA-like endoplasmic reticulum kinase (PERK)-induced apoptotic pathway is the main way; but its role in liver injury remains unclear. Yinchenhao decoction (YCHD) is a traditional Chinese medicine formula that alleviates liver injury and apoptosis, yet its mechanism is unknown. We undertook this study to investigate the effects of YCHD on the expression of ER stress proteins and hepatocyte apoptosis in rats with obstructive jaundice (OJ).

### AIM

To investigate whether YCHD can attenuate OJ-induced liver injury and hepatocyte apoptosis by inhibiting the PERK-CCAAT/enhancer-binding protein homologous protein (CHOP)-growth arrest and DNA damage-inducible protein 34 (GADD34) pathway and B cell lymphoma/leukemia-2 related X protein (Bax)/B cell lymphoma/leukemia-2 (Bcl-2) ratio.

### METHODS

For *in vivo* experiments, 30 rats were divided into three groups: control group, OJ model group, and YCHD-treated group. Blood was collected to detect the indicators of liver function, and liver tissues were used for histological analysis. For *in vitro* experiments, 30 rats were divided into three groups: G1, G2, and G3.

distribute, remix, adapt, build upon this work non-commercially, and license their derivative works on different terms, provided the original work is properly cited and the use is non-commercial. See: <http://creativecommons.org/licenses/by-nc/4.0/>

**Manuscript source:** Unsolicited manuscript

**Received:** August 8, 2019

**Peer-review started:** August 8, 2019

**First decision:** September 18, 2019

**Revised:** September 26, 2019

**Accepted:** October 17, 2019

**Article in press:** October 17, 2019

**Published online:** November 7, 2019

**P-Reviewer:** Exbrayat JM, Mizuguchi T, Slomiany BL

**S-Editor:** Tang JZ

**L-Editor:** Wang TQ

**E-Editor:** Ma YJ



The rats in group G1 had their bile duct exposed without ligation, the rats in group G2 underwent total bile duct ligation, and the rats in group G3 were given a gavage of YCHD. According to the serum pharmacology, serum was extracted and centrifuged from the rat blood to cultivate the BRL-3A cells. Terminal deoxynucleotidyl transferase mediated dUTP nick end-labelling (TUNEL) assay was used to detect BRL-3A hepatocyte apoptosis. Alanine aminotransferase (ALT) and aspartate transaminase (AST) levels in the medium were detected. Western blot and quantitative real-time polymerase chain reaction (qRT-PCR) analyses were used to detect protein and gene expression levels of PERK, CHOP, GADD34, Bax, and Bcl-2 in the liver tissues and BRL-3A cells.

## RESULTS

Biochemical assays and haematoxylin and eosin staining suggested severe liver function injury and liver tissue structure damage in the OJ model group. The TUNEL assay showed that massive BRL-3A rat hepatocyte apoptosis was induced by OJ. Elevated ALT and AST levels in the medium also demonstrated that hepatocytes could be destroyed by OJ. Western blot or qRT-PCR analyses showed that the protein and mRNA expression levels of PERK, CHOP, and GADD34 were significantly increased both in the rat liver tissue and BRL-3A rat hepatocytes by OJ. The Bax and Bcl-2 levels were increased, and the Bax/Bcl-2 ratio was also increased. When YCHD was used, the PERK, CHOP, GADD34, and Bax levels quickly decreased, while the Bcl-2 levels increased, and the Bax/Bcl-2 ratio decreased.

## CONCLUSION

OJ-induced liver injury and hepatocyte apoptosis are associated with the activation of the PERK-CHOP-GADD34 pathway and increased Bax/Bcl-2 ratio. YCHD can attenuate these changes.

**Key words:** Yinchenhao decoction; Obstructive jaundice; Liver injury; Apoptosis; Protein kinase RNA-like endoplasmic reticulum kinase; CCAAT/enhancer-binding protein homologous protein; Growth arrest and DNA damage-inducible protein 34; B cell lymphoma/leukemia-2 gene; B cell lymphoma/leukemia-2 gene related X protein

©The Author(s) 2019. Published by Baishideng Publishing Group Inc. All rights reserved.

**Core tip:** Chronic biliary obstruction results in ischaemia and hypoxia of hepatocytes and leads to apoptosis. The protein kinase RNA-like endoplasmic reticulum kinase (PERK)-induced apoptotic pathway is the main and important way, however, its role in liver injury and hepatocyte apoptosis remains unclear. Yinchenhao decoction (YCHD) can alleviate liver injury and apoptosis, but whether YCHD can attenuates obstructive jaundice (OJ)-induced liver injury and hepatocyte apoptosis by inhibiting the PERK-induced pathway is still unknown. In this research study, we found that OJ induced liver injury and hepatocyte apoptosis by activating the PERK- CCAAT/enhancer-binding protein homologous protein (CHOP)-growth arrest and DNA damage-inducible protein 34 (GADD34) pathway and upregulating the B cell lymphoma/leukemia-2 related X protein (Bax)/ B cell lymphoma/leukemia-2 (Bcl-2) ratio. YCHD attenuated these changes by inhibiting the PERK-CHOP-GADD34 pathway and Bax/Bcl-2 ratio.

**Citation:** Wu YL, Li ZL, Zhang XB, Liu H. Yinchenhao decoction attenuates obstructive jaundice-induced liver injury and hepatocyte apoptosis by suppressing protein kinase RNA-like endoplasmic reticulum kinase-induced pathway. *World J Gastroenterol* 2019; 25(41): 6205-6221

**URL:** <https://www.wjgnet.com/1007-9327/full/v25/i41/6205.htm>

**DOI:** <https://dx.doi.org/10.3748/wjg.v25.i41.6205>

## INTRODUCTION

Obstructive jaundice (OJ) is defined by evaluated serum bilirubin levels and characterized by increased conjugated bilirubin levels without influencing

unconjugated bilirubin levels<sup>[1]</sup>. Biliary obstruction can cause damage to all organs of the body, especially the liver. OJ affects tissues by releasing various inflammatory mediators that stimulate the inflammatory response and cytokine cascades. This can lead to reduced clearance of endotoxin, decreased immune function, vascular dysfunction, coagulation disorders, and even disseminated intravascular coagulation, impaired gastrointestinal mucosal barrier, damaged hepatic sinusoidal endothelium, and injured liver function<sup>[2,3]</sup>, which eventually can cause hepatocyte ischaemia, hypoxia, and acidosis.

Apoptosis is a programmed mechanism of cell death caused by various physiological and pathological conditions characterized by DNA damage<sup>[4]</sup>. In 2014, Kosar *et al.*<sup>[5]</sup> confirmed that serious cellular damage occurs in hepatocytes during OJ. If DNA damage in a cell cannot be resolved, apoptotic signaling mechanisms can be activated, forcing the cell to self-destruct<sup>[6]</sup>. There are three main apoptotic signaling pathways: The death receptor pathway, the mitochondrial pathway, and the endoplasmic reticulum (ER) stress pathway. The ER stress pathway, which is a newly characterized apoptotic signaling pathway, is considered a supplement of the mitochondrial pathway and is a research hotspot<sup>[7,8]</sup>. However, there are few studies on liver injury and hepatocyte apoptosis induced by OJ through activating the ER stress pathway.

The ER has three transmembrane receptors, inositol-requiring protein 1 (IRE1), protein kinase RNA-like endoplasmic reticulum kinase (PERK), and activating transcription factor 6 (ATF6), which collectively monitor the functions of the ER<sup>[9]</sup>. These three receptors represent three classical unfolded protein response (UPR) signaling pathways: The IRE1-XBP1 pathway, the PERK-eIF2 pathway, and the ATF6 pathway<sup>[10,11]</sup>. Cellular ischaemia and hypoxia can induce ER stress and activate the UPR to restore normal physiological function to the ER<sup>[12]</sup>. It is known that the UPR is a pro-survival response by reducing gene transcription, attenuating protein translation, enhancing protein folding, and promoting ER-associated degradation of misfolded proteins to resist ER stress and restore ER homeostasis<sup>[13]</sup>. However, if the ER stress is too prolonged or too severe, the UPR fails to control ER stress, resulting in a change from pro-survival to pro-apoptotic signaling and, eventually, cell apoptosis<sup>[14]</sup>.

However, these three signaling pathways do not directly induce apoptosis but activate apoptotic signaling molecules, including CCAAT/enhancer-binding protein homologous protein (CHOP), c-Jun NH<sub>2</sub> terminal kinase (JNK), and caspases. There are three apoptotic pathways induced by the UPR: The IRE1-ASK-JNK pathway, the PERK-eIF2-CHOP signaling pathway, and the caspase-12 pathway<sup>[15]</sup>. The expression of CHOP has significant importance in inducing pro-survival to pro-apoptosis<sup>[11]</sup>. CHOP interacts with other transcription regulators, including growth arrest and DNA damage-inducible protein 34 (GADD34), the B cell lymphoma/leukemia-2 (Bcl-2) family, endoplasmic reticulum oxidoreductase 1, and Tribbles-related protein 3 pseudokinase, to induce apoptosis changes<sup>[16]</sup>. The Bcl-2 family is not only an important regulator of cell apoptosis, but it is also the most important regulator of the mitochondrial apoptosis pathway.

Yinchenhao decoction (YCHD) is used as a complementary and alternative treatment to ameliorate clinical symptoms, improve liver function, reduce liver inflammation and fibrosis, and improve patient quality of life with a high degree of safety, few side effects, and low toxicity<sup>[17]</sup>. Liu *et al.*<sup>[18]</sup> compared five types of traditional Chinese medicine (TCM) and showed that YCHD exerted the most significant therapeutic effect in improving liver function in patients with liver cirrhosis. YCHD has been used for more than a thousand years to treat patients with viral hepatitis, cholestasis, primary biliary cirrhosis, and liver fibrosis<sup>[19]</sup>. Additionally, YCHD has been shown to inhibit hepatocyte apoptosis and promote the secretion and excretion of bile, which alleviates icterus<sup>[20]</sup>. YCHD consists of three herbal components: *Artemisia capillaris* Thunb (Herba Artemisiae Capillaris, Yin-Chen-Hao), *Gardenia jasminoides* Ellis (Fructus Gardeniae, Zhi-zi), and *Rheum officinale* Baill (Radix Rhei Officinalis, Da-huang) with a ratio of 3:2:1 in weight. Its major bioactive ingredients are geniposide, capillin, capilene, capillarisin, and rhein<sup>[17,21]</sup>. The YCHD components exert their effects on liver disease in a synergistic manner. For instance, capillarisin also acts as a choleric<sup>[17]</sup>. Rhein has been shown to inhibit hepatic stellate cell activation and reverse liver fibrosis<sup>[22]</sup>. Many experiments have confirmed that the main YCHD components alleviate liver damage and inhibit apoptosis, but the main mechanism of YCHD has not been clarified.

The pharmacological evaluation of serum, which was first proposed by Iwama Hiroko in 1987<sup>[23]</sup>, has become an important method to study the mechanisms of TCM. The core concept of serum pharmacology is to collect animal blood and to obtain serum after administering a TCM by gavage at defined times, followed by the addition of the serum to an *in vitro* tissue or cell system to study the



pharmacodynamics and mechanism of TCM. This method prevents interference of the *in vitro* experiment from the physical and chemical properties of crude TCM and allows the study of the metabolized pharmacologically active products, following the process of digestion and absorption of the TCM and its biological transformation in the gastrointestinal tract. Collectively, these features allow us to evaluate the true pharmacological effects of TCMs<sup>[24]</sup>. Compared with the evaluation of TCMs directly added in *in vitro* studies, the results of *in vitro* studies evaluating the pharmacological effects in serum, derived from an animal model, may be more reliable and representative of the true *in vivo* effects of the TCM compound being investigated.

Therefore, the aim of this study was to determine the role of the PERK-induced ER stress pathways in liver injury and hepatocyte apoptosis, and the mechanism by which YCHD alleviates apoptosis and improves liver injury.

## MATERIALS AND METHODS

### YCHD

According to the current version of the “Synopsis of Prescriptions of the Golden Chamber”<sup>[25]</sup>, the YCHD formula consists of 120 g of *Artemisia capillaris* Thunb (Herba Artemisiae Capillaris, Yin-Chen-Hao), 80 g of *Gardenia jasminoides* Ellis (Fructus Gardeniae, Zhi-zi), and 40 g of *Rheum officinale* Baill (Radix Rhei Officinalis, Dahuang), all of which were purchased from Tianjin Nankai Hospital. These herbals were mixed in water, decocted for 45 min and 30 min, successively, and then concentrated to 240 mL. As such, every 1 mL of liquid contains 1 g YCHD. The concentrated form of YCHD was stored at 4 °C.

### Rat model of OJ

Sixty male Wistar rats weighing 250-270 g were obtained from the Institute of the Environmental Medicine of the Chinese People’s Liberation Army Academy of Military Medical Sciences. The rats were housed under standard laboratory conditions, and provided with *ad libitum* food and water, with a 12-hour light/dark cycle, a mean humidity of  $50 \pm 5\%$ , a mean temperature of  $25 \pm 2$  °C, and external noise controlled to within 60 dB. The rats had one week of environmental adaptation.

Surgical common bile duct ligation is one of the most commonly used methods for the creation of an OJ animal model. In 2016, Aoki *et al*<sup>[26]</sup> showed that although total ligation of the bile duct resulted in a high mortality, this model also resulted in the conspicuous symptoms of jaundice and was suitable for short-term research studies. Tarcin *et al*<sup>[27]</sup> further showed that serum levels of alanine aminotransferase (ALT), aspartate transaminase (AST), alkaline phosphatase (ALP), gamma-glutamyl transpeptidase (GGT), and total bilirubin (TBIL), and direct bilirubin (DBIL) rose and peaked at day 7 after bile duct ligation before they began to decline. Therefore, in the current experiment, total bile duct ligation was selected as the surgical method, and all rats were sacrificed on day 7.

### Animals and treatment

Thirty rats were randomly selected and divided into three groups: A, control group ( $n = 10$ ); B, OJ model group ( $n = 10$ ); and C, YCHD-treated group ( $n = 10$ ). The rats in group A had their bile duct exposed without ligation. The rats in groups B and C underwent total bile duct ligation. One hour after operation, the rats in group C were given a gavage of 1 mL of YCHD per 100 g body weight for 7 d. Blood samples of all rats were collected on day 7 from the abdominal aorta and were tested for biochemical parameters. Liver tissues were quickly dissected and rinsed in ice-cold saline, frozen in liquid nitrogen, and stored at -80 °C for histopathology, Western blot, and quantitative real-time polymerase chain reaction (qRT-PCR) analyses. Samples from the group C rats were collected one hour after gavage.

The remaining 30 rats were randomly divided into three groups on average: G1, G2, and G3. On the day of surgery, the rats in group G1 had their bile duct exposed without ligation, and the rats in group G2 underwent total bile duct ligation, and the rats in group G3 were just given a gavage of 1 mL of YCHD per 100 g body weight every day for 7 d. Blood samples of all rats were collected on day 7 from the abdominal aorta and centrifuged. Plasma was retained and stored at 80 °C for cell study use.

### Liver function test

The rat blood was collected and centrifuged at 300 g for 10 min at 20 °C, and the supernatants were collected. ALT, AST, TBIL, DBIL, GGT, and ALP levels were then measured using an automatic clinical analyser (ACA).

**Histopathology analysis**

Liver tissues were fixed in 5% formaldehyde solution, embedded in paraffin, and sliced into 5-micron sections. Haematoxylin and eosin staining was performed to observe the histopathologic changes. Histological features were observed and captured with a light microscope.

**Culture of BRL-3A rat hepatocytes**

BRL-3A rat hepatocytes were purchased from the Cell Bank of the Chinese Academy of Sciences and cultured in Dulbecco's modified Eagle's medium (DMEM) (Gibco, United States) supplemented with 10% foetal bovine serum (Gibco, United States) and 1% penicillin-streptomycin solution (HyClone, United States) at 37 °C in a humidified atmosphere containing 5% CO<sub>2</sub>. The culture medium was replaced every 2 d. BRL-3A cells were divided into three groups: S, O, and M. In group S, BRL-3A cells were cultured in DMEM medium containing 10% serum from the G1 group with 1% penicillin-streptomycin solution. In group O, BRL-3A cells were cultured in DMEM medium containing 10% serum from the G2 group with 1% penicillin-streptomycin solution. In group M, BRL-3A cells were cultured in DMEM medium containing 10% serum from the G2 group and 10% serum from the G3 group with 1% penicillin-streptomycin solution. Cells were cultured for 6 h, 24 h, and 48 h. At each time point, cell culture medium was collected to detect the ALT and AST levels, and cultured BRL-3A cells were frozen in liquid nitrogen and stored at 80 °C for TUNEL assay, Western blot, and qRT-PCR analyses.

**ALT and AST levels in cell culture medium**

ALT and AST levels in the cell culture medium were measured using an ACA.

**Terminal deoxynucleotidyl transferase mediated dUTP nick end-labelling (TUNEL) assay**

BRL-3A cell apoptosis was detected by using an In-Situ Cell Death Detection Kit, Fluorescein (Roche-11684795910) (Sigma-Aldrich, United States) to perform TUNEL assay, according to the manufacturer's protocol. Biotinylated nucleotides detected DNA fragments through terminal deoxynucleotidyl transferase. Biotinylated nucleotides were detected by TACS Blue Label (Trevigen, United States). Following TUNEL staining, the BRL-3A cells were counterstained with 4'-6-diamidino-2-phenylindole to detect the nuclei, as shown by blue staining. TUNEL-positive cells were defined as cells with green staining (wavelength, 488 nm).

**Quantitative real-time PCR (qRT-PCR)**

qRT-PCR was performed to detect the mRNA expression levels of PERK, CHOP, GADD34, B cell lymphoma/leukemia-2 related X protein (Bax), and Bcl-2 both in rat liver tissues and BRL-3A rat hepatocytes. Total RNA was extracted from cells using TRIzol reagent (Invitrogen, United States) to detect the mRNA expression levels. cDNA was synthesized from RNA through reverse transcription (RT) by using the SuperScript III RT kit following the manufacturer's instructions. The RT conditions for each cDNA amplification were 42 °C for 60 min and 85 °C for 10 min, and then the cDNA was stored in a -20 °C freezer. qRT-PCR was performed in triplicate with SYBR qPCR mix (Invitrogen, United States) in a total volume of 20 µL on the 7900 HT Fast Real-Time PCR System (Applied Biosystems, United States) using the following cycling parameters: 95 °C for 2 min and 40 cycles of 94 °C for 20 s, 60 °C for 20 s, and 72 °C for 30 s. The primer sequences used are shown in Tables 1 and 2.  $\beta$ -actin and glyceraldehyde-3-phosphate dehydrogenase (GAPDH) were used as the reference genes. Experiments were repeated at least three times for each group.

**Western blot analysis**

Western blot analysis was performed to detect the protein expression levels of PERK, CHOP, GADD34, Bax, and Bcl-2 both in rat liver tissues and BRL-3A rat hepatocytes. Total protein was obtained from cells using protein extraction solution and quantified using a BCA Protein Assay kit (ThermoFisher Scientific, United States). Proteins were separated by 10% sodium dodecyl sulfate-polyacrylamide gel electrophoresis. Following electrophoresis, proteins were transferred onto polyvinylidene difluoride membranes (Millipore, United States). After blocking with 5% blocking buffer, the membranes were incubated overnight at 4 °C with primary antibodies against  $\beta$ -actin (1:1000), GAPDH (1:1000), PERK (1:1000), CHOP (1:1000), GADD34 (1:1000), Bax (1:1000), and Bcl-2 (1:1000). After washing, the membranes were incubated with horseradish peroxidase-conjugated secondary antibody for 1 h. The immune complexes were detected by the enhanced chemiluminescence method, and Western blots were measured with the ChemiDoc MP Imaging System (Bio-Rad, United States). Each experiment was repeated at least three times for each group.

**Table 1** Primer sequences used for quantitative real-time polymerase chain reaction for rat liver tissue

Gene	Forward primer (5'-3')	Reverse primer (5'-3')
<i>β-actin</i>	GTTACCAGGGCTGCCITTC	GGGTTTCCCCTTGATGACC
<i>PERK</i>	GTTTCATGGAGAATGGCGCTT	GACACTTGCACACCAGGTT
<i>CHOP</i>	ACACCACCACACCTGAAAGC	TGGACACTGTCTCAAAGGCG
<i>GADD34</i>	GTTTGACGAGATCGAAGCC	CCCTGAAAGCAGGGGTAAGG
<i>Bax</i>	CCGAAATGTTTGTGACG	AGCCGATCTCGAAGGAAGT
<i>Bcl-2</i>	ACCTGAATGACCACCTAGAGC	TCCGACTGAAGAGCGAAC

PERK: Endoplasmic reticulum-resident protein kinase; CHOP: CCAAT/enhancer-binding protein homologous protein; GADD34: Growth arrest- and DNA damage-inducible gene 34; Bcl-2: B cell lymphoma/leukemia-2 gene; Bax: Bcl-2 related X protein.

### Statistical analysis

Data are presented as the mean ± standard deviation. Statistical differences among multiple groups were compared by one-way analysis of variance (ANOVA) using SPSS version 21.0.  $P < 0.05$  was considered statistically significant.

## RESULTS

### YCHD attenuates liver tissue injury induced by OJ

Liver histopathologic changes were detected to investigate the effects of YCHD on liver tissue injury. As shown in [Figure 1](#), there were no abnormal liver tissue structure in the control group. The liver tissue in the OJ model group showed an unclear texture, the hepatic sinusoids were narrowed and congestive, and the hepatic lobule structures were disordered. Moreover, cholestasis, liver cell swelling, fatty degeneration and necrosis, cytoplasmic shrinkage, and hyperchromatic, inflammatory cell infiltration were observed. However, the histopathologic changes in the liver tissues were substantially ameliorated in the YCHD-treated group.

### YCHD attenuates liver function injury induced by OJ

We detected liver function by measuring serum TBIL, DBIL, ALT, AST, GGT, and ALP levels. As shown in [Figure 2](#), compared with the control group, these levels were remarkably increased in the OJ model group, but they decreased quickly after treatment with YCHD.

### Effect of YCHD on the protein and mRNA expression levels of PERK, CHOP, GADD34, Bax, and Bcl-2 in rat liver tissue

To investigate the mechanisms of YCHD in improving liver injury induced by OJ, both the protein and mRNA levels of PERK, CHOP, GADD34, Bax, and Bcl-2 in liver tissues were detected. As shown in [Figure 3](#), compared with the control group, the protein and mRNA expression levels of PERK, CHOP, and GADD34 were upregulated. Additionally, the Bax and Bcl-2 levels were increased, and the Bax/Bcl-2 ratio was also increased. However, after treatment with YCHD, the PERK, CHOP, GADD34, and Bax levels were downregulated and the Bcl-2 levels were upregulated; however, the Bax/Bcl-2 ratio decreased.

### Effect of YCHD on ALT and AST levels in cell culture medium

ALT and AST changes reflect hepatocyte injury. As shown in [Figure 4](#), the ALT and AST levels were increased in group O compared with group S, but they decreased quickly after YCHD treatment.

### Effect of YCHD on BRL-3A rat hepatocytes apoptosis

TUNEL assay was utilized to detect the cells apoptosis, and the results are shown in [Figure 5A](#). Normal cells are shown in blue, and TUNEL positive cells are shown in green. Quantitative results, using the apoptosis index, are shown in [Figure 5B](#). It is clear that the green staining and the apoptosis index increased significantly in group O; however, the green staining and apoptosis index decreased in group M.

### Effect of YCHD on the protein and mRNA expression levels of PERK, CHOP, GADD34, Bax, and Bcl-2 in BRL-3A rat hepatocytes

**Table 2** Primer sequences used for quantitative real-time polymerase chain reaction for BCL-3A rat hepatocytes

Gene	Forward primer (5'-3')	Reverse primer (5'-3')
<i>GADPH</i>	GTTACCAGGGCTGCCTTC	GGGTTCCCGTTGATGACC
<i>PERK</i>	GCTTGCTCCACATCGGATA	CTAAGGACCTGCCGCGAG
<i>CHOP</i>	GATACTCGCTCTCCGCTCCA	CTTCCTTCGGAACACTCTCTCC
<i>GADD34</i>	TTACCTGGACAGAAGCCAGC	AGTGCACCTTTCTACCTTCAG
<i>Bax</i>	TTGCTACAGGGTTTCATCCAGG	CACTCGCTCAGCTTCTTGGT
<i>Bcl-2</i>	AGGATAACGGAGGCTGGGATG	CTCACTTGTGGCCAGGTAT

GADPH: Glyceraldehyde 3-phosphate dehydrogenase; PERK: Endoplasmic reticulum-resident protein kinase; CHOP: CCAAT/enhancer-binding protein homologous protein; GADD34: Growth arrest- and DNA damage-inducible gene 34; Bcl-2: B cell lymphoma/leukemia-2 gene; Bax: B cell lymphoma/leukemia-2 gene related X protein.

Next, we evaluated the roles of YCHD in inhibiting hepatocyte apoptosis induced by OJ by examining changes in the protein and mRNA expression levels of PERK, CHOP, GADD34, Bax, and Bcl-2 in BRL-3A rat hepatocytes. In BRL-3A rat hepatocytes that were cultured with OJ rat serum for 6 h, 24 h and 48 h, both the protein and mRNA levels of PERK, CHOP, and GADD34 were upregulated. Additionally, the Bax and Bcl-2 levels were increased, and the Bax/Bcl-2 ratio was also increased. In contrast, the BRL-3A rat hepatocytes cultured with OJ rat serum and rat serum containing YCHD for 6 h, 24 h and 48 h, the protein and mRNA expression levels of PERK, CHOP, GADD34, and Bax were downregulated, the Bcl-2 levels were upregulated, and the Bax/Bcl-2 ratio also decreased (Figure 6).

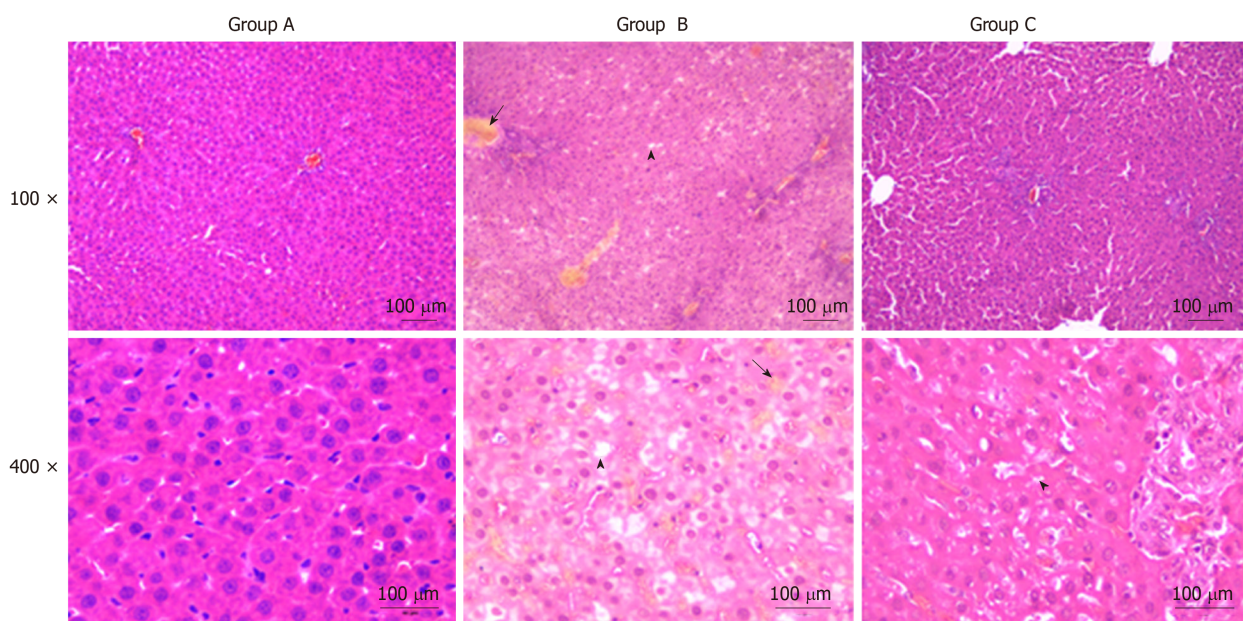
## DISCUSSION

OJ has several causes, including biliary atresia, cholangiolithiasis, pancreatic tumours, cholangiocarcinoma, gallbladder carcinoma, and liver tumours, which can lead to bile decrease or cessation<sup>[28]</sup>. Chronic biliary obstruction can lead to a dramatic increase in biliary pressure, which results in increased portal vein and hepatic sinus pressure, causing further reduction in liver blood perfusion. Ischaemia and hypoxia in liver cells cause hepatocyte damage, resulting in the release of intracellular liver enzymes, including ALT and AST, which are released into the blood. In the present study, TBIL, DBIL, ALT, AST, GGT, and ALP levels were all obviously elevated in group B. Additionally, the rat liver structure in group B was seriously damaged. The above experiments demonstrated that OJ can seriously influence liver morphology and function.

The ER is essential for secretion and synthesis of membrane proteins, post-translational modification, protein folding, and oligomerization<sup>[29]</sup>. Therefore, it is necessary for the ER to maintain homeostasis to perform normal physiological functions. Ischaemia, hypoxia, acidosis, disorders of calcium metabolism, and oxidative stress result in unfolded or misfolded protein accumulation, which can cause ER stress. The ability of cells to deal with this disturbance is a critical factor in cell survival<sup>[30]</sup>.

IRE1, PERK, and ATF6 activate a series of downstream signaling proteins that resist ER stress. Under normal physiological conditions, all three transducers are bound to an ER-resident chaperone, an immunoglobulin binding protein (Bip) also known as glucose regulating protein 78 (Grp78). When ER stress occurs, each transducer is activated and triggers downstream signaling cascades following Grp78/Bip dissociation to restore ER homeostasis<sup>[31,32]</sup>. However, if ER stress is prolonged or unresolved, cells become apoptotic. PERK is the key regulator of the response to ER stress<sup>[33]</sup>. PERK is a type I transmembrane protein with an ER luminal sensor and a cytoplasmic domain with Ser/Thr kinase activity. When dissociated from Grp78/Bip, PERK is activated by dimerization and autophosphorylation. Active PERK then phosphorylates a downstream factor, eukaryotic initiation factor 2 $\alpha$  (eIF2 $\alpha$ ) at Ser51<sup>[34]</sup>. In the initiation of protein synthesis, translation of eIF2 $\alpha$  combines with methionyl-tRNA to form a ternary complex, eIF2-GTP-tRNA<sup>met</sup>, to recognize AUG start codons. Inactive eIF2-GDP is then converted to active eIF2-GTP that requires the guanine nucleotide exchange factor, eIF2B<sup>[32]</sup>. When ER stress occurs, phosphorylated eIF2 $\alpha$ , which is activated by PERK, inhibits eIF2B translation of eIF2-GDP into eIF2-GTP,





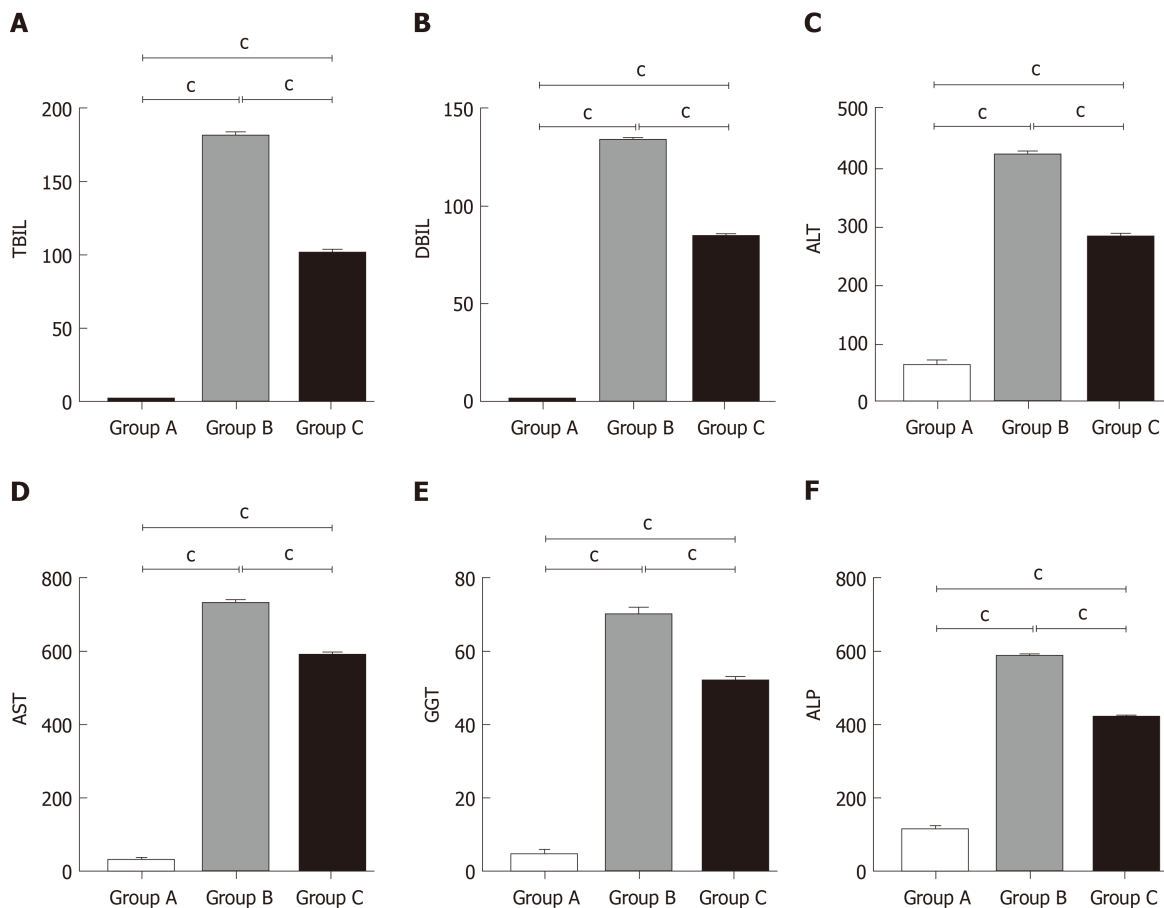
**Figure 1** Yinchenhao decoction improves the obstructive jaundice induced histopathological changes in liver tissue. The liver tissue in group B showed an unclear texture, and the hepatic lobule structures were disordered. Moreover, cholestasis and fatty degeneration were observed. Group A: Control group; Group B: Obstructive jaundice model group; Group C: Yinchenhao decoction-treated group.

thereby reducing protein synthesis<sup>[35]</sup>. At the same time, specific genes, such as activating transcription factor 4 (ATF4), contain small non-coding upstream open reading frames in their 5' untranslated region, which can bypass the eIF2 $\alpha$ -dependent translation block, and express increasingly through phosphorylated eIF2 $\alpha$ <sup>[36,37]</sup>. Fawcett *et al* showed that ATF4 could activate the downstream transcription factor, CHOP, *in vivo*<sup>[38]</sup>. CHOP is known as a key apoptosis factor, and the PERK-eIF2 $\alpha$ -ATF4 pathway is most important for CHOP activation in the three arms of the UPR. GADD34 has a catalytic subunit, protein phosphatase 1, which can dephosphorylate eIF2 $\alpha$  to restore the function of general Cap-dependent protein translation to resume protein synthesis and suppress ATF4 translation<sup>[39-41]</sup>. If the UPR fails in restoring ER homeostasis, increased protein synthesis leading to ATP depletion, oxidative stress, and cell death can occur (Han *et al*<sup>[42]</sup>, 2013). The expression of GADD34 is related to cell apoptosis, and its overexpression can initiate or enhance the cell apoptosis<sup>[43]</sup>.

CHOP can also induce apoptosis by regulating Bcl-2 family proteins. CHOP induces apoptosis by enhancing the expression of pro-apoptotic proteins and suppressing anti-apoptotic proteins. Bcl-2 and Bax are the most important and typical anti-apoptotic and pro-apoptotic proteins in the Bcl-2 family, respectively<sup>[44]</sup>. The Bax/Bcl-2 ratio plays a decisive role in the fate of cells. Bax and Bcl-2 regulate apoptosis by forming homodimers or heterodimers. Apoptotic signals activate Bax, which is transferred from the cytoplasm to the mitochondrial membrane. Bax is increased, and Bax/Bax homodimers promote cell apoptosis. When Bcl-2 is increased, Bcl-2/Bax heterodimers are formed, and the apoptosis trend is weakened; therefore, a function of Bcl-2 is to inhibit apoptosis<sup>[45,46]</sup>.

In the present study, the TUNEL assay showed that apoptotic cells in group O were more frequent, and the levels of ALT and AST in cell culture medium were increased, which indicated that liver cells could be destroyed by OJ. The Western blot and qRT-PCR analyses showed that the protein and mRNA expression of PERK, CHOP, and GADD34 both in group B rat liver tissues and BRL-3A rat liver cells of group O were increased significantly. Additionally, the protein and mRNA levels of Bax and Bcl-2 increased, and the Bax/Bcl-2 ratio also went up, which indicated that the Bax increase dominated. These results indicated that OJ could injure liver tissues and promote hepatocyte apoptosis by activating the PERK-CHOP-GADD34 pathways and upregulating the Bax/Bcl-2 ratio.

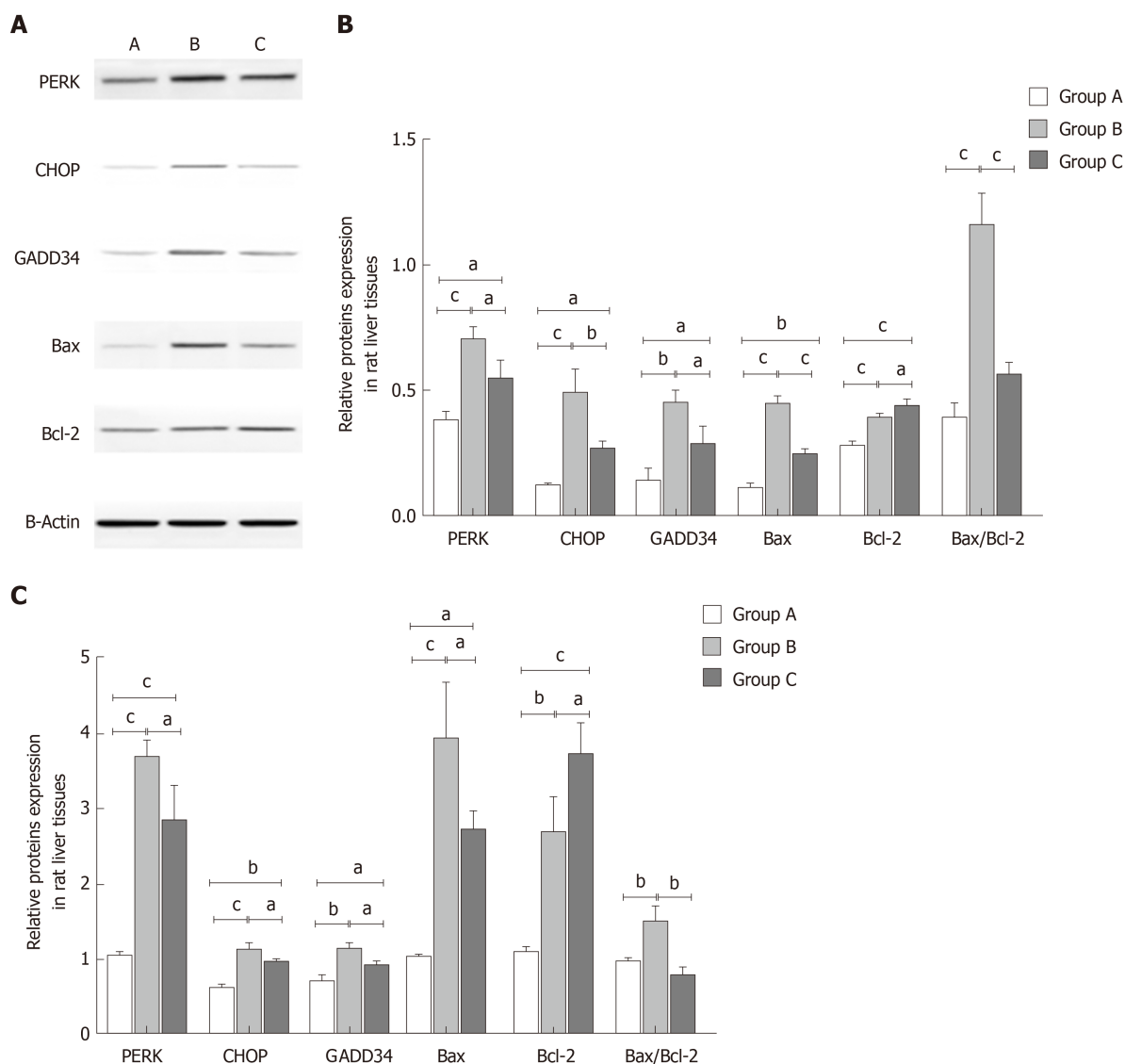
YCHD has a recognized role in increasing bile secretion and excretion, enhancing bile flow, treating inflammation, and promoting diuresis<sup>[47-49]</sup>. YCHD is not only used for treating jaundice and liver disorders but also for inhibiting hepatic cell apoptosis<sup>[19-21,50,51]</sup>. In the present study, after the YCHD treatment, the liver tissue structure, liver function, and hepatocytes apoptosis indices were obviously improved. Additionally, the protein and mRNA expression levels of PERK, CHOP, GADD34, and Bax both in the rat liver tissues and BRL-3A cells were downregulated; however,



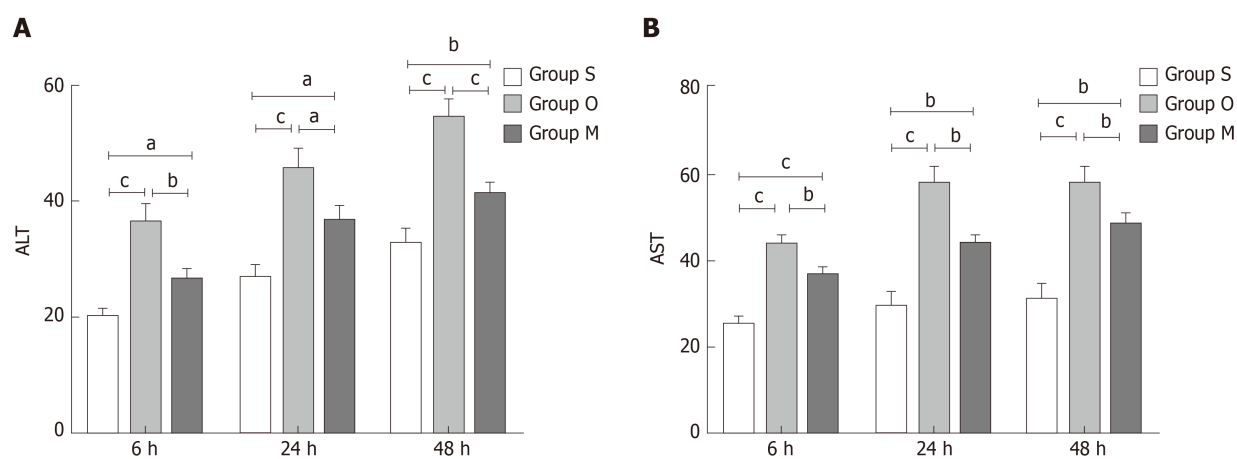
**Figure 2** Yinchenhao decoction relieves the hepatic injury induced by obstructive jaundice. A: Total bilirubin levels in the serum; B: Direct bilirubin levels in the serum; C: Alanine aminotransferase levels in the serum; D: Aspartate transaminase levels in the serum; E: Gamma-glutamyl transpeptidase levels in the serum; F: Alkaline phosphatase levels in the serum. Group A: Control group; Group B: Obstructive jaundice model group; Group C: Yinchenhao decoction;-treated group. <sup>a</sup> $P < 0.05$ , <sup>b</sup> $P < 0.01$ , <sup>c</sup> $P < 0.001$ . TBIL: Total bilirubin; DBIL: Direct bilirubin; ALT: Alanine aminotransferase; AST: Aspartate transaminase; GGT: Gamma-glutamyl transpeptidase; ALP: Alkaline phosphatase.

the protein and mRNA levels of Bcl-2 increased, while the Bax/Bcl-2 ratio decreased, indicating that the Bcl-2 levels dominated. These results further supported that YCHD could suppress liver injury, improve liver function, and alleviate hepatocyte apoptosis by inhibiting the PERK-CHOP-GADD34 pathways and downregulating the Bax/Bcl-2 ratio.

In conclusion, OJ can induce liver damage and hepatocyte apoptosis by activating the PERK-CHOP-GADD34 pathways and upregulating the Bax/Bcl-2 ratio. Additionally, YCHD can improve liver function and reduce hepatocyte apoptosis by inhibiting the activation of the PERK-CHOP-GADD34 pathways and downregulating the Bax/Bcl-2 ratio.

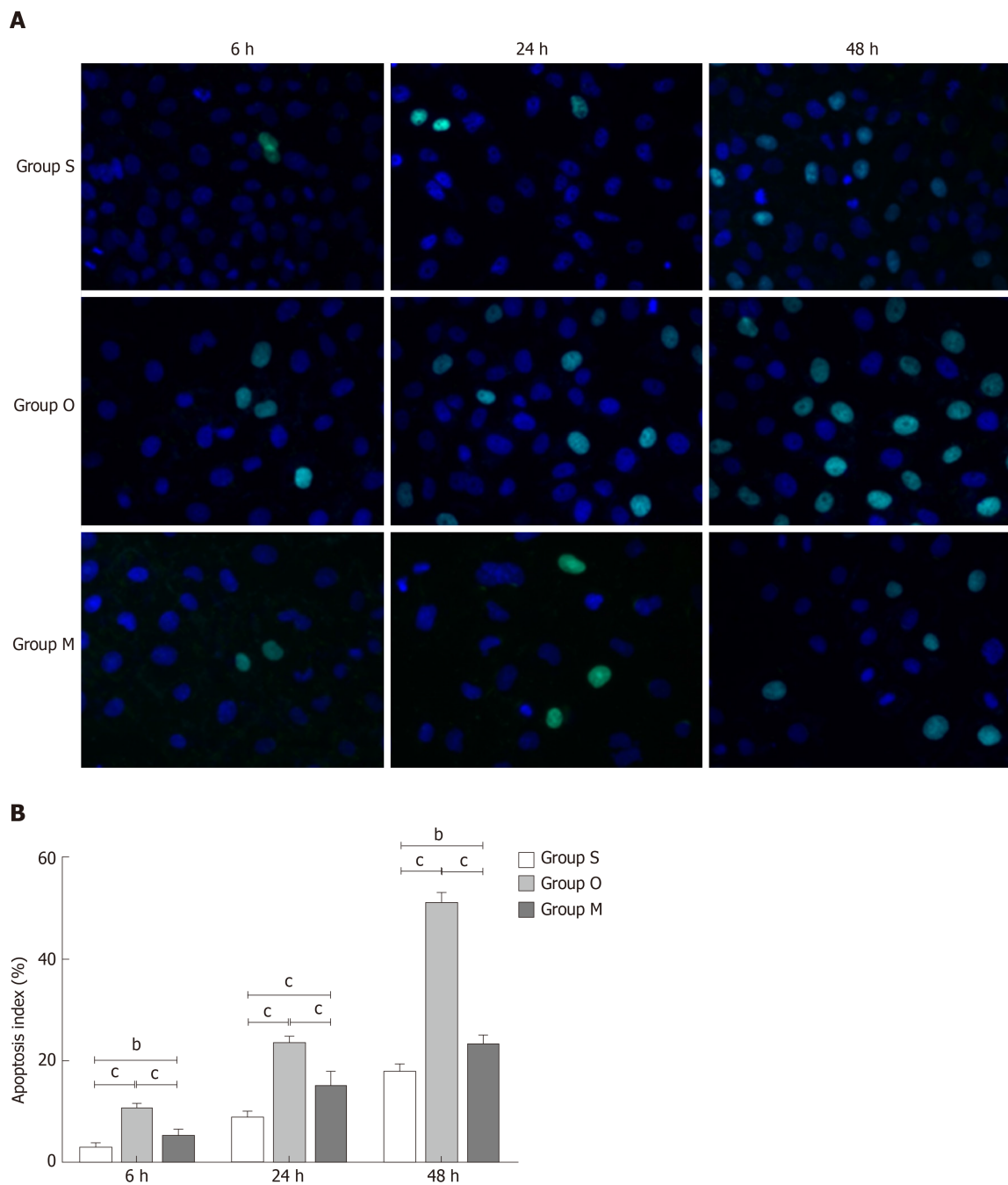


**Figure 3** Yinchanhao decoction regulates the protein kinase RNA-like endoplasmic reticulum kinase-induced apoptotic signaling pathway in rat liver tissue. **A:** Representative Western blot images of protein kinase RNA-like endoplasmic reticulum kinase (PERK), CCAAT/enhancer-binding protein homologous protein (CHOP), growth arrest and DNA damage-inducible protein 34 (GADD34), B cell lymphoma/leukemia-2 gene related X protein (Bax), and B cell lymphoma/leukemia-2 gene (Bcl-2) proteins; **B:** The protein expression levels of PERK, CHOP, GADD34, Bax, and Bcl-2; **C:** The gene expression levels of PERK, CHOP, GADD34, Bax, and Bcl-2. The mRNA levels were normalized to  $\beta$ -actin expression. Group A: Control group; Group B: Obstructive jaundice model group; Group C: Yinchanhao decoction-treated group. <sup>a</sup> $P < 0.05$ , <sup>b</sup> $P < 0.01$ , <sup>c</sup> $P < 0.001$ . PERK: Protein kinase RNA (PKR)-like endoplasmic reticulum kinase; CHOP: CCAAT/enhancer-binding protein homologous protein; GADD34: Growth arrest and DNA damage-inducible protein 34; Bcl-2: B cell lymphoma/leukemia-2 gene; Bax: Bcl-2 related X protein.

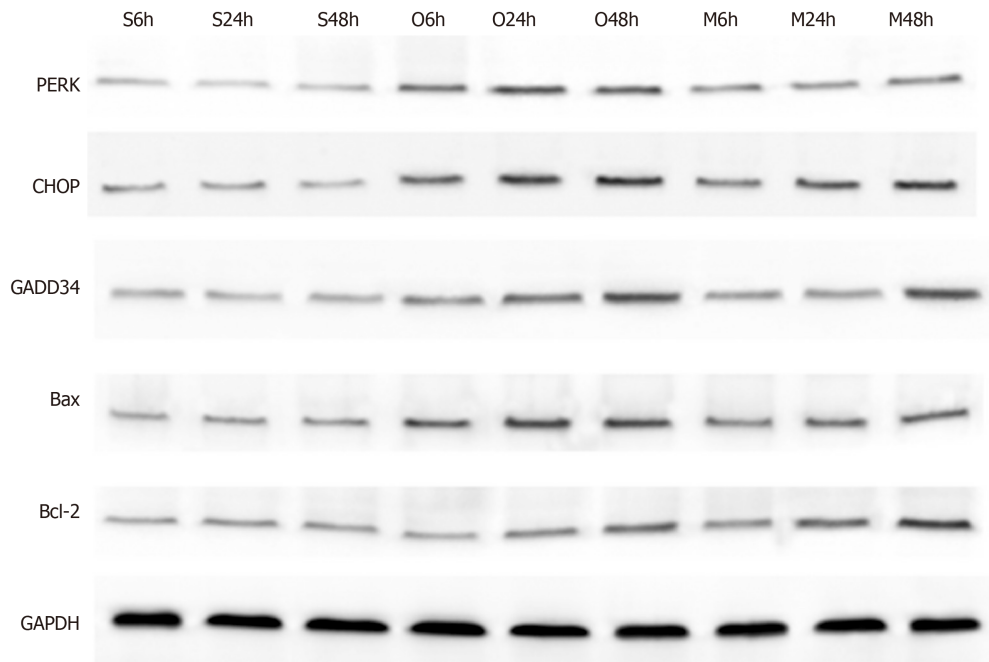
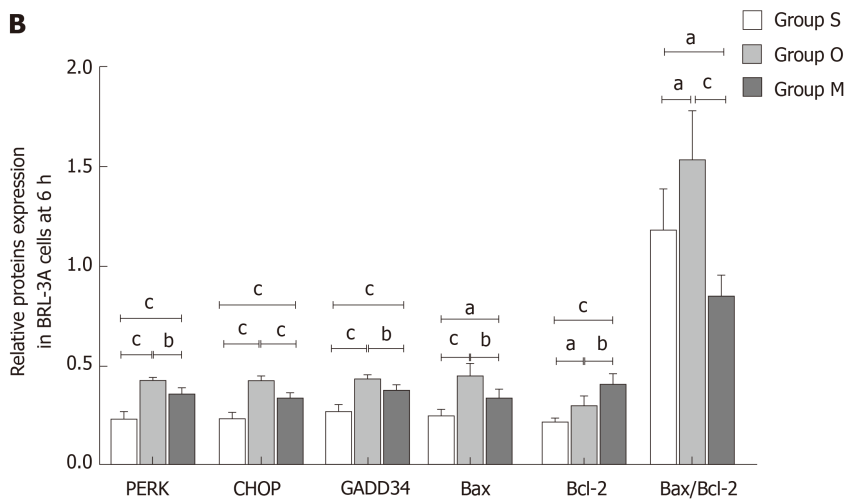
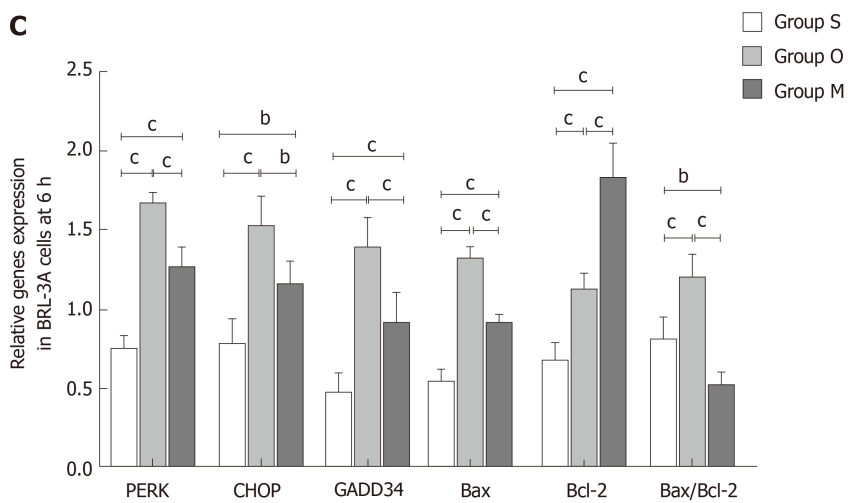


**Figure 4** Yinchenhao decoction alleviates BRL-3A rat hepatocyte injury. A: Alanine aminotransferase levels in cell culture medium; B: Aspartate transaminase levels in cell culture medium. Group S: BCL-3A rat hepatocytes incubated in rat serum of the G1 group; group O: BCL-3A rat hepatocytes incubated in rat serum of the G2 group; group M: BCL-3A rat hepatocytes incubated in rat serum of the G2 + G3 group. <sup>a</sup> $P < 0.05$ , <sup>b</sup> $P < 0.01$ , <sup>c</sup> $P < 0.001$ . ALT: Alanine aminotransferase; AST: Aspartate transaminase.

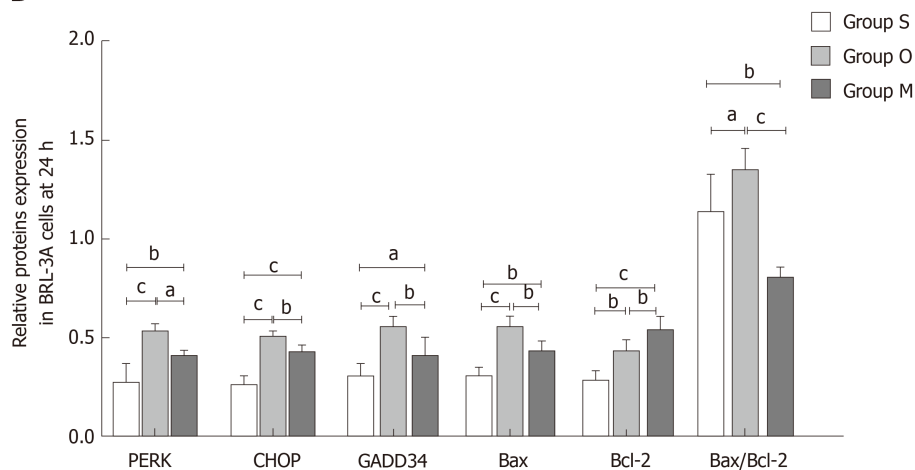




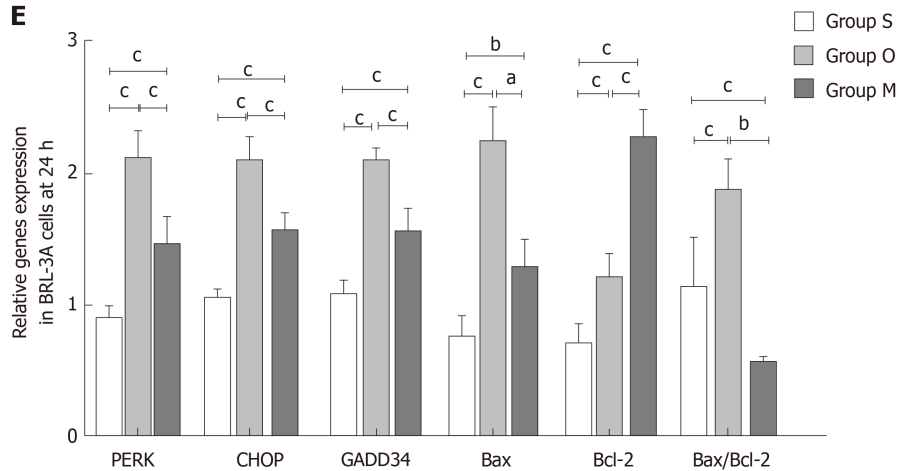
**Figure 5** Yinchenhao decoction inhibits BRL-3A rat hepatocyte apoptosis. A: TUNEL results of each group; B: Apoptosis index of each group at 6 h, 24 h, and 48 h. Group S: BCL-3A rat hepatocytes incubated in rat serum of the G1 group; group O: BCL-3A rat hepatocytes incubated in rat serum of the G2 group; group M: BCL-3A rat hepatocytes incubated in rat serum of the G2 + G3 group. <sup>a</sup> $P < 0.05$ , <sup>b</sup> $P < 0.01$ , <sup>c</sup> $P < 0.001$ .

**A**

**B**

**C**


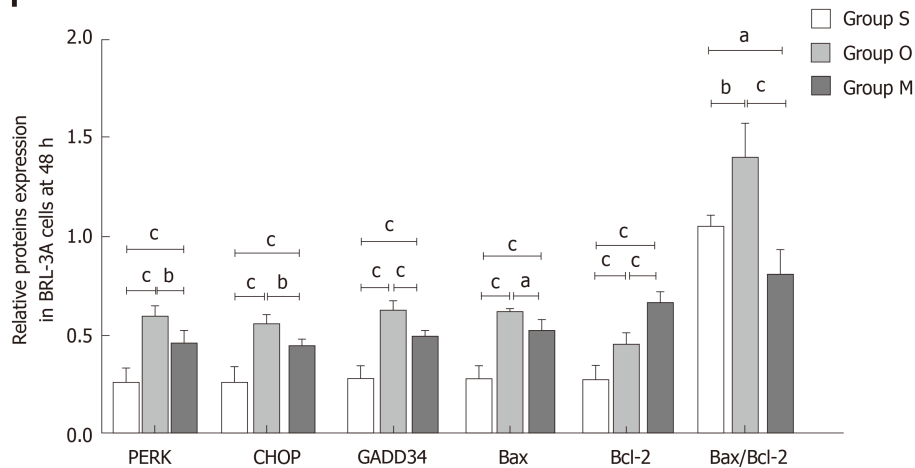
**D**

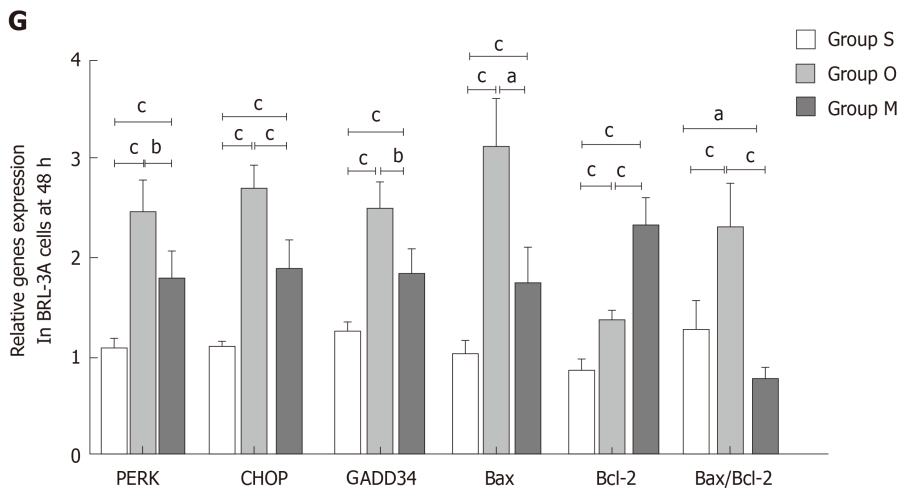


**E**



**F**





**Figure 6** Yinchanhao decoction regulates the protein kinase RNA-like endoplasmic reticulum kinase-induced apoptotic signaling pathway in BRL-3A rat hepatocytes. A: Representative Western blots of protein kinase RNA-like endoplasmic reticulum kinase, CCAAT/enhancer-binding protein homologous protein, growth arrest and DNA damage-inducible protein 34, B cell lymphoma/leukemia-2 gene related X protein, and B cell lymphoma/leukemia-2 gene proteins at 6 h, 24 h, and 48 h; B: Expression levels of the above proteins at 6 h; C: Expression levels of the corresponding genes at 6 h; D: Expression levels of the above proteins at 24 h; E: Expression levels of the corresponding genes at 24 h; F: Expression levels of the above proteins at 48 h; G: Expression levels of the corresponding genes at 48 h. The mRNA levels were normalized to GAPDH expression. Group S: BCL-3A rat hepatocytes incubated in rat serum of the G1 group; group O: BCL-3A rat hepatocytes incubated in rat serum of the G2 group; group M: BCL-3A rat hepatocytes incubated in rat serum of the G2 + G3 group. <sup>a</sup>*P* < 0.05, <sup>b</sup>*P* < 0.01, <sup>c</sup>*P* < 0.001. GAPDH: Glyceraldehyde 3-phosphate dehydrogenase; PERK: Protein kinase RNA (PKR)-like endoplasmic reticulum kinase; CHOP: CCAAT/enhancer-binding protein homologous protein; GADD34: Growth arrest and DNA damage-inducible protein 34; Bcl-2: B cell lymphoma/leukemia-2 gene; Bax: B cell lymphoma/leukemia-2 gene related X protein.

## ARTICLE HIGHLIGHTS

### Research background

Biliary obstruction can cause damage to all organs of the body, especially the liver. Chronic biliary obstruction results in ischaemia and hypoxia of hepatocytes and leads to apoptosis. Apoptosis is very important in regulating the homeostasis of the hepatobiliary system. Endoplasmic reticulum (ER) stress induced apoptosis is a hot research topic worldwide. However, there are few studies on liver injury and hepatocyte apoptosis induced by obstructive jaundice (OJ) through activating the ER stress pathway. Previous studies have confirmed that Yinchanhao decoction (YCHD) can effectively alleviate liver function injury and inhibit liver cell apoptosis, but the main mechanism of YCHD has not been clarified.

### Research motivation

To provide scientific evidence for clinical application of YCHD in OJ treatment.

### Research objectives

This study aimed to clarify the molecular mechanism of YCHD in alleviating OJ-induced liver injury and hepatocyte apoptosis.

### Research methods

In this study, the expression levels of protein kinase RNA-like endoplasmic reticulum-resident protein kinase (PERK), CCAAT/enhancer-binding protein homologous protein (CHOP), growth arrest- and DNA damage-inducible gene 34 (GADD34), B cell lymphoma/leukemia-2 gene (Bcl-2), and Bcl-2 related X protein (Bax) were detected in rats and BRL-3A rat hepatocytes, and the changes of PERK, CHOP, GADD34, Bax, and Bcl-2 were detected after the application of YCHD.

### Research results

We found that OJ induced liver injury and hepatocyte apoptosis by activating the PERK-CHOP-GADD34 pathways and upregulating Bax/Bcl-2 ratio, and YCHD attenuated these changes by inhibiting the PERK-CHOP-GADD34 pathways and downregulating Bax/Bcl-2 ratio.

### Research conclusions

YCHD can attenuate OJ-induced liver injury and hepatocyte apoptosis by inhibiting the PERK-CHOP-GADD34 pathways and downregulating Bax/Bcl-2 ratio. These findings support the clinical use of YCHD for OJ treatment.

### Research perspectives

YCHD is a traditional Chinese medicine (TCM) formula that has thousands of years of history for OJ treatment. The combination of TCM and modern medicine can effectively treat OJ.



## REFERENCES

- 1 **Kurniawan J**, Hasan I, Gani RA, Simadibrata M. Mortality-related Factors in Patients with Malignant Obstructive Jaundice. *Acta Med Indones* 2016; **48**: 282-288 [PMID: [28143989](#)]
- 2 **Qiu YD**, Bai JL, Xu FG, Ding YT. Effect of preoperative biliary drainage on malignant obstructive jaundice: a meta-analysis. *World J Gastroenterol* 2011; **17**: 391-396 [PMID: [21253401](#) DOI: [10.3748/wjg.v17.i3.391](#)]
- 3 **Sun C**, Yan G, Li Z, Tzeng CM. A meta-analysis of the effect of preoperative biliary stenting on patients with obstructive jaundice. *Medicine (Baltimore)* 2014; **93**: e189 [PMID: [25474436](#) DOI: [10.1097/MD.0000000000000189](#)]
- 4 **Sun EW**, Shi YF. Apoptosis: the quiet death silences the immune system. *Pharmacol Ther* 2001; **92**: 135-145 [PMID: [11916534](#) DOI: [10.1016/S0163-7258\(01\)00164-4](#)]
- 5 **Kosar NM**, Tosun M, Polat C, Kahraman A, Arikan Y. Hepatocyte apoptotic index and p53 expression in obstructive jaundice rats. *Bratisl Lek Listy* 2014; **115**: 352-356 [PMID: [25023425](#) DOI: [10.4149/BLL\\_2014\\_069](#)]
- 6 **Sherr CJ**. Tumor surveillance via the ARF-p53 pathway. *Genes Dev* 1998; **12**: 2984-2991 [PMID: [9765200](#) DOI: [10.1101/gad.12.19.2984](#)]
- 7 **Arora S**, Tandon S. Mushroom Extracts Induce Human Colon Cancer Cell (COLO-205) Death by Triggering the Mitochondrial Apoptosis Pathway and Go/G1-Phase Cell Cycle Arrest. *Arch Iran Med* 2015; **18**: 284-295 [PMID: [25959910](#) DOI: [10.51805/AIM.006](#)]
- 8 **Fujiwara N**, Inoue J, Kawano T, Tanimoto K, Kozaki K, Inazawa J. miR-634 Activates the Mitochondrial Apoptosis Pathway and Enhances Chemotherapy-Induced Cytotoxicity. *Cancer Res* 2015; **75**: 3890-3901 [PMID: [26216549](#) DOI: [10.1158/0008-5472.CAN-15-0257](#)]
- 9 **Walter P**, Ron D. The unfolded protein response: from stress pathway to homeostatic regulation. *Science* 2011; **334**: 1081-1086 [PMID: [22116877](#) DOI: [10.1126/science.1209038](#)]
- 10 **Sano R**, Reed JC. ER stress-induced cell death mechanisms. *Biochim Biophys Acta* 2013; **1833**: 3460-3470 [PMID: [23850759](#) DOI: [10.1016/j.bbamcr.2013.06.028](#)]
- 11 **Szegezdi E**, Logue SE, Gorman AM, Samali A. Mediators of endoplasmic reticulum stress-induced apoptosis. *EMBO Rep* 2006; **7**: 880-885 [PMID: [16953201](#) DOI: [10.1038/sj.embor.7400779](#)]
- 12 **Sovolyova N**, Healy S, Samali A, Logue SE. Stressed to death - mechanisms of ER stress-induced cell death. *Biol Chem* 2014; **395**: 1-13 [PMID: [24002662](#) DOI: [10.1515/hsz-2013-0174](#)]
- 13 **Tabas I**, Ron D. Integrating the mechanisms of apoptosis induced by endoplasmic reticulum stress. *Nat Cell Biol* 2011; **13**: 184-190 [PMID: [21364565](#) DOI: [10.1038/ncb0311-184](#)]
- 14 **Wang K**. Molecular mechanisms of liver injury: apoptosis or necrosis. *Exp Toxicol Pathol* 2014; **66**: 351-356 [PMID: [24867271](#) DOI: [10.1016/j.etp.2014.04.004](#)]
- 15 **Cao Y**, Hao Y, Li H, Liu Q, Gao F, Liu W, Duan H. Role of endoplasmic reticulum stress in apoptosis of differentiated mouse podocytes induced by high glucose. *Int J Mol Med* 2014; **33**: 809-816 [PMID: [24503896](#) DOI: [10.3892/ijmm.2014.1642](#)]
- 16 **Du K**, Herzig S, Kulkarni RN, Montminy M. TRB3: a tribbles homolog that inhibits Akt/PKB activation by insulin in liver. *Science* 2003; **300**: 1574-1577 [PMID: [12791994](#) DOI: [10.1126/science.1079817](#)]
- 17 **Wu L**, Zhou PQ, Xie JW, Zhu R, Zhou SC, Wang G, Wu ZX, Hao S. Effects of Yinchenhao decoction on self-regulation of renin-angiotensin system by targeting angiotensin converting enzyme 2 in bile duct-ligated rat liver. *J Huazhong Univ Sci Technolog Med Sci* 2015; **35**: 519-524 [PMID: [26223920](#) DOI: [10.1007/s11596-015-1463-9](#)]
- 18 **Liu C**, Sun M, Wang L, Wang G, Chen G, Liu C, Liu P. Effects of Yinchenhao Tang and related decoctions on DMN-induced cirrhosis/fibrosis in rats. *Chin Med* 2008; **3**: 1 [PMID: [18237412](#) DOI: [10.1186/1749-8546-3-1](#)]
- 19 **Wang X**, Zhang A, Wang P, Sun H, Wu G, Sun W, Lv H, Jiao G, Xu H, Yuan Y, Liu L, Zou D, Wu Z, Han Y, Yan G, Dong W, Wu F, Dong T, Yu Y, Zhang S, Wu X, Tong X, Meng X. Metabolomics coupled with proteomics advancing drug discovery toward more agile development of targeted combination therapies. *Mol Cell Proteomics* 2013; **12**: 1226-1238 [PMID: [23362329](#) DOI: [10.1074/mcp.M112.021683](#)]
- 20 **Zhang A**, Sun H, Qiu S, Wang X. Advancing drug discovery and development from active constituents of yinchenhao tang, a famous traditional chinese medicine formula. *Evid Based Complement Alternat Med* 2013; **2013**: 257909 [PMID: [24191164](#) DOI: [10.1155/2013/257909](#)]
- 21 **Arai M**, Yokosuka O, Fukai K, Kanda T, Kojima H, Kawai S, Imazeki F, Hirasawa H, Saisho H. A case of severe acute hepatitis of unknown etiology treated with the Chinese herbal medicine Inchinko-to. *Hepatol Res* 2004; **28**: 161-165 [PMID: [15036073](#) DOI: [10.1016/j.hepres.2003.09.004](#)]
- 22 **Guo MZ**, Li XS, Xu HR, Mei ZC, Shen W, Ye XF. Rhein inhibits liver fibrosis induced by carbon tetrachloride in rats. *Acta Pharmacol Sin* 2002; **23**: 739-744 [PMID: [12147197](#)]
- 23 **Iwama H**, Amagaya S, Ogihara Y. Effect of shosaikoto, a Japanese and Chinese traditional herbal medicinal mixture, on the mitogenic activity of lipopolysaccharide: a new pharmacological testing method. *J Ethnopharmacol* 1987; **21**: 45-53 [PMID: [3695555](#) DOI: [10.1016/0378-8741\(87\)90093-6](#)]
- 24 **Bochu W**, Liancai Z, Qi C. Primary study on the application of Serum Pharmacology in Chinese traditional medicine. *Colloids Surf B Biointerfaces* 2005; **43**: 194-197 [PMID: [15964749](#) DOI: [10.1016/j.colsurfb.2005.04.013](#)]
- 25 **Song SJ**, Li ZL, Zhang XB. Effect of Yinchenhao decoction on expression of IRE1 $\alpha$  protein in liver cells of rats with obstructive jaundice. *Shijie Huaren Xiaohua Zazhi* 2016; **24**: 2520-2524
- 26 **Aoki H**, Aoki M, Yang J, Katsuta E, Mukhopadhyay P, Ramanathan R, Woelfel IA, Wang X, Spiegel S, Zhou H, Takabe K. Murine model of long-term obstructive jaundice. *J Surg Res* 2016; **206**: 118-125 [PMID: [27916350](#) DOI: [10.1016/j.jss.2016.07.020](#)]
- 27 **Tarcin O**, Basaranoglu M, Tahan V, Tahan G, Sücüllü I, Yilmaz N, Sood G, Snyder N, Hilman G, Celikel C, Tözün N. Time course of collagen peak in bile duct-ligated rats. *BMC Gastroenterol* 2011; **11**: 45 [PMID: [21527001](#) DOI: [10.1186/1471-230X-11-45](#)]
- 28 **Unal Y**, Tuncal S, Kosmaz K, Kucuk B, Kismet K, Cavusoglu T, Celepli P, Senes M, Yildiz S, Hucumenoglu S. The Effect of Calcium Dobesilate on Liver Damage in Experimental Obstructive Jaundice. *J Invest Surg* 2019; **32**: 238-244 [PMID: [29589984](#) DOI: [10.1080/08941939.2018.1451936](#)]
- 29 **Ron D**, Hubbard SR. How IRE1 reacts to ER stress. *Cell* 2008; **132**: 24-26 [PMID: [18191217](#) DOI: [10.1016/j.cell.2007.12.017](#)]
- 30 **Ron D**, Walter P. Signal integration in the endoplasmic reticulum unfolded protein response. *Nat Rev Mol Cell Biol* 2007; **8**: 519-529 [PMID: [17565364](#) DOI: [10.1038/nrm2199](#)]
- 31 **Bertolotti A**, Zhang Y, Hendershot LM, Harding HP, Ron D. Dynamic interaction of BiP and ER stress

- transducers in the unfolded-protein response. *Nat Cell Biol* 2000; **2**: 326-332 [PMID: [10854322](#) DOI: [10.1038/35014014](#)]
- 32 **Shen Y**, Meunier L, Hendershot LM. Identification and characterization of a novel endoplasmic reticulum (ER) DnaJ homologue, which stimulates ATPase activity of BiP *in vitro* and is induced by ER stress. *J Biol Chem* 2002; **277**: 15947-15956 [PMID: [11836248](#) DOI: [10.1074/jbc.M112214200](#)]
- 33 **Ron D**, Harding HP. Protein-folding homeostasis in the endoplasmic reticulum and nutritional regulation. *Cold Spring Harb Perspect Biol* 2012; **4** [PMID: [23209157](#) DOI: [10.1101/cshperspect.a013177](#)]
- 34 **Donnelly N**, Gorman AM, Gupta S, Samali A. The eIF2 $\alpha$  kinases: their structures and functions. *Cell Mol Life Sci* 2013; **70**: 3493-3511 [PMID: [23354059](#) DOI: [10.1007/s00018-012-1252-6](#)]
- 35 **Harding HP**, Zhang Y, Ron D. Protein translation and folding are coupled by an endoplasmic-reticulum-resident kinase. *Nature* 1999; **397**: 271-274 [PMID: [9930704](#) DOI: [10.1038/16729](#)]
- 36 **Harding HP**, Novoa I, Zhang Y, Zeng H, Wek R, Schapira M, Ron D. Regulated translation initiation controls stress-induced gene expression in mammalian cells. *Mol Cell* 2000; **6**: 1099-1108 [PMID: [11106749](#) DOI: [10.1016/S1097-2765\(00\)00108-8](#)]
- 37 **Schröder M**, Kaufman RJ. The mammalian unfolded protein response. *Annu Rev Biochem* 2005; **74**: 739-789 [PMID: [15952902](#) DOI: [15952902](#)]
- 38 **Fawcett TW**, Martindale JL, Guyton KZ, Hai T, Holbrook NJ. Complexes containing activating transcription factor (ATF)/cAMP-responsive-element-binding protein (CREB) interact with the CCAAT/enhancer-binding protein (C/EBP)-ATF composite site to regulate Gadd153 expression during the stress response. *Biochem J* 1999; **339**: 135-141 [PMID: [10085237](#) DOI: [10.1042/bj3390135](#)]
- 39 **Novoa I**, Zeng H, Harding HP, Ron D. Feedback inhibition of the unfolded protein response by GADD34-mediated dephosphorylation of eIF2 $\alpha$ . *J Cell Biol* 2001; **153**: 1011-1022 [PMID: [11381086](#) DOI: [10.1083/jcb.153.5.1011](#)]
- 40 **Connor JH**, Weiser DC, Li S, Hallenbeck JM, Shenolikar S. Growth arrest and DNA damage-inducible protein GADD34 assembles a novel signaling complex containing protein phosphatase 1 and inhibitor 1. *Mol Cell Biol* 2001; **21**: 6841-6850 [PMID: [11564868](#) DOI: [10.1128/MCB.21.20.6841-6850.2001](#)]
- 41 **Ma Y**, Hendershot LM. Delineation of a negative feedback regulatory loop that controls protein translation during endoplasmic reticulum stress. *J Biol Chem* 2003; **278**: 34864-34873 [PMID: [12840028](#) DOI: [10.1074/jbc.M301107200](#)]
- 42 **Han J**, Back SH, Hur J, Lin YH, Gildersleeve R, Shan J, Yuan CL, Krokowski D, Wang S, Hatzoglou M, Kilberg MS, Sartor MA, Kaufman RJ. ER-stress-induced transcriptional regulation increases protein synthesis leading to cell death. *Nat Cell Biol* 2013; **15**: 481-490 [PMID: [23624402](#) DOI: [10.1038/ncb2738](#)]
- 43 **Adler HT**, Chinery R, Wu DY, Kussick SJ, Payne JM, Fornace AJ, Tkachuk DC. Leukemic HRX fusion proteins inhibit GADD34-induced apoptosis and associate with the GADD34 and hSNF5/INI1 proteins. *Mol Cell Biol* 1999; **19**: 7050-7060 [PMID: [10490642](#) DOI: [10.1128/mcb.19.10.7050](#)]
- 44 **Rossé T**, Olivier R, Monney L, Rager M, Conus S, Fellay I, Jansen B, Borner C. Bcl-2 prolongs cell survival after Bax-induced release of cytochrome c. *Nature* 1998; **391**: 496-499 [PMID: [9461218](#) DOI: [10.1038/35160](#)]
- 45 **Brooks C**, Dong Z. Regulation of mitochondrial morphological dynamics during apoptosis by Bcl-2 family proteins: a key in Bak? *Cell Cycle* 2007; **6**: 3043-3047 [PMID: [18073534](#) DOI: [10.4161/cc.6.24.5115](#)]
- 46 **Lalier L**, Cartron PF, Juin P, Nedelkina S, Manon S, Bechinger B, Vallette FM. Bax activation and mitochondrial insertion during apoptosis. *Apoptosis* 2007; **12**: 887-896 [PMID: [17453158](#) DOI: [10.1007/s10495-007-0749-1](#)]
- 47 **Wang YH**, Zhao CX, Chen BM, He M, Liu LQ, Li CY, Chen X. Reverse effect of Yinchenhao decoction in dimethyl nitrosamine-induced hepatic fibrosis in rats. *Zhongguo Zhong Yao Za Zhi* 2014; **39**: 1473-1478 [PMID: [25039185](#)]
- 48 **Lee TY**, Chang HH, Wu MY, Lin HC. Yin-Chen-Hao-Tang ameliorates obstruction-induced hepatic apoptosis in rats. *J Pharm Pharmacol* 2007; **59**: 583-590 [PMID: [17430643](#) DOI: [10.1211/jpp.59.4.0014](#)]
- 49 **Cai H**, Song YH, Xia WJ, Jin MW. Aqueous extract of Yin-Chen-Hao decoction, a traditional Chinese prescription, exerts protective effects on concanavalin A-induced hepatitis in mice through inhibition of NF- $\kappa$ B. *J Pharm Pharmacol* 2006; **58**: 677-684 [PMID: [16640837](#) DOI: [10.1211/jpp.58.5.0013](#)]
- 50 **Inao M**, Mochida S, Matsui A, Eguchi Y, Yulutuz Y, Wang Y, Naiki K, Kakinuma T, Fujimori K, Nagoshi S, Fujiwara K. Japanese herbal medicine Inchin-ko-to as a therapeutic drug for liver fibrosis. *J Hepatol* 2004; **41**: 584-591 [PMID: [15464238](#) DOI: [10.1016/j.jhep.2004.06.033](#)]
- 51 **Yamamoto M**, Miura N, Ohtake N, Amagaya S, Ishige A, Sasaki H, Komatsu Y, Fukuda K, Ito T, Terasawa K. Genipin, a metabolite derived from the herbal medicine Inchin-ko-to, and suppression of Fas-induced lethal liver apoptosis in mice. *Gastroenterology* 2000; **118**: 380-389 [PMID: [10648466](#) DOI: [10.1016/S0016-5085\(00\)70220-4](#)]



## Basic Study

# MiR-32-5p aggravates intestinal epithelial cell injury in pediatric enteritis induced by *Helicobacter pylori*

Jing Feng, Jian Guo, Jun-Ping Wang, Bao-Feng Chai

**ORCID number:** Jing Feng (0000-0001-9440-1136); Jian Guo (0000-0002-4409-0066); Jun-Ping Wang (0000-0002-1586-2776); Bao-Feng Chai (0000-0001-7625-8217).

**Author contributions:** Chai BF and Wang JP designed the research; Feng J and Guo J performed the research; Feng J and Chai BF analyzed the data; Feng J and Wang JP wrote the paper.

**Institutional review board statement:** The study was reviewed and approved by the Ethics Committee of Shanxi University and Ethics Committee of Shanxi Provincial People's Hospital, Shanxi Province, China.

**Conflict-of-interest statement:** There was no competing interest.

**Data sharing statement:** All the data in the current research are available from the corresponding author on reasonable request.

**Open-Access:** This article is an open-access article which was selected by an in-house editor and fully peer-reviewed by external reviewers. It is distributed in accordance with the Creative Commons Attribution Non Commercial (CC BY-NC 4.0) license, which permits others to distribute, remix, adapt, build upon this work non-commercially, and license their derivative works on different terms, provided the original work is properly cited and the use is non-commercial. See: <http://creativecommons.org/licenses/by-nc/4.0/>

**Manuscript source:** Unsolicited

**Jing Feng, Bao-Feng Chai,** Institute of Loess Plateau, Shanxi University, Taiyuan 030006, Shanxi Province, China

**Jing Feng, Jun-Ping Wang,** Department of Gastroenterology, Shanxi Provincial People's Hospital, The Affiliated People's Hospital of Shanxi Medical University, Taiyuan 030012, Shanxi Province, China

**Jian Guo,** Department of General Surgery, Shanxi Provincial People's Hospital, The Affiliated People's Hospital of Shanxi Medical University, Taiyuan 030012, Shanxi Province, China

**Corresponding author:** Bao-Feng Chai, MD, PhD, Professor, Institute of Loess Plateau, Shanxi University, No. 92, Wucheng Road, Taiyuan 030006, Shanxi Province, China.

[13644359409@163.com](mailto:13644359409@163.com)

**Telephone:** +86-13603583312

## Abstract

### BACKGROUND

Pediatric enteritis is one of the infectious diseases in the digestive system that causes a variety of digestive problems, including diarrhea, vomiting, and bellyache in children. Clinically, *Helicobacter pylori* (*H. pylori*) infection is one of the common factors to cause pediatric enteritis. It has been demonstrated that aberrant expression of microRNAs (miRNAs) is found in gastrointestinal diseases caused by *H. pylori*, and we discovered a significant increase of miR-32-5p in *H. pylori*-related pediatric enteritis. However, the exact role of miR-32-5p in it is still unknown.

### AIM

To investigate the role of aberrant miR-32-5p in pediatric enteritis induced by *H. pylori*.

### METHODS

MiR-32-5p expression was detected by quantitative real time-polymerase chain reaction. The biological role of miR-32-5p in *H. pylori*-treated intestinal epithelial cells was evaluated by Cell Counting Kit-8 assay and flow cytometry. The potential target of miR-32-5p was predicted with TargetScanHuman and verified by luciferase assay. The downstream mechanism of miR-32-5p was explored by using molecular biology methods.

### RESULTS

We found that miR-32-5p was overexpressed in serum of *H. pylori*-induced pediatric enteritis. Further investigation revealed that *H. pylori* infection

manuscript

**Received:** January 26, 2019**Peer-review started:** August 27, 2019**First decision:** September 19, 2019**Revised:** October 11, 2019**Accepted:** October 22, 2019**Article in press:** October 22, 2019**Published online:** November 7, 2019**P-Reviewer:** Cheng TH, Rodrigo L, Stanciu C, Sipos F**S-Editor:** Wang J**L-Editor:** Wang TQ**E-Editor:** Ma YJ

promoted the death of intestinal epithelial cells, and increased miR-32-5p expression. Moreover, miR-32-5p mimic further facilitated apoptosis and inflammatory cytokine secretion of intestinal epithelial cells. Further exploration revealed that SMAD family member 6 (SMAD6) was the direct target of miR-32-5p, and SMAD6 overexpression partially rescued cell damage induced by *H. pylori*. The following experiments showed that miR-32-5p/SMAD6 participated in the apoptosis of intestinal epithelial cells induced by transforming growth factor- $\beta$ -activated kinase 1 (TAK1)-p38 activation under *H. pylori* infection.

### CONCLUSION

Our work uncovered the crucial role of aberrant expression of miR-32-5p in *H. pylori*-related pediatric enteritis, and suggested that the TAK1-p38 pathway is involved in it.

**Key words:** MiR-32-5p; SMAD family member 6; Transforming growth factor- $\beta$ -activated kinase 1; Apoptosis; Enteritis; *Helicobacter pylori*

©The Author(s) 2019. Published by Baishideng Publishing Group Inc. All rights reserved.

**Core tip:** Our study demonstrated the harmful role of aberrant miR-32-5p in *Helicobacter pylori* (*H. pylori*)-infected intestinal epithelial cells. Further investigation showed that SMAD family member 6 (SMAD6) was the downstream of miR-32-5p and exerted an opposite role in this process. What's more, miR-32-5p/SMAD6 contributed to transforming growth factor- $\beta$ -activated kinase 1-p38 cascade activation in intestinal epithelial cells under *H. pylori* infection. These findings provide a novel insight into the pathogenesis of pediatric enteritis caused by *H. pylori*.

**Citation:** Feng J, Guo J, Wang JP, Chai BF. MiR-32-5p aggravates intestinal epithelial cell injury in pediatric enteritis induced by *Helicobacter pylori*. *World J Gastroenterol* 2019; 25(41): 6222-6237

**URL:** <https://www.wjnet.com/1007-9327/full/v25/i41/6222.htm>

**DOI:** <https://dx.doi.org/10.3748/wjg.v25.i41.6222>

## INTRODUCTION

Enteritis is a common disease of the digestive system in children among outpatients<sup>[1]</sup>. Etiologically, *Helicobacter pylori* (*H. pylori*) infection is one of the most important pathogenic factors to induce pediatric enteritis<sup>[2]</sup>. The stomach is the primary organ that is damaged by *H. pylori*. However, *H. pylori*-induced enteritis is seen with increasing incidence in recent years.

*H. pylori* infection is regarded as a class I carcinogen<sup>[3]</sup>. Normally, *H. pylori*-induced gastritis could lead to gastric ulcer, which is the major precancerous lesion if without treatment. Although mainly residing in stomach, *H. pylori* displays a strong ability of acid resistance. As a pathogen, *H. pylori* could attack and damage the mucosa of the digestive tract by recruiting and activating neutrophils<sup>[4]</sup>, inducing abnormal expression of key proteins<sup>[5]</sup> and microRNAs (miRNAs)<sup>[6]</sup>, and releasing cytotoxic substances<sup>[7]</sup>. A previous study showed that *H. pylori* infection accounted for 6% of children with duodenitis<sup>[8]</sup>. Moreover, Gimiga *et al*<sup>[9]</sup> found that gastritis and duodenitis contributed to half of children with upper gastrointestinal bleeding, and 36.89% of participants were diagnosed with *H. pylori* infection. These findings suggested a relatively high prevalence of children with *H. pylori* infection in the digestive system.

MicroRNAs (miRNAs) belong to non-coding RNA molecules that are abundant in eukaryotic organisms<sup>[10,11]</sup>. MiRNAs have no ability to encode proteins, but contribute to the modulation of gene expression<sup>[11,12]</sup>. A recent study revealed the upregulation of miR-146a and miR-155 in patients with gastritis induced by *H. pylori* infection<sup>[13]</sup>, with the similar findings demonstrated by another research group<sup>[14]</sup>. Cortés-Márquez *et al*<sup>[14]</sup> further grouped the patients with gastritis by age, and found that both children and adults with *H. pylori*-induced gastritis displayed higher levels of miR-145a and miR-155. Moreover, the cancerization tendency of *H. pylori*-induced gastritis was correlated with the upregulation of miR-146a and miR-155<sup>[13,14]</sup>. In addition, *H. pylori*



infection could result in the downregulation of miRNAs. The decreased expression of miR-24-3p was shown in *H. pylori*-induced gastritis tissue samples compared with the gastritis tissues without *H. pylori* infection<sup>[15]</sup>. Zou *et al*<sup>[16]</sup> demonstrated that gastric epithelial cells treated with miR-3178 mimic presented alleviated inflammation induced by *H. pylori*, and miR-3178 could block *H. pylori*-induced carcinogenesis by targeting the TRAF1-NF- $\kappa$ B pathway. Therefore, the relationship between miRNAs and *H. pylori* infection is not positively correlated. Except for causing gastric epithelial cell damage *via* abnormal expression of miRNAs, *H. pylori* infection-induced miRNAs might contribute to intestinal epithelial cell damage. However, little is currently known about miRNAs and *H. pylori*-related enteritis.

Herein, our research revealed significant upregulation of miR-32-5p by targeting SMAD family member 6 (SMAD6) in *H. pylori*-infected intestinal epithelial cells, which aggravated the damage of *H. pylori* to the cells and might contribute to the pathogenesis of pediatric enteritis induced by *H. pylori*.

## MATERIALS AND METHODS

### Participants

Serum samples were obtained from children with *H. pylori*-induced enteritis ( $n = 15$ ) and healthy controls ( $n = 15$ ), and the participants were from Shanxi Provincial People's Hospital. Procedures in this study were approved by the Ethics Committee of Shanxi University and Ethics Committee of Shanxi Provincial People's Hospital, and complied with the guidelines of Declaration of Helsinki. Both guardians of the children and the participants were informed of the purpose of the study, and signed an informed consent form.

### Cell culture and *H. pylori* strain

Human intestinal epithelial cell line HIEC-6 was cultured in RPMI 1640 medium with 10% fetal bovine serum (FBS). Human embryonic kidney cell line HEK-293T was cultured in DMEM medium with 10% FBS. The medium and FBS were purchased from ThermoFisher Scientific (United States). *H. pylori* strain T81213-NTB (ATCC 46396) was cultured as previously described<sup>[17]</sup>. The concentration of *H. pylori* was adjusted to  $1 \times 10^9$  CFU/mL, and  $1 \times 10^6$  CFU/mL was used in our experiments.

### Quantitative real time-polymerase chain reaction

Serum miRNAs were extracted using a miRNeasy Serum/Plasma Kit (QIAGEN, Germany), miRNAs of cells were obtained with a miRNeasy Mini Kit (QIAGEN, Germany), and total RNA of cells was extracted using TRIzol (Takara, Japan). cDNA was acquired from the extracted RNA, and quantitative real time-polymerase chain reaction (qRT-PCR) was carried out by using a SYBR Premix Ex Taq II Kit (Takara, Japan). The expression level was calculated by using  $2^{-\Delta\Delta CT}$  methods. Primers used in our study are displayed in Table 1.

### Cell transfection

SiRNAs, miRNA mimic and inhibitor, and overexpression vectors were obtained from Sangon Biotech (China). Cell transfection was carried out with Lipofectamine 3000 (Invitrogen, United States) according to the manufacturer's instructions. The sequences used are shown in Table 1.

### Detection of cell viability

Cell Counting Kit-8 (Beyotime, China) assay was utilized to evaluate cell viability according to the manufacturer's instructions. Cells were seeded followed by cell transfection in the presence or absence of *H. pylori*. Ten microliters of the reagents were added into each well at 37 °C for 1.5 h. The value of optical density (OD) was detected with a microplate reader (Bio-Rad, United States) at 450 nm.

### Flow cytometry

After cell transfection, cells were incubated with TAK1 inhibitor NG25 (5  $\mu$ mol/L, APExBio, United States) and p38 inhibitor (10  $\mu$ mol/L, Cell Signaling Technology, United States) in the presence or absence of *H. pylori*, harvested, and stained using an Annexin V-FITC/PI apoptosis kit (Beyotime, China) according to the manufacturer's instructions. The apoptotic rate is represented as the positive rate of cells labelled with Annexin V, and the results were analyzed by flow cytometry (Accuri C6, United States).

### Luciferase assay

HEK-293T cells were used to validate the binding between miR-32-5p and SMAD6.

**Table 1** Sequences of primers, siRNAs, microRNA mimic, and microRNA inhibitor used in this study

Gene	Sequence (5'-3')
miR-32-5p	Forward: CGGTATTGCACATTACTAAGTTGCA Reverse: CTCGCTTCGGCAGCACA
U6	Forward: AGGGGCCATCCACAGTCTTC Reverse: AACGCTTCACGAATTTGCGT
GAPDH	Forward: AAAAGGGCCCTGACAACCTCTT Reverse: ACCCTGTTGCTGTAGCCAAA
SMAD6	Forward: TTGTCATTAGGGACCCTCAGC Reverse: TTGGCAGGAAATGCAGGTTTG
TNF- $\alpha$	Forward: AAGATAGGGTGTCTGGCACA Reverse: CCCTGAGGTGTCTGGTTTCT
IL-6	Forward: AGCAGGCACCCCAGTTAAT Reverse: AATCCTTTGCACTGGAGGGA
SMAD6 siRNA	Forward: CCACAUUGUCUUACACUGAAACGGA Reverse: UCCGUUUCAGUGUAGACAAUGUGG
si-control	AAUUCUCCGAACGUGUCACGU
MiR-32-5p mimic	Forward: UAUUGCACAUAUACUAAAGUUGCA Reverse: CAACUUAGUAAUGUGCAAUAUU
Mimic NC	UUCUCCGAACGUGUCACUGUU
MiR-32-5p inhibitor	UGCAACUUAGUAAUGUGCAAUA
Inhibitor NC	CAGUACUUUUGUGUAGUACAA

U6: U6 small nuclear RNA; GAPDH: Glyceraldehyde-3-phosphate dehydrogenase; SMAD6: SMAD family member 6; NC: Negative control.

Wild type (WT) and mutant (Mut) SMAD6 containing predicted sites with miR-32-5p were obtained from Sangon Biotech (China). After transfection for 48 h, the cells were tested using the Bio-Glo Luciferase Assay System (Promega, United States).

### Western blot analysis

Western blot analysis was performed as previously described<sup>[16]</sup>. Primary antibodies (mouse monoclonal to SMAD6, Santa Cruz Biotechnology, United States; rabbit monoclonal to TAK1, Abcam, United States; rabbit monoclonal to TAK1, phosphor S439, Abcam; rabbit monoclonal to p38, Abcam; rabbit monoclonal to p38, phosphor T180, Abcam; mouse monoclonal to Actin, Beyotime, China) were used in our research. The ChemDoc XRS+ System (Bio-Rad, United States) was utilized to evaluate the protein bands.

### Statistical analysis

The data are expressed as the mean  $\pm$  standard deviation (SD) and analyzed by non-parametric *t*-tests using GraphPad Prism 6.0 software (GraphPad, United States). *P* < 0.05 was considered statistically significant.

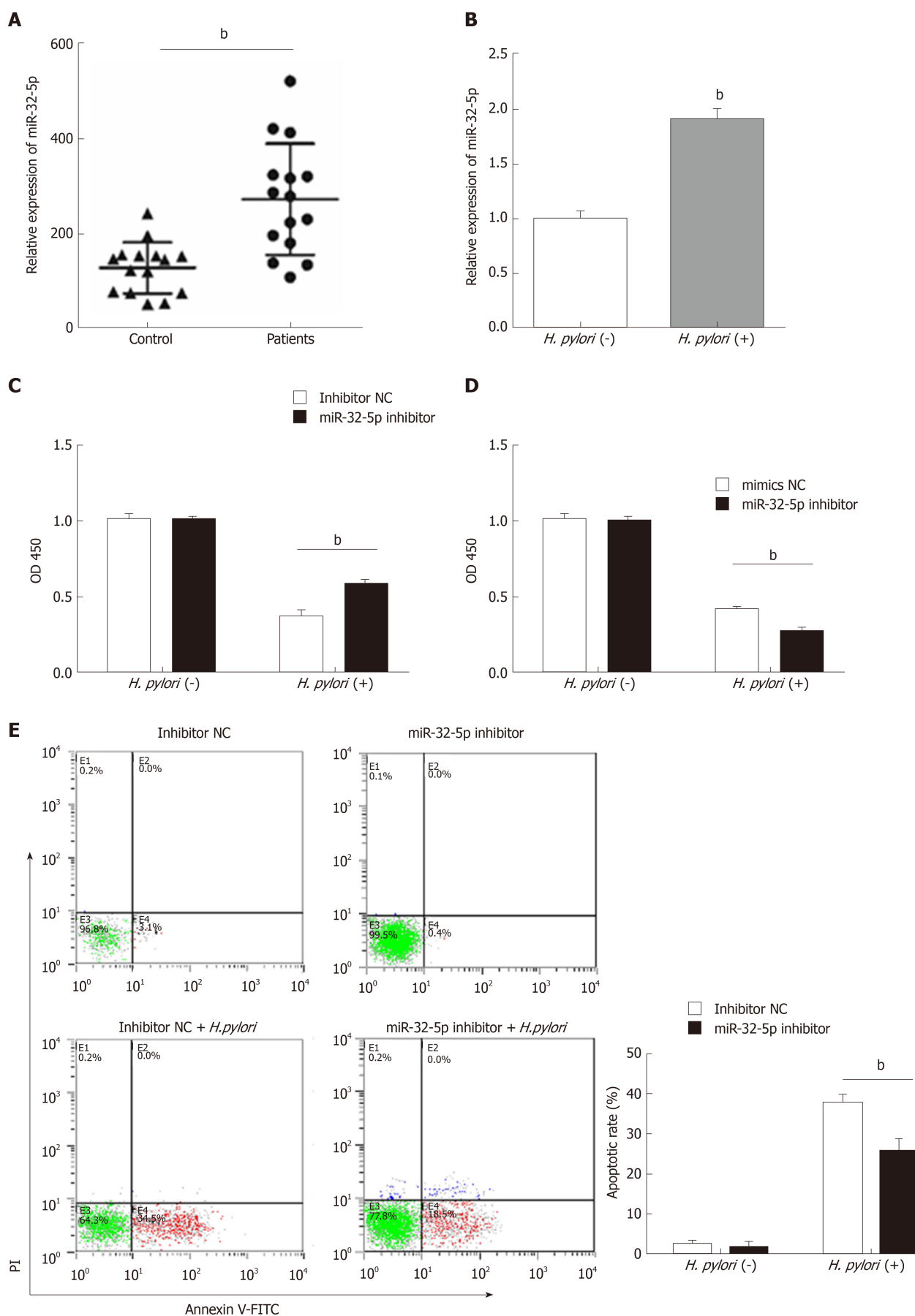
## RESULTS

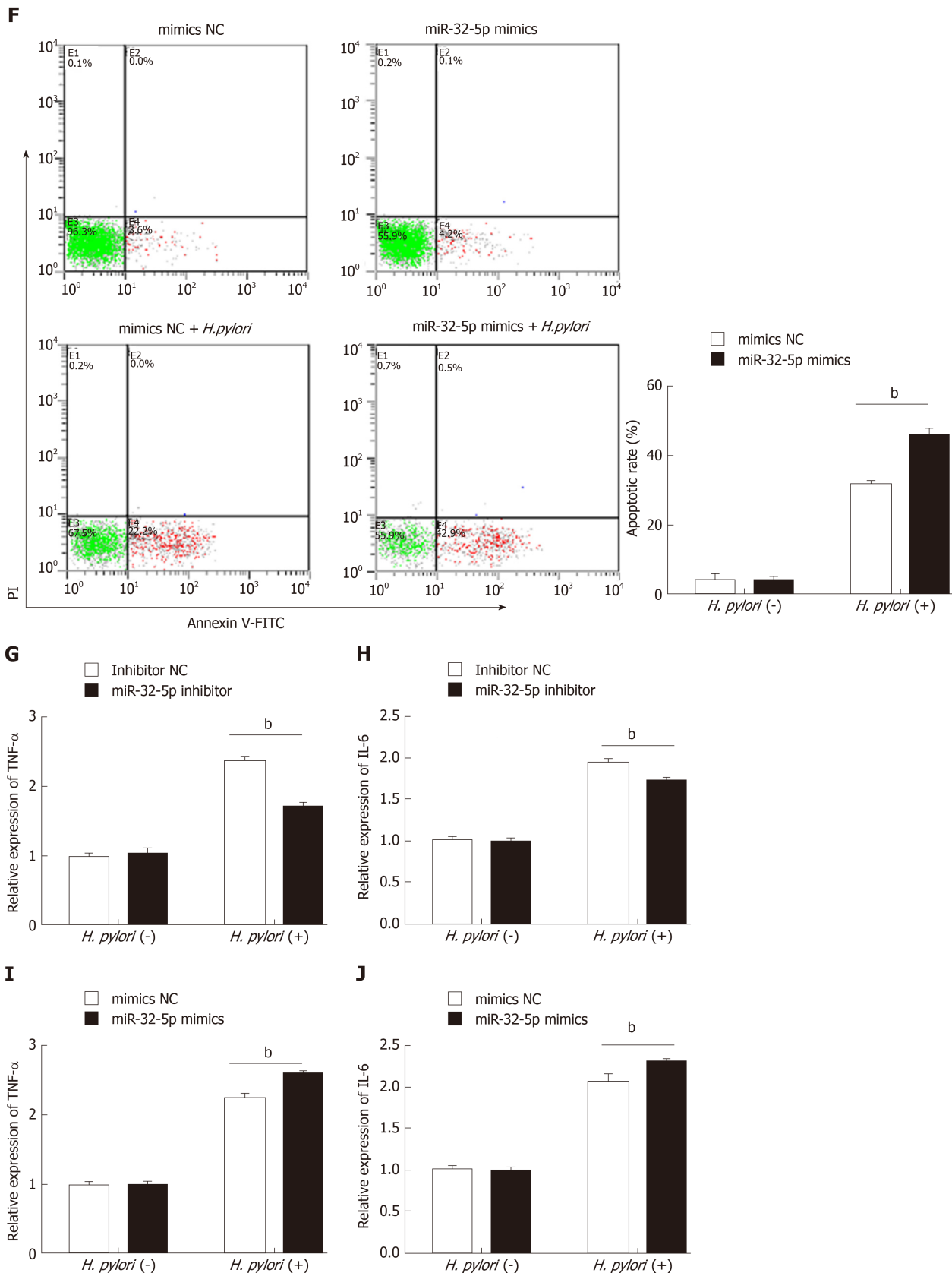
### MiR-32-5p is overexpressed in enteritis

To explore the potential role of miR-32-5p in pediatric enteritis, we first monitored the expression of miR-32-5p. After separating the serum from children with enteritis induced by *H. pylori* and healthy controls, we found that miR-32-5p was upregulated in serum of children with *H. pylori*-induced pediatric enteritis (Figure 1A). Next, we treated intestinal epithelial cells with *H. pylori*. The qRT-PCR results displayed that *H. pylori* led to a significant increase of miR-32-5p in intestinal epithelial cells (Figure 1B). These findings suggested that miR-32-5p might play a crucial role in *H. pylori*-related pediatric enteritis.

### MiR-32-5p regulates biological behavior of *H. pylori*-treated intestinal epithelial cells

Next, cell transfection with miR-32-5p inhibitor or miR-32-5p mimic was utilized to





**Figure 1** Aberrant expression of miR-32-5p in enteritis regulates biological function of intestinal epithelial cells. A: Expression of miR-32-5p in serum of pediatric enteritis; B: Expression of miR-32-5p in intestinal epithelial cells infected by *Helicobacter pylori* (*H. pylori*); C: Cell viability measurement in intestinal epithelial cells transfected with miR-32-5p inhibitor in the presence or absence of *H. pylori*; D: Viability measurement in intestinal epithelial cells transfected with miR-32-5p mimic in the presence or absence of *H. pylori*; E: Apoptosis of intestinal epithelial cells with miR-32-5p inhibitor transfection in the presence or absence of *H. pylori*; F: Apoptosis of intestinal epithelial cells with miR-32-5p mimic transfection in the presence or absence of *H. pylori*; G: The mRNA level of TNF- $\alpha$  in *H. pylori*-infected intestinal epithelial cells in the presence of miR-32-5p inhibitor; I: The mRNA level of TNF- $\alpha$  in *H. pylori*-infected intestinal epithelial cells in the presence of miR-32-5p mimic; H: The mRNA level of IL-6 in *H. pylori*-infected intestinal epithelial cells in the presence of miR-32-5p inhibitor; J: The mRNA level of IL-6 in *H. pylori*-infected intestinal epithelial cells in the presence of miR-32-5p mimic. <sup>b</sup>*P* < 0.01. *H. pylori*: *Helicobacter pylori*.



verify the role of miR-32-5p in cell viability in the presence or absence of *H. pylori*. We found that *H. pylori* impaired cell viability, and miR-32-5p inhibitor partially restored the viability of *H. pylori*-infected intestinal epithelial cells (Figure 1C). On the contrary, miR-32-5p mimic further caused the decrease of viability of *H. pylori*-infected intestinal epithelial cells (Figure 1D). In parallel, *H. pylori*-infected intestinal epithelial cells with miR-32-5p inhibitor displayed a lower apoptotic rate, and miR-32-5p mimic facilitated apoptosis of *H. pylori*-infected intestinal epithelial cells (Figure 1E and F). In addition, we found that TNF- $\alpha$  was upregulated in intestinal epithelial cells infected with *H. pylori*, which was decreased by miR-32-5p inhibitor transfection and further increased by miR-32-5p mimic (Figure 1G and I). IL-6 expression displayed the similar trend as TNF- $\alpha$  (Figure 1H and J).

### **SMAD6 is the direct target of miR-32-5p**

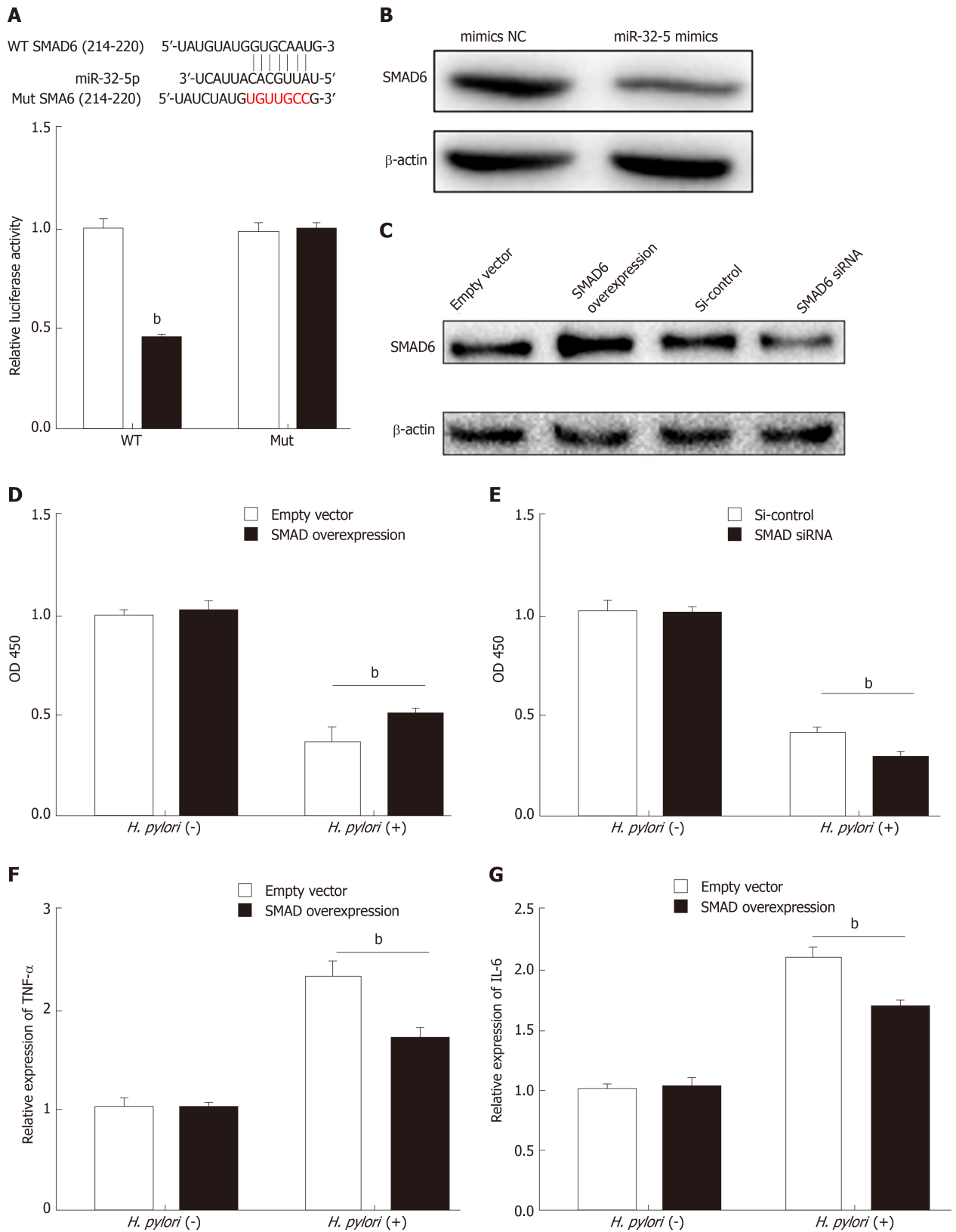
To further explore the downstream mechanism of miR-32-5p, we used TargetScanHuman 7.2 ([http://www.targetscan.org/vert\\_72/](http://www.targetscan.org/vert_72/)) to identify SMAD6, acting as a mediator of anti-inflammatory activity, as the potential target of miR-32-5p. The luciferase assay showed that SMAD6 was the direct target of miR-32-5p (Figure 2A). After transfecting with miR-32-5p mimic into intestinal epithelial cells, we found that the protein level of SMAD6 was downregulated (Figure 2B). Next, we performed cell transfection assay to make SMAD6 overexpress and knock down (Figure 2C). We further found that SMAD6 overexpression ameliorated the death of intestinal epithelial cells infected by *H. pylori* (Figure 2D). On the contrary, SMAD6 siRNA accelerated *H. pylori*-induced cell death (Figure 2E). In addition, SMAD6 could partially restrain the elevation of both TNF- $\alpha$  and IL-6 in intestinal epithelial cells infected by *H. pylori* (Figure 2F and G), while SMAD6 knockdown exerted an opposite role as SMAD6 overexpression did in the expression of TNF- $\alpha$  and IL-6 (Figure 2H and I). Therefore, these findings suggested that SMAD6 played a critical role in *H. pylori*-infected intestinal epithelial cells by acting as the downstream molecule of miR-32-5p.

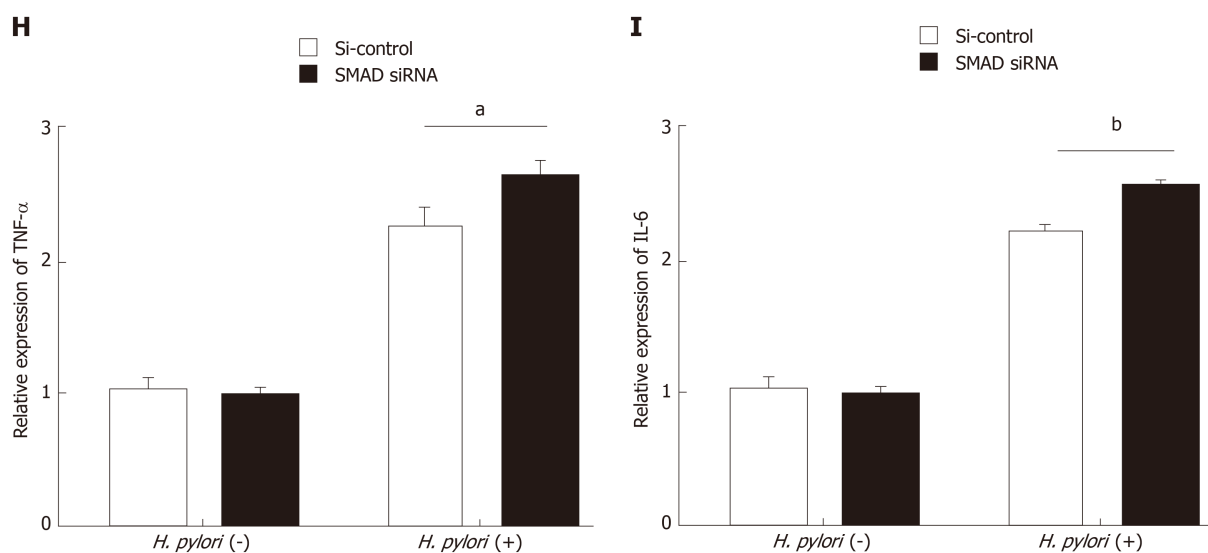
### **TGF- $\beta$ 1/p38 pathway is involved in apoptosis of *H. pylori*-infected intestinal epithelial cells**

SMAD6 is a downstream molecule of transforming growth factor- $\beta$ 1 (TGF- $\beta$ 1), and transforming growth factor- $\beta$ -activated kinase 1 (TAK1)-p38 cascade activation could be executed by TGF- $\beta$ 1<sup>[18,19]</sup>. We found that TGF- $\beta$ 1 treatment increased the apoptosis of intestinal epithelial cells, and both TAK1 inhibitor and p38 inhibitor could limit TGF- $\beta$ 1-induced apoptosis (Figure 3A). What's more, TGF- $\beta$ 1 led to the upregulation of phosphorylated TAK1 (p-TAK1) and phosphorylated p38 (p-p38), which could be restrained by TAK1 inhibitor (Figure 3B). However, TGF- $\beta$ 1-mediated phosphorylation of TAK1 was not inhibited by p38 inhibitor (Figure 3B). As shown in Figure 3C and D, TAK1 inhibitor and p38 inhibitor could partially increase the viability of intestinal epithelial cells infected with *H. pylori*, while miR-32-5p mimic, combined with either TAK1 inhibitor or p38 inhibitor, led to a marked decrease in the cell viability (Figure 3C). On the contrary, miR-32-5p further increased cell viability with either TAK1 inhibitor or p38 inhibitor under *H. pylori* infection (Figure 3D). Consistent with the findings in the cell viability, we found that both TAK1 inhibitor and p38 inhibitor could partially restrained the apoptosis of *H. pylori*-infected intestinal epithelial cells (Figure 3E and F). When miR-32-5p mimic was transfected into the cells with either TAK1 inhibitor or p38 inhibitor under *H. pylori* infection, apoptosis increased significantly (Figure 3E). However, miR-32-5p inhibitor transfection played an opposite role as miR-32-5p mimic did (Figure 3F). Thus, these results suggested that TGF- $\beta$ 1-TAK1-p38 cascade contributed to intestinal epithelial cell damage under *H. pylori* infection.

### **MiR-32-5p/SMAD6 contributes to TAK1-p38 pathway activation in intestinal epithelial cells infected by *H. pylori***

Next, we found the upregulation of p-TAK1 and p-p38 in intestinal epithelial cells with *H. pylori* infection (Figure 4A). SMAD6 is one of the inhibitory SMADs that could block TGF- $\beta$ 1 signaling<sup>[19]</sup>. Once SMAD6 overexpression plasmid was transfected into the cells, the activation of TAK1-p38 cascade was limited significantly (Figure 4B). Moreover, we stimulated intestinal epithelial cells with patient serum, and found that SMAD6 was downregulated (Figure 4C). When miR-32-5p antagonist was added into the patient serum, the downregulated expression of SMAD6 was reversed (Figure 4D). We also found that patient serum treatment activated TAK1 and p38 in intestinal epithelial cells compared with healthy control serum treatment (Figure 4E). However, miR-32-5p antagonist could result in downregulation of p-TAK1 and p-p38 in intestinal epithelial cells cultured in medium containing patient serum (Figure 4F).





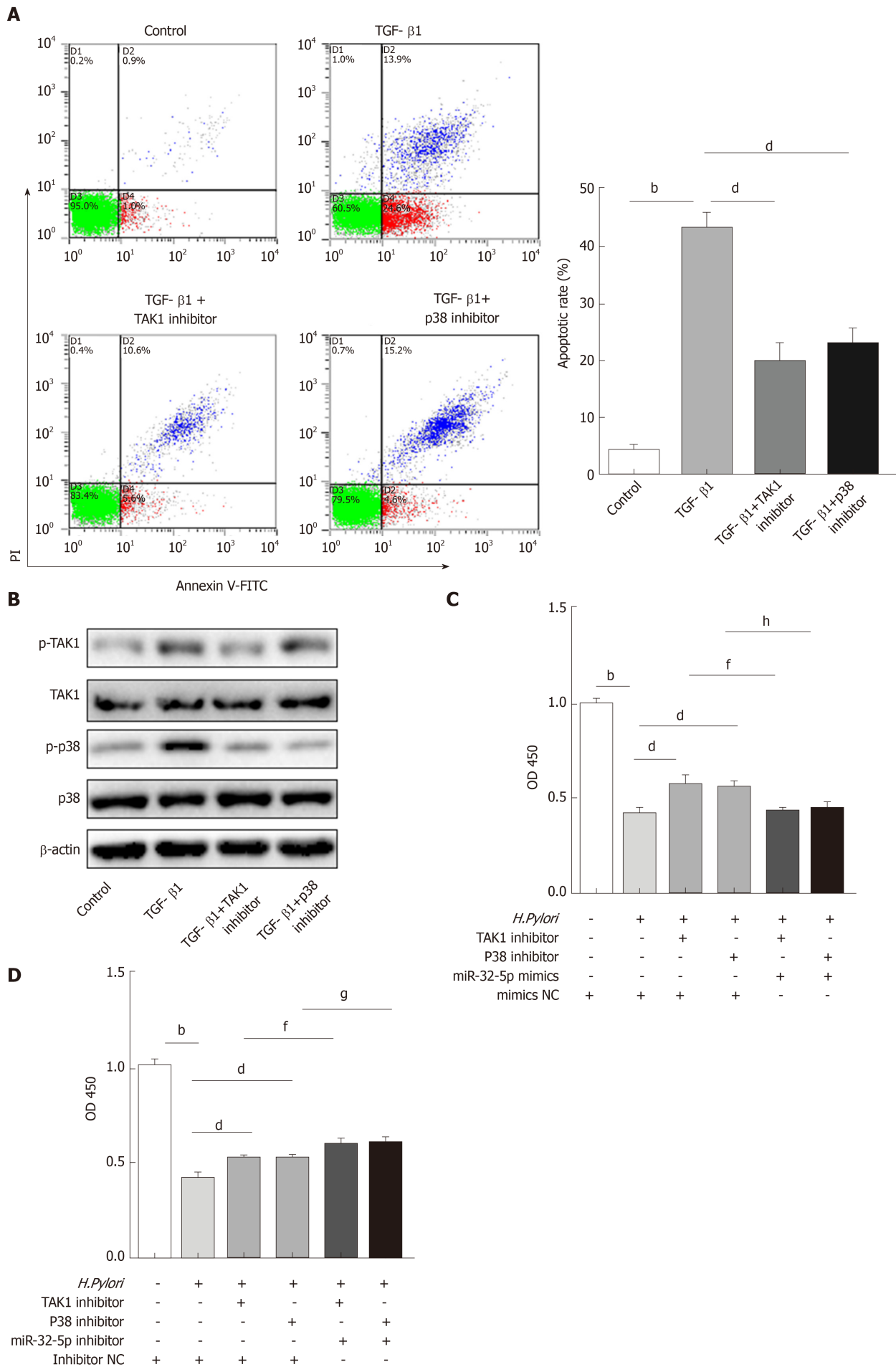
**Figure 2** SMAD family member 6 is sponged by miR-32-5p in intestinal epithelial cells. A: Luciferase assay for determining the binding between miR-32-5p and SMAD family member 6 (SMAD6); B: Protein level of SMAD6 in intestinal epithelial cells transfected with miR-32-5p mimic; C: Expression of SMAD6 in intestinal epithelial cells after SMAD6 overexpression and knockdown; D: Cell viability measurement in intestinal epithelial cells after SMAD6 overexpression in the presence or absence of *H. pylori*; E: Cell viability measurement in intestinal epithelial cells after SMAD6 knockdown in the presence or absence of *Helicobacter pylori* (*H. pylori*); F: The mRNA level of TNF-α in *H. pylori*-infected intestinal epithelial cells after SMAD6 overexpression; H: The mRNA level of TNF-α in *H. pylori*-infected intestinal epithelial cells after SMAD6 knockdown; G: IL-6 expression in *H. pylori*-infected intestinal epithelial cells after SMAD6 overexpression; I: IL-6 expression in *H. pylori*-infected intestinal epithelial cells after SMAD6 knockdown. <sup>a</sup>*P* < 0.05, <sup>b</sup>*P* < 0.01. SMAD6: SMAD family member 6; *H. pylori*: *Helicobacter pylori*.

## DISCUSSION

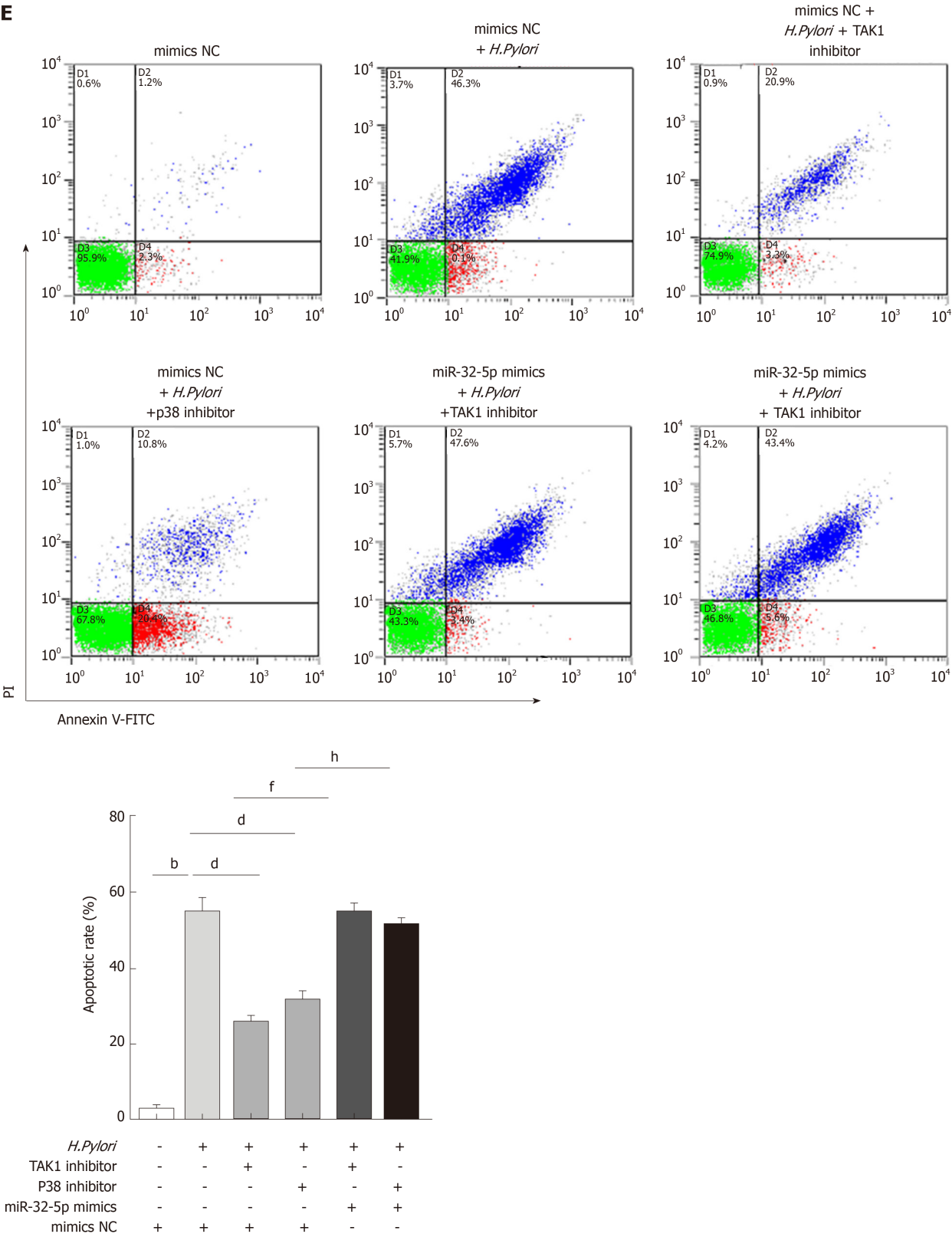
As a common digestive disease in children, enteritis could cause abdominal pain, diarrhea, and dyspepsia. If chronic enteritis results from the nonstandard treatment, children might display malnutrition, even severely affecting health and growth of children. Virus infection is regarded as the leading cause of pediatric enteritis worldwide<sup>[20,21]</sup>, which might lead to a local outbreak. However, what could not be ignored is that bacterial infection is also an important pathogenic factor resulting in pediatric enteritis. It has been reported that *H. pylori* infection displayed a remarkable correlation with pediatric enteritis<sup>[2,22]</sup>. However, there is a lack of systematic understanding about the correlation between *H. pylori* infection and the pathogenesis of pediatric enteritis.

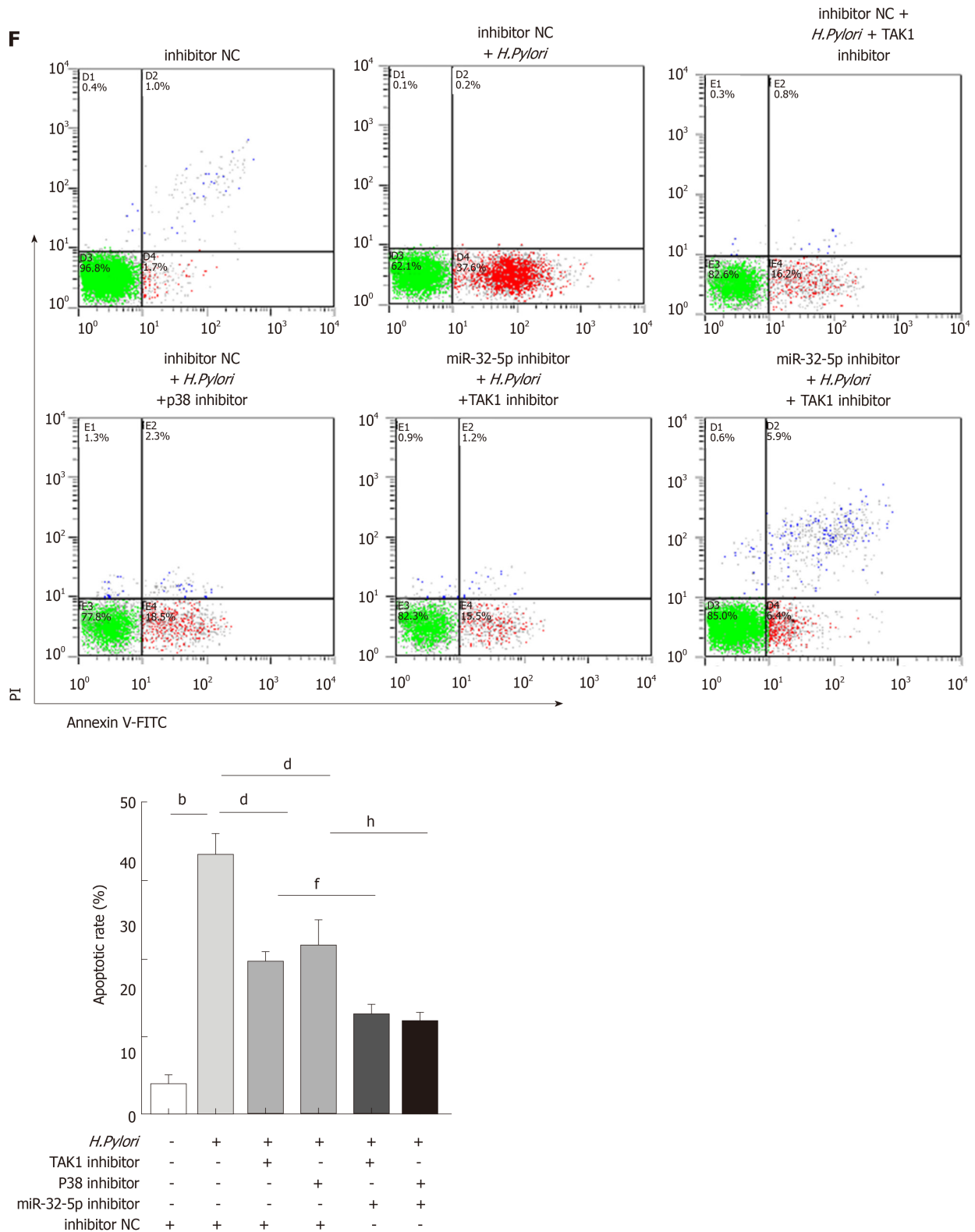
*H. pylori* is a common bacterium that could cause gastritis, gastric ulcer, and even gastric cancer<sup>[3,7,23]</sup>. A great deal of evidence has revealed that multiple factors contribute to *H. pylori* infection, including autophagy, miRNAs, and long non-coding RNAs (lncRNAs). *H. pylori* could promote autophagy of gastric adenocarcinoma epithelial cells, and increased antibiotic resistance of *H. pylori*-infected cells<sup>[24]</sup>. Yang *et al.*<sup>[25]</sup> reported that miR-30d regulated autophagy-related proteins to facilitate *H. pylori* survival within cells. An increasing number of miRNAs and lncRNAs were identified by different research groups, which displayed a tight relationship with *H. pylori* infection<sup>[6,14,26,27]</sup>. In the current study, we found the upregulation of miR-32-5p in serum of patients with *H. pylori*-related pediatric enteritis and *H. pylori*-infected intestinal epithelial cells. In addition, miR-32-5p inhibition could rescue intestinal epithelial cells infected with *H. pylori*, reduce *H. pylori*-induced apoptosis, and restrain the increase of inflammatory cytokines of *H. pylori*-infected cells, which inferred that miR-32-5p contributed to intestinal epithelial cell injury caused by *H. pylori* infection.

Currently, only a few studies focus on miR-32-5p, and these research findings are largely about the relationship between miR-32-5p and the pathogenesis of tumors, including cervical cancer<sup>[28]</sup>, prostate cancer<sup>[29]</sup>, hepatocellular carcinoma<sup>[30]</sup>, and pancreatic cancer<sup>[31]</sup>. Besides, Zhang and colleagues<sup>[32]</sup> discovered that *Mycobacterium tuberculosis* infection led to a significant increase of miR-32-5p in macrophages, which in turns promoted *Mycobacterium tuberculosis* survival in the infected cells by targeting the downstream molecules of miR-32-5p. We found that SMAD6 was a direct target of miR-32-5p to be involved in *H. pylori*-induced intestinal epithelial cell damage. It has been demonstrated that SMAD6 is one of the two inhibitory SMADs (*e.g.*, SMAD6 and SMAD7) downstream of TGF-β, and could inhibit inflammation and cell apoptosis<sup>[19,33,34]</sup>. Our findings revealed that SMAD6 overexpression could increase resistance of intestinal epithelial cells to *H. pylori*, and reduce inflammatory cytokines caused by *H. pylori*. Next, we found that TGF-β1-activated TAK1-p38 cascade

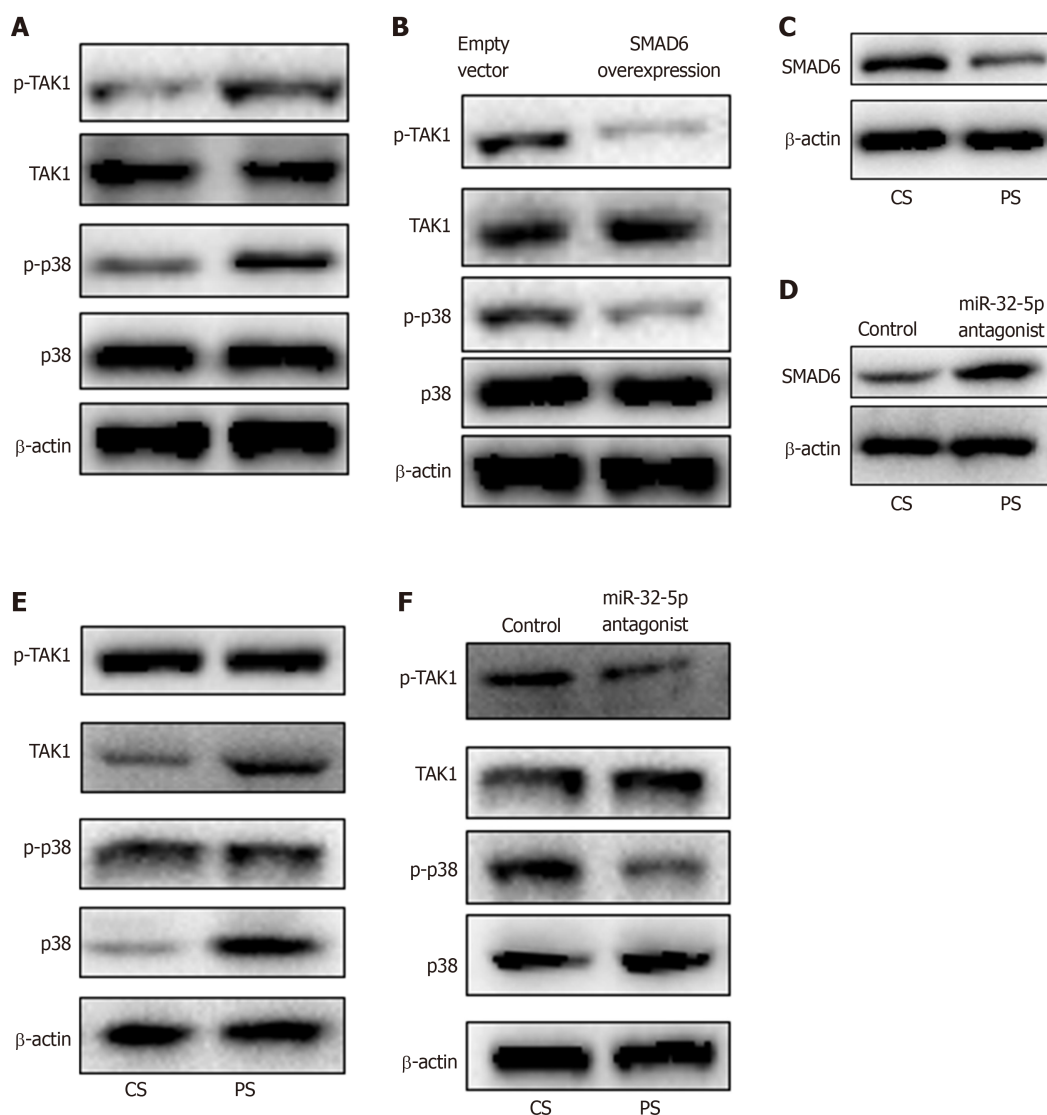








**Figure 3** Transforming growth factor- $\beta$ 1/p38 participates in apoptosis of intestinal epithelial cells infected by *Helicobacter pylori*. A: Apoptosis detection in transforming growth factor- $\beta$ 1 (TGF- $\beta$ 1)-treated intestinal epithelial cells in the presence of transforming growth factor- $\beta$ -activated kinase 1 (TAK1) inhibitor and p38 inhibitor; B: Protein levels of total TAK1, p38, phosphorylated TAK1, and phosphorylated p38 in TGF- $\beta$ 1-treated intestinal epithelial cells in the presence of TAK1 inhibitor and p38 inhibitor; C: Cell viability measurement in *Helicobacter pylori* (*H. pylori*)-infected intestinal epithelial cells with TAK1 inhibitor and p38 inhibitor treatment followed by transfection with miR-32-5p mimic; D: Cell viability measurement in *H. pylori*-infected intestinal epithelial cells with TAK1 inhibitor and p38 inhibitor treatment followed by transfection with miR-32-5p inhibitor; E: Apoptosis evaluation in *H. pylori*-infected intestinal epithelial cells with TAK1 inhibitor and p38 inhibitor treatment followed by transfection with miR-32-5p mimic; F: Apoptosis evaluation in *H. pylori*-infected intestinal epithelial cells with TAK1 inhibitor and p38 inhibitor treatment followed by transfection with miR-32-5p inhibitor. <sup>b</sup> $P < 0.01$ , <sup>d</sup> $P < 0.01$ , <sup>f</sup> $P < 0.01$ , <sup>h</sup> $P < 0.05$ , <sup>h</sup> $P < 0.01$ . TGF- $\beta$ 1: Transforming growth factor- $\beta$ 1; TAK1: Transforming growth factor- $\beta$ -activated kinase 1; *H. pylori*: *Helicobacter pylori*.



**Figure 4** MiR-32-5p/SMAD family member 6 is involved in transforming growth factor- $\beta$ -activated kinase 1-p38 pathway in intestinal epithelial cells. A: Detection of transforming growth factor- $\beta$ -activated kinase 1 (TAK1)-p38 activation in *Helicobacter pylori* (*H. pylori*)-treated intestinal epithelial cells by Western blot; B: Inhibition of TAK1-p38 activation in *H. pylori*-treated intestinal epithelial cells with SMAD6 overexpression as revealed by Western blot; C: SMAD6 expression in intestinal epithelial cells treated with control serum and patient serum (PS); D: SMAD6 expression in PS-treated intestinal epithelial cells with miR-32-5p antagonist transfection; E: TAK1-p38 activation in PS-treated intestinal epithelial cells as revealed by Western blot; F: Inhibition of TAK1-p38 activation in PS-treated intestinal epithelial cells with miR-32-5p antagonist transfection as revealed by Western blot. CS: Control serum; PS: Patient serum; SMAD6: SMAD family member 6; TAK1: Transforming growth factor- $\beta$ -activated kinase 1; *H. pylori*: *Helicobacter pylori*.

contributed to *H. pylori*-induced intestinal epithelial cell injury. Luo and colleagues reported that TGF- $\beta$ 1 mediated *H. pylori*-related gastritis, and blocking TGF- $\beta$ 1 could effectively alleviate gastritis<sup>[35]</sup>. As we verified, inhibition of TAK1 activation and p38 activation could partially protect epithelial cells from *H. pylori* infection. Moreover, miR-32-5p inhibition further improved the protective role of TAK1 inhibitor and p38 inhibitor in *H. pylori*-infected intestinal epithelial cells.

Recently, TGF- $\beta$  was determined to be involved in *H. pylori* infection. A recent study found that *H. pylori* facilitated the expression of TGF- $\beta$ , and induced downregulation of cystic fibrosis transmembrane conductance regulator (CFTR) and solute linked carrier 26 gene family A6 (SLC26A6) in the duodenum<sup>[36]</sup>. Patients with *H. pylori*-induced duodenal ulcers displayed significantly decreased expression of CFTR and SLC26A6, which displayed a remarkable correlation with the severity of the illness<sup>[37]</sup>. In addition to affecting the function of intestinal epithelial cells, *H. pylori* could modulate the role of immune cells in the intestinal tract. A previous study suggested that *H. pylori* led to the upregulation of heat shock protein 60 in macrophages to promote TGF- $\beta$  production, which contributed to the infiltration of regulatory T cells (Treg) to cause persistent infection<sup>[38]</sup>. Clinical data showed an increased number of Treg in children with *H. pylori* infection, and TGF- $\beta$  had a positive correlation with the increase of Treg<sup>[39]</sup>. In our study, we discovered a novel

manner involving TGF- $\beta$ 1 in which *H. pylori* infection damaged intestinal epithelial cells. Induction of miR-32-5p by *H. pylori* infection led to decreased expression of SMAD6, which weakened the inhibitory role of SMAD6 in TGF- $\beta$ 1-TAK1-p38 cascade activation, as demonstrated by the treatment of serum samples in intestinal epithelial cells.

Based on the above findings, we concluded that *H. pylori* infection promotes miR-32-5p upregulation to aggravate apoptosis and inflammation in intestinal epithelial cells by targeting SMAD6 and activating the TAK1-p38 pathway, highlighting a crucial role of miR-32-5p in the pathogenesis of pediatric enteritis caused by *H. pylori*.

## ARTICLE HIGHLIGHTS

### Research background

*Helicobacter pylori* (*H. pylori*) infection is a global issue that could cause a variety of diseases involving multiple organs. It is worth noting that the incidence of *H. pylori*-related enteritis in children increases, but the underlying mechanism is largely unknown. It has been reported that miR-32-5p is overexpressed in diseases associated with bacterial infection. However, the potential role of miR-32-5p in *H. pylori*-induced pediatric enteritis is not clear.

### Research motivation

To investigate the exact role of miR-32-5p in the pathogenesis of pediatric enteritis with *H. pylori* infection, and to find a novel target for *H. pylori*-related enteritis in children.

### Research objectives

To explore the aberrant expression and significance of miR-32-5p in children with *H. pylori*-related enteritis, especially in the damage of intestinal epithelial cells with *H. pylori* infection.

### Research methods

qRT-PCR was performed to detect the expression of miR-32-5p in clinical samples and *H. pylori*-infected intestinal epithelial cells. Cell Counting Kit-8 assay and flow cytometry were conducted to evaluate the role of miR-32-5p in *H. pylori*-infected intestinal epithelial cells. TargetScanHuman database and luciferase assay were utilized to verify the potential target of miR-32-5p. Western blot was employed to clarify the underlying mechanism of miR-32-5p in influencing *H. pylori*-infected intestinal epithelial cells.

### Research results

The present study discovered the aberrant expression of miR-32-5p in pediatric enteritis with *H. pylori* infection and *H. pylori*-treated intestinal epithelial cells. The *in vitro* experiments showed the significance of miR-32-5p in regulating cell viability and apoptosis of *H. pylori*-treated intestinal epithelial cells. We identified that SMAD family member 6 (SMAD6) was the direct target of miR-32-5p, and SMAD6 partially counteracted the harmful role of miR-32-5p by inhibiting the activation of TAK1-p38 cascade. However, *in vivo* assays are needed to further verify our *in vitro* findings and significance of miR-32-5p in *H. pylori*-induced pediatric enteritis.

### Research conclusions

Our research first identified the upregulation of miR-32-5p in *H. pylori*-related pediatric enteritis. Further exploration revealed that miR-32-5p inhibited SMAD6 to activate the TAK1-p38 signaling pathway, aggravating *H. pylori*-induced damage of intestinal epithelial cells. MiR-32-5p might be a potential target to overcome *H. pylori*-induced damage of intestinal epithelial cells in children.

### Research perspectives

Based on the clinical findings and *in vitro* experiments, miR-32-5p could be a novel therapeutic target for *H. pylori*-induced damage of intestinal epithelial cells in children. Further *in vivo* assays are of necessity to clarify the deleterious effects of miR-32-5p on *H. pylori*-infected intestinal epithelial cells, which is very meaningful and would contribute to clinical application.

## REFERENCES

1. Chen J, Wan CM, Gong ST, Fang F, Sun M, Qian Y, Huang Y, Wang BX, Xu CD, Ye LY, Dong M, Jin Y, Huang ZH, Wu QB, Zhu CM, Fang YH, Zhu QR, Dong YS. Chinese clinical practice guidelines for acute infectious diarrhea in children. *World J Pediatr* 2018; **14**: 429-436 [PMID: 30269306 DOI: 10.1007/s12519-018-0190-2]
2. Zhang SH, Zhu X. Advances in *Helicobacter pylori* in children. *Linchuang Erke Zazhi* 2015; **33**: 391-395
3. Vogiatzi P, Cassone M, Luzzi I, Lucchetti C, Otvos L, Giordano A. *Helicobacter pylori* as a class I carcinogen: physiopathology and management strategies. *J Cell Biochem* 2007; **102**: 264-273 [PMID: 17486575 DOI: 10.1002/jcb.21375]
4. Ren WK, Xu YF, Wei WH, Huang P, Lian DW, Fu LJ, Yang XF, Chen FJ, Wang J, Cao HY, Deng YH. Effect of patchouli alcohol on *Helicobacter pylori*-induced neutrophil recruitment and activation. *Int Immunopharmacol* 2019; **68**: 7-16 [PMID: 30599446 DOI: 10.1016/j.intimp.2018.12.044]
5. Li FY, Weng IC, Lin CH, Kao MC, Wu MS, Chen HY, Liu FT. *Helicobacter pylori* induces intracellular



- galectin-8 aggregation around damaged lysosomes within gastric epithelial cells in a host O-glycan-dependent manner. *Glycobiology* 2019; **29**: 151-162 [PMID: 30289459 DOI: 10.1093/glycob/cwy095]
- 6 Santos JC, Brianti MT, Almeida VR, Ortega MM, Fischer W, Haas R, Matheu A, Ribeiro ML. Helicobacter pylori infection modulates the expression of miRNAs associated with DNA mismatch repair pathway. *Mol Carcinog* 2017; **56**: 1372-1379 [PMID: 27862371 DOI: 10.1002/mc.22590]
- 7 Mnich E, Kowalewicz-Kulbat M, Sicińska P, Hinc K, Obuchowski M, Gajewski A, Moran AP, Chmiela M. Impact of Helicobacter pylori on the healing process of the gastric barrier. *World J Gastroenterol* 2016; **22**: 7536-7558 [PMID: 27672275 DOI: 10.3748/wjg.v22.i33.7536]
- 8 Alper A, Hardee S, Rojas-Velasquez D, Escalera S, Morotti RA, Pashankar DS. Prevalence and Clinical, Endoscopic, and Pathological Features of Duodenitis in Children. *J Pediatr Gastroenterol Nutr* 2016; **62**: 314-316 [PMID: 26252915 DOI: 10.1097/MPG.0000000000000942]
- 9 Gimiga N, Olaru C, Diaconescu S, Miron I, Burlea M. Upper gastrointestinal bleeding in children from a hospital center of Northeast Romania. *Minerva Pediatr* 2016; **68**: 189-195 [PMID: 27125439]
- 10 Bossi L, Figueroa-Bossi N. Competing endogenous RNAs: a target-centric view of small RNA regulation in bacteria. *Nat Rev Microbiol* 2016; **14**: 775-784 [PMID: 27640758 DOI: 10.1038/nrmicro.2016.129]
- 11 Beermann J, Piccoli MT, Viereck J, Thum T. Non-coding RNAs in Development and Disease: Background, Mechanisms, and Therapeutic Approaches. *Physiol Rev* 2016; **96**: 1297-1325 [PMID: 27535639 DOI: 10.1152/physrev.00041.2015]
- 12 Subramaniam S, Jeet V, Clements JA, Gunter JH, Batra J. Emergence of MicroRNAs as Key Players in Cancer Cell Metabolism. *Clin Chem* 2019; **65**: 1090-1101 [PMID: 31101638 DOI: 10.1373/clinchem.2018.299651]
- 13 Zabaglia LM, Sallas ML, Santos MPD, Orcini WA, Peruquetti RL, Constantino DH, Chen E, Smith MAC, Payão SM, Rasmussen LT. Expression of miRNA-146a, miRNA-155, IL-2, and TNF- $\alpha$  in inflammatory response to Helicobacter pylori infection associated with cancer progression. *Ann Hum Genet* 2018; **82**: 135-142 [PMID: 29250766 DOI: 10.1111/ahg.12234]
- 14 Cortés-Márquez AC, Mendoza-Elizalde S, Arenas-Huetero F, Trillo-Tinoco J, Valencia-Mayoral P, Consuelo-Sánchez A, Zarate-Franco J, Dionicio-Avendaño AR, Herrera-Esquivel JJ, Recinos-Carrera EG, Colín-Valverde C, Rivera-Gutiérrez S, Reyes-López A, Viguera-Galindo JC, Velázquez-Guadarrama N. Differential expression of miRNA-146a and miRNA-155 in gastritis induced by Helicobacter pylori infection in paediatric patients, adults, and an animal model. *BMC Infect Dis* 2018; **18**: 463 [PMID: 30219037 DOI: 10.1186/s12879-018-3368-2]
- 15 Li Q, Wang N, Wei H, Li C, Wu J, Yang G. miR-24-3p Regulates Progression of Gastric Mucosal Lesions and Suppresses Proliferation and Invasiveness of N87 Via Peroxiredoxin 6. *Dig Dis Sci* 2016; **61**: 3486-3497 [PMID: 27743162 DOI: 10.1007/s10620-016-4309-9]
- 16 Zou M, Wang F, Jiang A, Xia A, Kong S, Gong C, Zhu M, Zhou X, Zhu J, Zhu W, Cheng W. MicroRNA-3178 ameliorates inflammation and gastric carcinogenesis promoted by Helicobacter pylori new toxin, Tip- $\alpha$ , by targeting TRAF3. *Helicobacter* 2017; **22** [PMID: 27493095 DOI: 10.1111/hel.12348]
- 17 Beceiro S, Radin JN, Chaturvedi R, Piazuelo MB, Horvath DJ, Cortado H, Gu Y, Dixon B, Gu C, Lange I, Koomoa DL, Wilson KT, Algood HM, Partida-Sánchez S. TRPM2 ion channels regulate macrophage polarization and gastric inflammation during Helicobacter pylori infection. *Mucosal Immunol* 2017; **10**: 493-507 [PMID: 27435104 DOI: 10.1038/mi.2016.60]
- 18 Liao SJ, Luo J, Li D, Zhou YH, Yan B, Wei JJ, Tu JC, Li YR, Zhang GM, Feng ZH. TGF- $\beta$ 1 and TNF- $\alpha$  synergistically induce epithelial to mesenchymal transition of breast cancer cells by enhancing TAK1 activation. *J Cell Commun Signal* 2019; **13**: 369-380 [PMID: 30739244 DOI: 10.1007/s12079-019-00508-8]
- 19 Jung SM, Lee JH, Park J, Oh YS, Lee SK, Park JS, Lee YS, Kim JH, Lee JY, Bae YS, Koo SH, Kim SJ, Park SH. Smad6 inhibits non-canonical TGF- $\beta$ 1 signalling by recruiting the deubiquitinase A20 to TRAF6. *Nat Commun* 2013; **4**: 2562 [PMID: 24096742 DOI: 10.1038/ncomms3562]
- 20 Mursalova N, Shugayev N, Suleymanova J, Daniels DS, Wasley A, Cohen AL, Aliabadi N. Rotavirus gastroenteritis surveillance in Azerbaijan, 2011-2016. *Vaccine* 2018; **36**: 7790-7793 [PMID: 29784471 DOI: 10.1016/j.vaccine.2018.02.045]
- 21 Chen SY, Chiu CH. Worldwide molecular epidemiology of norovirus infection. *Paediatr Int Child Health* 2012; **32**: 128-131 [PMID: 22824658 DOI: 10.1179/2046905512Y.0000000031]
- 22 Bansal D, Patwari AK, Logani KB, Malhotra VL, Anand VK. Study of diagnostic modalities and pathology of Helicobacter pylori infection in children. *Indian J Pathol Microbiol* 1999; **42**: 311-315 [PMID: 10862290]
- 23 Reshetnyak VI, Reshetnyak TM. Significance of dormant forms of Helicobacter pylori in ulcerogenesis. *World J Gastroenterol* 2017; **23**: 4867-4878 [PMID: 28785141 DOI: 10.3748/wjg.v23.i27.4867]
- 24 Chu YT, Wang YH, Wu JJ, Lei HY. Invasion and multiplication of Helicobacter pylori in gastric epithelial cells and implications for antibiotic resistance. *Infect Immun* 2010; **78**: 4157-4165 [PMID: 20696835 DOI: 10.1128/IAI.00524-10]
- 25 Yang XJ, Si RH, Liang YH, Ma BQ, Jiang ZB, Wang B, Gao P. Mir-30d increases intracellular survival of Helicobacter pylori through inhibition of autophagy pathway. *World J Gastroenterol* 2016; **22**: 3978-3991 [PMID: 27099441 DOI: 10.3748/wjg.v22.i15.3978]
- 26 Yang L, Long Y, Li C, Cao L, Gan H, Huang K, Jia Y. Genome-wide analysis of long noncoding RNA profile in human gastric epithelial cell response to Helicobacter pylori. *Jpn J Infect Dis* 2015; **68**: 63-66 [PMID: 25420666 DOI: 10.7883/yoken.JJID.2014.149]
- 27 Sun F, Ni Y, Zhu H, Fang J, Wang H, Xia J, Ding F, Shen H, Shao S. microRNA-29a-3p, Up-Regulated in Human Gastric Cells and Tissues with H.Pylori Infection, Promotes the Migration of GES-1 Cells via A20-Mediated EMT Pathway. *Cell Physiol Biochem* 2018; **51**: 1250-1263 [PMID: 30485838 DOI: 10.1159/000495502]
- 28 Liu YJ, Zhou HG, Chen LH, Qu DC, Wang CJ, Xia ZY, Zheng JH. MiR-32-5p regulates the proliferation and metastasis of cervical cancer cells by targeting HOXB8. *Eur Rev Med Pharmacol Sci* 2019; **23**: 87-95 [PMID: 30657550 DOI: 10.26355/eurrev\_201901\_16752]
- 29 Zhang L, Li X, Chao Y, He R, Liu J, Yuan Y, Zhao W, Han C, Song X. KLF4, a miR-32-5p targeted gene, promotes cisplatin-induced apoptosis by upregulating BIK expression in prostate cancer. *Cell Commun Signal* 2018; **16**: 53 [PMID: 30176890 DOI: 10.1186/s12964-018-0270-x]
- 30 Fu X, Liu M, Qu S, Ma J, Zhang Y, Shi T, Wen H, Yang Y, Wang S, Wang J, Nan K, Yao Y, Tian T. Exosomal miR-32-5p induces multidrug resistance in hepatocellular carcinoma via the PI3K/Akt pathway. *J Exp Clin Cancer Res* 2018; **37**: 52 [PMID: 29530052 DOI: 10.1186/s13046-018-0677-7]
- 31 Gao ZQ, Wang JF, Chen DH, Ma XS, Wu Y, Tang Z, Dang XW. Long non-coding RNA GASS

- suppresses pancreatic cancer metastasis through modulating miR-32-5p/PTEN axis. *Cell Biosci* 2017; **7**: 66 [PMID: 29225772 DOI: 10.1186/s13578-017-0192-0]
- 32 **Zhang ZM**, Zhang AR, Xu M, Lou J, Qiu WQ. TLR-4/miR-32-5p/FSTL1 signaling regulates mycobacterial survival and inflammatory responses in Mycobacterium tuberculosis-infected macrophages. *Exp Cell Res* 2017; **352**: 313-321 [PMID: 28215633 DOI: 10.1016/j.yexcr.2017.02.025]
- 33 **Lee YS**, Park JS, Jung SM, Kim SD, Kim JH, Lee JY, Jung KC, Mamura M, Lee S, Kim SJ, Bae YS, Park SH. Inhibition of lethal inflammatory responses through the targeting of membrane-associated Toll-like receptor 4 signaling complexes with a Smad6-derived peptide. *EMBO Mol Med* 2015; **7**: 577-592 [PMID: 25766838 DOI: 10.15252/emmm.201404653]
- 34 **Zhang T**, Wu J, Ungvijanpunya N, Jackson-Weaver O, Gou Y, Feng J, Ho TV, Shen Y, Liu J, Richard S, Jin J, Hajishengallis G, Chai Y, Xu J. Smad6 Methylation Represses NFκB Activation and Periodontal Inflammation. *J Dent Res* 2018; **97**: 810-819 [PMID: 29420098 DOI: 10.1177/0022034518755688]
- 35 **Luo J**, Song J, Zhang H, Zhang F, Liu H, Li L, Zhang Z, Chen L, Zhang M, Lin D, Lin M, Zhou R. Melatonin mediated Foxp3-downregulation decreases cytokines production via the TLR2 and TLR4 pathways in *H. pylori* infected mice. *Int Immunopharmacol* 2018; **64**: 116-122 [PMID: 30173051 DOI: 10.1016/j.intimp.2018.08.034]
- 36 **Wen G**, Deng S, Song W, Jin H, Xu J, Liu X, Xie R, Song P, Tuo B. Helicobacter pylori infection downregulates duodenal CFTR and SLC26A6 expressions through TGFβ signaling pathway. *BMC Microbiol* 2018; **18**: 87 [PMID: 30119655 DOI: 10.1186/s12866-018-1230-8]
- 37 **Wen G**, Jin H, Deng S, Xu J, Liu X, Xie R, Tuo B. Effects of Helicobacter pylori Infection on the Expressions and Functional Activities of Human Duodenal Mucosal Bicarbonate Transport Proteins. *Helicobacter* 2016; **21**: 536-547 [PMID: 27004488 DOI: 10.1111/hel.12309]
- 38 **Hsu WT**, Ho SY, Jian TY, Huang HN, Lin YL, Chen CH, Lin TH, Wu MS, Wu CJ, Chan YL, Liao KW. Helicobacter pylori-derived heat shock protein 60 increases the induction of regulatory T-cells associated with persistent infection. *Microb Pathog* 2018; **119**: 152-161 [PMID: 29660522 DOI: 10.1016/j.micpath.2018.04.016]
- 39 **Yang YJ**, Chuang CC, Yang HB, Lu CC, Sheu BS. Susceptibility to pediatric Helicobacter pylori infection correlates with the host responses of regulatory and effector T cells. *Pediatr Infect Dis J* 2014; **33**: 1277-1282 [PMID: 25389709 DOI: 10.1097/INF.0000000000000464]



## Retrospective Study

# Bacterobilia in pancreatic surgery-conclusions for perioperative antibiotic prophylaxis

Colin Markus Krüger, Ulrich Adam, Thomas Adam, Axel Kramer, Claus D Heidecke, Frank Makowiec, Hartwig Riediger

**ORCID number:** Colin Markus Krueger (0000-0003-4976-870X); Ulrich Adam (0000-0002-6458-0513); Thomas Adam (0000-0002-7658-9240); Axel Kramer (0000-0003-4193-2149); Claus D Heidecke (0000-0001-8664-9537); Frank Makowiec (0000-0003-0012-3775); Hartwig Riediger (0000-0003-2615-8853).

**Author contributions:** Krueger CM contributed to design of the study, acquisition and analysis of data, and writing of manuscript; Adam U contributed to performing of procedures, acquisition of data, and critical review of manuscript; Adam T contributed to acquisition of data and critical review of manuscript; Kramer A contributed to design of the study, analysis of data, interpretation of data, writing of manuscript, and reviewing the manuscript; Heidecke CD contributed to interpretation of data and critical review of manuscript; Makowiec F contributed to interpretation of data and critical review of manuscript; Riediger H contributed to design of the study, performing of procedures, analysis and interpretation of data, and writing of manuscript.

### Institutional review board

**statement:** The study was only reviewed and approved by the Review Board of Brandenburg Medical School.

### Informed consent statement:

Patients were not required to give informed consent to the study because the analysis used

**Colin Markus Krüger**, Department of Surgery, Immanuel Hospital Rüdersdorf, Berlin 15562, Germany

**Ulrich Adam, Hartwig Riediger**, Department of General Surgery, Vivantes-Humboldt hospital, Berlin 13503, Germany

**Thomas Adam**, Department of Microbiology, Labor Berlin GmbH, Berlin 13353, Germany

**Axel Kramer**, Institute of Hygiene and Environmental Medicine, University Medicine Greifswald, Greifswald 17495, Mecklenburg Vorpommern, Germany

**Claus D Heidecke**, Department of Surgery, Clinic of General, Visceral, Vascular and Thoracic Surgery, University Medicine Greifswald, Greifswald 17475, Mecklenburg Vorpommern, Germany

**Frank Makowiec**, Section of clinical risk assessment, University hospital of Freiburg, Freiburg 79106, Baden-Württemberg, Germany

**Corresponding author:** Colin Markus Krüger, FACS, MD, PhD, Chief Physician, Postdoc, Surgeon, Department of Surgery, Immanuel Hospital Rüdersdorf, Seebad 82/83, Berlin 15562, Germany. [cm.krueger@immanuel.de](mailto:cm.krueger@immanuel.de)

**Telephone:** +49-1718-151480

## Abstract

### BACKGROUND

Jaundice or preoperative cholestasis (PC) are typical symptoms of pancreatic masses. Approximately 50% of patients undergo preoperative biliary drainage (PBD) placement. PBD is a common cause of bacterobilia (BB) and is a known surgical site infection risk factor. An adjustment of preoperative antibiotic prophylaxis (PAP) may be reasonable according to the profile of BB. For this, we examined the microbiological findings in routine series of patients.

### AIM

To investigate the incidence and profile of biliary bacterial colonization in patients undergoing pancreatic head resections.

### METHODS

In the period from January 2009 to December 2015, 285 consecutive pancreatic head resections were performed. Indications for surgery were malignancy (71%), chronic pancreatitis (18%), and others (11%). A PBD was in 51% and PC was in

anonymous data that were obtained after each patient agreed to treatment by written consent.

**Conflict-of-interest statement:** All authors declare no conflicts-of-interest related to this article.

**Data sharing statement:** No additional data are available.

**Open-Access:** This article is an open-access article which was selected by an in-house editor and fully peer-reviewed by external reviewers. It is distributed in accordance with the Creative Commons Attribution Non Commercial (CC BY-NC 4.0) license, which permits others to distribute, remix, adapt, build upon this work non-commercially, and license their derivative works on different terms, provided the original work is properly cited and the use is non-commercial. See: <http://creativecommons.org/licenses/by-nc/4.0/>

**Manuscript source:** Unsolicited manuscript

**Received:** July 12, 2019

**Peer-review started:** July 12, 2019

**First decision:** August 18, 2019

**Revised:** October 10, 2019

**Accepted:** October 17, 2019

**Article in press:** October 17, 2019

**Published online:** November 7, 2019

**P-Reviewer:** Kitamura K, Ueno M

**S-Editor:** Tang JZ

**L-Editor:** A

**E-Editor:** Ma YJ



42%. The standard PAP was ampicillin/sulbactam. Intraoperatively, a smear was taken from the hepatic duct. An analysis of the isolated species and resistograms was performed. Patients were categorized according to the presence or absence of PC (PC+/PC-) and PBD (PBD+/PBD-) into four groups. Antibiotic efficiency was analyzed for standard PAP and possible alternatives.

## RESULTS

BB was present in 150 patients (53%). BB was significantly more frequent in PBD+ ( $n=120$ ) than in PBD- ( $n=30$ ),  $P < 0.01$ . BB was present both in patients with PC and without PC: (PBD-/PC-: 18%, PBD-/PC+: 30%, PBD+/PC-: 88%, PBD+/PC+: 80%). BB was more frequent in malignancy (56%) than in chronic pancreatitis (45%). PBD, however, was the only independent risk factor in multivariate analysis. In total, 357 pathogens (342 bacteria and 15 fungi) were detected. The five most common groups ( $n=256$ , 74.8%) were *Enterococcus* spp. (28.4%), *Streptococcus* spp. (16.9%), *Klebsiella* spp. (12.6%), *Escherichia coli* (10.5%), and *Enterobacter* spp. (6.4%). A polymicrobial BB (PBD+: 77% vs PBD-: 40%,  $P < 0.01$ ) and a more frequent detection of *Enterococcus* ( $P < 0.05$ ) was significantly associated with PBD+. In PBD+, the efficiency of imipenem and piperacillin/tazobactam was significantly higher than that of the standard PAP ( $P < 0.01$ ).

## CONCLUSION

PBD-/PC- and PBD-/PC+ were associated with a low rate of BB, while PBD+ was always associated with a high rate of BB. In PBD+ patients, BB was polymicrobial and more often associated with *Enterococcus*. In PBD+, the spectrum of potential bacteria may not be covered by standard PAP. A more potent alternative for prophylactic application, however, was not found.

**Key words:** Pancreatic surgery; Bacteriobilia; Antibiotic prophylaxis; Cholestasis; Cholangiopancreatography; Endoscopic retrograde

©The Author(s) 2019. Published by Baishideng Publishing Group Inc. All rights reserved.

**Core tip:** The aim of our retrospective study was to analyze the microbial profile of bacteriobilia in patients undergoing pancreatic head resection ( $n=285$ ). Patients with preoperative biliary drainage (PBD+) had a significantly elevated risk of bacteriobilia. In those cases, the contamination was polymicrobial. *Enterococcus* was significantly more frequent in PBD+. Our standard preoperative antibiotic prophylaxis reaches an overall sensitivity rate of 60% and a resistance rate of 25% in 342 bacteria. The antibiotic efficiency of Imipenem and Piperacillin/Tazobactam is significantly higher in PBD+. The data on polymicrobial colonization of the biliary tract may be useful for the decision on antibiotic treatment in case of postoperative infection until the final results from the intraoperative smear are available. A more potent alternative for prophylactic application, however, was not found among the examined antibiotics.

**Citation:** Krüger CM, Adam U, Adam T, Kramer A, Heidecke CD, Makowiec F, Riediger H. Bacteriobilia in pancreatic surgery-conclusions for perioperative antibiotic prophylaxis. *World J Gastroenterol* 2019; 25(41): 6238-6247

**URL:** <https://www.wjgnet.com/1007-9327/full/v25/i41/6238.htm>

**DOI:** <https://dx.doi.org/10.3748/wjg.v25.i41.6238>

## INTRODUCTION

With modern tomography techniques that yield cross-sectional images, a sufficiently predictive prognosis for the operability of pancreatic masses is now possible. A purely diagnostic endoscopic retrograde cholangiopancreatography (ERCP) is thus obsolete. In preoperative cholestasis (PC), the indication for preoperative biliary drainage (PBD) may exist. Often, however, the indication for ERCP is made even before operability has been determined. For example, an analysis of Medicare patients (1992-2007) showed that one in two patients already has a PBD at the time of the surgical



consultation<sup>[1]</sup>. The disadvantage is that ERCP leads almost always to bacterobilia (BB)<sup>[2-4]</sup>. BB is a risk factor (up to factor 2) for surgical site infection<sup>[5-9]</sup>.

According to the current guideline recommendations for pancreatic carcinoma, preoperative ERCP shall only be carried out if cholangitis is present or if surgery cannot be performed soon. A basic indication for preoperative antibiotic prophylaxis (PAP) in pancreatic resections is given regardless of the PBD status<sup>[8]</sup>. In the present study, the collected microbiological data are used to investigate whether a differentiated recommendation for PAP can be derived.

## MATERIALS AND METHODS

In the period from January 2009 to December 2015, 285 pancreatic head resections were performed at the Vivantes-Humboldt-hospital in Berlin. Pylorus preserving pancreatoduodenectomy was the standard procedure ( $n = 259$ ; 91%) and Whipple was only performed in selected cases ( $n = 26$ ; 9%). The morbidity was 59% ( $n = 169$ ) and the mortality was 3.8% ( $n = 11$ ).

Intraoperatively, a standard aseptic smear of the bile fluid was obtained after the hepatocholedochal duct was severed on average 90 min after skin incision. It was then used for routine microbiological diagnostics.

During the study period, preoperative ERCP was performed in case of cholestasis due to evaluation of the initially treating gastroenterologist. Under surgical surveillance, it was always performed in patients with relevantly elevated bilirubin ( $> 8$  mg/dL) and if a pancreas head resection could not be performed promptly. According to earlier data, serum bilirubin above 5 mg/dL already reduces liver function and thus a PBD is recommended<sup>[10]</sup>.

During the study period, antibiotics were administered as follows: The standard PAP (ampicillin-sulbactam) was administered 30 min before the skin incision, with a second dose after 4 h of surgery. In the case of penicillin allergy, ciprofloxacin and metronidazole were used. If a postoperative infection was suspected, empirical treatment with piperacillin/tazobactam was carried out, which was adjusted after receiving the result of the smear.

The microbiological specimens were examined according to standard microbiological procedures. Sensitivity and resistance for the tested antibiotics were analyzed in this study. Intermediate sensitivity was considered as resistance according to clinical routine. The number of detected sensitivities and resistances was related to the number of bacteria in each group, even though not all antibiotics were tested for all genera. This procedure allowed comparability of the groups. The results are presented as "antimicrobial efficiency" (AE: Sensitivity in %/resistance in %).

All perioperative and microbiological data were collected in a local scientific database (IBM SPSS Statistics, IBM, version 22). For the significance calculation, both the Chi-squared and McNemar tests were used. An additional binary logistic regression analysis was performed. The graphs were created with the program "GraphPad Prism" (GraphPad Software). The workgroup affirms that the statistical review of the study was performed by a biomedical statistician.

The study defined the presence of a PC at a measured serum value above the bilirubin standard (1.2 mg/dL) in the final check prior to surgery. Some patients had a completely recovered cholestasis after placement of a biliary drainage. They were classified as PBD+ and PC-. Patient data were divided into 4 groups according to clinical criteria: PBD-/PC-, PBD-/PC+, PBD+/PC-, and PBD+/PC+.

## RESULTS

The surgical treatment data are summarized in Table 1. BB was present in 150 patients (53%). In multivariate analysis of all factors from Table 1, only PBD was disclosed as an independent risk factor ( $P < 0.01$ ).

A total of 357 isolates were cultivated (342 bacteria, 15 fungi). With PBD+, BB was significantly more common than with PBD- (BB for PBD+:  $n = 120$ , 83.3% vs BB for PBD-:  $n = 30$ , 21.4%,  $P < 0.01$ ). In the subgroup PBD+, the BB rate was high regardless of the presence of cholestasis (BB for PC+: 80% and with PC-: 88%). In the subgroup PC+ ( $n = 120$ ), the BB rate with PBD+ was significantly higher compared to PBD- (PBD+/PC+:  $n = 60$ , 80% vs PBD-/PC+:  $n = 13$ ; 30%,  $P < 0.01$ ). In the four clinical groups, the incidence of BB with PBD-/PC- was 18%, with PBD-/PC+ 30%, with PBD+/PC- 88% and with PBD+/PC+ 80% (Table 2).

Of 342 bacteria, the five most commonly isolated (TOP5;  $n = 256$ , 74.8%) represented about three-quarters of all pathogens, and included the following genera:

**Table 1** Surgical treatment data from 285 patients with pancreatic head resection

	All patients, n = 285 (%)	With bacteriobilia (BB+), n = 150 (%)	Without bacteriobilia (BB-), n = 135 (%)	P value
Indications				
Malignancy	n = 202 (71)	n = 114 (56) <sup>a</sup>	n = 88 (44)	< 0.05
cP <sup>1</sup>	n = 51 (18)	n = 23 (45)	n = 28 (55)	0.23
Others	n = 32 (11)	n = 13 (41)	n = 19 (59)	0.15
Biliary drainage				
PBD+	n = 144 (51)	n = 120 (83) <sup>b</sup>	n = 24 (17)	< 0.01
PBD-	n = 141 (49)	n = 30 (21) <sup>b</sup>	n = 111 (79)	
Cholestasis				
PC+	n = 120 (42)	n = 73 (61) <sup>c</sup>	n = 47 (39)	0.02
PC-	n = 165 (58)	n = 77 (47) <sup>c</sup>	n = 88 (53)	

<sup>1</sup>cP = Chronic pancreatitis.<sup>a</sup>P < 0.05 vs BB-;<sup>b</sup>P < 0.01 vs BB-;<sup>c</sup>P = 0.02 vs BB-. PBD: Preoperative biliary drainage; PC: Preoperative cholestasis; BB: Bacteriobilia.

*Enterococcus* (n = 97), *Streptococcus* (n = 58), *Klebsiella* (n = 43), *Escherichia* (n = 36), and *Enterobacter* spp. (n = 22). In contrast, there were 13 different genera with a smaller number of cases (Varia: n = 86, 25.2%): *Staphylococcus* (n = 21), *Citrobacter* (n = 14), *Bacteroides* (n = 11), *Prevotella* (n = 8), *Lactobacillus* (n = 5), *Pseudomonas* (n = 4), *Aeromonas* (n = 3), *Raoultella* (n = 3), *Morganella* (n = 2), *Clostridium* (n = 2), *Proteus* (n = 2), *Fusobacterium* (n = 2), *Hafnia* (n = 2), *Proteus* (n = 2), MRSA (n = 2), *Stenotrophomonas* (n = 1), *Achromobacter* (n = 1), *Lactococcus* (n = 1), *Gemella* (n = 1), and *Rothia* spp. (n = 1).

Four species were multi-resistant bacteria (two MRSA and two triple-resistant *Klebsiella pneumoniae*). Anaerobes [*Bacteroides* (n = 11), *Prevotella* (n = 8), *Clostridia* (n = 2) and *Fusobacteria* (n = 2)] were rare (total: n = 23, 6.7%). A fungal colonization (total: n = 15, 4%) was significantly more frequent with PBD+ (n = 13, 9%) than with PBD- (n = 2, 1%) (P < 0.01) and was always associated with the occurrence of at least one bacterial genus. Out of 15 fungi, 13 cases (87%) consisted of *Candida* spp.

With PBD+, there was a higher rate (86%) and variety of bacteria. The distribution of bacteria in the groups PBD-/PC- and PBD-/PC+ consisted of only 8 genera per group, but in among the PBD+, 18 genera were found for PBD+/PC- and 16 for PBD+/PC+. The TOP5 were most common in both PBD+ and PBD- [PBD+: n = 222 (75%) vs PBD-: n = 34 (74%), P = 0.87] (Table 2). In contrast, the Varia/other were found almost exclusively with PBD+ (n = 74, 86%). In Subgroup analysis of the most frequent (TOP5) bacteria, only *Enterococcus* was significantly more frequent in PBD+. A broad spectrum of bacteria and a polymicrobial colonization was significantly characteristic of patients with PBD+ (Table 3).

The antimicrobial efficacy (AE) of the tested antibiotics in the whole group (n = 342) was 84%/11% for imipenem, 74%/16% for piperacillin-tazobactam, 60%/26% for ampicillin-sulbactam, 43%/33% for ciprofloxacin, 59%/17% for moxifloxacin, 50%/22% for ceftriaxone, and 44%/39% cefuroxime. The outstanding AE of imipenem is also evident in the graphical representation of all four clinical groups. Piperacillin-tazobactam was only significantly more effective with PBD+/PC+ and PBD+/PC- than PAP with ampicillin-sulbactam. This in turn also differed significantly from ciprofloxacin, cefuroxime, and ceftriaxone. The sensitivity rates of the other substances were lower than those of the PAP. Moxifloxacin has a good AE similar to that of the PAP used (Figure 1 and Table 4).

Compared to the clinically relevant substances (ampicillin-sulbactam and piperacillin-tazobactam), there was no significant difference in AE in enterococci, streptococci and *Klebsiella* spp. (together: n = 198; 57%). However, in *Escherichia* and *Enterobacter* spp. as well as in the rarer genera (together: n = 144, 43%), a significant difference in the AE was found. The AE of PAP was lower in about half of the bacteria in direct comparison of the two named substances (Table 5).

## DISCUSSION

BB often occurs after interventions on the bile duct system. A preoperative ERCP is the typical trigger<sup>[7,11-13]</sup>. Prophylactic use of antibiotics as part of ERCP cannot reliably affect BB or cholangitis. Again, even biliary excreted Ciprofloxacin does not provide

**Table 2** Pathogen detection depending on horizontal drain (PBD+/PBD-) or presence of cholestasis (PC+/PC-)

Clinical group	Number of patients, (n)	Patients with bacterobilia, n (%)	Bacteria quantity, n	Fungi
PBD-/PC-No stent/no cholestasis	97	17 (18)	24	0
PBD-/PC+No stent/cholestasis	44	13 (30)	22	2
PBD+/PC-Stent/no cholestasis	68	60 (88)	146	4
PBD+/PC+Stent/cholestase	76	60 (80)	150	9
All groups	285	150 (53)	342	

PBD: Preoperative biliary drainage; PC: Preoperative cholestasis.

uniform protection against post-ERCP cholangitis<sup>[2]</sup>.

The suspended sphincter function of the papilla of Vater leads to colonization and a pathogen shift in the hepatobiliary system<sup>[1,14,15]</sup>. In only a few cases of our data, BB was detected without prior ERCP. However, a high BB rate is typical in patients with PBD+. This may have consequences for perioperative antibiotic prophylaxis (PAP). For pancreatic surgery, ampicillin-sulbactam is used for PAP in our clinic. It is not clear whether this strategy is sufficient for all patients prior to pancreatic resection. According to the recommendations of the guideline, no adaptation of the PAP depending on the PBD or PC status has been performed so far<sup>[8]</sup>.

The literature describes a BB rate of 87% and 98%, respectively, with PBD+ vs 21% and 55%, respectively, for PBD- and the frequent detection of a mixed flora with PBD+<sup>[12,16]</sup>, which is in line with our own data. The introduction of a drain represents a risk independent of the presence of a preoperative cholestasis<sup>[14]</sup>. As PBD leads to an increase in postoperative complications, it shall not be performed routinely but only in selected cases<sup>[9]</sup>.

In a study of 91 ERCP patients, 15 different pathogen groups are identified, with *Escherichia coli* (28%) being the largest group<sup>[17]</sup>. In intraoperative smears of the hepatic duct, *Klebsiella* (18%), and *enterococci spp.* (13%) are the most frequent pathogens<sup>[18]</sup>. In patients with ERCP, *enterococci spp.* (31%) are most frequently detected with PBD+ and *Escherichia coli* (17%) with PBD-<sup>[12]</sup>. The literature also describes a shift to a more aggressive pathogen spectrum with an increase of *E. cloacae* and *E. faecalis*. At the same time, there is a lower sensitivity to ampicillin-sulbactam<sup>[19]</sup>. Therefore, it is recommended that an empirical PAP should take into account the more aggressive pathogen spectrum with PBD+<sup>[13]</sup>. A significant increase of the mentioned genera was not found in our total of 342 bacteria. However, *Enterococcus* was significantly more frequent in PBD+ patients. The frequent detection of *Enterobacter* with PBD+ and the limited AE of ampicillin-sulbactam must be emphasized, too.

Of the antibiotics tested, imipenem is the most potent antibiotic substance. However, as it is an important reserve antibiotic, it should not be used for PAP. Our own data show a lower AE of ampicillin-sulbactam compared with piperacillin-tazobactam, depending on the implantation of a biliary drainage. The superiority of piperacillin-tazobactam is significantly detectable with PBD+. Same as Imipenem, this antibiotic has its place in treatment and not in prophylaxis. However, the AE of ampicillin-sulbactam stands out in comparison to the other substances examined and seems to be well suited to a PAP with PBD-.

Since anaerobes accounted for only 6% of the isolated genera, the administration of metronidazole in addition to the PAP does not seem to be necessary. In our data, the AE of moxifloxacin is comparable with that of the PAP. However, this substance has no indication with cholangitis.

In contrast to the guideline, adaptation of perioperative antibiotic therapy in the context of pancreatic surgery as a function of PBD status is recommended in the literature<sup>[8,20]</sup>. This is justified by an increase in infectious complications (especially wound infections) with PBD+<sup>[6,21]</sup>. However, severe complications or mortality are not affected by BB in this case<sup>[22]</sup>.

In our own data, there is often only one species with PBD-. In addition, the pathogen spectrum is less aggressive (rarely *Enterobacter spp.*). We categorize the group PBD-/PC- as a low risk group due to the low BB probability. There is a slightly higher risk (30%) of BB for PBD-/PC+ as well as a relative accumulation of rare pathogens, so that we assess the risk of this group as intermediate. We classify PBD+/PC- and PBD+/PC+ as high-risk groups, because BB with polymicrobial mixed flora is almost always found.

Based on the findings of the resistogram, the AE of the PAP is sufficient when used in low clinical-risk situations. It should be noted, however, that depending on the regional resistance situation, other preferences for the PAP may arise. Therefore,

**Table 3 Bacterial profile in patients with bacteriobilia, (n = 150)**

Patients with...	PBD-, n (%)	PBD+, n (%)	P value
	30 (20)	120 (80)	
Polymicrobial mixed flora (n = 104)	12 (40) <sup>d</sup>	92 (78)	< 0.01
Enterococci (n = 82)	9 (30) <sup>e</sup>	73 (61)	< 0.05
Streptococci (n = 41)	6 (20)	35 (29)	0.32
Klebsiella (n = 38)	6 (20)	32 (27)	0.45
Escherichia (n = 35)	8 (27)	27 (23)	0.60
Enterobacter (n = 21)	1 (3)	20 (17)	0.06
Multi-drug resistant bacteria (n = 4)	1 (3)	3 (3)	0.80

<sup>d</sup>P < 0.01 vs PBD+.<sup>e</sup>P < 0.05 vs PBD+. PBD: Preoperative biliary drainage.

continuous analysis and evaluation of the species isolated from the hepatocholedochus duct is recommended.

On the basis of our data, a risk-adapted intensification to PAP with piperacillin-tazobactam may be seriously considered. In the literature, even with high risk, the recommendation is a primary 5-d therapy with later adjustment to the microbiological findings<sup>[23]</sup>. However, in our opinion, our own microbiological data do not allow this clinical conclusion. This would require the detection of significantly increased postinterventional infections with pathogens sensitive to piperacillin-tazobactam in this patient group. It is necessary to further analyze our own clinical data in this respect. In case of postoperative infection, these data have to be reminded in the selection of antibiotic treatment until the final results from the intraoperative smear are available.

In conclusion, A smear should always be taken intraoperatively during a pancreas head resection. This allows targeted subsequent antibiotic therapy in the perioperative course. The data of the clinical groups yield the following consequences: Patients with PBD+ are at high risk for polymicrobial bacteriobilia. Standard PAP may not sufficiently cover all genera in those patients. A significantly better antibiotic efficiency exists only for Imipenem and Piperacillin/Tazobactam. Their administration, however, can not be recommended for prophylactic use. An adequate alternative to our standard PAP can not be derived from our data.



**Table 4** Frequency of sensitivity and resistance compared to standard antibiotic prophylaxis with ampicillin-sulbactam in 342 bacteria

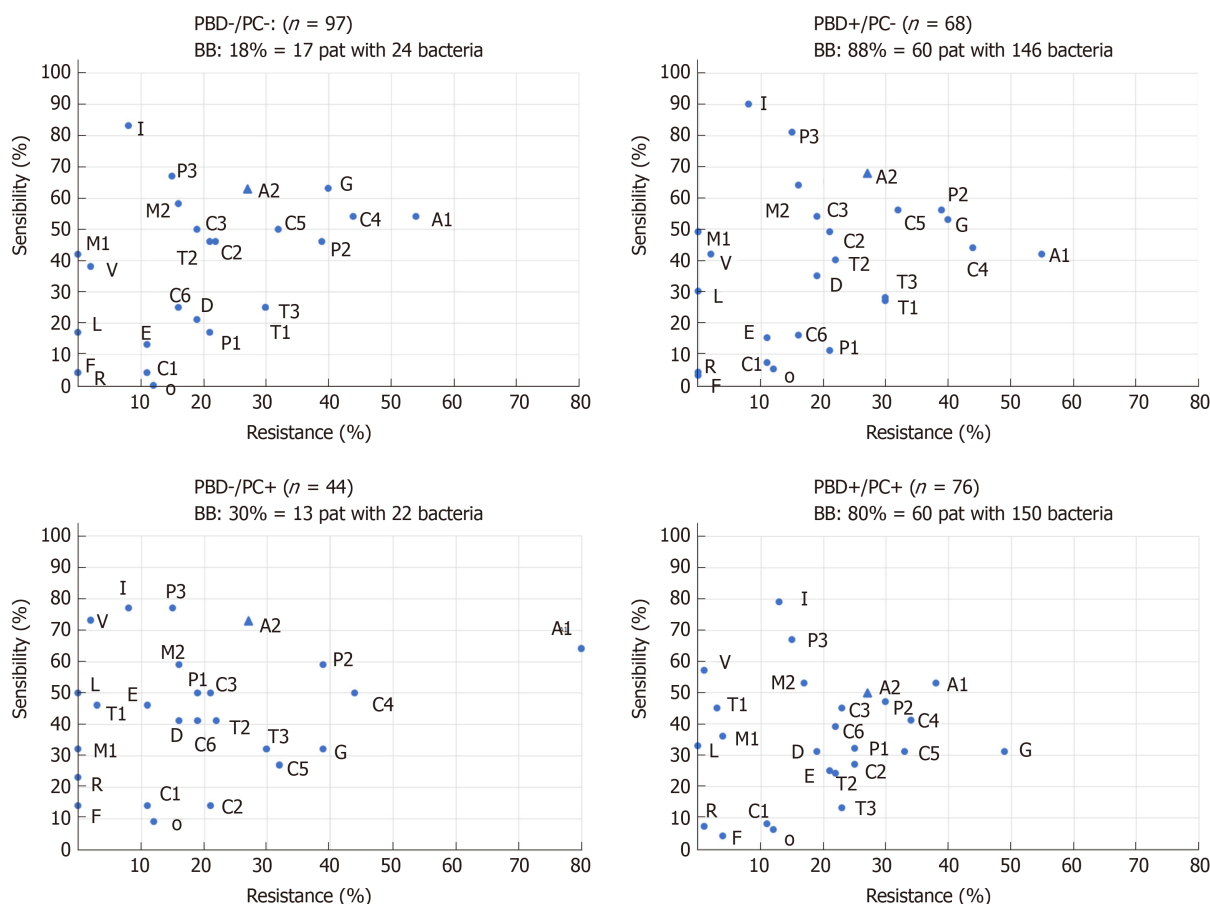
		Ampicillin Sulbactam	Imipenem	Piperacillin Tazobactam	Ciprofloxacin	Moxifloxacin	Ceftriaxon	Cefuroxim
PBD+ ( <i>n</i> = 296)	Sensitivity	174 (59)	249 (84) <sup>e</sup>	219 (74) <sup>e</sup>	129 (44) <sup>e</sup>	173 (58)	147 (50) <sup>f</sup>	126 (43) <sup>e</sup>
	Resistance	81 (27)	31 (11) <sup>e</sup>	45 (15) <sup>e</sup>	96 (32)	49 (17) <sup>e</sup>	62 (21) <sup>f</sup>	115 (39) <sup>e</sup>
PBD- ( <i>n</i> = 46)	Sensitivity	31 (67)	37 (80)	33 (72)	18 (39) +	27 (59)	23 (50) <sup>f</sup>	24 (52)
	Resistance	8 (17)	7 (15)	8 (17)	15 (33)	8 (17)	13 (28)	18 (39) <sup>f</sup>

Absolute numbers and percentages in brackets,

<sup>e</sup>*P* < 0.01,<sup>f</sup>*P* < 0.05. PBD: Preoperative biliary drainage.**Table 5** Antimicrobial efficacy of ampicillin-sulbactam and piperacillin-tazobactam in direct comparison with 342 bacteria

		Sensitivity (%)		Signifi- cance	Resistance (%)		Significance
		AS	PT	<i>P</i>	AS	PT	<i>P</i> value
TOP5( <i>n</i> = 256)	<i>Enterococci</i> ( <i>n</i> = 97)	71	70	NS	27	29	NS
	<i>Streptococci</i> ( <i>n</i> = 58)	60 <sup>g</sup>	88	< 0.01	0	0	NS
	<i>Klebsiella</i> ( <i>n</i> = 43)	86	98	NS	14 <sup>h</sup>	0	0.03
	<i>Escherichia</i> ( <i>n</i> = 36)	81 <sup>g</sup>	100	< 0.01	19 <sup>i</sup>	0	0.02
	<i>Enterobacter</i> ( <i>n</i> = 22)	5 <sup>g</sup>	91	< 0.01	95 <sup>g</sup>	0	< 0.01
Varia( <i>n</i> = 86)	Other genera	40 <sup>g</sup>	80	< 0.01	34 <sup>g</sup>	12	< 0.01

<sup>g</sup>*P* < 0.01 vs PT,<sup>h</sup>*P* = 0.03 vs PT,<sup>i</sup>*P* = 0.02 vs PT. AS: Ampicillin-sulbactam; PT: Piperacillin-tazobactam; NS: No significance.



**Figure 1 Proven sensitivities and resistances in the intraoperative smear of the hepatic duct.** Out of 285 patients, pathogens were not detected in 134 of them. In 150 patients, 342 bacteria were detected and the associated sensitivity and resistance tests were compiled. PBD+/- and PC+/- according to the defined clinical groups is used as subtitle of the figures. A1: Ampicillin; A2: Ampicillin/Sulbactam; C1: Cefazolin; C2 – Ceftazidim; C3: Ceftriaxon; C4: Cefuroxim; C5: Ciprofloxacin; C6: Clindamycin; D: Doxycyclin; E: Erythromycin; F: Fosfomycin; G: Gentamycin; I: Imipenem; L: Linezolid; M1: Meropenem; M2: Moxifloxacin; O: Oxacillin; P1: Penicillin; P2: Piperacillin; P3: Piperacillin/Tazobactam; R: Rifampicin; T1: Tigecyclin; T2: Trimethoprim/Sulfamethoxazol; T3: Tobramycin; V: Vancomycin. PBD: Preoperative biliary drainage; PC: Preoperative cholestasis.

## ARTICLE HIGHLIGHTS

### Research background

Preoperative biliary drainage (PBD) is a common cause of bacterobilia (BB) and is a known surgical site infection risk factor, especially in pancreatoduodenectomies.

### Research motivation

An adjustment of preoperative antibiotic prophylaxis (PAP) may be reasonable according to the profile of BB. However, current guidelines do not recommend an adoption of the PAP according to the PBD status.

### Research objectives

The objective of this study was to analyze the bacterial profile in routine patients undergoing pancreatic surgery and to find out, if our PAP is adequate for our patients. Antibiotic efficiency was analyzed for standard PAP and possible alternatives.

### Research methods

In the period from January 2009 to December 2015, 285 consecutive pancreatic head resections were performed. Indications for surgery were malignancy (71%), chronic pancreatitis (18%), and others (11%). A PBD was in 51% and preoperative cholestasis (PC) was in 42%. The standard PAP was ampicillin/sulbactam. Intraoperatively, a smear was taken from the hepatic duct. Patients were categorized according to the existence or lack of PC (PC+/PC-) and PBD (PBD+/PBD-).

### Research results

BB was present in 150 patients (53%). BB was significantly more frequent in PBD+ ( $n = 120$ ) than in PBD- ( $n = 30$ ),  $P < 0.01$ . BB was more frequent in malignancy (56%) than in chronic pancreatitis (45%). PBD, however, was the only independent risk factor for BB in multivariate analysis ( $P <$

0.01). The five most common groups ( $n = 256$ , 74.8%) were *Enterococcus* spp. (28.4%), *Streptococcus* spp. (16.9%), *Klebsiella* spp. (12.6%), *Escherichia coli* (10.5%), and *Enterobacter* spp. (6.4%). A polymicrobial BB (PBD+: 77% vs PBD-: 40%,  $P < 0.01$ ) and a more frequent detection of *Enterococcus* ( $P < 0.05$ ) was significantly associated with PBD+. In PBD+, the efficiency of imipenem and piperacillin/tazobactam was significantly higher than that of the standard PAP ( $P < 0.01$ ).

### Research conclusions

PBD-/PC- and PBD-/PC+ were associated with a low rate of BB, while PBD+ was always associated with a high rate of BB. In PBD+ patients, BB was polymicrobial and more often associated with *Enterococcus*. In PBD+, the spectrum of potential bacteria may not be covered by standard PAP. A more potent alternative for prophylactic application, however, was not found.

### Research perspectives

The perspective of this study is to show more differentiated ways of perioperative antibiotic prophylaxis and to stratify patient groups according to PBD and PC status. As patients with PBD+ are not full covered by standard PAP, these patients have a well-known high risk for infectious complications. A more proper PAP is required. In these selected patients a primary antibiotic treatment adopted to the (suspected) resistogramm.

## REFERENCES

- 1 **Jenkins LJ**, Parmar AD, Han Y, Duncan CB, Sheffield KM, Brown KM, Riall TS. Current trends in preoperative biliary stenting in patients with pancreatic cancer. *Surgery* 2013; **154**: 179-189 [PMID: 23889947 DOI: 10.1016/j.surg.2013.03.016]
- 2 **Ratanachu-ek T**, Prajanphanit P, Leelawat K, Chantawibul S, Panpimanmas S, Subwongcharoen S, Wannaprasert J. Role of ciprofloxacin in patients with cholestasis after endoscopic retrograde cholangiopancreatography. *World J Gastroenterol* 2007; **13**: 276-279 [PMID: 17226908 DOI: 10.1155/2015/204508]
- 3 **Bai Y**, Gao F, Gao J, Zou DW, Li ZS. Prophylactic antibiotics cannot prevent endoscopic retrograde cholangiopancreatography-induced cholangitis: a meta-analysis. *Pancreas* 2009; **38**: 126-130 [PMID: 19238021 DOI: 10.1097/MPA.0b013e318189f6d]
- 4 **Ceyssens C**, Frans JM, Christiaens PS, Van Steenberghe W, Peetermans WE. Recommendations for antibiotic prophylaxis before ERCP: can we come to workable conclusions after review of the literature? *Acta Clin Belg* 2006; **61**: 10-18 [PMID: 16673611 DOI: 10.1179/acb.2006.003]
- 5 **Mezhir JJ**, Brennan MF, Baser RE, D'Angelica MI, Fong Y, DeMatteo RP, Jarnagin WR, Allen PJ. A matched case-control study of preoperative biliary drainage in patients with pancreatic adenocarcinoma: routine drainage is not justified. *J Gastrointest Surg* 2009; **13**: 2163-2169 [PMID: 19774424 DOI: 10.1007/s11605-009-1046-9]
- 6 **Sahora K**, Morales-Oyarvide V, Ferrone C, Fong ZV, Warshaw AL, Lillemoe KD, Fernández-del Castillo C. Preoperative biliary drainage does not increase major complications in pancreaticoduodenectomy: a large single center experience from the Massachusetts General Hospital. *J Hepatobiliary Pancreat Sci* 2016; **23**: 181-187 [PMID: 26768943 DOI: 10.1002/jhbp.322]
- 7 **Nomura T**, Shirai Y, Hatakeyama K. Enterococcal bactibilia in patients with malignant biliary obstruction. *Dig Dis Sci* 2000; **45**: 2183-2186 [PMID: 11215736 DOI: 10.1023/a:1026640603312]
- 8 **Adler G**, Seufferlein T, Bischoff SC, Brambs HJ, Grabenbauer G, Hahn S, Heinemann V, Hohenberger W, Langrehr JM, Lutz MP, Micke O, Neuhaus H, Neuhaus P, Oettle H, Schlag PM, Schmid R, Schmiegel W, Schlottmann K, Werner J, Wiedenmann B, Kopp I. [S3-Guidelines "Exocrine pancreatic cancer" 2007]. *Z Gastroenterol* 2007; **45**: 487-523 [PMID: 17607616 DOI: 10.1055/s-2007-963224]
- 9 **van der Gaag NA**, Rauws EA, van Eijck CH, Bruno MJ, van der Harst E, Kubben FJ, Gerritsen JJ, Greve JW, Gerhards MF, de Hingh IH, Klinkenbijl JH, Nio CY, de Castro SM, Busch OR, van Gulik TM, Bossuyt PM, Gouma DJ. Preoperative biliary drainage for cancer of the head of the pancreas. *N Engl J Med* 2010; **362**: 129-137 [PMID: 20071702 DOI: 10.1056/NEJMoa0903230]
- 10 **Kawarada Y**, Higashiguchi T, Yokoi H, Vaidya P, Mizumoto R. Preoperative biliary drainage in obstructive jaundice. *Hepatogastroenterology* 1995; **42**: 300-307 [PMID: 8586359]
- 11 **Negm AA**, Schott A, Vonberg RP, Weismueller TJ, Schneider AS, Kubicka S, Strassburg CP, Manns MP, Suerbaum S, Wedemeyer J, Lankisch TO. Routine bile collection for microbiological analysis during cholangiography and its impact on the management of cholangitis. *Gastrointest Endosc* 2010; **72**: 284-291 [PMID: 20541201 DOI: 10.1016/j.gie.2010.02.043]
- 12 **Rerknimitr R**, Fogel EL, Kalayci C, Esber E, Lehman GA, Sherman S. Microbiology of bile in patients with cholangitis or cholestasis with and without plastic biliary endoprosthesis. *Gastrointest Endosc* 2002; **56**: 885-889 [PMID: 12447303 DOI: 10.1067/mge.2002.129604]
- 13 **Scheufele F**, Aichinger L, Jäger C, Demir IE, Schorn S, Sargut M, Erkan M, Kleeff J, Friess H, Ceyhan GO. Effect of preoperative biliary drainage on bacterial flora in bile of patients with periampullary cancer. *Br J Surg* 2017; **104**: e182-e188 [PMID: 28121036 DOI: 10.1002/bjs.10450]
- 14 **Johnson RC**, Ahrendt SA. The case against preoperative biliary drainage with pancreatic resection. *HPB (Oxford)* 2006; **8**: 426-431 [PMID: 18333097 DOI: 10.1080/13651820600840124]
- 15 **Ertz-Archambault N**, Keim P, Von Hoff D. Microbiome and pancreatic cancer: A comprehensive topic review of literature. *World J Gastroenterol* 2017; **23**: 1899-1908 [PMID: 28348497 DOI: 10.3748/wjg.v23.i10.1899]
- 16 **Herzog T**, Belyaev O, Akkuzu R, Hölling J, Uhl W, Chromik AM. The Impact of Bile Duct Cultures on Surgical Site Infections in Pancreatic Surgery. *Surg Infect (Larchmt)* 2015; **16**: 443-449 [PMID: 26110464 DOI: 10.1089/sur.2014.104]
- 17 **Kaya M**, Beştaş R, Bacalan F, Bacaksız F, Arslan EG, Kaplan MA. Microbial profile and antibiotic sensitivity pattern in bile cultures from endoscopic retrograde cholangiography patients. *World J Gastroenterol* 2012; **18**: 3585-3589 [PMID: 22826624 DOI: 10.3748/wjg.v18.i27.3585]
- 18 **Fathi AH**, Jackson T, Barati M, Eghbalieh B, Siegel KA, Siegel CT. Extended Perioperative Antibiotic

- Coverage in Conjunction with Intraoperative Bile Cultures Decreases Infectious Complications after Pancreaticoduodenectomy. *HPB Surg* 2016; **2016**: 3031749 [PMID: [27147813](#) DOI: [10.1155/2016/3031749](#)]
- 19 **Scheufele F**, Schorn S, Demir IE, Sargut M, Tieftrunk E, Calavrezos L, Jäger C, Friess H, Ceyhan GO. Preoperative biliary stenting versus operation first in jaundiced patients due to malignant lesions in the pancreatic head: A meta-analysis of current literature. *Surgery* 2017; **161**: 939-950 [PMID: [28043693](#) DOI: [10.1016/j.surg.2016.11.001](#)]
- 20 **Sudo T**, Murakami Y, Uemura K, Hashimoto Y, Kondo N, Nakagawa N, Ohge H, Sueda T. Perioperative antibiotics covering bile contamination prevent abdominal infectious complications after pancreatoduodenectomy in patients with preoperative biliary drainage. *World J Surg* 2014; **38**: 2952-2959 [PMID: [25022981](#) DOI: [10.1007/s00268-014-2688-7](#)]
- 21 **Mohammed S**, Evans C, VanBuren G, Hodges SE, Silberfein E, Artinyan A, Mo Q, Issazadeh M, McElhany AL, Fisher WE. Treatment of bacteriobilia decreases wound infection rates after pancreaticoduodenectomy. *HPB (Oxford)* 2014; **16**: 592-598 [PMID: [23992045](#) DOI: [10.1111/hpb.12170](#)]
- 22 **Morris-Stiff G**, Tamijmarane A, Tan YM, Shapey I, Bhati C, Mayer AD, Buckels JA, Bramhall SR, Mirza DF. Pre-operative stenting is associated with a higher prevalence of post-operative complications following pancreatoduodenectomy. *Int J Surg* 2011; **9**: 145-149 [PMID: [21029795](#) DOI: [10.1016/j.ijssu.2010.10.008](#)]
- 23 **Sourrouille I**, Gaujoux S, Lacave G, Bert F, Dokmak S, Belghiti J, Paugam-Burtz C, Sauvanet A. Five days of postoperative antimicrobial therapy decreases infectious complications following pancreaticoduodenectomy in patients at risk for bile contamination. *HPB (Oxford)* 2013; **15**: 473-480 [PMID: [23458261](#) DOI: [10.1111/hpb.12012](#)]



## Retrospective Study

# Tumor-infiltrating platelets predict postoperative recurrence and survival in resectable pancreatic neuroendocrine tumor

Shuai-Shuai Xu, Hua-Xiang Xu, Wen-Quan Wang, Shuo Li, Hao Li, Tian-Jiao Li, Wu-Hu Zhang, Liang Liu, Xian-Jun Yu

**ORCID number:** Shuai-Shuai Xu (0000-0001-8766-8529); Hua-Xiang Xu (0000-0002-5346-2335); Shuo Li (0000-0001-9804-8448); Wen-Quan Wang (0000-0001-9434-8013); Hao Li (0000-0002-1624-8970); Tian-Jiao Li (0000-0001-5429-1016); Wu-Hu Zhang (0000-0002-5182-9850); Liang Liu (0000-0002-8003-0503); Xian-Jun Yu (0000-0002-6697-7143).

**Author contributions:** Xu SS, Wang WQ, and Li S contributed equally to this work, in conducting clinical observations, analyzing the data, and writing the manuscript; Xu SS, Xu HX, Wang WQ, Li S, Li H, Li TJ, and Zhang WH performed the research; Xu HX, Liu L, and Yu XJ contributed equally to this work, in designing the research, revising the manuscript, and providing valuable suggestions for this study.

**Supported by** grants from the National Science Foundation for Distinguished Young Scholars of China, No. 81625016; the National Natural Science Foundation of China, No. 81871941, No. 81872366, No. 81827807, No. 81802675, and No. 81702341; the Outstanding Academic Leader Program of the “Technological Innovation Action Plan” in Shanghai Science and Technology Commission, No. 18XD1401200; and the Young Talented Specialist Training Program of Shanghai.

### Institutional review board

**statement:** This study was reviewed and approved by the Human Research Ethics Committee of Fudan University Shanghai Cancer Center.

Shuai-Shuai Xu, Hua-Xiang Xu, Wen-Quan Wang, Shuo Li, Hao Li, Tian-Jiao Li, Wu-Hu Zhang, Liang Liu, Xian-Jun Yu, Department of Pancreatic Surgery, Fudan University Shanghai Cancer Center, Shanghai 20032, China

Shuai-Shuai Xu, Hua-Xiang Xu, Wen-Quan Wang, Shuo Li, Hao Li, Tian-Jiao Li, Wu-Hu Zhang, Liang Liu, Xian-Jun Yu, Department of Oncology, Shanghai Medical College, Fudan University, Shanghai 200032, China

Shuai-Shuai Xu, Hua-Xiang Xu, Wen-Quan Wang, Shuo Li, Hao Li, Tian-Jiao Li, Wu-Hu Zhang, Liang Liu, Xian-Jun Yu, Shanghai Pancreatic Cancer Institute, Shanghai 200032, China

Shuai-Shuai Xu, Hua-Xiang Xu, Wen-Quan Wang, Shuo Li, Hao Li, Tian-Jiao Li, Wu-Hu Zhang, Liang Liu, Xian-Jun Yu, Pancreatic Cancer Institute, Fudan University, Shanghai 200032, China

**Corresponding author:** Liang Liu, MD, PhD, Professor, Surgeon, Surgical Oncologist, Department of Pancreatic Surgery, Fudan University Shanghai Cancer Center, 270 Dong An Road, Shanghai 200032, China. [liuliang@fudanpci.org](mailto:liuliang@fudanpci.org)

**Telephone:** +86-21-64031446

**Fax:** +86-21-64031446

## Abstract

### BACKGROUND

Platelets have been reported to participate in tumor cell growth, extravasation, epithelial-mesenchymal transition, metastasis, and drug resistance. However, the importance of platelets in pancreatic neuroendocrine tumor (pNET) lacks adequate literature support. The predictive value of tumor-infiltrating platelets (TIPs) in pNET remains unclear.

### AIM

To investigate the relationship between TIPs and the prognosis of patients with pNET following radical resection.

### METHODS

In total, 113 patients who had undergone radical surgical resection with a pathologic diagnosis of pNET were enrolled in this study. Immunohistochemical analysis of cluster of differentiation 42b (CD42b) expression in the tumor specimens was performed to determine the presence of TIPs. Univariate and multivariate analyses were used to analyze the prognostic value of TIPs.

### RESULTS



**Informed consent statement:**

Written informed consent has been acquired from each patient.

**Conflict-of-interest statement:**

All authors declare no conflicts of interest related to this article.

**Data sharing statement:**

No additional data are available.

**Open-Access:**

This article is an open-access article which was selected by an in-house editor and fully peer-reviewed by external reviewers. It is distributed in accordance with the Creative Commons Attribution Non Commercial (CC BY-NC 4.0) license, which permits others to distribute, remix, adapt, build upon this work non-commercially, and license their derivative works on different terms, provided the original work is properly cited and the use is non-commercial. See: <http://creativecommons.org/licenses/by-nc/4.0/>

**Manuscript source:**

Invited manuscript

**Received:** May 22, 2019

**Peer-review started:** May 22, 2019

**First decision:** June 16, 2019

**Revised:** July 8, 2019

**Accepted:** July 19, 2019

**Article in press:** June 16, 2019

**Published online:** November 7, 2019

**P-Reviewer:** Neri V, Tsolakis AV, Vagholkar KR

**S-Editor:** Ma RY

**L-Editor:** Filipodia

**E-Editor:** Ma YJ



TIPs were observed in intratumoral areas in 54 patients. Neither basic characteristics nor preoperative platelet-associated indicators showed a significant relationship with the presence of TIPs (all  $P > 0.05$ ). Patients with positive intratumoral CD42b expression had worse overall survival ( $P = 0.005$ ) and recurrence-free survival ( $P < 0.001$ ) than those with negative intratumoral CD42b expression. Multivariate analysis demonstrated that TIPs were independent prognostic factors for overall survival ( $P = 0.049$ ) and recurrence-free survival ( $P = 0.003$ ). Nevertheless, platelet count, mean platelet volume, and platelet-to-lymphocyte ratio were not associated with postoperative survival or recurrence in pNET patients (all  $P > 0.05$ ).

**CONCLUSION**

TIPs are a useful prognostic biomarker for patients with resectable pNET, and their detection represents a promising tool for pNET treatment strategy decisions.

**Key words:** Tumor-infiltrating platelets; Pancreatic neuroendocrine tumor; Survival; Recurrence; Platelet count; Mean platelet volume; Platelet-to-lymphocyte ratio

©The Author(s) 2019. Published by Baishideng Publishing Group Inc. All rights reserved.

**Core tip:** We uncovered the importance of platelets in pancreatic neuroendocrine tumors and investigated the association between clinical outcome and preoperative platelet-associated indicators and tumor-infiltrating platelets in pancreatic neuroendocrine tumors. Platelet count, mean platelet volume, and platelet-to-lymphocyte ratio determined by preoperative blood tests were not related to overall survival or recurrence-free survival. Thus, tumor-infiltrating platelets are potential independent indicators of survival and recurrence in patients with resectable pancreatic neuroendocrine tumors.

**Citation:** Xu SS, Xu HX, Wang WQ, Li S, Li H, Li TJ, Zhang WH, Liu L, Yu XJ. Tumor-infiltrating platelets predict postoperative recurrence and survival in resectable pancreatic neuroendocrine tumor. *World J Gastroenterol* 2019; 25(41): 6248-6257

**URL:** <https://www.wjnet.com/1007-9327/full/v25/i41/6248.htm>

**DOI:** <https://dx.doi.org/10.3748/wjg.v25.i41.6248>

**INTRODUCTION**

Pancreatic neuroendocrine tumor (pNET) is the second most common malignancy among all pancreatic tumors, and its incidence has been increasing over the years<sup>[1]</sup>. Surgery remains the preferred treatment for pNET<sup>[2,3]</sup>. However, patient prognoses after surgery differ because of the inherent heterogeneity of these tumors. Various guidelines have been modified to classify the prognosis of pNET patients. Most studies have concentrated on the significance of tumor cells, but few have focused on the importance of the tumor microenvironment in pNET.

Platelets are an important component of the tumor microenvironment. They participate in growth, extravasation, epithelial-mesenchymal transition, and metastasis of tumor cells by secreting microparticles and exosomes<sup>[4]</sup>. They also mediate the interaction between tumor cells and immune cells<sup>[5]</sup>. Moreover, platelets reportedly influence the prognosis and drug resistance of different tumors and can serve as treatment carriers<sup>[6,7]</sup>.

Nevertheless, the ability of platelet-associated indicators determined by blood tests to predict clinical outcome is in dispute. Although one study identified platelet count as a risk factor for recurrence and 3-year survival probability in resectable pNET<sup>[8]</sup>, another study reported that platelet count was not associated with overall survival (OS) in inoperable advanced or metastatic pNET<sup>[9]</sup>. Other platelet-associated indicators, such as mean platelet volume (MPV) and platelet-to-lymphocyte ratio (PLR), have been described as distinguishable serous indicators of pNET risk and prognosis<sup>[10,11]</sup>. However, in another study, MPV and PLR in pNET were reported not to be independent recurrence risk factors for patients with radical resection<sup>[12]</sup>. Tumor-infiltrating platelets (TIPs) are educated and activated by tumor cells, and their distribution promotes metastasis of tumor cells. A previous study revealed the prognostic significance of TIPs in resectable pancreatic cancer<sup>[13]</sup>. However, the role of

TIPs in pNET remains unclear.

In this study, we evaluated the potential value of TIPs assessment as a biomarker to predict survival and recurrence outcome in patients with pNET undergoing radical resection.

## MATERIALS AND METHODS

### Patients

In total, 113 patients who had undergone radical surgical resection from 2012 to 2017 at our institution were retrospectively enrolled. All specimens were selected *via* pathologic diagnosis as pNET without distant metastasis or other tumor history. None of the patients had received any preoperative chemotherapy or radiotherapy or died of postoperative complications within 30 d. All cases included complete clinical preoperative and postoperative data, and all patients received therapy at Fudan University Shanghai Cancer Center. This study was approved by the Human Research Ethics Committee of Fudan University Shanghai Cancer Center and was performed in accordance with the tenets of the World Medical Association Declaration of Helsinki.

Age referred to the time when a patient was definitively diagnosed with pNET. Tumor location was divided into pancreatic head or pancreatic body with tail. Tumor grade was classified according to the Ki-67 labeling index of the World Health Organization in 2017, and Tumor Nodes Metastases (TNM) staging was assessed as the eighth edition norm of the American Joint Committee on Cancer. Preoperative platelet-associated indicators, including platelet count, MPV, and PLR, were measured and calculated *via* blood tests within 3 d before surgery.

Postoperative patients were routinely evaluated according to clinical manifestations and auxiliary examinations, including tumor markers (carbohydrate antigen 19-9, cancer antigen 125, and carcinoembryonic antigen, among others) and imaging examinations (enhanced computed tomography, enhanced magnetic resonance imaging, *etc*). All patients were strictly followed up until the last follow-up in January 2019. OS was defined as the interval from the date of surgery to death or the last follow-up. Recurrence-free survival (RFS) was defined as the interval from the date of surgery to the date of tumor recurrence or the last follow-up.

### Histopathological assessment

Formalin-fixed and paraffin-embedded serial pathological sections of surgical resection specimens were utilized to perform immunostaining. Immunohistochemistry is described in detail below. Baked slides were deparaffinized in xylene and rehydrated in an ethanol concentration gradient. Endogenous peroxidase activity was inhibited with a 3% methanol solution of hydrogen peroxide in an aqueous chamber at 37 °C, and antigen retrieval was conducted using high-pressure heated induction in citrate buffer (pH 6.0, G1201, Servicebio, Wuhan, China). Then, nonspecific binding was blocked with 10% normal goat serum, and primary monoclonal anti-CD42b antibody (diluted 1:150, anti-CD42b, EPR6995; Abcam, Cambridge, MA, United States) was applied to detect the platelet-specific marker CD42b. Slides were incubated with secondary antibody along with the 3,3'-diaminobenzidine chromogen using a Secondary Antibody Kit (G1210-2-A, Servicebio). Next, nuclei were stained with hematoxylin (G1004, Servicebio). Finally, the slices were sequentially exposed to an ethanol concentration gradient and xylene and were then sealed airtight with neutral resin and coverslips.

The immunostaining images of the whole slide from each case were evaluated under low-power scanning magnification ( $\times 100$ ). Hotspot images were defined as the areas in the tumor with the highest number of cells with immunoreactive staining. Under high-power magnification ( $\times 200$ ), five representative photographs of the hotspot were captured to identify the number of TIPs. The results were independently reviewed by two blinded, independent, clinically experienced pathologists. Positive tests were performed with pancreatic adenocarcinoma that definitively showed CD42b staining. Negative controls were treated identically but with the primary antibodies omitted. The evaluation criteria were that positive referred to an immunostained platelet distribution that accounted for  $\geq 10\%$  of the intratumoral region and negative referred to an immunostained platelet distribution that accounted for  $< 10\%$  of intratumoral region; furthermore, samples with platelet immunostaining limited to intratumoral vessels or the peritumoral area were also regarded as negative<sup>[13-15]</sup>. In the study, we evaluated 5%, 10%, and 20% as the cut-off values for CD42b expression. The proportion of positive CD42b expression at cut-off values of 5%, 10%, and 20% was 60.18%, 47.79%, and 25.66%, respectively. The *P* value for

survival comparison between patients with positive CD42b expression and those with negative CD42b expression were 0.042, 0.005, and 0.771, respectively, at cut-off values of 5%, 10%, and 20%. The cut-off value of 10% had the best survival discrimination and was chosen as the cut-off value.

### Statistical analysis

Correlations between TIP expression and clinicopathologic characteristics were analyzed using a chi-square test. Kaplan–Meier survival curves were used to display OS and RFS, and differences between groups were compared with a log-rank test. Univariate and multivariate Cox regression analyses were used to identify independent prognostic factors for recurrence and survival. All tests were two sided, and  $P < 0.05$  was considered statistically significant. Statistical analyses were performed using SPSS 24.0 software (SPSS Inc., Armonk, NY, United States).

## RESULTS

### Clinicopathologic characteristics of patients

The clinicopathologic characteristics of all the patients are shown in Table 1. The median age was 54 years, and 50 (44.24%) patients were males. There were 66 (58.41%) patients with pancreatic head tumors, and 5 (4.42%) patients with functional pNET, all belonging to insulinoma. The majority (58.41%) of patients was stage 1 and stage 2, and the rest were stage 3. Similarly, 101 (89.38%) tumors were grade 1, and the remaining were grade 2. The median preoperative platelet count, MPV, and PLR were  $225 \times 10^9/L$ , 11.1 fL, and 130.7, respectively. At the last follow-up, 13 patients (11.50%) had died, and 41 patients (36.28%) had recurrence. Furthermore, the 1-year, 3-year, and 5-year mortality rates were 3.6%, 8.8%, and 14.2%, respectively, and the 1-year, 3-year, and 5-year recurrence rates were 8.0%, 15.7%, and 27.7%, respectively.

### Presence of TIPs was associated with poor OS and RFS

Positive CD42b (a platelet-specific marker) expression was seen in the intratumoral spaces surrounding cancer cells (Figure 1A and B); in contrast, negative CD42b staining referred to an absence of intratumoral CD42b expression or positive CD42b expression only in intratumoral vessels (Figure 1C and D). Positive CD42b expression was observed in 47.79% of the patients. As shown in Table 2, neither basic characteristics nor preoperative platelet count, MPV, or PLR showed a statistical relationship with CD42b expression (all  $P > 0.05$ ). Kaplan–Meier survival curves revealed that patients with positive CD42b expression showed worse OS ( $P = 0.005$ ) and RFS ( $P < 0.001$ ) than those with negative CD42b expression (Figure 2), indicating that the presence of TIPs was associated with poorer clinical outcomes.

### Presence of TIPs was an independent prognosis factor for patients

As shown in Table 3, univariate analysis showed that TNM stage (OS:  $P = 0.005$ ; RFS:  $P = 0.001$ ), tumor grade (OS:  $P < 0.001$ ; RFS:  $P < 0.001$ ), and CD42b expression (OS:  $P = 0.015$ ; RFS:  $P = 0.001$ ) were associated with patient clinical outcomes, while platelet count, MPV, and PLR were not associated with patient OS or RFS (all  $P > 0.05$ ). Multivariate analysis (Table 4) showed that CD42b expression was an independent prognostic factor for both OS ( $P = 0.049$ ) and RFS ( $P = 0.003$ ). Tumor grade and TNM stage were also independently associated with patient prognosis. The above results demonstrate that the presence of TIPs is a predictor of poor OS and RFS.

## DISCUSSION

In this study, platelet count determined by a blood test had no significant value in prediction of survival and recurrence in pNET. Similar results were observed with other platelet-associated indicators determined by a blood test. Notably, we demonstrated that the presence of TIPs in the tumor microenvironment in pNET exhibited potential as a risk biomarker to predict the prognosis of pNET following radical resection. The determination of TIPs in tumors could improve prognostic classification of pNET after resection.

Several reasons were attributed to the irrelative association between preoperative platelet count, MPV, and PLR determined by blood tests and clinical outcome in resectable pNET. First, these indicators themselves might not be appropriate to predict prognosis. Platelet count, MPV, and PLR provide limited information concerning the malignant features of pNET, and their levels remained unchanged even after tumor recurrence<sup>[12]</sup>. Second, preoperative platelet count, MPV, and PLR

**Table 1 Clinical characteristics of patients**

Clinical characteristics	
Age in yrs, as median (range)	54 (25, 82)
Gender, male/female	50/63
Tumor location, head/body, tail	66/47
Tumor diameter, as median (range)	3.8 (1.0, 10.5) cm
Extend of disease, localized/nodal	66/47
Tumor grade, 1/2	101/12
TNM stage, 1, 2/3	66/47
Functional pNET, no/yes	108/5
MPV, as median (range)	11.1 (9.1, 13.8) fL
PLR, as median (range)	130.7 (13.6, 413.3)
Platelet count, as median (range)	225 (79, 436) $\times 10^9/L$
Death, no/yes	100/13
Recurrence, no/yes	72/41

MPV: Mean platelet volume; PLR: Platelet lymphoid ratio; pNET: Pancreatic neuroendocrine tumor; TNR: Tumor, nodes, metastases.

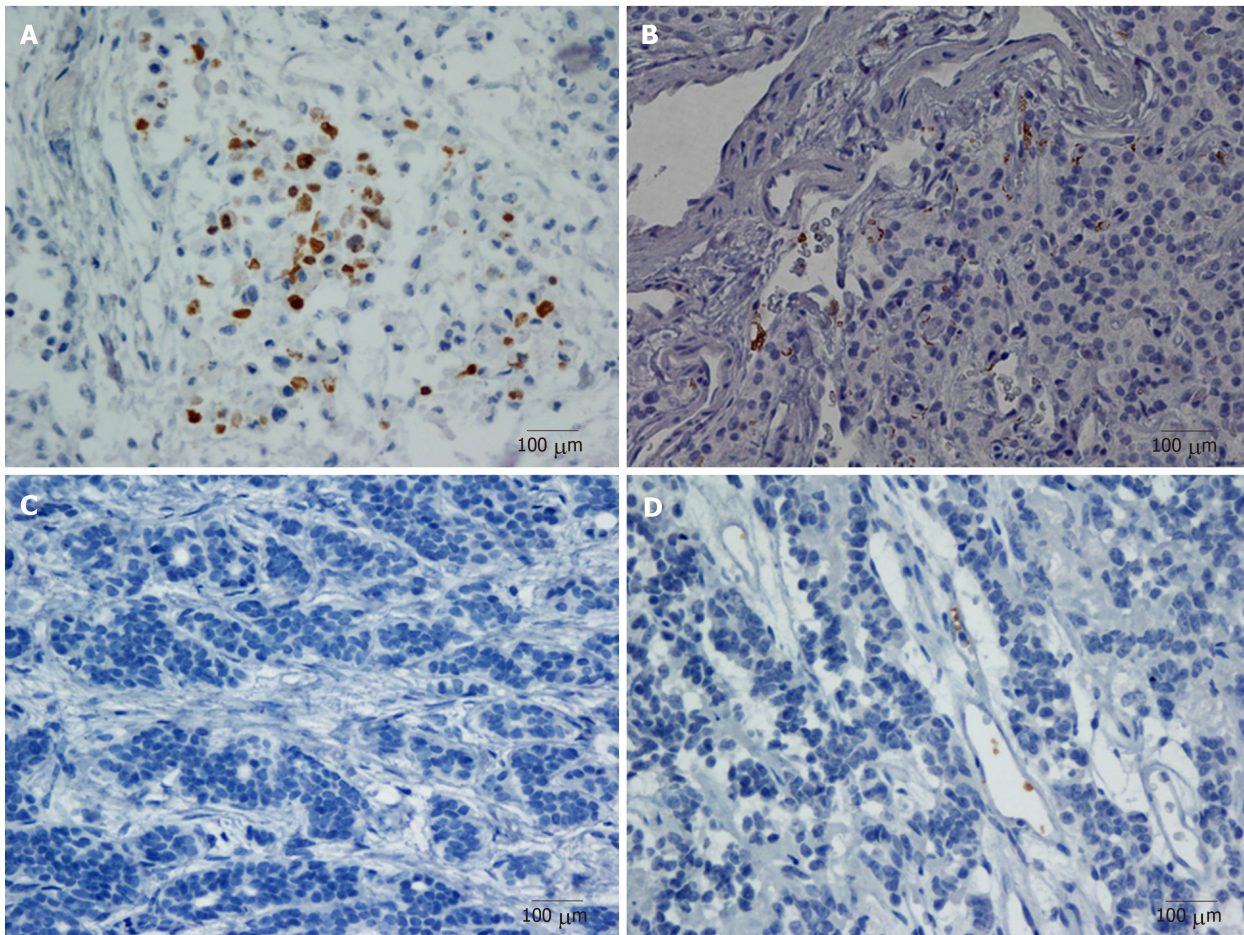
determined by blood tests are easily affected by other diseases, such as hematopoietic disease, hypersplenism, and common cardiovascular and cerebrovascular diseases. They can also be influenced by drugs, such as aspirin<sup>[16]</sup>. Last, platelet count, MPV, and PLR detected as systemic indicators might not accurately reflect the specific regional details of the tumor microenvironment. Minor changes in the tumor microenvironment cannot be determined by systemic indicators.

TIPs exhibit the activated and agminated status of intratumoral platelets, which are enticed by tumor cells into sustaining stability. They are induced by tumor cells *via* direct and indirect mechanisms through a series of indispensable processes that can be divided into penetration, activation, and aggregation<sup>[17]</sup>. TIPs travel easily through tumor-associated vessels due to the fragility of these vessels, which are characterized by overexpressed, abnormal, and leaky tumor vasculature<sup>[18]</sup>. They are subsequently activated by cancer-released factors, cancer-surface molecules, or cancer-induced aggregation<sup>[19]</sup>. TIPs gather around tumor cells and further motivate other platelets through the process of platelet coagulation<sup>[20]</sup>. TIPs are seldom affected by changes in blood contents because TIPs are formed by activated platelets that are primarily attracted from the bloodstream into the tumor region by tumor cells. Thus, no statistical relationship was observed between TIPs and platelet count, MPV, or PLR (Table 2).

The presence of TIPs is considered a potential biomarker for predicting prognosis outcome in resectable pNET, which is attributed to the interaction between platelets and tumor cells. Not only can tumor cells stimulate platelets, but platelets can also communicate with tumor cells by releasing numerous proteins, growth factors, microparticles, and microRNAs to promote tumor progression<sup>[17]</sup>. Platelets enhance tumor proliferation by secreting transforming growth factor- $\beta$ <sup>[21]</sup>, promote tumor invasion *via* secretion of microRNA-223<sup>[22]</sup>, and facilitate tumor metastasis through activation of YAP1 signaling in tumor cells<sup>[23]</sup>. Activated platelets rely on paracrine activation of the epidermal growth factor receptor and downstream DNA-dependent protein kinase to motivate the anti-apoptosis response of tumor cells<sup>[24]</sup>. Platelets produce the proangiogenic proteins vascular endothelial growth factors, which contribute to the neovascularization process that assists tumor cells in obtaining sufficient nutrition and aid in further extravasation<sup>[17,25]</sup>. The antitumor reactivity of natural killer cells can also be impaired by platelets through platelet-derived transforming growth factor- $\beta$ <sup>[26]</sup>. In addition, platelets induce cisplatin resistance through the Akt/Bad/Bcl-2 signaling pathway under endoplasmic reticulum stress<sup>[7]</sup>. The interaction between platelets and tumor cells forms a mutually reinforcing cycle that promotes tumor metastasis. Thus, a reduction in platelet infiltration in the tumor microenvironment might be a potential treatment strategy for pNET. In addition, one of the mechanisms underlying the antitumor effect of aspirin in pNET with multiple endocrine neoplasia type 1 was attributed to targeted therapy of platelets<sup>[27]</sup>.

Our study has some limitations. First, the nature of a retrospective study with a limited sample size restricts the level of evidence. Another prospective study with a larger sample size needs be conducted with multicenter cooperation. Next, the





**Figure 1 Representative microphotographs of CD42b staining.** A: Positive, CD42b expression aggregating around and embracing tumor cells; B: Positive, CD42b expression surrounding tumor cells and intratumoral blood vessels; C: Negative, no CD42b staining in intratumoral region; D: Negative, CD42b staining only in intratumoral vessels. All magnifications  $\times 400$ . Positive staining appears brown.

mechanism by which platelets influence the recurrence of patients with resectable pNET was not thoroughly investigated, and thus, additional experiments to examine the mechanism need to be implemented.

In conclusion, we found that TIPs were potential pNET prognosis indicators. In addition, therapy targeting platelets in pNET could improve the long-term survival of patients.



**Table 2** The relationship between CD42b expression and clinicopathologic characteristics of patients

Factor	CD42b expression		P value
	Negative	Positive	
Age in yr			0.157
< 54	33	23	
≥ 54	26	31	
Gender			0.968
Male	26	24	
Female	33	30	
Tumor location			0.186
Head	31	35	
Body, Tail	28	19	
Tumor grade			0.439
1	54	47	
2	5	7	
TNM stage			0.556
1, 2	36	30	
3	23	24	
Functional pNET			1.00
No	56	52	
Yes	3	2	
Platelet count, as $\times 10^9/L$			0.928
< 225	29	27	
≥ 225	30	27	
MPV in fL			0.298
< 11.1	32	24	
≥ 11.1	27	30	
PLR			0.507
< 130.7	31	25	
≥ 130.7	28	29	

$P < 0.05$  was statistically significant. pNET: Pancreatic neuroendocrine tumor; MPV: Mean platelet volume; PLR: Platelet lymphoid ratio; TNM: Tumor, nodes, metastases.

**Table 3** Univariate Cox regression analyses of overall survival and recurrence-free survival with clinicopathologic characteristics in resectable pancreatic neuroendocrine tumor patients

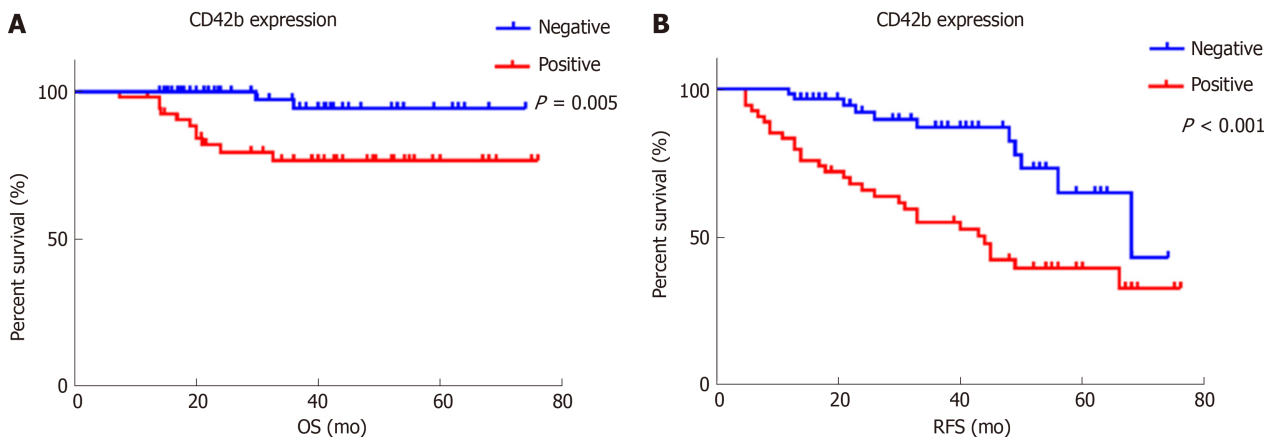
Factor	OS			RFS		
	HR	95%CI	P value	HR	95%CI	P value
Age, < 54/≥ 54	1.790	0.585-5.481	0.308	0.995	0.538-1.840	0.987
Gender, male/female	2.689	0.740-9.770	0.133	0.972	0.526-1.796	0.929
Tumor location, head/body, tail	0.760	0.233-2.482	0.650	1.026	0.531-1.982	0.939
Tumor grade, 1/2	13.403	4.332-41.466	< 0.001	5.509	2.299-13.199	< 0.001
TNM stage, 1, 2/3	8.861	1.960-40.064	0.005	2.892	1.527-5.477	0.001
Functional pNET, no/yes	0.046	0.000-5340.899	0.606	0.412	0.056-3.007	0.382
Platelet count, as $\times 10^9/L$ , < 225/≥ 225	2.497	0.768-8.114	0.128	1.188	0.642-2.201	0.583
MPV in fL, < 11.1/≥ 11.1)	1.442	0.472-4.411	0.521	1.547	0.827-2.893	0.172
PLR, < 130.7/≥ 130.7	1.217	0.409-3.624	0.724	1.043	0.564-1.927	0.894
CD42b expression, negative/positive	6.432	1.425-29.025	0.015	3.203	1.603-6.400	0.001

$P < 0.05$  was statistically significant. pNET: Pancreatic neuroendocrine tumor; CI: Confidence interval; HR: Hazard ratio; OS: Overall survival; RFS: Recurrence-free survival; MPV: Mean platelet volume; PLR: Platelet lymphoid ratio.

**Table 4** Multivariate Cox regression analyses of overall survival and recurrence-free survival with clinicopathologic characteristics in resectable pancreatic neuroendocrine tumor patients

Factor	OS			RFS		
	HR	95%CI	P value	HR	95%CI	P value
Tumor grade, 1/2	5.882	1.848-18.719	0.003	3.283	1.345-8.016	0.009
TNM stage, 1, 2/3	5.136	1.062-24.842	0.042	2.366	1.219-4.591	0.011
CD42b expression, negative/positive	4.601	1.004-21.095	0.049	2.893	1.439-5.817	0.003

$P < 0.05$  was statistically significant. pNET: Pancreatic neuroendocrine tumor; CI: Confidence interval; HR: Hazard ratio; OS: Overall survival; RFS: Recurrence-free survival.



**Figure 2** The relationship between CD42b expression and overall survival and recurrence-free survival. A: OS ( $P = 0.005$ ); B: RFS ( $P < 0.001$ ). Patients with positive CD42b expression had worse OS and RFS than those with negative CD42b expression.  $P$  values were calculated by Kaplan–Meier estimations. OS: Overall survival; RFS: Recurrence-free survival.

## ARTICLE HIGHLIGHTS

### Research background

Pancreatic neuroendocrine tumor (pNET) is the second most common malignancy among pancreatic tumors. Most studies have primarily concentrated on the significance of tumor cells, but few have focused on the importance of the tumor microenvironment in pNET. Platelets are an important component of the tumor microenvironment. However, the importance of platelets in pNET lacks adequate literature support.

### Research motivation

To assess the potential clinical meaning of platelets in pNET and offer evidence concerning a potential anti-platelet therapeutic strategy for pNET.

### Research objectives

Tumor-infiltrating platelets are potential independent indicators of survival and recurrence outcome for patients with resectable pNET.

### Research methods

In total, 113 patients who had undergone radical surgical resection were retrospectively enrolled. All the specimens were selected *via* pathologic diagnosis of pNET without distant metastasis or other tumor history. None of the patients had received any preoperative chemotherapy or radiotherapy or died of postoperative complications within 30 d. Immunohistochemical analysis of CD42b expression in tumor specimens was performed to determine the presence of TIPs. Univariate and multivariate analyses were applied to analyze the prognostic value of tumor-infiltrating platelets.

### Research results

Tumor-infiltrating platelets were observed in intratumoral areas in 54 patients. Neither basic characteristics nor preoperative platelet count, mean platelet volume, or platelet lymphoid ratio showed a statistical relationship with CD42b expression. Platelet count, mean platelet volume, and platelet-to-lymphocyte ratio determined by preoperative blood tests were not related to overall survival or recurrence-free survival. Tumor-infiltrating platelets were found to be potential independent indicators of survival and recurrence outcome for patients with resectable

pNET. The major limitations were that the nature of a retrospective study with a limited sample size restricts the level of evidence and that the mechanism by which platelets influence the recurrence of patients was not thoroughly investigated.

### Research conclusions

We uncovered a relationship between tumor-infiltrating platelets and the prognosis of patients with pNET following radical resection. We found that tumor-infiltrating platelets were potential pNET prognosis indicators. In addition, therapy targeting platelets in pNET could improve long-term survival. We further provide the clinical meaning of platelets in the tumor microenvironment in pNET.

### Research perspectives

A further prospective study with a large sample size should be conducted with multicenter cooperation, and additional experiments to assess the mechanism need to be implemented. If possible, we recommend a randomized double-blind controlled clinical trial for platelet-targeted therapy for pNET.

## ACKNOWLEDGEMENTS

We appreciate the support and help from Dr. Ya-Fei Chen, Dr. Houpu Xu, Dr. Dan Huang, and Dr. Cong Tan.

## REFERENCES

- 1 Lee MR, Harris C, Baeg KJ, Aronson A, Wisnivesky JP, Kim MK. Incidence Trends of Gastroenteropancreatic Neuroendocrine Tumors in the United States. *Clin Gastroenterol Hepatol* 2018 [PMID: 30580091 DOI: 10.1016/j.cgh.2018.12.017]
- 2 Öberg K, Knigge U, Kwekkeboom D, Perren A; ESMO Guidelines Working Group. Neuroendocrine gastro-entero-pancreatic tumors: ESMO Clinical Practice Guidelines for diagnosis, treatment and follow-up. *Ann Oncol* 2012; 23 Suppl 7: vii124-vii130 [PMID: 22997445 DOI: 10.1093/annonc/mds295]
- 3 Kaderli RM, Spanjol M, Kollár A, Bütikofer L, Gloy V, Dumont RA, Seiler CA, Christ ER, Radojewski P, Briel M, Walter MA. Therapeutic Options for Neuroendocrine Tumors: A Systematic Review and Network Meta-analysis. *JAMA Oncol* 2019; [Epub ahead of print] [PMID: 30763436 DOI: 10.1001/jamaoncol.2018.6720]
- 4 Haemmerle M, Stone RL, Menter DG, Afshar-Kharghan V, Sood AK. The Platelet Lifeline to Cancer: Challenges and Opportunities. *Cancer Cell* 2018; 33: 965-983 [PMID: 29657130 DOI: 10.1016/j.ccell.2018.03.002]
- 5 Placke T, Örgel M, Schaller M, Jung G, Rammensee HG, Kopp HG, Salih HR. Platelet-derived MHC class I confers a pseudonormal phenotype to cancer cells that subverts the antitumor reactivity of natural killer immune cells. *Cancer Res* 2012; 72: 440-448 [PMID: 22127925 DOI: 10.1158/0008-5472.CAN-11-1872]
- 6 Rao L, Bu LL, Ma L, Wang W, Liu H, Wan D, Liu JF, Li A, Guo SS, Zhang L, Zhang WF, Zhao XZ, Sun ZJ, Liu W. Platelet-Facilitated Photothermal Therapy of Head and Neck Squamous Cell Carcinoma. *Angew Chem Int Ed Engl* 2018; 57: 986-991 [PMID: 29193651 DOI: 10.1002/anie.201709457]
- 7 Wang Z, Fang M, Li J, Yang R, Du J, Luo Y. High Platelet Levels Attenuate the Efficacy of Platinum-Based Treatment in Non-Small Cell Lung Cancer. *Cell Physiol Biochem* 2018; 48: 2456-2469 [PMID: 30121639 DOI: 10.1159/000492683]
- 8 Kaltenborn A, Matzke S, Kleine M, Krech T, Ramackers W, Vondran FW, Klempnauer J, Bektas H, Schrem H. Prediction of survival and tumor recurrence in patients undergoing surgery for pancreatic neuroendocrine neoplasms. *J Surg Oncol* 2016; 113: 194-202 [PMID: 26709239 DOI: 10.1002/jso.24116]
- 9 Zou J, Li Q, Kou F, Zhu Y, Lu M, Li J, Lu Z, Shen L. Prognostic value of inflammation-based markers in advanced or metastatic neuroendocrine tumours. *Curr Oncol* 2019; 26: e30-e38 [PMID: 30853807 DOI: 10.3747/co.26.4135]
- 10 Karaman K, Bostanci EB, Aksoy E, Kurt M, Celep B, Ulas M, Dalgic T, Surmelioglu A, Hayran M, Akoglu M. The predictive value of mean platelet volume in differential diagnosis of non-functional pancreatic neuroendocrine tumors from pancreatic adenocarcinomas. *Eur J Intern Med* 2011; 22: e95-e98 [PMID: 22075321 DOI: 10.1016/j.ejim.2011.04.005]
- 11 Salman T, Kazaz SN, Varol U, Oflazoglu U, Unek IT, Kucukzeybek Y, Alacacioglu A, Atag E, Semiz HS, Cengiz H, Oztup I, Tarhan MO. Prognostic Value of the Pretreatment Neutrophil-to-Lymphocyte Ratio and Platelet-to-Lymphocyte Ratio for Patients with Neuroendocrine Tumors: An Izmir Oncology Group Study. *Chemotherapy* 2016; 61: 281-286 [PMID: 27070366 DOI: 10.1159/000445045]
- 12 Gaitanidis A, Patel D, Nilubol N, Tirosh A, Sadowski S, Kebebew E. Markers of Systemic Inflammatory Response are Prognostic Factors in Patients with Pancreatic Neuroendocrine Tumors (PNETs): A Prospective Analysis. *Ann Surg Oncol* 2018; 25: 122-130 [PMID: 29134377 DOI: 10.1245/s10434-017-6241-4]
- 13 Zhang SR, Yao L, Wang WQ, Xu JZ, Xu HX, Jin W, Gao HL, Wu CT, Qi ZH, Li H, Li S, Ni QX, Yu XJ, Fu DL, Liu L. Tumor-Infiltrating Platelets Predict Postsurgical Survival in Patients with Pancreatic Ductal Adenocarcinoma. *Ann Surg Oncol* 2018; 25: 3984-3993 [PMID: 30171511 DOI: 10.1245/s10434-018-6727-8]
- 14 Saito H, Fushida S, Miyashita T, Oyama K, Yamaguchi T, Tsukada T, Kinoshita J, Tajima H, Ninomiya I, Ohta T. Potential of extravasated platelet aggregation as a surrogate marker for overall survival in patients with advanced gastric cancer treated with preoperative docetaxel, cisplatin and S-1: a retrospective observational study. *BMC Cancer* 2017; 17: 294 [PMID: 28449652 DOI: 10.1186/s12885-017-3279-4]
- 15 Ishikawa S, Miyashita T, Inokuchi M, Hayashi H, Oyama K, Tajima H, Takamura H, Ninomiya I, Ahmed AK, Harman JW, Fushida S, Ohta T. Platelets surrounding primary tumor cells are related to

- chemoresistance. *Oncol Rep* 2016; **36**: 787-794 [PMID: 27349611 DOI: 10.3892/or.2016.4898]
- 16 **Yang J**, Zhou X, Fan X, Xiao M, Yang D, Liang B, Dai M, Shan L, Lu J, Lin Z, Liu R, Liu J, Wang L, Zhong M, Jiang Y, Bai X. mTORC1 promotes aging-related venous thrombosis in mice via elevation of platelet volume and activation. *Blood* 2016; **128**: 615-624 [PMID: 27288518 DOI: 10.1182/blood-2015-10-672964]
- 17 **Wojtukiewicz MZ**, Sierko E, Hempel D, Tucker SC, Honn KV. Platelets and cancer angiogenesis nexus. *Cancer Metastasis Rev* 2017; **36**: 249-262 [PMID: 28681240 DOI: 10.1007/s10555-017-9673-1]
- 18 **Ronca R**, Benkheil M, Mitola S, Struyf S, Liekens S. Tumor angiogenesis revisited: Regulators and clinical implications. *Med Res Rev* 2017; **37**: 1231-1274 [PMID: 28643862 DOI: 10.1002/med.21452]
- 19 **Miao S**, Shu D, Zhu Y, Lu M, Zhang Q, Pei Y, He AD, Ma R, Zhang B, Ming ZY. Cancer cell-derived immunoglobulin G activates platelets by binding to platelet FcγRIIa. *Cell Death Dis* 2019; **10**: 87 [PMID: 30692520 DOI: 10.1038/s41419-019-1367-x]
- 20 **Zhang Y**, Qiu Y, Blanchard AT, Chang Y, Brockman JM, Ma VP, Lam WA, Salaita K. Platelet integrins exhibit anisotropic mechanosensing and harness piconewton forces to mediate platelet aggregation. *Proc Natl Acad Sci USA* 2018; **115**: 325-330 [PMID: 29269394 DOI: 10.1073/pnas.1710828115]
- 21 **Cho MS**, Bottsford-Miller J, Vasquez HG, Stone R, Zand B, Kroll MH, Sood AK, Afshar-Kharghan V. Platelets increase the proliferation of ovarian cancer cells. *Blood* 2012; **120**: 4869-4872 [PMID: 22966171 DOI: 10.1182/blood-2012-06-438598]
- 22 **Liang H**, Yan X, Pan Y, Wang Y, Wang N, Li L, Liu Y, Chen X, Zhang CY, Gu H, Zen K. MicroRNA-223 delivered by platelet-derived microvesicles promotes lung cancer cell invasion via targeting tumor suppressor EPB41L3. *Mol Cancer* 2015; **14**: 58 [PMID: 25881295 DOI: 10.1186/s12943-015-0327-z]
- 23 **Haemmerle M**, Taylor ML, Gutschner T, Pradeep S, Cho MS, Sheng J, Lyons YM, Nagaraja AS, Dood RL, Wen Y, Mangala LS, Hansen JM, Rupaimoole R, Gharpure KM, Rodriguez-Aguayo C, Yim SY, Lee JS, Ivan C, Hu W, Lopez-Berestein G, Wong ST, Karlan BY, Levine DA, Liu J, Afshar-Kharghan V, Sood AK. Platelets reduce anoikis and promote metastasis by activating YAP1 signaling. *Nat Commun* 2017; **8**: 310 [PMID: 28827520 DOI: 10.1038/s41467-017-00411-z]
- 24 **Au AE**, Sashindranath M, Borg RJ, Kleinfeld O, Andrews RK, Gardiner EE, Medcalf RL, Samson AL. Activated platelets rescue apoptotic cells via paracrine activation of EGFR and DNA-dependent protein kinase. *Cell Death Dis* 2014; **5**: e1410 [PMID: 25210793 DOI: 10.1038/cddis.2014.373]
- 25 **Jiang L**, Luan Y, Miao X, Sun C, Li K, Huang Z, Xu D, Zhang M, Kong F, Li N. Platelet releasate promotes breast cancer growth and angiogenesis via VEGF-integrin cooperative signalling. *Br J Cancer* 2017; **117**: 695-703 [PMID: 28697175 DOI: 10.1038/bjc.2017.214]
- 26 **Kopp HG**, Placke T, Salih HR. Platelet-derived transforming growth factor-beta down-regulates NKG2D thereby inhibiting natural killer cell antitumor reactivity. *Cancer Res* 2009; **69**: 7775-7783 [PMID: 19738039 DOI: 10.1158/0008-5472.CAN-09-2123]
- 27 **Manoharan J**, Fendrich V, Di Fazio P, Bollmann C, Roth S, Joos B, Mintziras I, Albers MB, Ramaswamy A, Bertolino P, Zhang CX, Slater EP, Bartsch DK, Lopez-Lopez CL. Chemoprevention with Enalapril and Aspirin in Men1(+/-T) Knockout Mouse Model. *Neuroendocrinology* 2018; **107**: 257-266 [PMID: 30025403 DOI: 10.1159/000492224]



## Retrospective Study

# Blood parameters score predicts long-term outcomes in stage II-III gastric cancer patients

Jian-Xian Lin, Yi-Hui Tang, Jia-Bin Wang, Jun Lu, Qi-Yue Chen, Long-Long Cao, Mi Lin, Ru-Hong Tu, Chang-Ming Huang, Ping Li, Chao-Hui Zheng, Jian-Wei Xie

**ORCID number:** Jian-Xian Lin (0000-0002-5006-4454); Yi-Hui Tang (0000-0003-1959-0728); Jia-Bin Wang (0000-0002-2023-0183); Jun Lu (0000-0002-8459-4867); Qi-Yue Chen (0000-0001-6391-4043); Long-Long Cao (0000-0003-3144-3050); Mi Lin (0000-0001-7299-6159); Ru-Hong Tu (0000-0002-7491-3879); Chang-Ming Huang (0000-0002-0019-885X); Ping Li (0000-0002-9418-9339); Chao-Hui Zheng (0000-0003-0157-5167); Jian-Wei Xie (0000-0002-4291-2644).

**Author contributions:** Lin JX and Tang YH contributed equally to his work and should be considered co-first authors; Li P, Zheng CH, Xie JW, Lin JX, and Tang YH conceived of the study and analyzed the data; Wang JB, Lu J, Chen QY, Cao LL, Lin M, and Tu RH helped collect the data and design the study; Lin JX and Tang YH wrote the manuscript; Li P, Zheng CH, Xie JW, Lin JX, Wang JB, Lu J, and Chen QY helped revise the manuscript critically for important intellectual content; all authors read and approved the final manuscript.

**Supported by** the Scientific and Technological Innovation Joint Capital Projects of Fujian Province, No. 2016Y9031; the Minimally Invasive Medical Center of Fujian Province, No. [2017]171; the Science Foundation of Fujian Province, No. 2018J01307; and the Startup Fund for Scientific Research, Fujian Medical University, No. 2016QH024.

**Institutional review board statement:** This study was

Jian-Xian Lin, Yi-Hui Tang, Jia-Bin Wang, Jun Lu, Qi-Yue Chen, Long-Long Cao, Mi Lin, Ru-Hong Tu, Chang-Ming Huang, Ping Li, Chao-Hui Zheng, Jian-Wei Xie, Department of Gastric Surgery, Fujian Medical University Union Hospital, Fuzhou 350001, Fujian Province, China

Jian-Xian Lin, Jia-Bin Wang, Jun Lu, Qi-Yue Chen, Long-Long Cao, Chang-Ming Huang, Ping Li, Chao-Hui Zheng, Jian-Wei Xie, Key Laboratory of Ministry of Education of Gastrointestinal Cancer, Fujian Medical University, Fuzhou 350108, Fujian Province, China

**Corresponding author:** Jian-Wei Xie, MD, PhD, Doctor, Department of Gastric Surgery, Fujian Medical University Union Hospital, No. 29, Xinquan Road, Fuzhou 350001, Fujian Province, China. [xjwhw2019@163.com](mailto:xjwhw2019@163.com)

**Telephone:** +86-591-83363366

**Fax:** +86-591-83363366

## Abstract

### BACKGROUND

Increasing numbers of laboratory blood parameters (BPM) have been reported to greatly affect the long-term outcomes of gastric cancer (GC) patients. However, the existing prognostic models do not comprehensively analyze these predictors.

### AIM

To construct a new prognostic tool, based on all the prognostic BPM, to achieve more accurate prognosis prediction for GC.

### METHODS

We retrospectively assessed 850 consecutive patients who underwent curative resection for stage II-III GC from January 2010 to April 2013. The patients were classified into developing ( $n = 567$ ) and validation ( $n = 283$ ) cohorts using computer-generated random numbers. A scoring system, namely BPM score, was then constructed using least absolute shrinkage and selection operator (LASSO) Cox regression model in the developing cohort, and validated in the validation cohort. A nomogram consisting of BPM score and tumor-lymph node-metastasis (TNM) stage was further created. The discrimination and calibration of the nomogram were evaluated *via* Harrell's C-statistic and the Hosmer-Lemeshow test.

### RESULTS

Using the LASSO model, we established the BPM score based on five BPM: Albumin, lymphocyte-to-monocyte ratio, neutrophil-to-lymphocyte ratio,



reviewed and approved by the Fujian Medical University Union Hospital (FMUHH) Institutional Review Board.

#### Informed consent statement:

Patients were not required to give informed consent to the study because the analysis used anonymous clinical data that were obtained after each patient agreed to treatment by written consent.

**Conflict-of-interest statement:** We have no financial relationships to disclose.

**Data sharing statement:** No additional data are available.

**Open-Access:** This article is an open-access article which was selected by an in-house editor and fully peer-reviewed by external reviewers. It is distributed in accordance with the Creative Commons Attribution Non Commercial (CC BY-NC 4.0) license, which permits others to distribute, remix, adapt, build upon this work non-commercially, and license their derivative works on different terms, provided the original work is properly cited and the use is non-commercial. See: <http://creativecommons.org/licenses/by-nc/4.0/>

**Manuscript source:** Unsolicited manuscript

**Received:** July 11, 2019

**Peer-review started:** July 12, 2019

**First decision:** August 18, 2019

**Revised:** September 6, 2019

**Accepted:** September 11, 2019

**Article in press:** September 11, 2019

**Published online:** November 7, 2019

**P-Reviewer:** Merrett ND, Silsirivanit A, Young CJ

**S-Editor:** Tang JZ

**L-Editor:** Wang TQ

**E-Editor:** Ma YJ



carcinoembryonic antigen, and carbohydrate antigen 19-9. The BPM scores were divided into high- and low-BPM groups based on a cut-off value of -0.93. High-BPM patients were significantly older and had more advanced, larger tumors. In the developing cohort, significant differences were found in 5-year overall survival (OS) and 5-year disease-specific survival between the high-BPM and low-BPM patients. Similar results were found in the validation group. Multivariable analysis showed that the BPM score was an independent predictor of OS. High-BPM patients had a poorer 5-year OS for each subgroup. Furthermore, a nomogram that combined the BPM score and TNM stage had significantly better prognostic value compared with TNM stage alone.

#### CONCLUSION

The BPM score provides more accurate prognosis prediction in stage II-III GC patients and is an effective complement to the TNM staging system.

**Key words:** Blood parameters score; Gastric cancer; Long-term survival; Nomogram; Discrimination and calibration

©The Author(s) 2019. Published by Baishideng Publishing Group Inc. All rights reserved.

**Core tip:** The study aimed to select the optimal combination of blood parameters (BPM) and to establish a novel prognostic classifier. Using the least absolute shrinkage and selection operator model, we established the BPM score based on five BPM: Albumin, lymphocyte-to-monocyte ratio, neutrophil-to-lymphocyte ratio, carcinoembryonic antigen, and carbohydrate antigen 19-9. The BPM score provides more accurate prognosis prediction in stage II-III gastric cancer patients and is an effective complement to the tumor-lymph node-metastasis staging system.

**Citation:** Lin JX, Tang YH, Wang JB, Lu J, Chen QY, Cao LL, Lin M, Tu RH, Huang CM, Li P, Zheng CH, Xie JW. Blood parameters score predicts long-term outcomes in stage II-III gastric cancer patients. *World J Gastroenterol* 2019; 25(41): 6258-6272

**URL:** <https://www.wjnet.com/1007-9327/full/v25/i41/6258.htm>

**DOI:** <https://dx.doi.org/10.3748/wjg.v25.i41.6258>

## INTRODUCTION

Gastric cancer (GC) remains an important malignancy worldwide; there were over 1000000 new cases of GC and an estimated 783000 deaths caused by GC (equating to 1 in every 12 deaths globally) in 2018, making it the fifth most frequently diagnosed cancer and the third leading cause of cancer death<sup>[1]</sup>. The tumor-lymph node-metastasis (TNM) staging system is the most commonly used criteria to predict GC patients' long-term outcomes<sup>[2]</sup>. However, clinical outcomes can vary in patients with GC who have the same TNM stage and similar treatment regimens<sup>[3-5]</sup>, indicating that this anatomy-based system provides incomplete prognostic information. Hence, the identification of potential predictors of risk stratification and treatment selection has become a hot topic in recent years.

There is growing evidence that the patient's immune and nutritional statuses are closely related to long-term survival in patients with various malignancies<sup>[5-14]</sup>. Over the past decades, the lymphocyte count and serum albumin have been the most widely used biomarkers for defining the immune and nutritional statuses. As a result, several scoring systems, including the prognostic nutritional index (PNI), the modified Glasgow prognostic score (mGPS), and the controlling nutritional status (CONUT) score, have been constructed and commonly used to predict the outcomes in patients with GC<sup>[9-11]</sup>. However, these scores contain limited blood parameters (BPM) and may provide inadequate prognostic information<sup>[11,15-16]</sup>. Ongoing work is seeking other prognostic biomarkers. To date, several ratios based on circulating blood cell counts, such as the neutrophil-to-lymphocyte ratio (NLR), lymphocyte-to-monocyte ratio (LMR), and platelet-to-lymphocyte ratio (PLR), have been developed to predict the outcome of GC<sup>[12-14]</sup>. In addition, tumor markers, including carcinoembryonic antigen (CEA) and carbohydrate antigen (CA) 19-9, are routinely applied in the early detection and postoperative follow-up of GC. Some studies have

proved their prognostic value in GC<sup>[17-18]</sup>. Therefore, we hypothesized that a new scoring system, based on all available laboratory BPM, would provide more accurate prognostic information in patients with GC.

In the present study, we used the least absolute shrinkage and selection operator (LASSO) Cox regression model to select the optimal combination of BPM and to establish a novel prognostic classifier, namely, the BPM score, in order to predict outcomes in patients with stage II-III GC.

## MATERIALS AND METHODS

### Study population

We retrospectively assessed patients undergoing curative resection for GC at the Fujian Medical University Union Hospital (FMUHU) between January 2010 and April 2013. Patients who met the following criteria were included: (1) Aged  $\geq 18$  years; (2) Stage II-III gastric adenocarcinoma confirmed by histopathology; and (3) No pre-operative chemoradiotherapy. The following patients were excluded: (1) Distant metastasis; (2) Malignant disease of other organs; (3) R1 resection; (4) Acute infections or other inflammatory conditions within 7 days before surgery; and (5) Incomplete medical records or follow-up data. Finally, 850 patients were enrolled in this study. All surviving patients had a follow-up period of at least 5 years. The patients were classified into developing ( $n = 567$ ) and validation ( $n = 283$ ) cohorts using computer-generated random numbers. All surgical procedures, including lymph node dissection, were performed according to the guidelines of the Japanese Research Society for the Study of GC<sup>[19]</sup>, while staging was performed according to the TNM classification (AJCC, 8th edition). All patients were routinely recommend to receive 5-fluorouracil (5-FU) based adjuvant chemotherapy after surgery<sup>[4]</sup>.

### Data collection

Data on patient demographics and pathological results were obtained from a large-scale prospective database. Routine blood tests were carried out during 1 wk before surgery, including hemoglobin, serum albumin, total cholesterol level, total peripheral neutrophils, lymphocyte count, monocyte count, platelet count, CEA, CA 19-9, and fibrinogen. LMR was calculated by dividing lymphocyte count by monocyte count. NLR was calculated by dividing neutrophil count by lymphocyte count. PLR was calculated by dividing platelet count by lymphocyte count. We used widely accepted thresholds to define the dichotomous forms of these BPM: hemoglobin (males 120 g/L; females 110 g/L), albumin (35 g/L), cholesterol (4.6 mmol/L or 180 mg/dL), CEA (5 ng/mL), CA 19-9 (37 U/mL), and fibrinogen (400 mg/dL)<sup>[8,17,21-22]</sup>. According to the X-tile program (3.6.1 software 20, <http://medicine.yale.edu/lab/rimm/research/software.aspx>), NLR, LMR, and PLR cut-off values for overall survival (OS) were 3.9, 3.2, and 161, respectively<sup>[23]</sup>. The utility of clinical data was approved by the FMUHU Institutional Review Board.

### Follow-up investigation

All patients were followed postoperatively by physical examination and laboratory tests (including CEA, CA 19-9, and CA 72-4), every 3 mo for 2 years, every 6 mo during years 2-5, and annually thereafter. In addition, examinations, including chest radiography, abdominal computed tomography, and endoscopy, were performed at least once per year. The follow-up period was completed in April 2018 or to the date of death of patients. OS was defined as the time interval from surgery to death from any cause or to the last follow-up. Disease-specific survival (DSS) was defined as the time interval from surgery to death from GC or to the follow-up.

### Model development

As assays may vary between hospitals, all the BPM are expressed as ratio of lower limit of normal (including hemoglobin, albumin, and cholesterol), upper limit of normal (including fibrinogen, CEA, and CA 19-9), or cut-off values (including NLR, LMR, and PLR). The relation between the BPM (as continuous variables) and OS was investigated in univariate Cox models with restricted cubic splines (RCS)<sup>[24]</sup>. Additional variable transformation was performed if strong nonlinear effects were shown. Next, we calculated the Akaike information criterion (AIC) scores of the continuous form and the dichotomous form of each blood parameter to determine the form in which the blood parameter was analyzed<sup>[25]</sup>. Finally, we used the LASSO Cox regression model to select the most useful predictors among the candidate BPM in the developing cohort<sup>[26,27]</sup>. A risk score based on multiple BPM, the BPM score, was then constructed to predict the prognosis of GC. Details of methods are described in the [Supplementary Materials](#).

### Statistical methods

Continuous variables were compared using the Student's *t*-test, and categorical variables were assessed using the  $\chi^2$  test or the Fisher exact test. The Kaplan-Meier method was used to analyze OS and DSS, and the differences were assessed by log-rank tests. The time-dependent receiver operating characteristic (ROC) curve was generated to assess the discriminatory power of indicators for time-dependent disease outcomes<sup>[28]</sup>. Univariate and multivariate analyses were performed using the Cox proportional hazards model. A nomogram consisting of the BPM score and TNM stage was created to translate model parameter estimates into a visual scoring system to calculate the estimated survival probability. The discriminative power of the nomogram was assessed *via* Harrell's C-statistic<sup>[29]</sup>. The calibration of the nomogram was evaluated by the Hosmer-Lemeshow test to assess the goodness of fit<sup>[30]</sup>. Decision curve analysis was used to examine the usefulness and benefit of the nomogram<sup>[31]</sup>. Two-tailed *P* values < 0.05 were considered statistically significant. All statistical analyses were conducted with SPSS software, version 18.0 (SPSS Inc., Chicago, IL, United States) and R software, version 3.1.2 (R Foundation for Statistical Computing, Vienna, Austria).

## RESULTS

### Patient characteristics

Overall, 850 patients were included in the study. There were 656 (77.2%) males and 194 (22.8%) females. The median age at the time of surgery was 62 years (range, 20-91 years). According to the TNM classification, 285 (33.5%) were classified as having stage II and 565 (66.5%) as having stage III, respectively. The majority of the patients (*n* = 645, 75.8%) received adjuvant chemotherapy. The median follow-up time was 61 mo (range, 1-102 mo). Patient characteristics in the developing and validation cohorts are detailed in [Table 1](#).

### Derivation of the BPM score

It was observed that the relationship between total cholesterol level and OS followed a U-shaped pattern, with a turning point approximately  $1.5 \times \text{LLN}$ . Therefore, the values for this variable were transformed by taking the absolute distance between cholesterol (in unit  $\times \text{LLN}$ ) and the turning point. Similarly, CEA and CA 19-9 were transformed to the form of  $\ln \text{CEA}$  and  $\ln \text{CA 19-9}$ . After transforming, no strong nonlinear effect was observed in all BPM ([Supplementary Figure 1](#)). Then, we calculated AIC scores and Harrell's C-statistics of 9 BPM as continuous variables ([Supplementary Table 1](#)) and as dichotomous variables. It was found that only hemoglobin, albumin,  $\ln \text{CEA}$ , and fibrinogen had smaller AIC scores as well as significantly higher Harrell's C-statistics in their continuous forms ([Supplementary Table 2](#)). So, they were further analyzed as continuous variables, with the others analyzed as dichotomous variables.

Using LASSO Cox regression analysis, we identified five out of the nine BPM in the developing cohort: Albumin, LMR, NLR, CEA, and CA 19-9, and derived a formula to calculate the BPM score for each patient:  $\text{BPM} = -0.86259331 \times \text{Albumin} (\times \text{LLN}) + 0.08074780 \times \text{Low\_LMR} + 0.06002645 \times \text{High\_NLR} + 0.05939068 \times \text{High\_CA19-9} + 0.04007563 \times \ln \text{CEA} (\times \text{ULN})$  ([Figure 1A and B](#)).

In this formula, LMR, NLR, and CA 19-9 were valued as 0 or 1;  $\text{LMR} \leq 3.2$ ,  $\text{NLR} \geq 3.9$ , and  $\text{CA 19-9} \geq 37 \text{ U/mL}$  were assigned a score of 1, and a value of 0 otherwise. The optimum cutoff value for BPM score was selected on the basis of the association with the patients' OS by using X-tile plots (-0.93). We then assigned patients to a high-BPM (BPM score  $\geq -0.93$ ) or low-BPM (BPM score < -0.93) group by this value.

### Correlations between clinicopathological findings and BPM score

[Table 1](#) shows the relationship between clinicopathological factors and the BPM score. In both the developing and validation cohorts, high-BPM status was related to older age ( $P < 0.001$  for both), higher tumor stage ( $P < 0.001$  and  $P = 0.004$ , respectively), and larger tumor size ( $P < 0.001$  and  $P = 0.014$ , respectively), compared with low-BPM status. In addition, although the high-BPM patients had a smaller body mass index (BMI) ( $P = 0.038$ ) than the low-BPM patients in the developing cohort, it did not reach statistical significance in the validation cohort ( $P = 0.285$ ).

### Prognostic value of BPM score

In the developing cohort, the 5-year OS rates in the low-BPM and high-BPM groups were 70.0% and 41.6%, and the 5-year DSS rates were 72.4% and 46.4% (log-rank  $P < 0.001$ , [Figure 2A](#)). We performed the same analyses in the validation cohort. The 5-

**Table 1** Clinicopathological characteristics of patients according to the blood parameters score in the developing and validation cohorts

Variable	Developing cohort (n = 567)				Validation cohort (n = 283)			
	Total	Low-BPM (%)	High-BPM (%)	P value	Total	Low-BPM (%)	High-BPM (%)	P value
Age (yr, mean ± SD)		58.8 (± 11.3)	64.6 (± 10.1)	< 0.001		59.5 (± 11.5)	65.5 (± 9.5)	< 0.001
Sex				0.409				0.193
Male	430	218 (74.4)	212 (77.4)		226	113 (76.9)	113 (83.1)	
Female	137	75 (25.6)	62 (22.6)		57	34 (23.1)	23 (16.9)	
Body mass index (mean ± SD)		22.3 (± 2.8)	21.8 (± 3.0)	0.038		22.1 (± 2.6)	21.7 (± 3.1)	0.285
Tumor stage				< 0.001				0.004
II a	86	58 (19.8)	79 (28.8)		61	39 (26.5)	22 (16.2)	
II b	93	42 (14.3)	51 (18.6)		45	25 (17.0)	20 (14.7)	
III a	142	89 (30.4)	53 (19.3)		63	33 (22.4)	30 (22.1)	
III b	148	71 (24.2)	77 (28.1)		66	33 (22.4)	30 (22.1)	
III c	98	33 (11.3)	65 (23.7)		48	17(11.6)	31 (22.8)	
Tumor location				0.363				0.553
Lower	222	121 (41.3)	101 (36.9)		109	62 (42.2)	47 (34.6)	
Middle	112	50 (17.1)	62 (22.6)		50	26 (17.7)	24 (17.6)	
Upper	156	80 (27.3)	76 (27.7)		74	36 (24.5)	38 (27.9)	
Mixed	77	42 (14.3)	35 (12.8)		50	23 (15.6)	27 (19.9)	
Tumor size (mm, mean ± SD)		45.9 (± 22.3)	56.7 (± 26.6)	< 0.001		47.2 (± 22.9)	54.2 (24.8)	0.014
Histologic type				0.902				0.613
Differentiated	92	47 (16.0)	45 (16.4)		52	25 (17.0)	27 (19.9)	
Undifferentiated	475	246 (84.0)	229 (83.6)		231	122 (83.0)	109 (80.1)	
Lymphovascular invasion				0.662				0.910
No	394	206 (70.3)	188 (68.6)		178	159 (65.4)	33 (53.2)	
Yes	173	87 (29.7)	86 (31.4)		113	84 (34.6)	29 (46.8)	
Adjuvant chemotherapy				0.346				0.355
No	137	66 (22.5)	71 (25.9)		68	32 (21.8)	36 (26.5)	
Yes	430	227 (77.5)	203 (74.1)		215	115 (78.2)	100 (73.5)	

SD: Standard deviation; BPM: Blood parameters.

year OS rates in the low-BPM and high-BPM groups were 67.3% and 39.7%, and the 5-year DSS rates were 70.1% and 41.9% (log-rank  $P < 0.001$ , **Figure 2B**). In the multivariate analysis, BPM score remained an independent prognostic factor for OS ( $P < 0.001$  and  $P = 0.004$ , respectively) in both the developing and validation cohorts (**Table 2**).

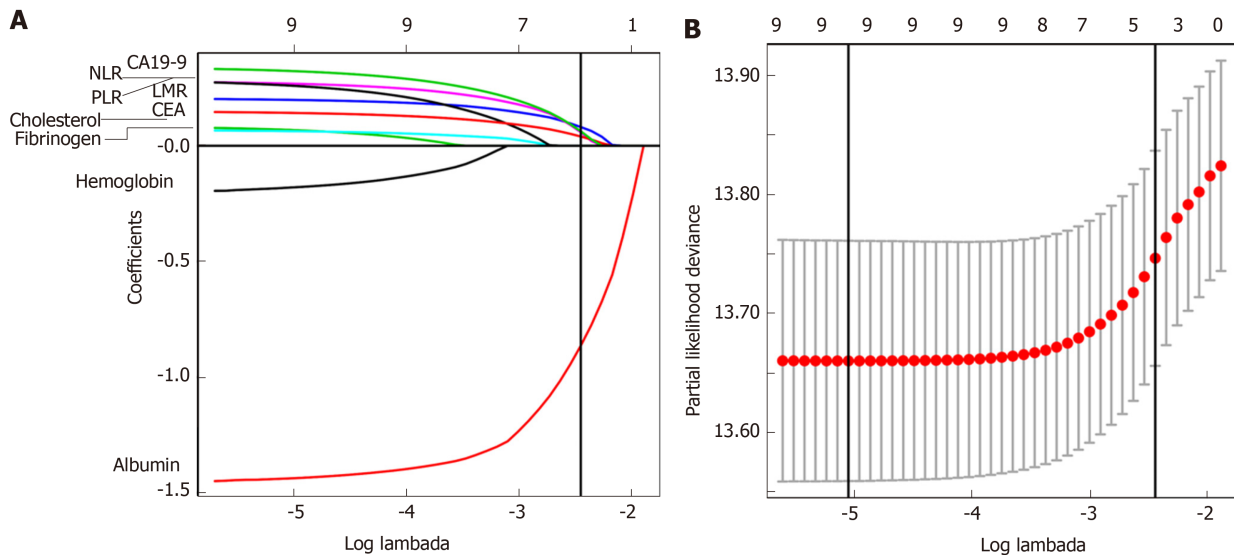
To confirm whether the BPM score has more benefits than using only one marker, we compared their areas under the curves (AUC) using ROC analysis in the entire cohort. The BPM score exhibited a higher prognostic accuracy (0.680) than each individual marker, including albumin (0.640,  $P < 0.001$ ), LMR (0.580,  $P < 0.001$ ), NLR (0.546,  $P < 0.001$ ), CEA (0.578,  $P < 0.001$ ), and CA 19-9 (0.565,  $P < 0.001$ ). Furthermore, the time-dependent ROC curves calculated at different time points for BPM score (as a dichotomous variable) and other scoring systems [including PNI, CONUT score, and modified systemic inflammation score (mSIS)<sup>[32]</sup>] clearly showed that the BPM score was continuously superior to the other scoring systems at each time point (**Figure 2C**).

Next, we used multivariate Cox models by means of RCS to further analyze the relationship between BPM score and OS with adjustment for the clinicopathologic factors (including age, BMI, tumor stage, tumor size, lymphovascular invasion, and adjuvant chemotherapy, which reached statistical significance in the univariate analysis). A continuous linear association between BPM score and OS was observed in the analysis of the developing, validation, and entire cohorts (Supplementary Figure 2).

### **BPM score has stable prognostic value in different subgroups of patients**

We performed stratified analyses of GC patients in the entire cohort. High-BPM patients with stages IIa, IIb, IIIa, IIIb, and IIIc disease had a shorter OS and DSS compared with low-BPM patients (log-rank  $P < 0.05$  for all, **Figure 3**). A forest plot





**Figure 1 Construction of the blood parameters score, a classifier comprising five blood parameters.** A: Least absolute shrinkage and selection operator (LASSO) coefficient profiles of the nine blood parameters. The vertical line indicates the value chosen by 10-fold cross-validation; B: Ten-fold cross-validation for tuning parameter selection in the LASSO Cox model. Solid vertical lines represent partial likelihood deviance  $\pm$  standard error. We plotted the partial likelihood deviance vs log ( $\lambda$ ), where  $\lambda$  is the tuning parameter. The vertical lines are drawn at the optimal values by minimum criteria and 1 - S.E. criteria.

based on 5-year OS was further established, and the results confirmed that high-BPM patients had a poor prognosis among each subgroup (Figure 4). Furthermore, we assigned patients to an adjuvant chemotherapy (AC) or a non-AC group based on the receipt of postoperative adjuvant chemotherapy and then performed the Kaplan-Meier survival analysis. The results revealed that high-BPM patients had a poorer prognosis compared with low-BPM patients in both the AC and non-AC groups (log-rank  $P < 0.001$  for all, Supplementary Figure 3).

#### Prognostic value of TNM + BPM

To make individualized prediction of the survival probability in stages II and III GC patients, we established a nomogram that combined the BPM score and TNM stage in the entire cohort (Figure 5A). The Harrell's C-statistic of this nomogram was significantly higher than that of TNM stage alone (0.727 vs 0.697,  $P < 0.001$ ). The Hosmer-Lemeshow test showed that the model had good fit for 1-, 3-, and 5-year OS ( $P = 0.979$ ,  $P = 0.853$ , and  $P = 0.655$ , respectively). The decision curve analysis revealed that TNM + BPM had better clinical utility than TNM stage alone at 1, 3, and 5 years (Figure 5B-D).

## DISCUSSION

A growing body of evidence has demonstrated the potential of some laboratory BPM as prognostic markers to predict the oncologic outcomes in human malignancies<sup>[5-14,17-18,21-22]</sup>. However, how to comprehensively use these predictors to predict the long-term prognosis of patients with GC remains unclear. So far, researchers have established PNI, mGPS, CONUT, and mSIS as scoring systems that reflect immunological and nutritional statuses to more accurately predict clinical outcomes and to administer individualized treatment<sup>[9-11,32]</sup>. However, the clinical usefulness of these scoring systems is still controversial. Liu *et al*<sup>[15]</sup> found that low PNI was marginally associated with 5-year OS in patients with stage III GC, but the prognostic value was not significant in stages I and II GC. A retrospective study of 416 patients reported that a high CONUT score was strongly associated with 5-year OS in both pStage I and pStage II patients but not in pStage III patients<sup>[11]</sup>. Similarly, previous studies showed that the utility of mGPS and mSIS in patients with GC was also controversial<sup>[16,32]</sup>. A possible explanation was that these scores did not include all valuable BPM for comprehensive analysis, resulting in their limited prognostic value.

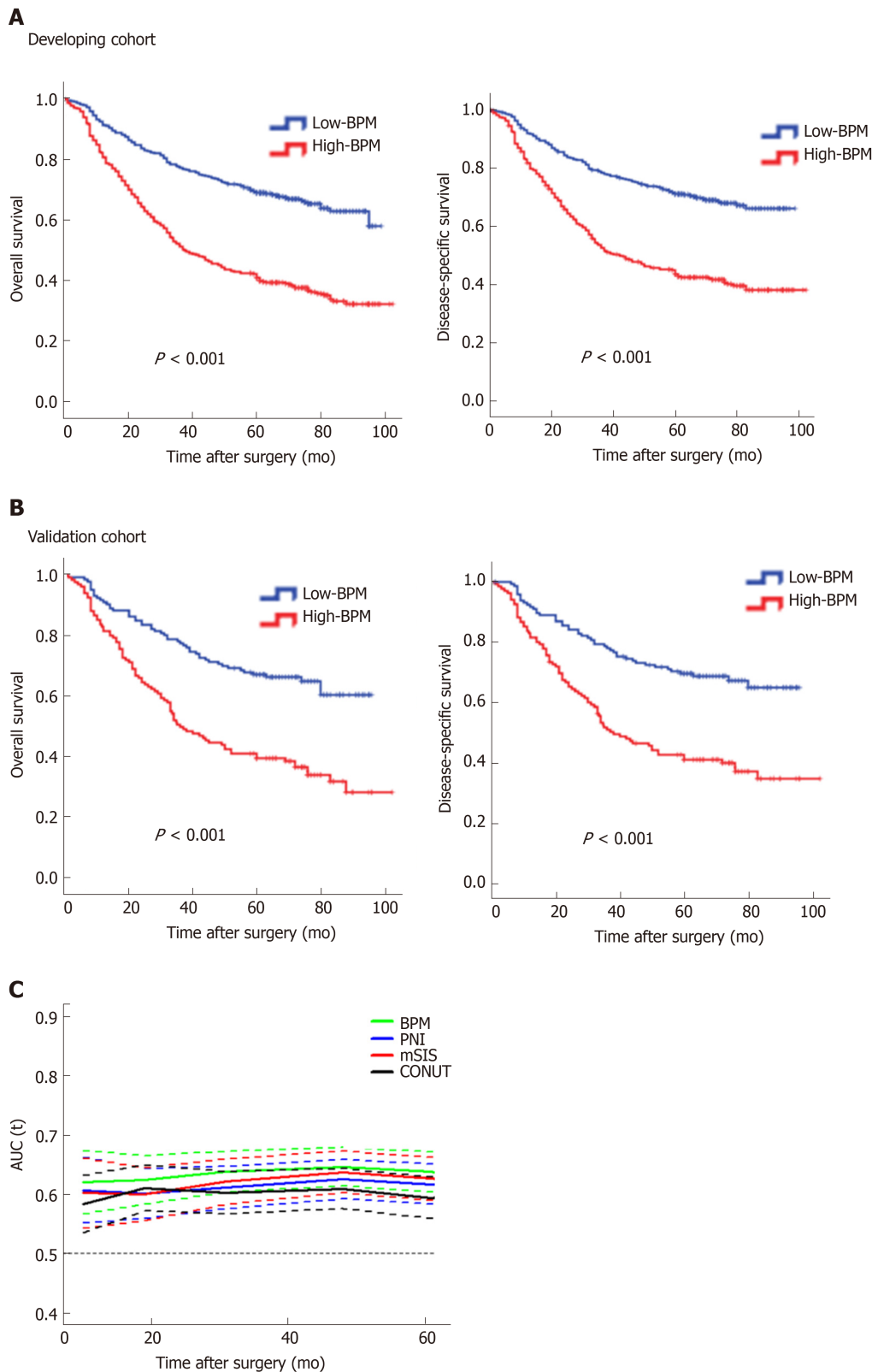
In addition, in the pursuit of simplicity, some of the current scoring systems handle the BPM in a categorical manner when they are, in fact, generated as continuous variables. It was reported that dichotomisation of continuous variables in a multiple regression procedure may be associated with considerable loss of statistical power and introduction of bias<sup>[33,34]</sup>. However, we should acknowledge that considering an



**Table 2** Univariate and multivariate analyses for overall survival in the developing and validation cohorts

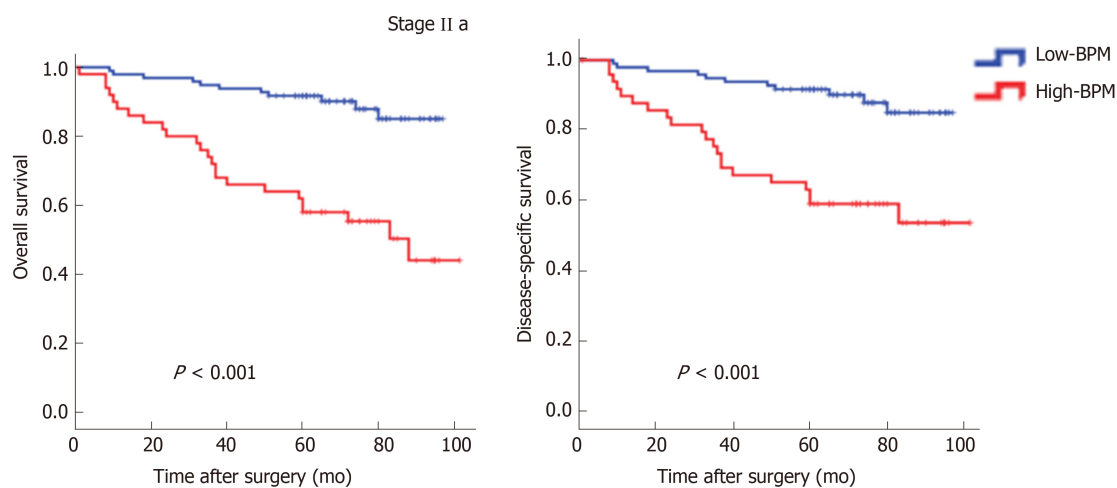
Variables	Developing cohort (n = 567)				Validation cohort (n = 283)			
	Univariate analysis		Multivariate analysis		Univariate analysis		Multivariate analysis	
	HR (95%CI)	P value	HR (95%CI)	P value	HR (95%CI)	P value	HR (95%CI)	P value
Age (yr)		0.005		0.144		0.001		0.008
< 60	Reference		Reference		Reference		Reference	
≥ 60	1.432 (1.115-1.838)		1.215 (0.936-1.579)		1.758 (1.262-2.449)		1.617 (1.132-2.311)	
Gender		0.502				0.900		
Male	Reference		Not included		Reference		Not included	
Female	1.098 (0.835-1.444)				0.974 (0.644-1.473)			
Body mass index		0.058				0.025		0.241
< 18.5	Reference		Not included		Reference		Reference	
18.5-23.9	0.734 (0.509-1.060)				0.551 (0.325-0.934)		0.720 (0.415-1.247)	
> 23.9	0.597 (0.390-0.913)				0.413 (0.217-0.788)		0.645 (0.328-1.270)	
BPM score		< 0.001		< 0.001		< 0.001		0.004
Low	Reference		Reference		Reference		Reference	
High	2.429 (1.893-3.117)		1.993 (1.534-2.589)		2.363 (1.677-3.330)		1.717 (1.913-2.470)	
Tumor stage		< 0.001		< 0.001		< 0.001		< 0.001
Ia	Reference		Reference		Reference		Reference	
Ib	1.422 (0.772-2.621)		1.220 (0.659-2.260)		0.942 (0.453-1.957)		0.778 (0.373-1.624)	
IIa	2.007 (1.161-3.471)		1.988 (1.143-3.458)		1.725 (0.953-3.121)		1.609 (0.876-2.956)	
IIb	4.776 (2.851-8.000)		3.977 (2.348-6.737)		3.526 (2.030-6.125)		3.116 (1.749-5.553)	
IIc	7.713 (4.550-13.074)		5.709 (3.299-9.882)		6.234 (3.535-10.993)		4.251 (2.294-7.878)	
Tumor size		< 0.001		0.034		0.004		0.638
≤40 mm	Reference		Reference		Reference		Reference	
>40 mm	1.987 (1.542-2.560)		1.332 (1.022-1.735)		1.647 (1.176-2.308)		0.913 (0.624-1.336)	
Tumor location		0.002		0.596		0.001		0.043
Lower	Reference		Reference		Reference		Reference	
Middle	1.307 (0.935-1.827)		1.103 (0.786-1.547)		1.319 (0.795-2.189)		1.313 (0.776-2.221)	
Upper	1.209 (0.888-1.647)		1.125 (0.822-1.539)		1.710 (1.117-2.618)		1.819 (1.518-2.857)	
Mixed	1.963 (1.396-2.762)		1.279 (0.896-1.825)		2.448 (1.554-3.857)		1.805 (1.052-3.096)	
Histologic type		0.344				0.871		
Differentiated	Reference		Not included		Reference		Not included	
Undifferentiated	1.176 (0.841-1.646)				0.966 (0.635-1.469)			
Lymphovascular invasion		0.006		0.832		0.102		
No	Reference		Reference		Reference		Not included	
Yes	1.422 (1.108-1.825)		1.029 (0.793-1.334)		1.324 (0.945-1.854)			
Adjuvant chemotherapy		< 0.001		0.003		0.001		0.022
No	Reference		Reference		Reference		Reference	
Yes	0.626 (0.481-0.814)		0.664 (0.508-0.868)		0.551 (0.385-0.787)		0.650 (0.450-0.939)	

HR: Hazard ratio; CI: Confidence interval; BPM: Blood parameters.

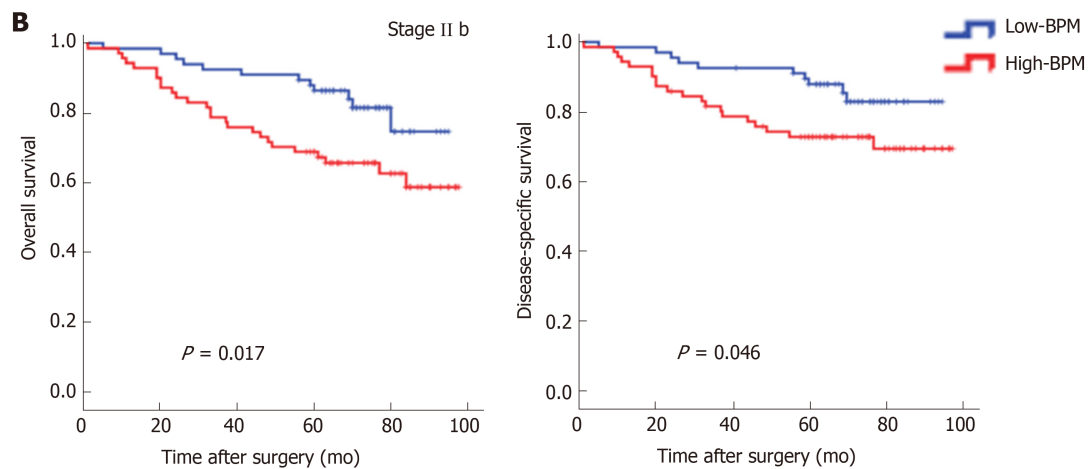


**Figure 2 Survival impact of the blood parameters score measured by Kaplan-Meier survival.** A: Survival impact of the blood parameters (BPM) score measured by Kaplan-Meier survival in the developing cohort; B: Survival impact of the BPM score measured by Kaplan-Meier survival in the validation cohort. We calculated  $P$  values using the log-rank test; C: Time-dependent receiver operating characteristic curves of BPM score, prognostic nutritional index (PNI), controlling nutritional status (CONUT), and modified systemic inflammation score (mSIS) for the prediction of overall survival. PNI indicates prognostic nutritional index calculated as follows:  $10 \times \text{serum albumin (g/L)} + 0.005 \times \text{lymphocyte count (/mm}^3\text{)}$ . CONUT indicates controlling nutritional status, a scoring system calculated by summing the value of serum albumin, total cholesterol, and total lymphocyte count. mSIS indicates modified systemic inflammation score developed based on serum albumin and lymphocyte-monocyte ratio. PNI: Prognostic nutritional index; CONUT: Controlling nutritional status; mSIS: Modified systemic inflammation score; BPM: Blood parameters.

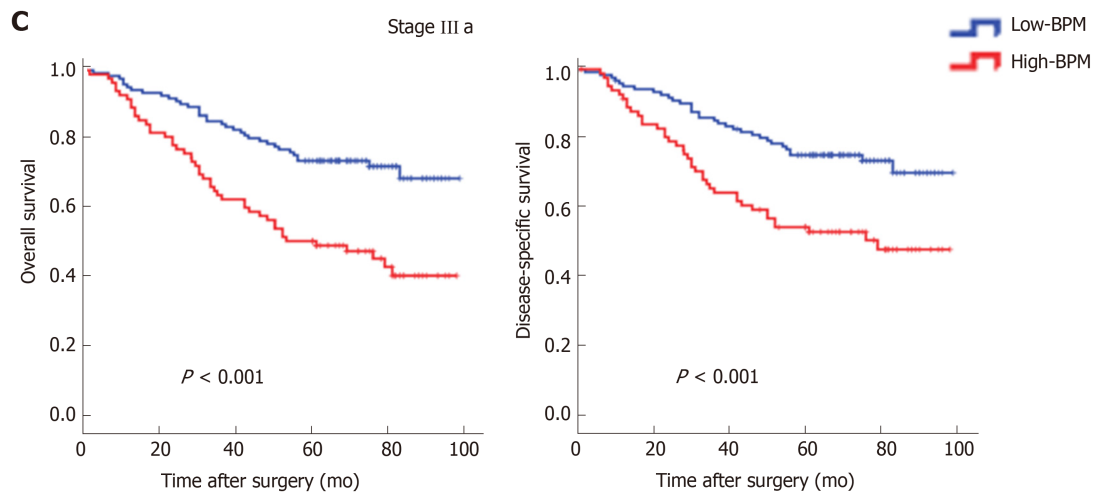
**A**

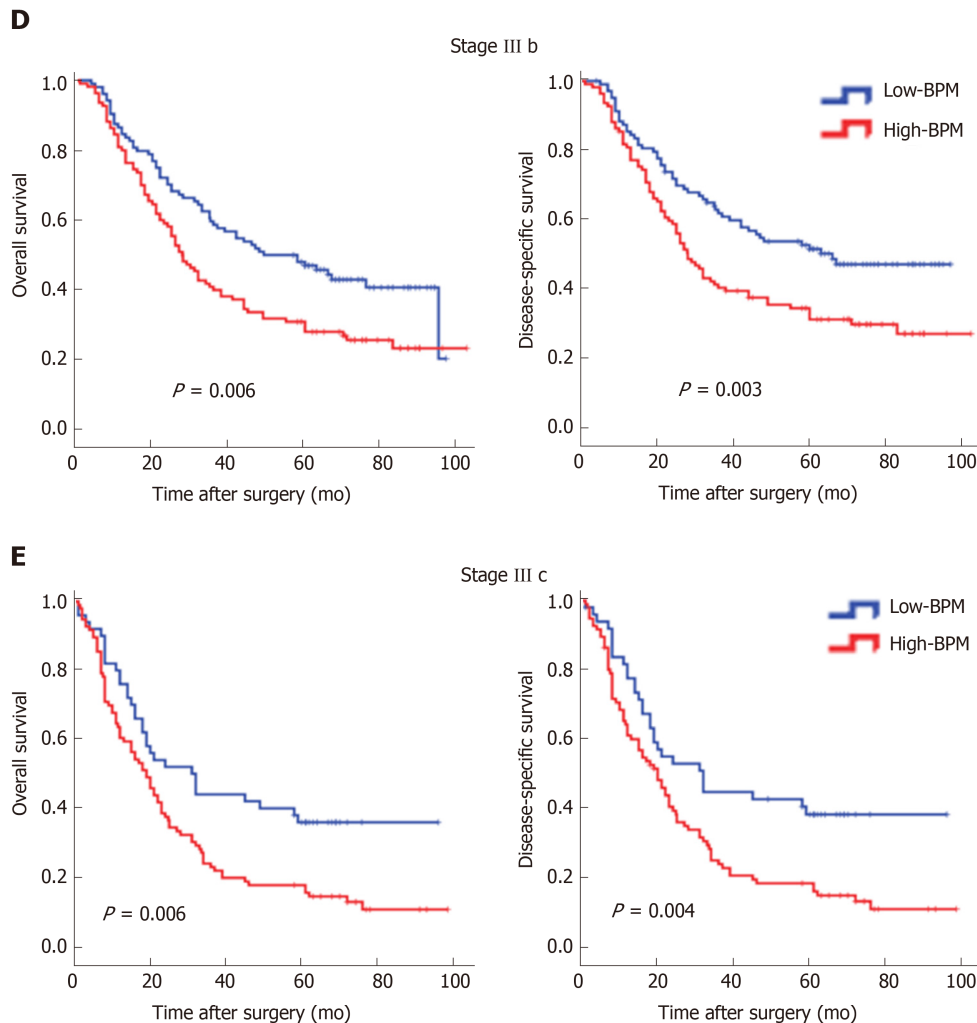


**B**



**C**

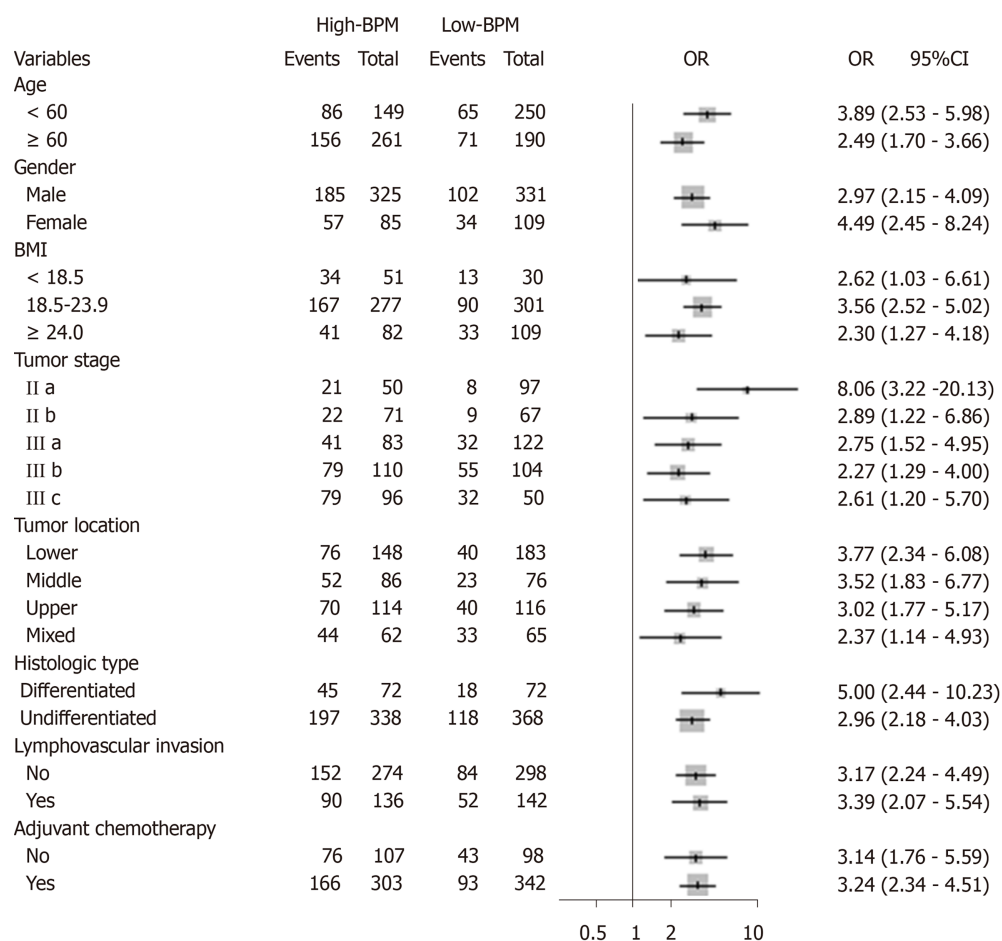




**Figure 3** Kaplan-Meier curves for overall survival and disease-specific survival in the high-blood parameters or low-blood parameters groups for different stages. A: Stage IIa; B: Stage IIb; C: Stage IIIa; D: Stage IIIb; E: Stage IIIc. BPM: Blood parameters.

indicator as a continuous variable does not necessarily improve the prediction accuracy. At the same time, it may not be easy to use in the clinical decision-making process<sup>[35]</sup>. Therefore, in the present study, we separately calculated and compared the AIC score and Harrell's C-statistic of each blood parameter in the dichotomous and continuous forms to determine which form was better for this indicator. It was found that only the continuous form of hemoglobin, albumin, fibrinogen, and CEA had smaller AIC scores than their dichotomous form, with significantly stronger discriminative power. So, we further analyzed them as continuous variables, while the remaining indicators (including cholesterol, LMR, NLR, PLR, and CA 19-9) were valued as 0 or 1 according to their cut-off values.

The prognostic influence of perioperative laboratory BPM may be difficult to discern in patients with stage I GC, who experience fewer cases of DSS, and in patients with stage IV GC, who experience extremely lower survival rates<sup>[5]</sup>. Therefore, the present study enrolled stage II-III GC patients based on a prospectively collected database of a high-volume center in order to provide a novel prognostic model for these patients with resectable locally advanced GC. Using LASSO Cox regression analysis, we established the BPM score based on five objectively measured, easily obtained BPM covering inflammatory, nutritional, and tumor markers: Albumin, LMR, NLR, CEA, and CA 19-9. To our knowledge, the link of malnutrition and systemic inflammation with carcinogenesis, tumor growth, and cancer progression has been demonstrated in several cancers, including GC<sup>[5-16,36-39]</sup>. In addition, tumor markers, as circulating substances that can be measured quantitatively, have a causal relationship with malignant diseases and are currently applied in prognosis prediction of GC patients<sup>[17,18,40]</sup>. A comparison of the clinicopathological variables between high-BPM and low-BPM patients revealed that a high BPM score was associated with older age, higher tumor stage, and larger tumor



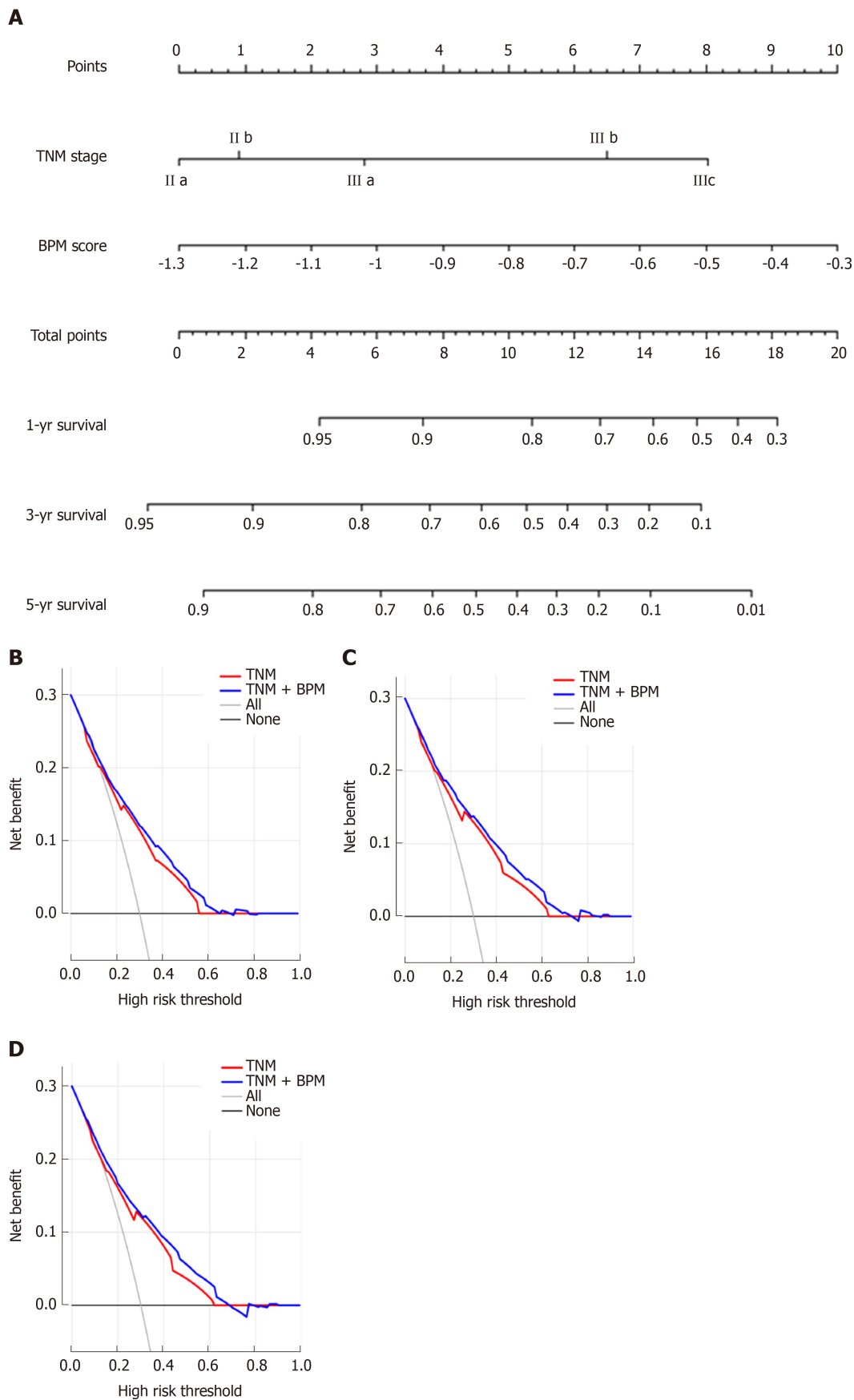
**Figure 4** Forest plot showing the impact of blood parameters score on 5-year overall survival stratified by different clinicopathological factors. Odds ratios with 95% confidence intervals are shown for the high-blood parameters (BPM) group vs low-BPM group. CI: Confidence interval; OR: Odds ratios; BMI: Body mass index; BPM: Blood parameters.

size. Multivariate analysis showed that the BPM score was an independent risk factor, had a stable prognostic ability among patients in each subgroup, and had better predictive accuracy than the traditional scoring systems. More importantly, the BPM score proved to be a supplement to the TNM staging system. Therefore, we recommend the use of the TNM + BPM scoring system incorporating preoperative albumin, LMR, NLR, CEA, and CA 19-9 levels for multimodality treatment planning and risk stratification in prospective studies.

In this study, we found that the BPM score, a novel scoring system based on five BPM, was predictive of long-term outcomes in stage II-III GC patients. This tool may have important uses in prognostic stratification, therapeutic intervention, and postoperative surveillance strategies, especially after incorporating TNM stage. For example, patients with a high BPM score will be recommended to receive postoperative multimodality treatment, such as chemotherapy, immunotherapy, and targeted therapy. And more regular follow-up schedule will be offered to early detect recurrence, which may provide survival benefit<sup>[41]</sup>. A patient example of how the model can be used in clinical practice is provided in the [Supplementary Materials](#).

This study has some limitations. First, as a retrospective, single-institution study, it may have been subject to selection bias. However, all data were derived from a prospectively collected database of a high-volume center, which can reduce this bias. Second, because C-reactive protein and prealbumin were not routinely tested before surgery in our institution, we did not include these potentially valuable biomarkers. Third, the validity and generalizability of the BPM score need to be established by testing it in other locations and groups of patients<sup>[42]</sup>.





**Figure 5 Prediction and analysis of 1-, 3-, and 5-year overall survival in patients.** A: A nomogram combining blood parameters score and tumor-lymph node-metastasis stage for predicting 1-, 3-, and 5-year overall survival (OS) in patients with stage II-III gastric cancer; B: Decision curve analysis of the nomogram for 1-year OS; C: Decision curve analysis of the nomogram for 3-year OS; D: Decision curve analysis of the nomogram for 5-year OS. TNM: Tumor-lymph node-metastasis; BPM: Blood parameters.

## ARTICLE HIGHLIGHTS

**Research background**

Increasing numbers of laboratory blood parameters (BPM) have been reported to greatly affect the long-term outcomes of gastric cancer (GC) patients. However, the existing prognostic models, including the prognostic nutritional index, the modified Glasgow prognostic score, and the controlling nutritional status score, contain limited BPM and provide inadequate prognostic information.

**Research motivation**

We hypothesized that a new scoring system, based on all available BPM, would provide more accurate prognostic information in patients with GC.

**Research objectives**

The present study aimed to construct a new prognostic tool, based on all the prognostic BPM, to achieve more accurate prognosis prediction for GC.

**Research methods**

We retrospectively assessed 850 consecutive patients who underwent curative resection for stage II-III GC from January 2010 to April 2013. The patients were classified into developing ( $n = 567$ ) and validation ( $n = 283$ ) cohorts using computer-generated random numbers. A scoring system, namely BPM score, was then constructed using the least absolute shrinkage and selection operator (LASSO) Cox regression model. A nomogram consisting of the BPM score and tumor-lymph node-metastasis (TNM) stage was created. The discrimination and calibration of the nomogram were evaluated *via* Harrell's C-statistic and the Hosmer-Lemeshow test.

**Research results**

Using the LASSO model, we established the BPM score based on five BPM: Albumin, lymphocyte-to-monocyte ratio, neutrophil-to-lymphocyte ratio, carcinoembryonic antigen, and carbohydrate antigen 19-9. The BPM scores were divided into high-BPM and low-BPM groups based on a cut-off value of -0.93. High-BPM patients were significantly older and had more advanced, larger tumors. In the developing cohort, significant differences were found in 5-year overall survival (OS) and 5-year disease-specific survival between the high-BPM and low-BPM patients. Similar results were found in the validation group. Multivariable analysis showed that the BPM score was an independent predictor of OS. High-BPM patients had a poorer 5-year OS for each subgroup. Furthermore, a nomogram that combined the BPM score and TNM stage had significantly better prognostic value compared with TNM stage alone.

**Research conclusions**

The BPM score provides more accurate prognosis prediction in stage II-III GC patients and is an effective complement to the TNM staging system. Therefore, we recommend the use of the BPM score for multimodality treatment planning and risk stratification in the future clinical work.

**Research perspectives**

Although we confirmed that the BPM score can accurately predict the outcomes in stage II-III GC patients, the efficiency of this novel scoring system need to be investigated in a prospective multicenter trial.

## REFERENCES

- Bray F, Ferlay J, Soerjomataram I, Siegel RL, Torre LA, Jemal A. Global cancer statistics 2018: GLOBOCAN estimates of incidence and mortality worldwide for 36 cancers in 185 countries. *CA Cancer J Clin* 2018; **68**: 394-424 [PMID: 30207593 DOI: 10.3322/caac.21492]
- Van Cutsem E, Sagaert X, Topal B, Haustermans K, Prenen H. Gastric cancer. *Lancet* 2016; **388**: 2654-2664 [PMID: 27156933 DOI: 10.1016/S0140-6736(16)30354-3]
- Sasako M, Inoue M, Lin JT, Khor C, Yang HK, Ohtsu A. Gastric Cancer Working Group report. *Jpn J Clin Oncol* 2010; **40**: i28-i37 [PMID: 20870917 DOI: 10.1093/jjco/hyq124]
- Noh SH, Park SR, Yang HK, Chung HC, Chung JJ, Kim SW, Kim HH, Choi JH, Kim HK, Yu W, Lee JI, Shin DB, Ji J, Chen JS, Lim Y, Ha S, Bang YJ; CLASSIC trial investigators. Adjuvant capecitabine plus oxaliplatin for gastric cancer after D2 gastrectomy (CLASSIC): 5-year follow-up of an open-label, randomised phase 3 trial. *Lancet Oncol* 2014; **15**: 1389-1396 [PMID: 25439693 DOI: 10.1016/S1470-2045(14)70473-5]
- Shen Q, Liu W, Quan H, Pan S, Li S, Zhou T, Ouyang Y, Xiao H. Prealbumin and lymphocyte-based prognostic score, a new tool for predicting long-term survival after curative resection of stage II/III gastric cancer. *Br J Nutr* 2018; **120**: 1359-1369 [PMID: 30370885 DOI: 10.1017/S0007114518002854]
- Dolan RD, McSorley ST, Park JH, Watt DG, Roxburgh CS, Horgan PG, McMillan DC. The prognostic value of systemic inflammation in patients undergoing surgery for colon cancer: comparison of composite ratios and cumulative scores. *Br J Cancer* 2018; **119**: 40-51 [PMID: 29789606 DOI: 10.1038/s41416-018-0095-9]
- Hirahara N, Tajima Y, Fujii Y, Kaji S, Yamamoto T, Hyakudomi R, Taniura T, Miyazaki Y, Kishi T, Kawabata Y. Preoperative Prognostic Nutritional Index Predicts Long-Term Surgical Outcomes in Patients with Esophageal Squamous Cell Carcinoma. *World J Surg* 2018; **42**: 2199-2208 [PMID: 29290069 DOI: 10.1007/s00268-017-4437-1]
- Harimoto N, Yoshizumi T, Inokuchi S, Itoh S, Adachi E, Ikeda Y, Uchiyama H, Utsunomiya T, Kajiyama K, Kimura K, Kishihara F, Sugimachi K, Tsujita E, Ninomiya M, Fukuzawa K, Maeda T, Shirabe K,

- Maehara Y. Prognostic Significance of Preoperative Controlling Nutritional Status (CONUT) Score in Patients Undergoing Hepatic Resection for Hepatocellular Carcinoma: A Multi-institutional Study. *Ann Surg Oncol* 2018; **25**: 3316-3323 [PMID: 30051372 DOI: 10.1245/s10434-018-6672-6]
- 9 Yang Y, Gao P, Song Y, Sun J, Chen X, Zhao J, Ma B, Wang Z. The prognostic nutritional index is a predictive indicator of prognosis and postoperative complications in gastric cancer: A meta-analysis. *Eur J Surg Oncol* 2016; **42**: 1176-1182 [PMID: 27293109 DOI: 10.1016/j.ejso.2016.05.029]
- 10 Nozoe T, Iguchi T, Egashira A, Adachi E, Matsukuma A, Ezaki T. Significance of modified Glasgow prognostic score as a useful indicator for prognosis of patients with gastric carcinoma. *Am J Surg* 2011; **201**: 186-191 [PMID: 20832047 DOI: 10.1016/j.amjsurg.2010.01.030]
- 11 Kuroda D, Sawayama H, Kurashige J, Iwatsuki M, Eto T, Tokunaga R, Kitano Y, Yamamura K, Ouchi M, Nakamura K, Baba Y, Sakamoto Y, Yamashita Y, Yoshida N, Chikamoto A, Baba H. Controlling Nutritional Status (CONUT) score is a prognostic marker for gastric cancer patients after curative resection. *Gastric Cancer* 2018; **21**: 204-212 [PMID: 28656485 DOI: 10.1007/s10120-017-0744-3]
- 12 Wang SC, Chou JF, Strong VE, Brennan MF, Capanu M, Coit DG. Pretreatment Neutrophil to Lymphocyte Ratio Independently Predicts Disease-specific Survival in Resectable Gastroesophageal Junction and Gastric Adenocarcinoma. *Ann Surg* 2016; **263**: 292-297 [PMID: 25915915 DOI: 10.1097/SLA.0000000000001189]
- 13 Hsu JT, Wang CC, Le PH, Chen TH, Kuo CJ, Lin CJ, Chou WC, Yeh TS. Lymphocyte-to-monocyte ratios predict gastric cancer surgical outcomes. *J Surg Res* 2016; **202**: 284-290 [PMID: 27229102 DOI: 10.1016/j.jss.2016.01.005]
- 14 Gu X, Gao XS, Cui M, Xie M, Peng C, Bai Y, Guo W, Han L, Gu X, Xiong W. Clinicopathological and prognostic significance of platelet to lymphocyte ratio in patients with gastric cancer. *Oncotarget* 2016; **7**: 49878-49887 [PMID: 27409665 DOI: 10.18632/oncotarget.10490]
- 15 Liu X, Qiu H, Kong P, Zhou Z, Sun X. Gastric cancer, nutritional status, and outcome. *Onco Targets Ther* 2017; **10**: 2107-2114 [PMID: 28442919 DOI: 10.2147/OTT.S132432]
- 16 Wen J, Bedford M, Begum R, Mitchell H, Hodson J, Whiting J, Griffiths E. The value of inflammation based prognostic scores in patients undergoing surgical resection for oesophageal and gastric carcinoma. *J Surg Oncol* 2018; **117**: 1697-1707 [PMID: 29761518 DOI: 10.1002/jso.25057]
- 17 Kochi M, Fujii M, Kanamori N, Kaiga T, Kawakami T, Aizaki K, Kasahara M, Mochizuki F, Kasakura Y, Yamagata M. Evaluation of serum CEA and CA19-9 levels as prognostic factors in patients with gastric cancer. *Gastric Cancer* 2000; **3**: 177-186 [PMID: 11984734]
- 18 Zhou YC, Zhao HJ, Shen LZ. Preoperative serum CEA and CA19-9 in gastric cancer—a single tertiary hospital study of 1,075 cases. *Asian Pac J Cancer Prev* 2015; **16**: 2685-2691 [PMID: 25854347 DOI: 10.7314/apjcp.2015.16.7.2685]
- 19 Japanese Gastric Cancer Association. Japanese gastric cancer treatment guidelines 2014 (ver. 4). *Gastric Cancer* 2017; **20**: 1-19 [PMID: 27342689 DOI: 10.1007/s10120-016-0622-4]
- 20 Ajani JA, In H, Sano T, Gaspar LE, Erasmus JJ, Tang LH, Washington MK, Gerdes H, Wittekind CW, Mansfield PF, Rimmer C, Hofstetter WL, Kelsen D, Amin MB, Edge SB, Greene FL, Brierley JD. Stomach. Amin MB, Edge SB, Greene FL, Brierley JD. *AJCC cancer staging manual*. New York: Springer 2017; 203-350
- 21 Liu X, Qiu H, Huang Y, Xu D, Li W, Li Y, Chen Y, Zhou Z, Sun X. Impact of preoperative anemia on outcomes in patients undergoing curative resection for gastric cancer: a single-institution retrospective analysis of 2163 Chinese patients. *Cancer Med* 2018; **7**: 360-369 [PMID: 29341506 DOI: 10.1002/cam4.1309]
- 22 Yu W, Wang Y, Shen B. An elevated preoperative plasma fibrinogen level is associated with poor overall survival in Chinese gastric cancer patients. *Cancer Epidemiol* 2016; **42**: 39-45 [PMID: 27010728 DOI: 10.1016/j.canep.2016.03.004]
- 23 Camp RL, Dolled-Filhart M, Rimm DL. X-tile: a new bio-informatics tool for biomarker assessment and outcome-based cut-point optimization. *Clin Cancer Res* 2004; **10**: 7252-7259 [PMID: 15534099 DOI: 10.1158/1078-0432.CCR-04-0713]
- 24 Durrleman S, Simon R. Flexible regression models with cubic splines. *Stat Med* 1989; **8**: 551-561 [PMID: 2657958 DOI: 10.1002/sim.4780080504]
- 25 Akaike H. A new look at the statistical model identification. *IEEE Trans Autom Contr*. CA 1974; **19**: 716-723 [DOI: 10.1109/TAC.1974.1100705]
- 26 Jiang Y, Zhang Q, Hu Y, Li T, Yu J, Zhao L, Ye G, Deng H, Mou T, Cai S, Zhou Z, Liu H, Chen G, Li G, Qi X. ImmunoScore Signature: A Prognostic and Predictive Tool in Gastric Cancer. *Ann Surg* 2018; **267**: 504-513 [PMID: 28002059 DOI: 10.1097/SLA.0000000000002116]
- 27 de Vries EM, Wang J, Williamson KD, Leeftang MM, Boonstra K, Weersma RK, Beuers U, Chapman RW, Geskus RB, Ponsioen CY. A novel prognostic model for transplant-free survival in primary sclerosing cholangitis. *Gut* 2018; **67**: 1864-1869 [PMID: 28739581 DOI: 10.1136/gutjnl-2016-313681]
- 28 Heagerty PJ, Lumley T, Pepe MS. Time-dependent ROC curves for censored survival data and a diagnostic marker. *Biometrics* 2000; **56**: 337-344 [PMID: 10877287 DOI: 10.1111/j.0006-341X.2000.00337.x]
- 29 Harrell FE, Lee KL, Mark DB. Multivariable prognostic models: issues in developing models, evaluating assumptions and adequacy, and measuring and reducing errors. *Stat Med* 1996; **15**: 361-387 [PMID: 8668867 DOI: 10.1002/(SICI)1097-0258(19960229)15:4<361::AID-SIM168>3.0.CO;2-4]
- 30 Lemeshow S, Hosmer DW. A review of goodness of fit statistics for use in the development of logistic regression models. *Am J Epidemiol* 1982; **115**: 92-106 [PMID: 7055134 DOI: 10.1093/oxfordjournals.aje.a113284]
- 31 Vickers AJ, Elkin EB. Decision curve analysis: a novel method for evaluating prediction models. *Med Decis Making* 2006; **26**: 565-574 [PMID: 17099194 DOI: 10.1177/0272989X06295361]
- 32 Lin JX, Lin JP, Xie JW, Wang JB, Lu J, Chen QY, Cao LL, Lin M, Tu R, Zheng CH, Huang CM, Li P. Prognostic importance of the preoperative modified systemic inflammation score for patients with gastric cancer. *Gastric Cancer* 2019; **22**: 403-412 [PMID: 29982861 DOI: 10.1007/s10120-018-0854-6]
- 33 Del Priore G, Zandieh P, Lee MJ. Treatment of continuous data as categorical variables in Obstetrics and Gynecology. *Obstet Gynecol* 1997; **89**: 351-354 [PMID: 9052583 DOI: 10.1016/S0029-7844(96)00504-2]
- 34 Royston P, Altman DG, Sauerbrei W. Dichotomizing continuous predictors in multiple regression: a bad idea. *Stat Med* 2006; **25**: 127-141 [PMID: 16217841 DOI: 10.1002/sim.2331]
- 35 Amri R, Bordeianou LG, Sylla P, Berger DL. Preoperative carcinoembryonic antigen as an outcome predictor in colon cancer. *J Surg Oncol* 2013; **108**: 14-18 [PMID: 23681672 DOI: 10.1002/jso.23352]
- 36 Candido J, Hagemann T. Cancer-related inflammation. *J Clin Immunol* 2013; **33** Suppl 1: S79-S84

- [PMID: 23225204 DOI: 10.1007/s10875-012-9847-0]
- 37 **Mei Z**, Liu Y, Liu C, Cui A, Liang Z, Wang G, Peng H, Cui L, Li C. Tumour-infiltrating inflammation and prognosis in colorectal cancer: systematic review and meta-analysis. *Br J Cancer* 2014; **110**: 1595-1605 [PMID: 24504370 DOI: 10.1038/bjc.2014.46]
  - 38 **Galdiero MR**, Bonavita E, Barajon I, Garlanda C, Mantovani A, Jaillon S. Tumor associated macrophages and neutrophils in cancer. *Immunobiology* 2013; **218**: 1402-1410 [PMID: 23891329 DOI: 10.1016/j.imbio.2013.06.003]
  - 39 **Van Cutsem E**, Arends J. The causes and consequences of cancer-associated malnutrition. *Eur J Oncol Nurs* 2005; **9** Suppl 2: S51-S63 [PMID: 16437758 DOI: 10.1016/j.ejon.2005.09.007]
  - 40 **Lin JX**, Wang W, Lin JP, Xie JW, Wang JB, Lu J, Chen QY, Cao LL, Lin M, Tu R, Zheng CH, Huang CM, Zhou ZW, Li P. Preoperative Tumor Markers Independently Predict Survival in Stage III Gastric Cancer Patients: Should We Include Tumor Markers in AJCC Staging? *Ann Surg Oncol* 2018; **25**: 2703-2712 [PMID: 29971670 DOI: 10.1245/s10434-018-6634-z]
  - 41 **Fujiya K**, Tokunaga M, Makuuchi R, Nishiwaki N, Omori H, Takagi W, Hirata F, Hikage M, Tanizawa Y, Bando E, Kawamura T, Terashima M. Early detection of nonperitoneal recurrence may contribute to survival benefit after curative gastrectomy for gastric cancer. *Gastric Cancer* 2017; **20**: 141-149 [PMID: 27778124 DOI: 10.1007/s10120-016-0661-x]
  - 42 **Justice AC**, Covinsky KE, Berlin JA. Assessing the generalizability of prognostic information. *Ann Intern Med* 1999; **130**: 515-524 [PMID: 10075620 DOI: 10.7326/0003-4819-130-6-199903160-00016]



## Observational Study

# Increased circulating circular RNA\_103516 is a novel biomarker for inflammatory bowel disease in adult patients

Yu-Lan Ye, Juan Yin, Tong Hu, Li-Ping Zhang, Long-Yun Wu, Zhi Pang

**ORCID number:** Yu-Lan Ye (0000-0001-6378-5675); Juan Yin (0000-0003-2750-4201); Tong Hu (0000-0002-4983-7448); Li-Ping Zhang (0000-0003-0085-9838); Long-Yun Wu (0000-0003-2007-6187); Pang Zhi (0000-0002-1164-5838).

**Author contributions:** Ye YL and Pang Z contributed to study conception and design; Ye YL contributed to data acquisition, analysis, and interpretation and writing of the article; Yin J, Hu T, Zhang LP, Wu LY, and Pang Z contributed to the editing and review of the article. All authors read and approved the final manuscript.

**Supported by** the Natural Science Foundation of Jiangsu Province, No. BK20161232; and the Suzhou Special Project of Diagnosis and Treatment for Key Clinical Disease, No. LCZX201715.

**Institutional review board statement:** The study was reviewed and approved by the Ethics Committee of the Affiliated Suzhou Hospital of Nanjing Medical University.

**Informed consent statement:** All participants signed an informed consent form prior to study enrolment.

**Conflict-of-interest statement:** The authors have no conflicts of interest to declare.

**Data sharing statement:** No additional data are available.

**STROBE statement:** The guidelines of the STROBE Statement were

Yu-Lan Ye, Juan Yin, Tong Hu, Li-Ping Zhang, Long-Yun Wu, Zhi Pang, Department of Gastroenterology, the North District of the Affiliated Suzhou Hospital of Nanjing Medical University, Suzhou 215008, Jiangsu Province, China

**Corresponding author:** Zhi Pang, MD, Chief Doctor, Full Professor, Department of Gastroenterology, the North District of the Affiliated Suzhou Hospital of Nanjing Medical University, No. 242, Guangji Road, Suzhou 215008, Jiangsu Province, China.  
[pangzhi0273@sina.com](mailto:pangzhi0273@sina.com)

**Telephone:** +86-512-62363008

**Fax:** +86-512-62362502

## Abstract

### BACKGROUND

Increasing evidence demonstrates that by acting as microRNA sponges modulating gene expression at the transcriptional or post-transcriptional level, circular RNAs (circRNAs) participate in the pathogenesis of a variety of diseases and are considered ideal biomarkers of human disease.

### AIM

To examine the expression of circRNA\_103516 in inflammatory bowel disease (IBD) and its associations with clinical phenotypes and inflammatory cytokines.

### METHODS

Peripheral blood mononuclear cells (PBMCs) were obtained from patients with IBD, healthy controls (HCs), and patient controls (PCs). Expression of circRNA\_103516 and hsa-miR-19b-1-5p was assessed by quantitative reverse transcription-polymerase chain reaction. Crohn's disease activity index (CDAI), Mayo score, C-reactive protein (CRP) level, and erythrocyte sedimentation rate (ESR) were measured. To assess the inflammatory cytokines tumour necrosis factor  $\alpha$  (TNF- $\alpha$ ), interferon- $\gamma$  (IFN- $\gamma$ ), and interleukin-10 (IL-10), blood samples were analysed by flow cytometry.

### RESULTS

Ninety Crohn's disease (CD) and 90 ulcerative colitis (UC) patients, 80 HCs, and 35 PCs were included in the study. CircRNA\_103516 was upregulated in CD and UC patients compared with HCs and PCs ( $P < 0.05$ ). The area under the curve of circRNA\_103516 for diagnosing CD and UC was 0.790 and 0.687, respectively. In addition, circRNA\_103516 levels were increased in active CD and UC compared with remittent groups ( $P = 0.027$ ,  $P = 0.045$ ). Furthermore, in CD, circRNA\_103516 correlated positively with CDAI ( $P < 0.001$ ), CRP ( $P < 0.001$ ),



adopted for this manuscript.

**Open-Access:** This article is an open-access article which was selected by an in-house editor and fully peer-reviewed by external reviewers. It is distributed in accordance with the Creative Commons Attribution Non Commercial (CC BY-NC 4.0) license, which permits others to distribute, remix, adapt, build upon this work non-commercially, and license their derivative works on different terms, provided the original work is properly cited and the use is non-commercial. See: <http://creativecommons.org/licenses/by-nc/4.0/>

**Manuscript source:** Unsolicited manuscript

**Received:** August 19, 2019

**Peer-review started:** August 19, 2019

**First decision:** September 10, 2019

**Revised:** September 23, 2019

**Accepted:** October 17, 2019

**Article in press:** October 17, 2019

**Published online:** November 7, 2019

**P-Reviewer:** Berezin AE, Gazouli M

**S-Editor:** Tang JZ

**L-Editor:** Wang TQ

**E-Editor:** Ma YJ



ESR ( $P < 0.001$ ), TNF $\alpha$  ( $P < 0.001$ ), and IFN- $\gamma$  ( $P < 0.001$ ) and negatively correlated with IL-10 ( $P = 0.006$ ). In UC patients, circRNA\_103516 correlated with Mayo score ( $P < 0.001$ ), CRP ( $P < 0.001$ ), ESR ( $P < 0.001$ ), TNF $\alpha$  ( $P < 0.001$ ), IFN- $\gamma$  ( $P = 0.011$ ), and IL-10 ( $P = 0.002$ ). Additionally, circRNA\_103516 correlated positively with stricturing ( $P = 0.018$ ) and penetrating ( $P = 0.031$ ) behaviour. Moreover, hsa-miR-19b-1-5p correlated negatively with circRNA\_103516 in CD.

## CONCLUSION

CircRNA\_103516 levels in PBMCs can be considered an ideal candidate biomarker for diagnosing IBD. Dysregulation of circRNA\_103516 may participate in the molecular mechanism of IBD through hsa-miR-19b-1-5p sponging.

**Key words:** Circular RNA; Circular RNA\_103516; Inflammatory bowel diseases; Biomarker

©The Author(s) 2019. Published by Baishideng Publishing Group Inc. All rights reserved.

**Core tip:** The study aimed to assess circular RNA (circRNA)\_103516 in peripheral blood mononuclear cells of inflammatory bowel disease (IBD) patients and evaluate its potential as a biomarker in Crohn's disease and ulcerative colitis patients with regard to clinical phenotype and inflammatory cytokines. Our results showed that PBMC circRNA\_103516 levels may be considered an ideal candidate biomarker for the diagnosis of IBD and have the ability to predict clinical outcomes in IBD. Dysregulation of circRNA\_103516 may participate in the molecular mechanism of IBD through hsa-miR-19b-1-5p sponging.

**Citation:** Ye YL, Yin J, Hu T, Zhang LP, Wu LY, Pang Z. Increased circulating circular RNA\_103516 is a novel biomarker for inflammatory bowel disease in adult patients. *World J Gastroenterol* 2019; 25(41): 6273-6288

**URL:** <https://www.wjgnet.com/1007-9327/full/v25/i41/6273.htm>

**DOI:** <https://dx.doi.org/10.3748/wjg.v25.i41.6273>

## INTRODUCTION

Inflammatory bowel disease (IBD), including ulcerative colitis (UC) and Crohn's disease (CD), comprises chronic inflammatory disorders of the gastrointestinal tract. IBD pathogenesis is believed to involve a complex interplay among immunology, genetic predisposition, and environmental risk factors<sup>[1-3]</sup>. Due to the characteristic of repeated recurrence, the disease activity of IBD must be assessed and monitored repeatedly. However, as most conventional detection methods are invasive, current detection methods are not suitable for repeated clinical applications. To overcome this limitation, serological biomarkers may constitute an optimal alternative choice for evaluating and screening disease activity in IBD.

Circular RNAs (circRNAs) are covalently closed continuous single-stranded RNA molecules that have advantageous properties because their circular structure enables rolling circle RNA replication and producing multiple genomic copies once a single initiation event occurs<sup>[4,5]</sup>. However, the characteristics of circRNAs are much less clear than those of microRNAs (miRNAs) and long noncoding RNAs (lncRNAs). Nonetheless, research on their functions has recently emerged, and increasing evidence demonstrates that circRNAs can modulate gene expression at the transcriptional or post-transcriptional level by sponging miRNAs or by interacting with other molecules<sup>[6]</sup>. Furthermore, circRNAs are evolutionally conserved, and their expression is relatively stable in the cytoplasm; these features indicate that circRNAs may be ideal biomarkers in human disease<sup>[7]</sup>. Although much remains to be revealed regarding circRNA biology and gene regulatory mechanisms, studies have elucidated their function in a variety of cancers<sup>[8]</sup>, cardiovascular disease<sup>[9]</sup>, autoimmune disease<sup>[10]</sup>, and nervous system disorders<sup>[11]</sup>, among others.

To date, little is known about the relationships between circRNAs and IBD. Our previous research based on microarray analysis identified 155 upregulated circRNAs and 229 downregulated circRNAs in peripheral blood mononuclear cells (PBMCs) from CD patients compared with healthy controls (HCs). Moreover, some aberrantly

expressed circRNAs were chosen for evaluation of their potential use in the diagnosis of CD<sup>[12]</sup>.

In this study, we focused on circRNA\_103516, which is located at chr3: 171969049-172028671 and spliced from *FNDC3B*. It was reported that *FNDC3B* might play a role in the epithelial-to-mesenchymal transition and activates several cancer pathways, including phosphoinositide 3-kinase/Akt, retinoblastoma 1, and transforming growth factor (TGF)  $\beta$  signalling<sup>[13]</sup>. Our bioinformatics analysis showed that hsa\_circRNA\_103516 is predicted to harbour hsa-miR-147b, hsa-miR-19b-1-5p, hsa-miR-134-3p, hsa-miR-576-5p, and hsa-miR-493-5p. Among them, miR-19b was found to be decreased in the serum and intestinal tissue of IBD patients<sup>[14]</sup>. Thus, in the present study, we explored the link between circRNA\_103516 and hsa-miR-19b-1-5p in PBMCs from IBD patients and determined its possible correlations with the clinical phenotypes of CD and UC.

## MATERIALS AND METHODS

### Patient samples

Between January 2018 and December 2018, 180 IBD patients (90 with CD and 90 with UC) were prospectively recruited from the Department of Gastroenterology of the North District of the Affiliated Suzhou Hospital of Nanjing Medical University (Jiangsu, China). Eighty HCs and 35 patient controls (PCs) were also included. The age and sex of all groups were matched. The inclusion criteria were: (1) A diagnosis of IBD established based on clinical manifestations, radiological findings, and endoscopic and histological criteria; (2) Age from 17 to 75 years old; and (3) Demographic and clinical information collected by experienced clinicians reviewing and completing medical questionnaires. Patients with irritable bowel syndrome were used as the PCs. The exclusion criteria were as follows: (1) Isolated upper digestive tract involvement; (2) Other coexisting autoimmune diseases, including systemic lupus erythematosus, rheumatoid arthritis, and asthma; and (3) A history of malignant tumour or severe infection (Figure 1). Disease activity was identified according to the CD activity index (CDAI) for CD and the Mayo score for UC<sup>[15,16]</sup>. Active IBD was defined as CDAI above 150 points or Mayo clinical score above 2. The sites and behaviour of the disease were defined according to the Montreal classification<sup>[17]</sup>. For assessing circRNA\_103516, hsa-miR-19b-1-5p, C-reactive protein (CRP), erythrocyte sedimentation rate (ESR), TNF- $\alpha$ , interferon- $\gamma$  (IFN- $\gamma$ ), and interleukin-10 (IL-10), blood samples were collected into ethylenediamine tetraacetic acid tubes for testing within one week before or after endoscopy.

### Ethics statement

The present study was approved by the Ethics Committees of the Affiliated Suzhou Hospital of Nanjing Medical University (Jiangsu, China). All IBD patients and control subjects signed an informed consent form, in accordance with the relevant guidelines and regulations.

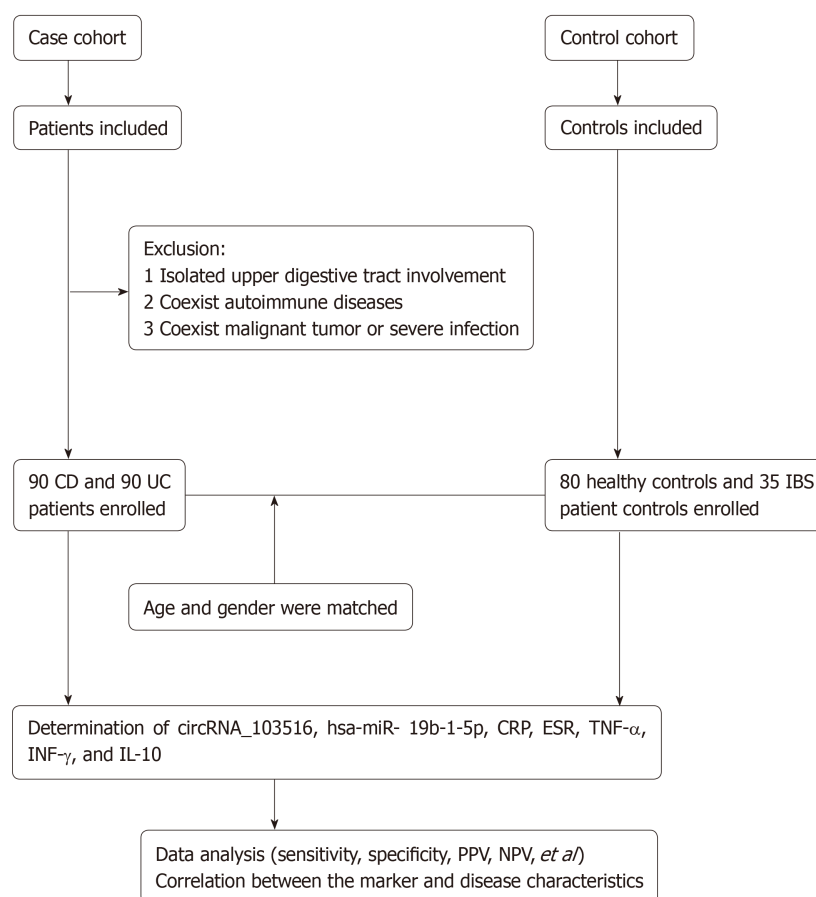
### Extraction of total RNA from PBMCs

PBMCs were immediately separated after blood sample collection from each donor according to the manufacturer's protocol (GE Healthcare, Uppsala, Sweden). Two millilitres of blood diluted in 2 mL of saline solution was layered onto 4 mL of Ficoll-Paque PLUS. After centrifugation for 30 min at 400 g at room temperature, the interlayer was collected by washing twice with the same volume of saline solution. The precipitate was gathered by centrifuging for 15 min at 90 g at room temperature. PBMCs were then frozen at -80 °C. TRIzol reagent (Invitrogen, Carlsbad CA, United States) was utilized for total RNA extraction from the PBMCs.

### Quantitative reverse transcription-polymerase chain reaction (qRT-PCR) determination of circRNA\_103516 levels

Total RNA was reverse transcribed using a PrimerScript Realtime Reagent Kit (Takara Bio Inc., TaKaRa, Shiga, Japan), and expression of circRNA\_103516 was quantitated with TB Green™ Premix Ex Taq™ II (Tli RNaseH Plus; TaKaRa, Shiga, Japan) and a LightCycler 480II real-time PCR system (Roche, Rotkreuz, Switzerland). The 2<sup>- $\Delta\Delta$ Ct</sup> method was employed to analyse the data.  $\beta$ -actin was used as an internal reference. The primer sequences are presented in Table 1. In total, the cycling parameters for PCR were 30 s for 95 °C, followed by 40 cycles of denaturation at 95 °C for 5 s and annealing and extension at 60 °C for 30 s.

### TNF- $\alpha$ , IFN- $\gamma$ , and IL-10 measurements by flow cytometry



**Figure 1** Flow chart of patient selection in the study and main study procedures. CD: Crohn's disease; UC: Ulcerative colitis; IBS: Irritable bowel syndrome; CRP: C reactive protein; ESR: Erythrocyte sedimentation rate; TNF- $\alpha$ : Tumor necrosis factor  $\alpha$ ; INF- $\gamma$ : Interferon  $\gamma$ ; IL-10: Interleukin-10; PPV: Positive predictive value; NPV: Negative predictive value.

According to the manufacturer's instructions, TNF $\alpha$ , IFN- $\gamma$ , and IL-10 levels in plasma samples from IBD patients were measured using flow cytometry (FCM) kits (Hangzhou Cellgene Biotechco, LTD, China).

### Annotation of circRNA/miRNA interaction

TargetScan (<http://www.targetscan.org/>) and miRanda (<http://www.microrna.org/>) were used to predict circRNA/miRNA interactions. Differential expression of circRNA\_103516, as identified by qRT-PCR, was annotated in detail with the circRNA/miRNA interactions. Additionally, the sequences of MREs and predicted miRNA targets were examined.

### Hsa-miR-19b-1-5p determination by qPCR

Expression of miR-19b-1-5p (predicted from annotations) in PBMCs from the 90 patients with CD and 90 patients with UC was detected using a Hairpin-it<sup>TM</sup> qRT-PCR miRNA Kit (GenePharma, LTD, China). U6 was used as an internal reference. The primer sequences used for hsa-miR-19b-1-5p are: 5'-UGUGCAAAUCCAUGCAAAACUG-3' (forward) and 5'-GCTCACTGCAACCTCCTCCTCC-3' (reverse). The primer sequences used for U6 are 5'-GCTTCGGCAGCACATA-TACTAAAAT-3' (forward) and 5'-CGCT-TCACGAATTTGCGTGTTCAT-3' (reverse). The PCR conditions included predenaturation at 95 °C for 3 min, followed by 40 cycles of denaturation at 95 °C for 12 s and annealing and elongation at 62 °C for 40 s. The 2<sup>- $\Delta\Delta$ Ct</sup> method was used to analyse the data.

### Statistical analysis

The results are reported as the mean  $\pm$  standard deviation or median (25%75%); assays were performed in triplicate. The unpaired *t*-test or Mann-Whitney U-test was applied to compare continuous variables for two groups. Multiple comparisons were assessed by one-way analysis of variance or the  $\chi^2$  test. Spearman's analysis was performed to determine linear correlation in different groups. Receiver operating characteristic curve analysis was employed to evaluate the clinical diagnostic value of

**Table 1** Sequences of primers used for quantitative reverse transcription–polymerase chain reaction

Gene	Primer sequence	Produce size (bp)
$\beta$ -actin	F: 5'GTGGCCGAGGACTTTGATTG 3' R: 5'CCTGTAACAACGCATCTCATATT-3'	73
circRNA_103516	F: 5'-GCACCAATTGACAACGGTTC-3' R: 5'-CTGGTCTTCTCGGGTGATGT-3'	123

Circular RNA: CircRNA; F: Forward; R: Reverse.

candidate circRNAs. Logistic regression was used to identify risk factors. A *P* value < 0.05 was considered statistically significant. The statistical analyses were performed using the package SPSS 19.0 (SPSS Inc., IBM, United States) for windows and GraphPad Prism 7.04 (GraphPad Software, San Diego, CA, United States).

## RESULTS

### Characteristics

The demographic and clinical data of the IBD patients and health controls and PCs are listed in **Table 2**. There were 90 CD patients [48 males (53.3%), mean age 39.94 years], 90 UC patients [38 males (42.2%), mean age 41.69 years], 80 HCs [46 males (57.5%), mean age 37.64 years], and 35 PCs [19 males (54.3%), mean age 42.40 years]. Age and sex were not significantly different among the four groups (*P* > 0.05). CD and UC activity was classified as remission, mild, moderate, or severe according to CDAI and the Mayo score. Laboratory test results (CRP, ESR, TNF- $\alpha$ , INF- $\gamma$ , and IL-10) and disease activity are shown in **Table 3**.

### CircRNA\_103516 expression in PBMCs from IBD patients and controls

Expression of circRNA\_103516 in PBMCs was increased in CD patients [2.085 (1.1953.510)] compared with that in UC patients [1.385 (0.9252.599), *P* = 0.003], HCs [0.901 (0.7241.376), *P* < 0.001], and PCs [0.901 (0.7421.375), *P* < 0.001]. The expression level of circRNA\_103516 was higher in PBMCs from the UC group compared with those of the HC (*P* = 0.004) and PC (*P* = 0.025) groups. However, there was no significant difference between the HC and PC groups (*P* = 0.998) (**Figure 2**).

The diagnostic value of circRNA\_103516 in differentiating the CD group from the HC group [area under the curve (AUC) = 0.790, 95% confidence interval (CI): 0.722–0.857] and the UC group (AUC = 0.631, 95%CI: 0.550–0.712) was also examined (**Figure 3A and C**, **Table 4**). Overall, circRNA\_103516 may be considered a predictive factor in differentiating UC from HC (AUC = 0.687, 95%CI: 0.608–0.767) (**Figure 3B**, **Table 4**). The level of circRNA\_103516 was considered positive at a cutoff value > 1.412 for CD and > 1.151 for UC (**Table 4**).

### Correlations of circRNA\_103516 expression with disease activity in IBD

The expression level of circRNA\_103516 was markedly increased, with values 2.614-fold and 1.953-fold higher in PBMCs from active CD and active UC, respectively (*P* < 0.001 and *P* < 0.001, respectively). However, expression was only 1.639-fold and 1.319-fold higher in CD and UC patients who were in remission, respectively (*P* < 0.001 and *P* = 0.024, respectively) (**Figure 4A**), and circRNA\_103516 levels in active CD and UC were higher than those in remittent CD and UC (*P* = 0.027, *P* = 0.045) (**Figure 4A and B**).

Additionally, circRNA\_103516 levels exhibited a positive correlation with disease activity and laboratory tests. In CD patients, circRNA\_103516 correlated positively with CDAI (*r* = 0.554, *P* < 0.001), CRP (*r* = 0.470, *P* < 0.001) and ESR (*r* = 0.466, *P* < 0.001) (**Figure 5A–C**); in UC patients, circRNA\_103516 correlated with the Mayo score (*r* = 0.460, *P* < 0.001), CRP (*r* = 0.424, *P* < 0.001), and ESR (*r* = 0.407, *P* < 0.001) (**Figure 5D and F**).

### Correlations of circRNA\_103516 expression with inflammatory cytokines in IBD

CircRNA\_103516 levels showed a positive correlation with TNF $\alpha$  and INF- $\gamma$ , though negative correlations were found for circRNA\_103516 with IL-10.

In CD patients, circRNA\_103516 correlated positively with TNF $\alpha$  (*r* = 0.637, *P* < 0.001) and INF- $\gamma$  (*r* = 0.595, *P* < 0.001) and negatively with IL-10 (*r* = -0.287, *P* = 0.006) (**Figure 6A–C**). Similarly, we observed a correlation of circRNA\_103516 with TNF $\alpha$  (*r*

**Table 2 Clinical characteristics of patients and controls**

Characteristic	CD (n = 90)	UC (n = 90)	HCs (n = 80)	PCs (n = 35)
Male/female	48/42	38/52	46/34	19/16
Mean age (yr)	39.94 ± 11.80	41.69 ± 12.40	37.64 ± 9.30	42.40 ± 10.20
Range (yr)	17-67	20-73	20-72	18-70
Tobacco smoking (n)				
Never	60	67	50	20
Past or current use	30	23	30	15
Disease duration (yr)	5.1 ± 3.1	5.1 ± 3.4		
Disease location: CD, n (%)				
L1	37 (41.1)			
L2	20 (22.2)			
L3	33 (36.7)			
Disease activity: CDAL, n (%)				
Remission	16 (17.8)			
Mild	19 (21.1)			
Moderate	40 (44.4)			
Severe	15 (16.7)			
Disease behavior:CD, n (%)				
B1	39 (43.3)			
B2	33 (36.7)			
B3	18 (20.0)			
Disease location: UC, n (%)				
E1		36 (40.0)		
E2		29 (32.2)		
E3		25 (27.8)		
Disease severity, n (%)				
Remission		14 (15.6)		
Mild		30 (33.3)		
Moderate		31 (34.4)		
Severe		15 (16.7)		
Medications, n (%)				
5-ASA	80 (88.9)	87 (96.7)		
Corticosteroids	50 (11.7)	41 (45.5)		
Immunosuppressants	28 (31.1)	14 (15.6)		
Anti-TNF-α	13 (14.4)	4 (4.4)		
Surgery	4 (4.4)	1 (1.1)		

The data are presented as the mean ± SD. Patients with isolated upper disease (L4) were excluded. L1: Terminal ileum; L2: Colon; L3: Ileocolon; B1: Non-stricture and non-penetrating; B2: Stricturing; B3: Penetrating; E1: Rectum; E2: Left side; E3: Extensive. CD: Crohn's disease; UC: Ulcerative colitis; HCs: Healthy controls; PCs: Patient controls; 5-ASA: 5-aminosalicylic acid; TNF-α: Tumor necrosis factor α.

= 0.412,  $P < 0.001$ ), IFN-γ ( $r = 0.267$ ,  $P = 0.011$ ), and IL-10 ( $r = -0.330$ ,  $P = 0.002$ ) in UC patients (Figure 6E and F).

### Correlations of circRNA\_103516 status with subgroups of IBD

The disease phenotypes of CD compared with the corresponding circRNA\_103516 status are listed in Table 5. The prevalence of circRNA\_103516 positivity was higher in patients with moderate and severe CD than in patients with mild disease (82.5%, 80.0% *vs* 47.4%,  $P = 0.008$ ,  $P = 0.025$ ). After adjustment for sex, age, and smoking, bivariate logistic analysis showed that positive circRNA\_103516 was independently associated with an increased risk of disease activity [moderate: odds ratio (OR) = 4.886, 95%CI: 1.383-17.251,  $P = 0.014$ ; severe: OR = 4.416, 95%CI: 0.084-22.054,  $P = 0.043$ ]. Additionally, circRNA\_103516 positivity was more frequently detected in patients with complicated CD (B2/B3) compared with those with the simple phenotype (B1) (78.8%, 77.8% *vs* 48.7%,  $P = 0.011$ ,  $P = 0.045$ ). After adjusting for clinical factors, logistic analysis also identified that circRNA\_103516 correlated



**Table 3 Laboratory measures and disease activity scores of inflammatory bowel disease patients and control groups**

Parameter	CD (n = 90)	UC (n = 90)	HCs (n = 80)	PCs (n = 35)
CRP (mg/L)	79.95 (18.47-121.22)	58.10 (16.43-123.67)	3.49 (3.30-6.09)	5.73 (3.84-7.94)
ESR (mm/H)	38.50 (17.75-67.00)	30.00 (15.00-58.00)	12.02 (4.87-14.25)	17.32 (3.87-26.85)
TNF- $\alpha$ (pg/mL)	6.83 (3.89-12.26)	6.70 (3.45-9.45)	--	--
INF- $\gamma$ (pg/mL)	9.29 (5.77-12.35)	6.70 (4.4-10.65)	--	--
IL-10 (pg/mL)	10.99 (6.21-19.27)	11.3 (6.66-25.08)	--	--
CDAI score	270.15 (170.60-376.58)	--	--	--
Mayo score	--	5.00 (3.00-10.00)	--	--

The data are presented as medians (1/4-3/4 quarters). CD: Crohn's disease; UC: Ulcerative colitis; HCs: Healthy controls; PCs: Patient controls; CRP: C reactive protein; ESR: Erythrocyte sedimentation rate; TNF- $\alpha$ : Tumor necrosis factor  $\alpha$ ; INF- $\gamma$ : Interferon  $\gamma$ ; IL-10: Interleukin-10; CDAI: Crohn's disease activity index.

independently with an increased risk of stricturing (OR = 3.641, 95%CI: 1.245-10.650,  $P = 0.018$ ) and penetrating (OR = 4.375, 95%CI: 1.147-16.690,  $P = 0.031$ ) behaviour. In contrast, circRNA\_103516 showed no correlation with disease location or medications.

In UC, circRNA\_103516 positivity was associated with an increased risk of more severe disease behaviour (OR = 10.803, 95%CI: 1.171-94.687) (Table 6), though statistical power was not high due to the small number of patients with severe UC. No correlation of circRNA\_103516 positivity with any other variable in UC was observed.

#### Interaction between circRNA\_103516 and miRNAs

Using miRNA target prediction software targetScan and miRanda, we investigated the top five predicted miRNA targets for circRNA\_103516. The candidate hsa\_circRNA\_103516 is predicted to harbour sites for hsa-miR-147b, hsa-miR-19b-1-5p, hsa-miR-134-3p, hsa-miR-576-5p, and hsa-miR-493-5p, with different seed region types (*i.e.*, 8mer, 7mer-m8, offset 6mer, and imperfect, respectively). We chose hsa-miR-19b-1-5p for detailed investigation of a correlation with circRNA\_103516.

#### Correlation of circRNA\_103516 expression with hsa-miR-19b-1-5p in IBD

The expression level of circRNA\_103516 correlated negatively with hsa-miR-19b-1-5p.

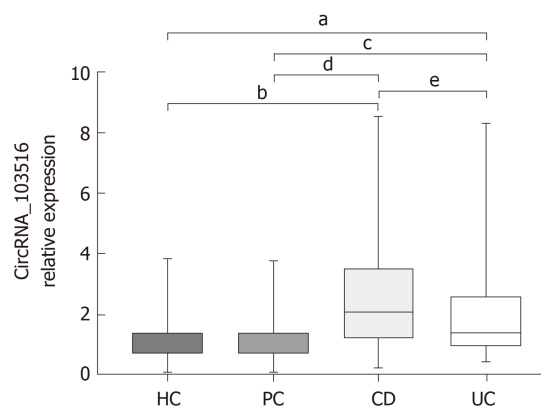
In CD patients, circRNA\_103516 showed a negative correlation with hsa-miR-19b-1-5p ( $r = -0.395$ ,  $P < 0.001$ ) (Figure 7A). In contrast, there was no significant correlation between circRNA\_103516 and hsa-miR-19b-1-5p in patients with UC ( $r = -0.167$ ,  $P = 0.116$ ) (Figure 7B).

## DISCUSSION

The diagnosis and therapy of IBD involve enormous challenges that can only be addressed by obtaining a better understanding of the molecular mechanisms of IBD. Currently, owing to the advent of high-density microarrays, numerous noncoding RNAs are being considered as novel and potent regulators of gene expression. Noncoding RNAs comprise miRNAs, lncRNAs, circular RNAs, ribosomal RNAs, and snRNPs as well as a variety of regulatory RNAs<sup>[18]</sup>. Among them, circRNAs are ideal diagnostic and therapeutic candidates due to their stability and conservation<sup>[19]</sup>. The most profound studies between circRNAs and diseases are with regard to tumours<sup>[20]</sup>. For example, circEXOC6B and circN4BP2L2 are considered novel prognostic biomarkers in epithelial ovarian cancer<sup>[21]</sup>. Circ\_0001451 was found to be downregulated in clear cell renal cell carcinoma and a potential biomarker for treatment of the disease<sup>[22]</sup>. Furthermore, sponging of miR-200a by circular RNA 101368 regulates the migration of hepatocellular carcinoma cells *via* the HMGB1/RAGE pathway<sup>[23]</sup>.

Hundreds of miRNAs and lncRNAs have been reported to participate in IBD pathogenesis and can be considered as biomarkers for these patients<sup>[24,25]</sup>. Nevertheless, the roles of circRNA in IBD have only begun to be elucidated.

Our previous research investigated circRNA microarray profiles in peripheral blood from adults with CD, revealing 384 differential circRNAs in CD *vs* HCs, with 155 increased circRNAs and 229 decreased circRNAs; thus, these molecules have great potential for investigating the pathogenesis of CD. In the present study, we focused on circRNA\_103516 and validated it by real-time PCR in a larger IBD cohort. First,



**Figure 2** Circular RNA\_103516 relative expression in patients with Crohn's disease, patients with ulcerative colitis, healthy controls, and patient controls. Circular RNA (circRNA)\_103516 was increased in Crohn's disease (CD) and ulcerative colitis (UC) patients compared with healthy controls (HC) and patient controls (PC). A significant difference in circRNA\_103516 was detected between CD and UC groups. Comparing the relative circRNA levels between two groups was performed by the Mann Whitney U-test. <sup>a</sup> $P < 0.05$  vs HC and <sup>b</sup> $P < 0.001$  vs HC; <sup>c</sup> $P < 0.05$  vs PC; <sup>d</sup> $P < 0.001$  vs PC; <sup>e</sup> $P < 0.05$  vs UC.  $P < 0.05$  was considered statistically significant. CD: Crohn's disease, UC: Ulcerative colitis, HC: Healthy controls, PC: Patient controls; CircRNA: Circular RNA.

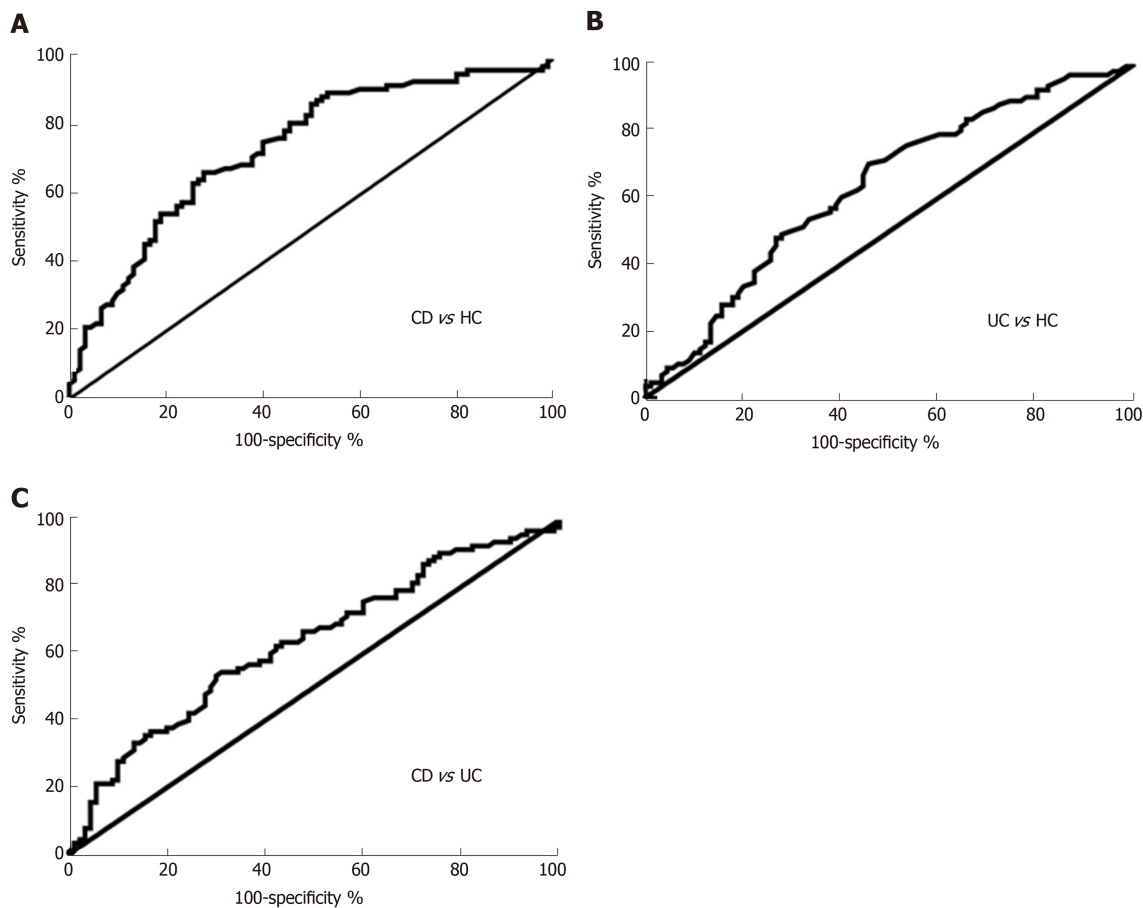
circRNA\_103516 exhibited strong clinical diagnostic value for CD and UC, suggesting that circRNA\_103516 may be considered a novel biomarker for IBD. Second, circRNA\_103516 was significantly more upregulated in the active stage than in the remission stage of both CD and UC, with positive correlations with disease activity (CDAI, Mayo, CRP, and ESR). Third, circRNA\_103516 correlated positively with proinflammatory cytokines (TNF- $\alpha$  and INF- $\gamma$ ) in CD and UC patients and negatively with anti-inflammatory cytokines (IL-10). Fourth, logistic regression analysis revealed that circRNA\_103516 was independently associated with an increased risk of disease activity in CD and UC. These data indicate that circRNA\_103516 may have a proinflammatory role.

Given the roles of circRNAs as miRNA sponges and gene regulators<sup>[6,26]</sup>, we investigated the top five predicted miRNA targets for circRNAs and identified that circRNA\_103516 may target hsa-miR-147b, hsa-miR-19b-1-5p, hsa-miR-134-3p, hsa-miR-576-5p, and hsa-miR-493-5p, competitively restraining miRNA activity. We chose hsa-miR-19b-1-5p to further evaluate the correlation with circRNA\_103516 in detail. The current study showed that circRNA\_103516 correlated negatively with hsa-miR-19b-1-5p in CD patients.

Interestingly, previous studies have identified that miR-19b levels are decreased in the serum and intestinal tissue of IBD patients<sup>[14,27]</sup>, which is consistent with our study. Research has also shown that miR-19b may participate in abnormal inflammatory reactions by inhibiting suppressor of cytokine signalling 3 to regulate chemokine production in intestinal epithelial cells<sup>[27]</sup>. Furthermore, miR-19 and its family members modulate the chronic inflammatory process by activating NF- $\kappa$ B signalling in rheumatoid arthritis<sup>[28]</sup>. The NF- $\kappa$ B signalling pathway plays a vital role in autoimmune diseases by regulating T cell and macrophage development and function, ultimately participating in the inflammatory process and immune regulation<sup>[29]</sup>. Moreover, miRNA19b modulates Th17 cell development by targeting thymic stromal lymphopoietin<sup>[30]</sup> and has a vital function by suppressing the IL-10 level in peripheral dendritic cells<sup>[31]</sup>. Thus, we suggest that circRNA\_103516 acts as a proinflammatory gene by sponging miRNA19b and is involved in the pathogenesis of IBD by mediating inflammation and immune-related signalling pathways.

Previous studies have shown that serum levels of miR-19 correlated negatively with stricturing CD<sup>[14]</sup>. The groups of Zhao and Zou attempted to explain these results by uncovering a new mechanism in which miR-19b depresses fibrogenesis by targeting TGF-beta receptor 2 in biliary atresia-related fibrosis<sup>[32]</sup> and myocardial fibrosis<sup>[33]</sup>. However, our study identified that circRNA\_103516 positivity may be an independent risk factor for CD stricture and penetrating behaviour. Indeed, a higher prevalence of circRNA\_103516 positivity was found in patients with complicated CD (stricturing and penetrating). These results further suggest that circRNA\_103516 may play a significant role in the development and progression of CD by acting as a microRNA19b sponge. Nevertheless, elucidation of the precise function of miRNA-circRNA interactions in CD pathogenesis requires further research.

To the best of our knowledge, this is the first study to identify the relationship



**Figure 3** Receiver operating characteristic analysis of circular RNA\_103516 in peripheral blood mononuclear cells from patients with Crohn's disease and ulcerative colitis. A: Circular RNA (circRNA)\_103516 was able to differentiate CD from HC; B: CircRNA\_103516 could differentiate UC from HCs; C: CircRNA\_103516 was able to differentiate CD from UC. CD: Crohn's disease; UC: Ulcerative colitis; HCs: Healthy controls.

between circRNA\_103516 expression in PBMCs and disease activity and the risk of IBD and inflammatory cytokines. Nonetheless, certain limitations in our study should not be neglected. First, the number of subjects was not large, which might have affected the results. In addition, a more diverse disease control group is needed for a more applicable conclusion. Second, we identified miRNA-circRNA interactions only by functional analysis and not by experimental verification. Thus, further research is needed.

In conclusion, we verified that increased circRNA\_103516 levels are a prospective candidate marker for IBD diagnosis and correlate positively with disease activity and behaviour in CD patients. Moreover, circRNA\_103516 may participate in the molecular mechanism of CD by sponging miR-19b. The precise molecular mechanisms underlying circRNA functions in CD require further investigation.

**Table 4 Receiver-operating characteristic analysis of circular RNA\_103516 in peripheral blood mononuclear cells from inflammatory bowel disease**

Group	AUC (95%CI)	P value	Cutoff value	Sensitivity (95%CI)	Specificity (95%CI)	PPV	NPV	LR +	LR -	Diagnostic accuracy
CD <i>vs</i> HC	0.790 (0.722-0.857)	< 0.001	1.412	66.67 (55.95%-76.26%)	78.75 (68.17%-87.11%)	77.63%	67.02%	3.137	0.423	71.76%
UC <i>vs</i> HC	0.687 (0.608-0.767)	< 0.001	1.151	66.67 (55.95%-76.26%)	62.50 (50.96%-73.08%)	66.67%	62.50%	1.778	0.533	64.71%
CD <i>vs</i> UC	0.631 (0.550-0.712)	0.002	1.963	54.44 (43.6%-64.98%)	68.89 (58.26% to 78.23%)	55.05%	55.75%	1.750	0.661	59.41%

AUC: Area under the curve; CD: Crohn's disease; UC: Ulcerative colitis; HC: Healthy control; PPV: Positive predictive value; NPV: Negative predictive value; LR +: Positive likelihood ratio; LR -: Negative likelihood ratio.

**Table 5 Univariate logistic regression analysis showing the disease phenotypes of Crohn's disease in correlation to circular RNA\_103516 status as dependent variable**

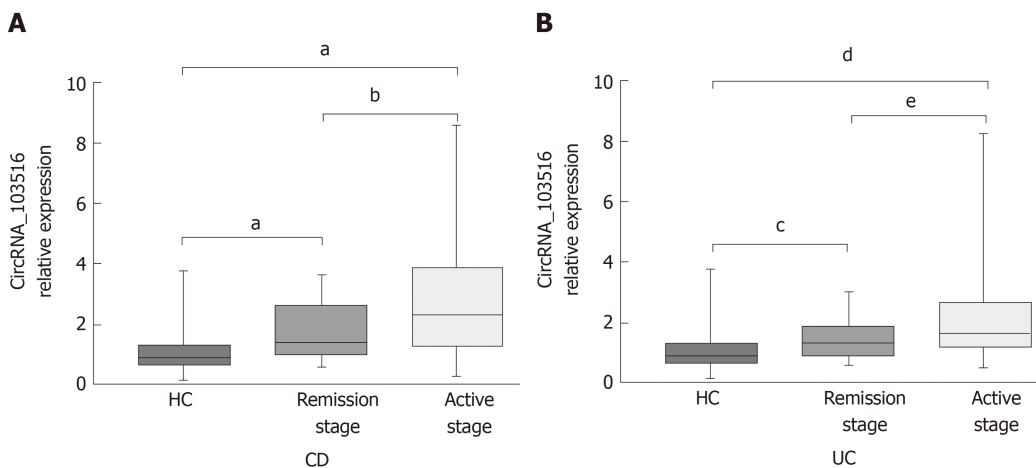
Clinical variable	n	CircRNA_103765 + (%)	Crude		Adjusted			
			OR	95%CI	P value	OR	95%CI	P value
Gender								
Male	48	66.7						
Female	42	64.3	1.11	0.465-2.655	0.813	NS		
Age								
< 40 yr	47	57.4						
≥ 40 yr	43	74.4	2.155	0.879-5.281	0.093	NS		
Smoking status								
Never	60	68.3						
Past or current use	30	60.0	1.439	0.579-3.577	0.434	NS		
Disease location of CD								
L1	37	64.7						
L2	20	64.7	0.524	0.094-2.930	0.462	NS		
L3	33	63.3	0.522	0.082-3.364	0.496			
Disease activity of CD								
Mild	19	47.4						
Moderate	40	82.5	5.238	1.554-17.653	0.008	4.886	1.384-17.251	0.014
Severe	15	80.0	4.444	0.941-21.001	0.025	4.416	0.084-22.054	0.043
Disease behavior of CD								
B1	39	48.7						
B2	33	78.8	3.910	1.376-11.110	0.011	3.641	1.245-10.650	0.018
B3	18	77.8	3.684	1.028-13.202	0.045	4.375	1.147-16.690	0.031
Medications								
5-ASA	80	73.8	1.309	0.340-5.035	0.696	NS		
Corticosteroids	50	74.0	2.329	0.959-5.655	0.062	NS		
Immunosuppressants	28	67.9	1.161	0.450-2.998	0.758	NS		
Anti-TNF-α	13	76.9	1.905	0.483-7.505	0.357	NS		
Surgery	4	75.0	1.607	0.160-16.130	0.687	NS		

The data are shown with crude and adjusted odds ratios and 95% confidence intervals accordingly. L1: Terminal ileum; L2: Colon; L3: Ileocolon; B1: Non-stricture and non-penetrating; B2: Stricturing; B3: Penetrating; CD: Crohn's disease; 5-ASA: 5-aminosalicylic acid; TNF-α: Tumor necrosis factor α; NS: No significance; OR: Odds ratio; CI: Confidence interval; CircRNA: Circular RNA.

**Table 6** Univariate logistic regression analysis showing the disease phenotypes of ulcerative colitis in correlation to circular RNA\_103516 status as dependent variable

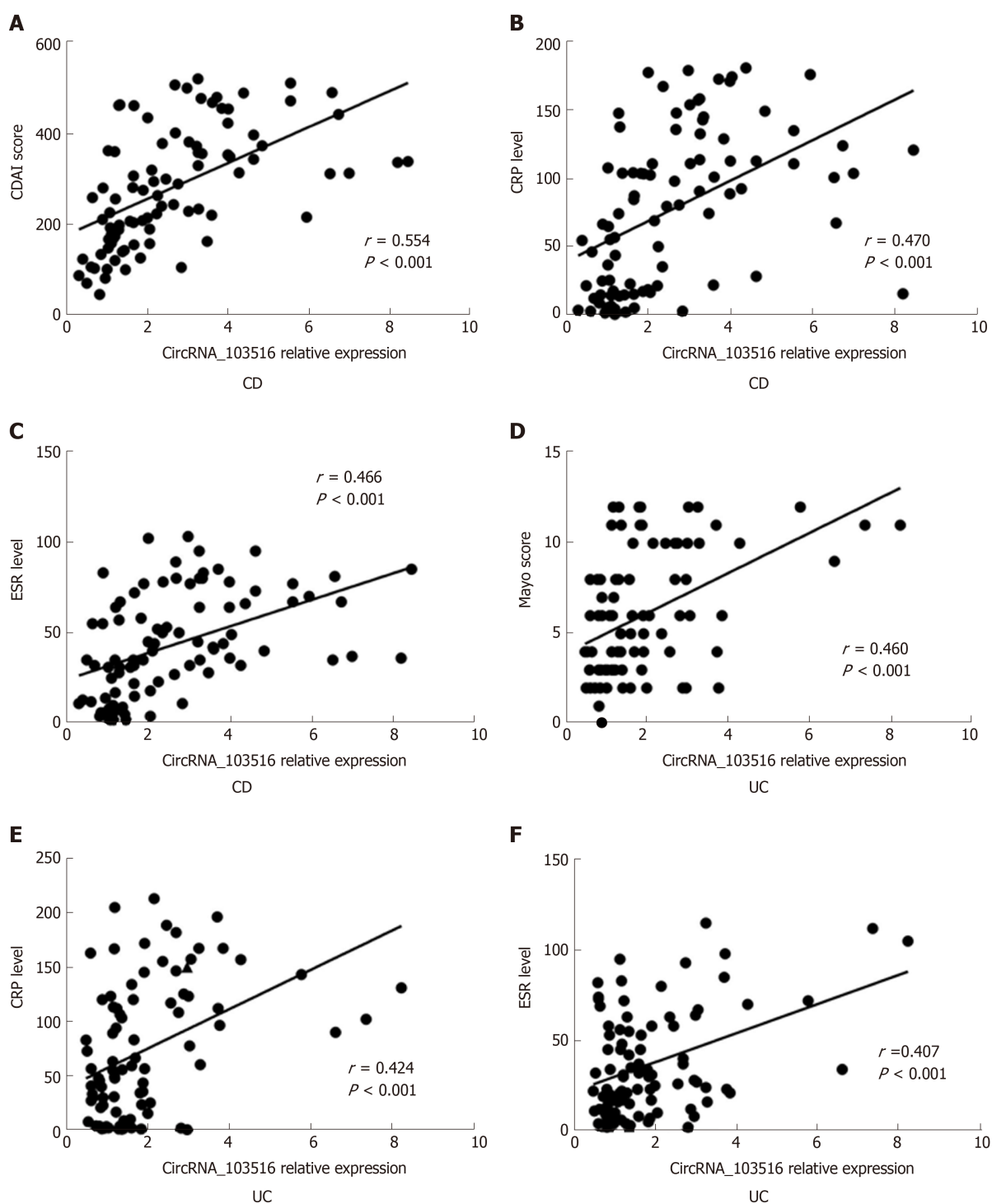
Clinical variable	n	CircRNA_103765 + (%)	Crude			Adjusted		
			OR	95%CI	P value	OR	95%CI	P value
Gender								
Male	38	52.6%						
Female	52	59.6%	1.329	0.571-3.090	0.509	NS		
Age								
< 40 yr	40	60.0%						
≥ 40 yr	50	54.0%	0.783	0.337-1.817	0.568	NS		
Smoking status								
Never	67	69.7%						
Past or current use	23	47.8%	0.619	0.239-1.604	0.323	NS		
Disease location of UC								
E1	36	44.4%						
E2	30	60.0%	1.875	0.702-5.009	0.210	NS		
E3	24	70.8%	3.036	1.012-9.107	0.048			
Disease severity of UC								
Mild	30	60.0%						
Moderate	31	70.9%	1.630	0.562-4.729	0.369	NS		
Severe	15	93.3%	9.333	1.080-80.627	0.042	10.803	1.171-94.687	0.036
Medications: n (%)								
5-ASA	87	57.5%	0.786	0.143-2.037	0.342	NS		
Corticosteroids	41	70.7%	1.827	0.762-5.234	0.084	NS		
Immunosuppressants	14	71.4%	1.234	0.673-3.238	0.705	NS		
Anti-TNF-α	4	50.0%	0.385	0.051-2.919	0.355	NS		
Surgery	1	0.0%	0.000	0.000-	1.000	NS		

The data are shown with crude and adjusted odds ratios and 95% confidence intervals accordingly. E1: Rectum; E2: Left side; E3: Extensive; UC: Ulcerative colitis; 5-ASA: 5-aminosalicylic acid; TNF-α: Tumor necrosis factor α; NS: No significance; OR: Odds ratios; CI: Confidence intervals; CircRNA: Circular RNA.

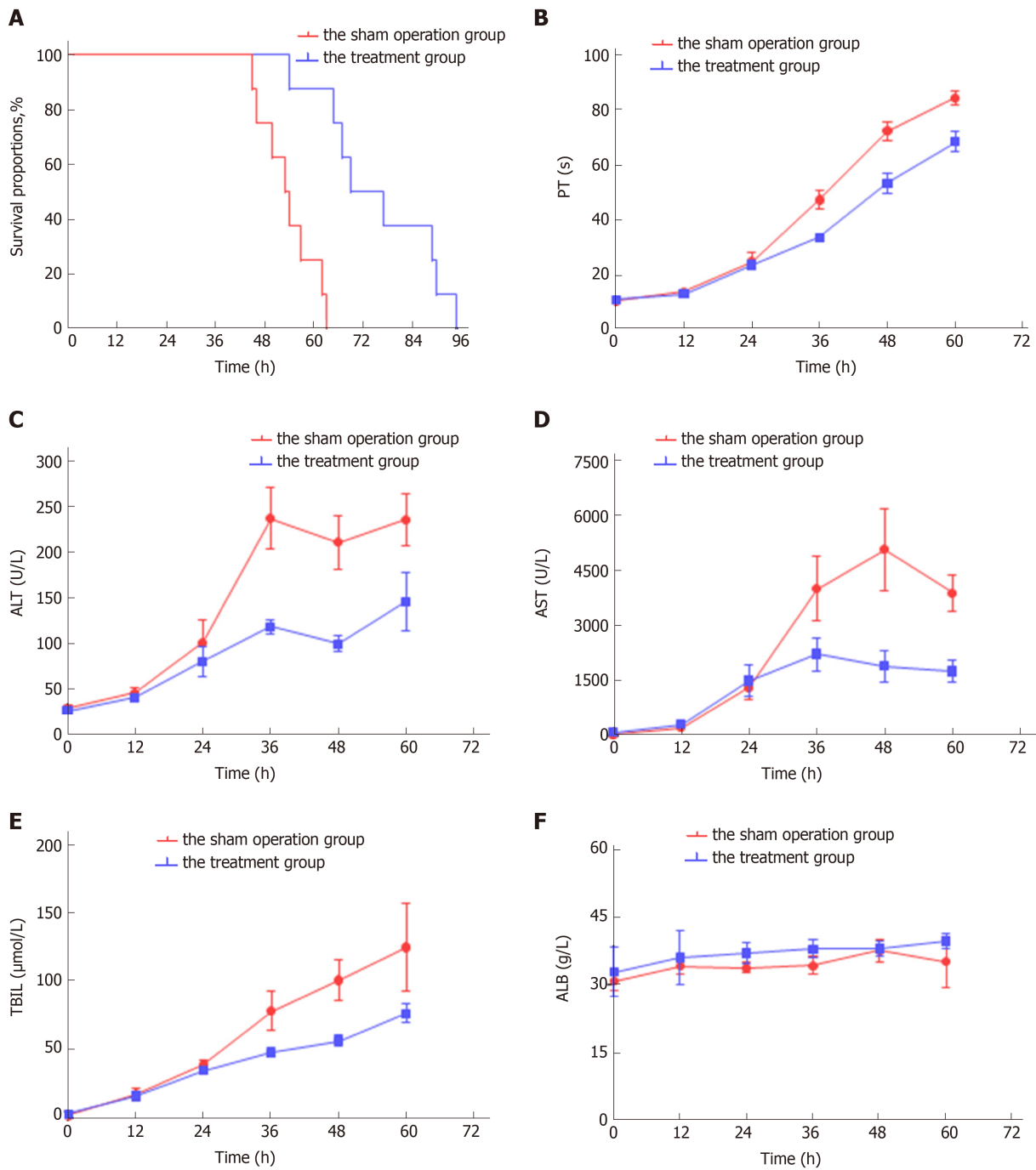


**Figure 4** Expression of circular RNA\_103516 in peripheral blood mononuclear cells from inflammatory bowel disease patients at different stages. A: Circular RNA (circRNA)\_103516 in CD patients at different stages. <sup>a</sup> $P < 0.001$  vs HCs; <sup>b</sup> $P < 0.05$ , remission stage vs active stage. B: CircRNA\_103516 in UC patients at different stage. <sup>c</sup> $P < 0.05$  vs HCs; <sup>d</sup> $P < 0.001$  vs HCs; <sup>e</sup> $P < 0.05$ , remission stage vs active stage.  $P < 0.05$  was considered statistically significant. CD: Crohn's disease; UC: Ulcerative colitis; CircRNA: Circular RNA.

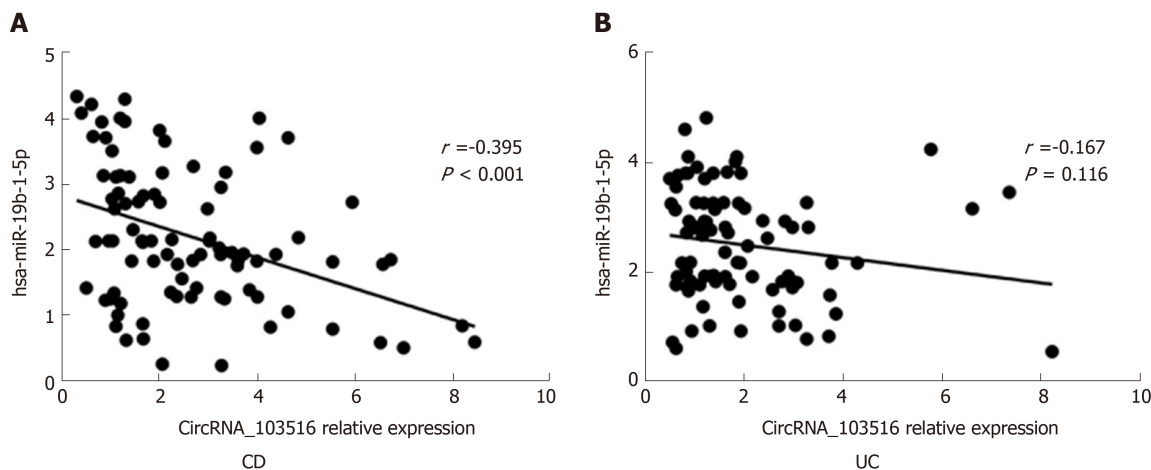




**Figure 5** Correlations of circular RNA\_103516 expression with Crohn's disease activity index, Mayo score, C reactive protein, and erythrocyte sedimentation rate in inflammatory bowel disease patients. Spearman's analysis was applied to test the correlation of circular RNA (circRNA)\_103516 expression with disease activity. A-C: Correlations of circRNA\_103516 expression with disease activity in patients with CD; D-F: Correlations of circRNA\_103516 expression with disease activity in patients with UC.  $P < 0.05$  was considered statistically significant. CD: Crohn's disease; UC: Ulcerative colitis; CDAI: Crohn's disease activity index; CRP: C reactive protein; ESR: Erythrocyte sedimentation rate; CircRNA: Circular RNA.



**Figure 6** Correlations of circular RNA\_103516 expression with inflammatory cytokines in inflammatory bowel disease. A-C: Correlations of circular RNA (circRNA)\_103516 expression with TNF $\alpha$ , IFN- $\gamma$ , and IL-10 in CD; D-F: Correlations of circRNA\_103516 expression with TNF $\alpha$ , IFN- $\gamma$ , and IL-10 in UC.  $P < 0.05$  was considered statistically significant. CD: Crohn's disease; UC: Ulcerative colitis; TNF- $\alpha$ : Tumor necrosis factor  $\alpha$ ; IFN- $\gamma$ : Interferon  $\gamma$ ; IL-10: Interleukin-10; CircRNA: Circular RNA.



**Figure 7 Correlations of circular RNA\_103516 expression with hsa-miR-19b-1-5p in inflammatory bowel disease.** A: Correlation of circular RNA (circRNA)\_103516 expression with hsa-miR-19b-1-5p in CD; B: Correlation of circRNA\_103516 expression with hsa-miR-19b-1-5p in UC.  $P < 0.05$  was considered statistically significant. CD: Crohn's disease; UC: Ulcerative colitis; CircRNA: Circular RNA.

## ARTICLE HIGHLIGHTS

### Research background

Inflammatory bowel disease (IBD), including ulcerative colitis (UC) and Crohn's disease (CD), comprises chronic gastrointestinal tract inflammatory disorders. Due to the characteristic of repeated recurrence, the disease activity of IBD must be assessed and monitored repeatedly. Accordingly, non-invasive serological biomarkers may constitute an optimal alternative choice for evaluating and screening disease activity in IBD. Increasing evidence demonstrates that circular RNAs (circRNAs) participate in the pathogenesis of a variety of diseases by modulating gene expression at the transcriptional or post-transcriptional level and are considered ideal biomarkers in human disease.

### Research motivation

To date, little is known about the relationships between circRNAs and IBD. Our previous research identified 155 upregulated circRNAs and 229 downregulated circRNAs by microarray analysis of peripheral blood mononuclear cells (PBMCs) from CD patients compared with healthy controls (HCs). Moreover, bioinformatics analysis predicted that hsa\_circRNA\_103516 might participate in the pathogenesis of IBD by sponging hsa-miR-19b-1-5p.

### Research objectives

The aim of this study was to identify expression of circRNA\_103516 in IBD and its association with clinical phenotypes and inflammatory cytokines.

### Research methods

We performed an observational study. PBMCs were obtained from patients with IBD, HCs, and patient controls. Expression of circRNA\_103516 and hsa-miR-19b-1-5p was assessed by quantitative reverse transcription-polymerase chain reaction. Crohn's disease activity index (CDAI), Mayo score, C-reactive protein (CRP) level, and erythrocyte sedimentation rate (ESR) were measured. Flow cytometry was used to examine blood samples for the measurement of the inflammatory cytokines tumour necrosis factor- $\alpha$ , interferon- $\gamma$  (IFN- $\gamma$ ), and interleukin-10 (IL-10). Spearman correlation analysis was performed to determine linear correlations for different groups. Receiver operating characteristic curve analysis was used to assess the clinical diagnostic value of candidate circRNAs. Logistic regression analysis was used to identify risk factors.

### Research results

CircRNA\_103516 was upregulated in CD and UC. Furthermore, circRNA\_103516 correlated positively with CDAI, Mayo score, CRP, ESR, TNF $\alpha$ , and IFN- $\gamma$  and negatively with IL-10 in IBD. Additionally, circRNA\_103516 correlated positively with stricturing and penetrating behaviour. The predicted hsa-miR-19b-1-5p correlated negatively with circRNA\_103516 in CD.

### Research conclusions

CircRNA\_103516 in PBMCs can be considered an ideal candidate for the diagnosis of IBD. Dysregulation of circRNA\_103516 may participate in the molecular mechanism of IBD through hsa-miR-19b-1-5p sponging.

### Research perspectives

More large prospective multicentre clinical studies need to be performed for a more applicable conclusion. In addition, miRNA-circRNA interactions were conducted by functional analysis and

not by experimental verification. It is imperative to further explore their respective molecular mechanisms and genetic changes to achieve better diagnostic and treatment strategies in the future.

## REFERENCES

- Karantanos T, Gazouli M. Inflammatory bowel disease: recent advances on genetics and innate immunity. *Ann Gastroenterol* 2011; **24**: 164-172 [PMID: 24713780]
- Xavier RJ, Podolsky DK. Unravelling the pathogenesis of inflammatory bowel disease. *Nature* 2007; **448**: 427-434 [PMID: 17653185 DOI: 10.1038/nature06005]
- Sartor RB. Genetics and environmental interactions shape the intestinal microbiome to promote inflammatory bowel disease versus mucosal homeostasis. *Gastroenterology* 2010; **139**: 1816-1819 [PMID: 21029802 DOI: 10.1053/j.gastro.2010.10.036]
- Diener TO. Circular RNAs: relics of precellular evolution? *Proc Natl Acad Sci U S A* 1989; **86**: 9370-9374 [PMID: 2480600 DOI: 10.1073/pnas.86.23.9370]
- Zhang XO, Wang HB, Zhang Y, Lu X, Chen LL, Yang L. Complementary sequence-mediated exon circularization. *Cell* 2014; **159**: 134-147 [PMID: 25242744 DOI: 10.1016/j.cell.2014.09.001]
- Hansen TB, Jensen TI, Clausen BH, Bramsen JB, Finsen B, Damgaard CK, Kjems J. Natural RNA circles function as efficient microRNA sponges. *Nature* 2013; **495**: 384-388 [PMID: 23446346 DOI: 10.1038/nature11993]
- Jeck WR, Sharpless NE. Detecting and characterizing circular RNAs. *Nat Biotechnol* 2014; **32**: 453-461 [PMID: 24811520 DOI: 10.1038/nbt.2890]
- Xin Z, Ma Q, Ren S, Wang G, Li F. The understanding of circular RNAs as special triggers in carcinogenesis. *Brief Funct Genomics* 2017; **16**: 80-86 [PMID: 26874353 DOI: 10.1093/bfgp/eltw001]
- Gomes CPC, Salgado-Somoza A, Creemers EE, Dieterich C, Lustrek M, Devaux Y; Cardioline™ network. Circular RNAs in the cardiovascular system. *Noncoding RNA Res* 2018; **3**: 1-11 [PMID: 30159434 DOI: 10.1016/j.ncrna.2018.02.002]
- Zheng F, Yu X, Huang J, Dai Y. Circular RNA expression profiles of peripheral blood mononuclear cells in rheumatoid arthritis patients, based on microarray chip technology. *Mol Med Rep* 2017; **16**: 8029-8036 [PMID: 28983619 DOI: 10.3892/mmr.2017.7638]
- Kumar L, Shamsuzzama, Haque R, Baghel T, Nazir A. Circular RNAs: the Emerging Class of Non-coding RNAs and Their Potential Role in Human Neurodegenerative Diseases. *Mol Neurobiol* 2017; **54**: 7224-7234 [PMID: 27796758 DOI: 10.1007/s12035-016-0213-8]
- Yin J, Hu T, Xu L, Li P, Li M, Ye Y, Pang Z. Circular RNA expression profile in peripheral blood mononuclear cells from Crohn disease patients. *Medicine (Baltimore)* 2019; **98**: e16072 [PMID: 31261517 DOI: 10.1097/MD.00000000000016072]
- Cai C, Rajaram M, Zhou X, Liu Q, Marchica J, Li J, Powers RS. Activation of multiple cancer pathways and tumor maintenance function of the 3q amplified oncogene FNDC3B. *Cell Cycle* 2012; **11**: 1773-1781 [PMID: 22510613 DOI: 10.4161/cc.20121]
- Lewis A, Mehta S, Hanna LN, Rogalski LA, Jeffery R, Nijhuis A, Kumagai T, Biancheri P, Bundy JG, Bishop CL, Feakins R, Di Sabatino A, Lee JC, Lindsay JO, Silver A. Low Serum Levels of MicroRNA-19 Are Associated with a Strictureing Crohn's Disease Phenotype. *Inflamm Bowel Dis* 2015; **21**: 1926-1934 [PMID: 25985247 DOI: 10.1097/MIB.0000000000000443]
- Best WR, Beckett JM, Singleton JW, Kern F. Development of a Crohn's disease activity index. National Cooperative Crohn's Disease Study. *Gastroenterology* 1976; **70**: 439-444 [PMID: 1248701 DOI: 10.1016/S0016-5085(76)80163-1]
- Paine ER. Colonoscopic evaluation in ulcerative colitis. *Gastroenterol Rep (Oxf)* 2014; **2**: 161-168 [PMID: 24879406 DOI: 10.1093/gastro/gou028]
- Satsangi J, Silverberg MS, Vermeire S, Colombel JF. The Montreal classification of inflammatory bowel disease: controversies, consensus, and implications. *Gut* 2006; **55**: 749-753 [PMID: 16698746 DOI: 10.1136/gut.2005.082909]
- Yang S, Sun Z, Zhou Q, Wang W, Wang G, Song J, Li Z, Zhang Z, Chang Y, Xia K, Liu J, Yuan W. MicroRNAs, long noncoding RNAs, and circular RNAs: potential tumor biomarkers and targets for colorectal cancer. *Cancer Manag Res* 2018; **10**: 2249-2257 [PMID: 30100756 DOI: 10.2147/CMAR.S166308]
- Zhang Z, Yang T, Xiao J. Circular RNAs: Promising Biomarkers for Human Diseases. *EBioMedicine* 2018; **34**: 267-274 [PMID: 30078734 DOI: 10.1016/j.ebiom.2018.07.036]
- Xu XY, Zhou LL, Yu C, Shen B, Feng JF, Yu SR. Advances of circular RNAs in carcinoma. *Biomed Pharmacother* 2018; **107**: 59-71 [PMID: 30077838 DOI: 10.1016/j.biopha.2018.07.164]
- Ning L, Long B, Zhang W, Yu M, Wang S, Cao D, Yang J, Shen K, Huang Y, Lang J. Circular RNA profiling reveals circEXOC6B and circN4BP2L2 as novel prognostic biomarkers in epithelial ovarian cancer. *Int J Oncol* 2018; **53**: 2637-2646 [PMID: 30272264 DOI: 10.3892/ijo.2018.4566]
- Wang G, Xue W, Jian W, Liu P, Wang Z, Wang C, Li H, Yu Y, Zhang D, Zhang C. The effect of Hsa\_circ\_0001451 in clear cell renal cell carcinoma cells and its relationship with clinicopathological features. *J Cancer* 2018; **9**: 3269-3277 [PMID: 30271486 DOI: 10.7150/jca.25902]
- Li S, Gu H, Huang Y, Peng Q, Zhou R, Yi P, Chen R, Huang Z, Hu X, Huang Y, Tang D. Circular RNA 101368/miR-200a axis modulates the migration of hepatocellular carcinoma through HMGB1/RAGE signaling. *Cell Cycle* 2018; **17**: 2349-2359 [PMID: 30265210 DOI: 10.1080/15384101.2018.1526599]
- Cao B, Zhou X, Ma J, Zhou W, Yang W, Fan D, Hong L. Role of MiRNAs in Inflammatory Bowel Disease. *Dig Dis Sci* 2017; **62**: 1426-1438 [PMID: 28391412 DOI: 10.1007/s10620-017-4567-1]
- Zacharopoulou E, Gazouli M, Tzouvala M, Vezakis A, Karamanolis G. The contribution of long non-coding RNAs in Inflammatory Bowel Diseases. *Dig Liver Dis* 2017; **49**: 1067-1072 [PMID: 28869157 DOI: 10.1016/j.dld.2017.08.003]
- Salzman J. Circular RNA Expression: Its Potential Regulation and Function. *Trends Genet* 2016; **32**: 309-316 [PMID: 27050930 DOI: 10.1016/j.tig.2016.03.002]
- Cheng X, Zhang X, Su J, Zhang Y, Zhou W, Zhou J, Wang C, Liang H, Chen X, Shi R, Zen K, Zhang CY, Zhang H. miR-19b downregulates intestinal SOCS3 to reduce intestinal inflammation in Crohn's disease. *Sci Rep* 2015; **5**: 10397 [PMID: 25997679 DOI: 10.1038/srep10397]
- Gantier MP, Stunden HJ, McCoy CE, Behlke MA, Wang D, Kaparakis-Liaskos M, Sarvestani ST, Yang

- YH, Xu D, Corr SC, Morand EF, Williams BR. A miR-19 regulon that controls NF- $\kappa$ B signaling. *Nucleic Acids Res* 2012; **40**: 8048-8058 [PMID: [22684508](#) DOI: [10.1093/nar/gks521](#)]
- 29 **Yue Y**, Stone S, Lin W. Role of nuclear factor  $\kappa$ B in multiple sclerosis and experimental autoimmune encephalomyelitis. *Neural Regen Res* 2018; **13**: 1507-1515 [PMID: [30127103](#) DOI: [10.4103/1673-5374.237109](#)]
- 30 **Wang Z**, Chen Y, Xu S, Yang Y, Wei D, Wang W, Huang X. Aberrant decrease of microRNA19b regulates TSLP expression and contributes to Th17 cells development in myasthenia gravis related thymomas. *J Neuroimmunol* 2015; **288**: 34-39 [PMID: [26531692](#) DOI: [10.1016/j.jneuroim.2015.08.013](#)]
- 31 **Luo XQ**, Shao JB, Xie RD, Zeng L, Li XX, Qiu SQ, Geng XR, Yang LT, Li LJ, Liu DB, Liu ZG, Yang PC. Micro RNA-19a interferes with IL-10 expression in peripheral dendritic cells of patients with nasal polyposis. *Oncotarget* 2017; **8**: 48915-48921 [PMID: [28388587](#) DOI: [10.18632/oncotarget.16555](#)]
- 32 **Zhao D**, Luo Y, Xia Y, Zhang JJ, Xia Q. MicroRNA-19b Expression in Human Biliary Atresia Specimens and Its Role in BA-Related Fibrosis. *Dig Dis Sci* 2017; **62**: 689-698 [PMID: [28083843](#) DOI: [10.1007/s10620-016-4411-z](#)]
- 33 **Zou M**, Wang F, Gao R, Wu J, Ou Y, Chen X, Wang T, Zhou X, Zhu W, Li P, Qi LW, Jiang T, Wang W, Li C, Chen J, He Q, Chen Y. Autophagy inhibition of hsa-miR-19a-3p/19b-3p by targeting TGF- $\beta$  R II during TGF- $\beta$ 1-induced fibrogenesis in human cardiac fibroblasts. *Sci Rep* 2016; **6**: 24747 [PMID: [27098600](#) DOI: [10.1038/srep24747](#)]





Published By Baishideng Publishing Group Inc  
7041 Koll Center Parkway, Suite 160, Pleasanton, CA 94566, USA  
Telephone: +1-925-2238242  
E-mail: [bpgoffice@wjgnet.com](mailto:bpgoffice@wjgnet.com)  
Help Desk: <http://www.f6publishing.com/helpdesk>  
<http://www.wjgnet.com>

